Proteomic analysis of cell models of ovarian cancer tumour suppression

John Sinclair
Department of Gynaecological Oncology
University College London

This thesis is submitted in partial fulfillment of the requirements for the degree of Doctor of Philosophy from University College London

I, John Sinclair confirm that the work presented in this thesis is my own. Where information has been derived from other sources, I confirm that this has been indicated in the thesis.

ABSTRACT

Epithelial ovarian cancer (EOC) is the most common form of gynaecological malignancy in the developed world. Identifying molecular markers of disease may provide novel approaches to screening and could enable targeted treatment and the design of novel therapies. In previous work, 141 primary ovarian tumours were analysed using metaphase comparative genomic hybridization to identify complete or partial chromosome deletions that may harbour tumour and/or metastasis suppressor genes. Chromosome 18 (Ch18) was found to have deletions in 50% of the tumours. Microcell-mediated chromosome transfer (MMCT) of normal Ch18 material into EOC cell lines resulted in hybrids that displayed significant suppression of anchorage-independent growth, invasiveness and reduced tumour growth in nude mice.

The major aim of this project was to identify protein changes associated with the tumour suppression observed in the EOC Ch18 MMCT cell models. The project involves a detailed quantitative proteomic comparison of two parental ovarian cancer cell lines (derived from primary endometrioid and clear cell carcinomas) and their MMCT-derived Ch18 hybrid clones. The cellular, secreted and surface proteomes were probed in order to gain comprehensive coverage and to improve the likelihood of useful biomarker identification.

A combination of quantitative two-dimensional difference gel electrophoresis (2D-DIGE), affinity chromatography and two-dimensional-liquid chromatography and tandem mass spectrometry (2D-LC-MS/MS) have been employed to examine the whole cell, secreted and cell surface proteomes of the parental and hybrid cell models to identify differentially expressed proteins as potential markers of tumour suppression.

Proteins of interest have been validated using immune-based detection methods in the parental cell lines, Ch18 hybrids, revertant cell lines, a panel of cancer cell lines and normal ovarian surface epithelium cell lines and in serum from a set of ovarian cancer cases and healthy controls.

ACKNOWLEDGEMENTS

Firstly, I would like to thank my supervisors: Dr John Timms, Dr Simon Gayther and Dr Dimitra Dafou for giving me the opportunity to carry out the work presented in this thesis. I would especially like to thank my primary supervisor, Dr John Timms, for introducing me to the field of proteomics and mass spectrometry and his guidance throughout my research.

Finally, I would also like to thank my present and past colleagues at the Cancer Proteomics Laboratory for their friendship and for making the laboratory an enjoyable place to work.

TABLE OF CONTENTS

LIST OF FIGURES & TABLES

ABBREVIATIONS

Chemicals and reagents

ACN	acetonitrile
AEBSF	4-(2-aminoethyl)benzenesulfonyl fluoride hydrochloride
AmBic	ammonium bicarbonate
BCA	bicinchoninic acid
CHAPS	(3-[(3-cholamidopropyl)dimethylammonio]-1-propanesulfonate
CHCA	α-cyano-4-hydroxycycinnamic acid
DHB	2,5-dihydroxybenzoic acid
DMSO	dimethyl sulfoxide
DTT	dithiothreitol
EDTA	ethylenediaminetetraacetic acid
FA	formic acid
FCS	foetal calf serum
HCL	hydrogen chloride
HEPES	N-[2-hydroxyethyl]piperazine-N'[2-ethanesulphonic acid]
IAM	iodoacetamide
KCL	potassium chloride
MgCl2	magnesium chloride
NaCl	sodium chloride
NaH_2PO_4	sodium phosphate
NP-40	nonidet P-40
PBS	phosphate-buffered saline
SDS	sodium dodecyl sulphate
TBS	tris buffered saline
TCEP	tris(2-carboxyethyl)phosphine
TEAB	triethylammoniumbicarbonate
TFA	trifluoroacetic acid
Tris	tris-(hydroxymethyl)aminomethane

General

1DE	one-dimensional gel electrophoresis
2D-DIGE	2D-differential in-gel electrophoresis
2DE	two-dimensional gel electrophoresis
Ab	antibody (mAb: monoclonal Ab; pAb: polyclonal Ab)
AQUA™	absolute quantitation
BAC	bacterial artificial chromosome
CCB	coomassie-colloidal blue
CFE	colony forming efficiency
CGH	comparative genomic hybridization
CID	collision induced dissociation
DC	direct current
DNA	deoxyribonucleic acid
ECL	enhanced chemiluminescence
ECM	extracellular matrix
ELISA	enzyme-linked immunosorbent assay
EmPAI	exponentially modified protein abundance index
EOC	epithelial ovarian cancer
ER	endoplasmic reticulum
ESI	electospray ionisation
FDR	false discovery rate
FISH	fluorescence in situ hybridization
FT	fourier transform
HCD	higher-energy collision-dissociation
HPLC	high performance liquid chromatography
ICAT	isotope-coded affinity tags
IEF	isoelectric focussing
IPG	immobilised pH gradient
IT	ion trap
iTRAQ	isobaric tags for relative and absolute quantitation
kDa	kilodalton
LC	liquid chromatography
LMP	low malignant potential
MALDI	matrix-assisted laser desorption ionisation
MARS	multiple affinity removal system
MMCT	microcell-mediated chromosome transfer
MOSE	mouse ovarian surface epithelium
MRM	multi-reaction monitoring
mRNA	messenger RNA
MS	mass spectrometry

MudPIT	multiple dimension protein identification technology
MWCO	molecular weight cut off
NHS	N-hydroxysuccinimidyl
NSCLC	non small cell lung cancer
OC	ovarian cancer
OSE	ovarian surface epithelium
PAGE	polyacrylamide gel electrophoresis
pI	isoelectric point
PMF	peptide mass fingerprinting
PSD	post source decay
PTM	post translational modification
PVDF	polyvinylidene fluoride
Q	quadrupole
RF	radio frequency
RNA	ribonucleic acid
RP	reverse phase
SCX	strong cation exchange
SELDI	surface-enhanced laser desorption ionisation
SNP	single nucleotide polymorphism
TCL	total cell lysate
TMA	tissue microarrays
TMT	tandem mass tags
TOF	time-of-flight
TVS	transvaginal sonography
UKCTOCS	united kingdom collaborative trial for ovarian cancer screening
XIC	extracted ion chromatogram

Proteins

ADH1A1	aldehyde dehydrogenase A1
ANXA1	annexin A1
BSA	bovine serum albumin
BTF3	basic transcription factor 3
COL3A1	collagen alpha-1 (III) chain
CRT	calreticulin
CYB5B	cytochrome b5 outer membrane precursor
DLD	dihydrolipoyl dehydrogenase
EGF	epidermal growth factor
EGFR	epidermal growth factor receptor
EIF4E	translation initiation factor 4E

EIF5A	translation initiation factor 5A
ERK	extracellular signal regulated kinase
ERp29	endoplasmic reticulum protein ERp29 precursor
FRP	follistatin-related protein
FSCN1	fascin 1
GRB2	growth factor receptor bound-2
HSP90A	heat shock protein 90 alpha
IGFBP	insulin-like growth factor binding protein
LDHB	lactate dehydrogenase B
MAPK	mitogen activated protein kinase
MMP10	stromelysin-2
Tp53	tumour protein 53
PCNA	proliferating cell nuclear antigen
PDI	protein disulphide isomerase
PEDGF	pigment epithelium-derived growth factor
PHB	prohibitin
PI3K	phosphatidylinostitol 3-kinase
PIG3	tumour protein p53 inducible protein 3
PRDX6	peroxiredoxin 6
PTPLAD1	protein tyrosine phosphatase-like protein
SACM1L	transcolase 2 and phosphatidylinositide phosphatase SAC1
SERPINF1	pigment epithelium-derived growth factor
TIMP1	tissue inhibitor metalloproteinase 1
TMEFF1	tomoregulin-1
UCLH1	ubiquitin carboxyl terminal esterase L1
VCP	valosine-containing protein
VEGF	vascular endothelial growth factor

Chapter 1 Introduction

1.1 Epithelial Ovarian Cancer

Background

Epithelial Ovarian cancer is the most lethal form of gynaecological malignancy in the western world and the ovary is the seventh most common site of cancer in women. Overall incidence rates of ovarian cancer are increasing although they show a high degree of variation geographically. In Europe, the USA and Canada, observed rates are highest whilst the lowest rates are observed in Asia, Africa and Latin America. Every year in the UK, nearly 7000 new cases of ovarian cancer are diagnosed and the disease accounts for more than 4400 deaths annually (CRUK 2006 http://info.cancerresearchuk.org/cancerstats/types/ovary/).

Most ovarian cancers occur after menopause when the ovaries have little or no physiological role. As a consequence, abnormal ovarian function has few symptoms and combined with the anatomical location of the ovaries deep in the pelvis, ovarian cancer is usually diagnosed at an advanced stage. Patients with early stage ovarian cancer, in whom the disease is confined to one or both of the ovaries (stage I; Table 2.1), have good prognoses (5 year survival rate >80%). Patients with advanced disease, in whom the tumour has spread within or beyond the abdominal cavity, (stage III and

IV) have a significantly poorer prognosis (20% of patients surviving 5 years). The overall survival rate is as low as 30%, mostly due to this late detection in presenting patients (Breedlove and Busenhart 2005).

Most ovarian tumours are epithelial in origin (80-90%), the remaining tumours arise from germ-cell or sex cord/stromal cells. The epithelial tumours are grouped into histological sub-types with the most common being serous adenocarcinoma (42%), undifferentiated carcinoma (17%), endometrioid carcinoma (15%), mucinous cystadenocarcinoma (12%), and clear cell carcinoma (6%).

Epithelial ovarian cancers are clonal neoplasms and it is thought that multiple genetic alterations must occur during their malignant transformation. Gene expression profiling or microarray analysis have enabled the measurement of thousands of genes in a single RNA sample. Despite its huge potential, gene expression profiling of EOC has been confounded by a lack of understanding of the cellular origin and pathways to EOC. The difficulty lies in the limited availability of early stage tumours, the heterogeneity, and the genetic instability of tumours, which makes it difficult to distinguish the occurrence of early or late stage mutations. In the literature it has been hypothesized that there maybe several cells of origin and precursor ovarian states, prior to transformation to malignancy. It is believed that EOC emerges via transformation of the cells lining inclusion cysts or directly from the ovarian surface epithelium (OSE) (Auersperg, Maines-Bandiera et al. 1997; Auersperg, Edelson et al. 1998; Auersperg, Wong et al.

2001) or other epithelial sources such as the fallopian tubes, endometrium, or endoocervix (Dubeau 1999).

Surrounding the ovary is a single layer of phenotypically undifferentiated cells known as the OSE. The OSE, mesothelial lining of the peritoneal cavity and the reproductive tract tissues are all derived during development from the coelomic layer. However, the OSE develops from the epithelium overlying the gonadal ridge whilst the reproductive tract tissues originate from the mullerian ducts, arising from an invagination of the coelomic epithelium beside the coelomic ridge. It has been observed that after metaplastic transformation, the OSE shares characteristics of mullerian duct-derived tissues such as the fallopian tubes, cervix and endometrium (Auersperg, Pan et al. 1999). This aberrant differentiation forms the basis for ovarian cancer classification (Bell 2005). An additional source of ovarian epithelial cells is the rete ovarii, a reticulum of tubules thought to develop from the mesonephric tubules. Mesonephric cells migrate towards and into the undifferentiated gonad during ovarian development, resulting in an extension of mesonephric tubules through the mesovarian.

It is known a significant fraction of ovarian cancer (10%) is hereditary. A few highly penetrant genes that contribute to genetic susceptibility have been identified. Women with germline mutations in the *BRCA1* gene or *BRCA2* gene and women harbouring such mutations are at a 20-60% risk of developing ovarian cancer in their lifetimes (Aunoble, Sanches et al. 2000; Welcsh, Owens et al. 2000; Welcsh, Lee et al. 2002). Mutations in the hereditary non-polyposis colorectal cancer genes, *MSH2* and *MLH1*

(Taylor, Charlton et al. 2003), also increase the risk of invasive EOC substantially, particularly of the endometrioid subtype (Ichikawa, Lemon et al. 1999). Association studies, considering the effect of common single nucleotide polymorphisms (SNPs) and risk of EOC, suggest that other lower penetrance mutations exist that have subtle effects on risk of EOC (Ramus, Vierkant et al. 2008; Quaye, Song et al. 2009). Furthermore, there are many reports that suggest the genetic and epigenetic changes that occur during ovarian tumourigenisis differ among the different subtypes of EOC (Duggan and Dubeau 1998).

The genes that may contribute to the tumourigenesis of sporadic ovarian cancers fall into two categories: oncogenes and tumour suppressors. Oncogenes are dominant transforming genes in that their activation occurs by the alteration of a single allele. Activation of oncogenes occurs through a variety of mechanisms such as point mutation, gene amplification, deletion of a regulatory domain or gene fusion through chromosomal translocation. The normal counterparts of oncogenes, proto-oncogenes, are involved in controlling critical cellular events such as survival and cell proliferation (Aunoble, Sanches et al. 2000; Hanahan and Weinberg 2000). Tumour suppressor genes behave recessively. This involves the loss or inactivation of both copies of a tumour suppressor gene that normally confers constraints on cell proliferation, survival, DNA damage repair etc. Although oncogenes and tumour suppressors may influence ovarian cancer, little is known about their role in the transformation of ovarian surface epithelial cells and the relative contributions of multiple mutations. A few genes have been reported as frequently altered in sporadic epithelial ovarian cancers. For example

the tumour suppressor gene *p53*, is mutated in approximately 50% of advanced stage cancers, the oncogene *K-RAS*, is mutated in 20-50% of borderline/low malignant potential (LMP) tumours (Aunoble, Sanches et al. 2000; Liu, Yang et al. 2004), the oncogenic receptor tyrosine kinases *HER2*/*ERBB2* and *fms* are overexpressed in 20-50% of ovarian tumours (Auersperg, Maines-Bandiera et al. 1997; Auersperg, Edelson et al. 1998) and the tumour suppressor lipid phosphatase *PTEN* is frequently mutated in endometrioid type ovarian carcinomas (Kurose, Zhou et al. 2001).

EOC risk increases with age with as much as 50% of all ovarian cancers being found in woman over the age of 63 (CRUK 2006 http://info.cancerresearchuk.org/cancerstats/types/ovary/). A link has been reported between the number of menstrual cycles in a woman's reproductive lifetime and her risk of developing EOC (Parazzini, La Vecchia et al. 1989; Schildkraut, Bastos et al. 1997; Purdie, Bain et al. 2003). This has been supported by evidence of a decrease in EOC risk with decreased lifetime ovulation number through pregnancy or oral contraceptive use (Tavani, Ricci et al. 2000). In addition, some studies suggest that the use of estrogen replacement therapy may promote EOC in women who have been through the menopause (Folsom, Anderson et al. 2004; Rossing, Cushing-Haugen et al. 2007), whilst, women who have never been pregnant because of infertility have a 40% higher risk of developing EOC compared to women who have never attempted to become pregnant. Moreover, the use of the progestin-only contraceptive pill has been shown to be even more protective against EOC than the combined contraceptive pill (Rodriguez 2003). Further studies have identified a protective effect of the high levels

of progesterone during pregnancy (Mukherjee, Syed et al. 2005). The role of inflammation during ovulation has also been proposed as a risk factor where the associated cytokine release, influx of inflammatory cells and tissue reconstruction has been postulated to stress OSE cells such that they become predisposed to genetic damage and malignant transformation (Rae and Hillier 2005). Consistent with this are findings that patients with chronic aspirin, nonsteroidal anti-inflammatory drug or acetaminophen use display decreased risk of EOC (Altinoz and Korkmaz 2004).

1.1.2 Staging and Treatment

All ovarian cancers are classified according to the terms of the staging scheme (I through IV) developed by the International Federation of Gynaecological and Obstetrics (FIGO) and the classification system developed by the American Joint Committee on Cancer (AJCC, TNM system), which indicate likely prognosis and help to define treatment (Table 1).

Stage	Description
I	Cancer is in one (IA) or both of the ovaries (IB) and has not spread onto the outer surface of the ovary. Cancer is present in one or both of the ovaries and present on the outer surface of at least one of the ovaries or the tumour may have ruptured (IC). The disease has not spread to the abdomen or pelvis.
II	Cancer is one or both of the ovaries and has grown onto or into other pelvic organs. Cancer has spread onto or into the uterus or the fallopian tubes, or both (IIA). Cancer has spread onto or grown into the tissue within the pelvis (IIB). Cancer has spread to the uterus, fallopian tubes, or other tissues within the pelvis (IIC).
III	The cancer is in one or both of the ovaries and has spread to the abdominal lining but can't be seen (IIIA) or small deposits observed (IIIB). Cancer has spread to the lymph nodes and deposits maybe visible in the abdomen (IIIC).
IV	The cancer has spread outside the pelvic region to distant sites such as inside the liver, the lungs, or other organs.

Table 1.1.1 Ovarian cancer is staged using the AJCC and FIGO system. This system defines cancers by Roman numerals I through IV. The higher the number, the more the cancer has spread. The stages of cancer and their definitions are shown.

Almost all women with EOC will have some kind of surgery in the course of their treatment. The purpose of surgery is first to diagnose by pathological examination of ovarian and other tissues to define the nature of the tumour and its stage. Staging is performed by examining histological sections of tissue samples and cytological assessment of fluid samples. EOC tumours display a spectrum of pathological changes. Tumours can be benign, borderline (low malignant potential or atypical proliferating lesions) or malignant. The success of treatment depends upon stage and grade of the disease, the histopathologic type and the patient's age and overall health. Where early disease is detected (confined to the ovaries) in woman who wish to preserve their fertility, 'conservative' surgery that leaves tumour-free reproductive organs intact is considered. This is dependent on the tumour being confined to an ovary (usually not serous or endometrioid sub-type, which tend to be bilateral tumours) and a wedge biopsy of the opposite ovary shows no evidence of disease involvement. Conservative surgery carries an increased risk of relapse, therefore a total hysterectomy and salpingo-oophorectomy is recommended immediately after child bearing is complete. The removal of the ovaries before the incidence of EOC reduces the risk to zero. The decision whether or not to proceed is often influenced by the fact that most women with increased risk of ovarian cancer are also at increased risk of breast cancer and there is clear evidence that oophorectomy reduces breast cancer risk in these cases. In advanced cases of EOC, where disease has spread beyond the ovaries, treatment involves surgery and chemotherapy. A total hysterectomy (removal of the uterus), bilateral salpingo-opphorectomy (removal of fallopian tubes and ovaries on both sides), omentectomy (removal of the fatty tissues that covers the bowel), lymph adenectomy

(removal of one or more lymph nodes) may be performed. Often with late stage cancers women will undergo debulking surgeries, which involves removing as much of the disease as possible. Sometimes patients will have their surgery performed after having 3 cycles of chemotherapy. Ovarian cancer is a chemosensitive disease, and the use of immediate first line platinum-based chemotherapy improves prognosis for patients with advanced disease. The platinum-based drugs cisplatin and carboplatin are equally effective in the treatment of EOC. Whilst ovarian tumours initially respond very well, eventually between 70-80% of advanced stage ovarian cancer patients develop a resistance to these drugs. Indeed, ovarian cancer cells that have developed secondary mutations on the *BRCA2* gene that restore the genes ability to repair DNA, confers a subsequent resistance to chemotherapy (Sakai, Swisher et al. 2008). Radiation treatment is also used in the treatment of EOC where high energy X-rays are used to kill cancer cells, ease the pain of metastases and stop tumours from bleeding. Patients are monitored for recurrence after treatment. Regular check-ups would continue from treatment and include a combination of bimanual pelvic examinations, serial measurements of the serum cancer antigen CA125 and radiographic imaging.

1.1.3 Screening for ovarian cancer

Ovarian cancer is often described as a silent killer because the symptoms are not specific and common to other diseases and disorders. Since most cases are diagnosed at late stage when treatment is less successful, there is an absolute necessity for early detection methods to reduce mortality. At present however, there is no screening test

that is reliable enough to use for ovarian cancer detection in the general population. The tumour marker, serum CA-125, is only approved for use in monitoring disease recurrence (Skates, Horick et al. 2004; Bast, Badgwell et al. 2005). 80% of women presenting with advanced stage disease have elevations in CA-125. However, it is elevated in only 50-60% of women with early stage disease and can be elevated in other non-cancerous gynaecological complications such as benign ovarian neoplasms, endometriosis, pelvis inflammatory disease and liver disease. The glycoprotein, CA-125 can also be elevated in other malignant conditions including cancers of the pancreas, breast, lung and colon. Despite this, a large randomised trial of ovarian cancer screening in the general population is currently underway to evaluate the use of an algorithm that incorporates the rate of change of CA-125 over time from intial marker levels with estimated age adjusted ovarian cancer prevalence rates in order to increase sensitivity and specificity and includes an ultrasound modality (Jacobs, Skates et al. 1999; Menon, Gentry-Maharaj et al. 2008). There is preliminary evidence that such a screening technique will reduce the mortality from ovarian cancer (Neesham 2007).

Transabdominal ultrasound and transvaginal ultrasonography (TVS) have been studied as non-invasive screening tools. TVS is currently the preferred modality. However, the specificity of ultrasonography is not adequate for use as a single screening modality. Therefore, there is an urgent requirement for better early diagnostic markers of EOC.

1.2 Cell models of Disease

Experimental cell models are of vital importance not only to understand the biological and genetic factors that influence the phenotypic characteristics of EOC, but also to develop robust early detection and intervention strategies. Cell models have remained a vital resource for understanding the underlying events that accompany oncogenesis. The use of cell lines carries a number of advantages including the purity of the research material, the ability to generate sufficient research material (DNA/RNA/protein) for numerous experiments and the ability to genetically manipulate cell lines allowing a wide range of *in vitro* and *in vivo* studies. The past 6 years has seen the development of ovarian surface epithelial cell models with inactivation/activation of different signalling pathways giving rise to transformed cells with different phenotypes (Davies, Steele et al. 2003; Liu, Yang et al. 2004; Mei, Young et al. 2005; Young, Mei et al. 2005). While these models offer the benefits of studying a simple and well-characterised system, the degree to which transformation of human cells *in vitro* represents the process *in vivo* remains unknown.

Xenografting of human cancer cells into immune deficient mice has been essential for analysing the tumourigenicity of cells, the histology of the tumours they form and the evaluation of therapeutics (Han, Begemann et al. 1996; Hu, McCrea et al. 2000; Oktem and Oktay 2007). While xenograft models using human cancer cell lines may reveal the nature and behaviour of advanced human ovarian cancer, they do not allow study of the

earlier steps in ovarian cancer development or provide meaningful information about human host-tumour interactions.

The use of mouse ovarian surface epithelium (MOSE) creates the opportunity for studying disease progression and therapeutic response in immune-competent animals (Fig 1.1.1). The role of the immune system on tumour progression is a factor that should not be ignored. Cancers that develop in immune deficient mice are very immunogenic when transplanted back into immune-competent mice, compared to the poor immunogenicity of spontaneous tumours arising directly in immune-competent mice. Immunosurveillance protects the host against tumour development and can shape the immunogenic phenotype of a developing tumour. Despite this, chronic inflammation as a result of immune response has for a long time been associated with cancer development. For example, macrophages produce many factors that promote growth and survival of tumours, angiogenesis, tissue invasion and metastases. A dual role exists for immunosurveillance in protection against and promotion of tumour development. Retroviral transduction to introduce various oncogenes or tumour suppressors in MOSE can lead to transgenic models in which tumours initiate and progress in situ (Roberts, Mottillo et al. 2005).

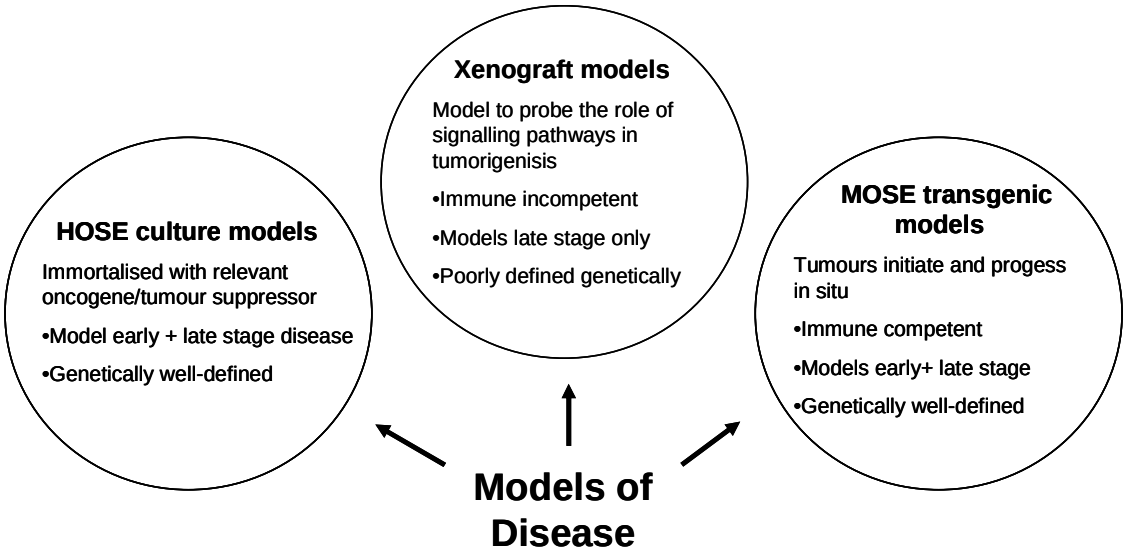

Figure 1.1.1 Summary of models used to characterize tumour development and progression.

1.3 Expression profiling of EOC

Traditionally, tumours have been categorised on the basis of histology. However, staining of cancer cells viewed under the microscope gives insufficient information on the underlying molecular events that drive the neoplastic process. The chromosomal abnormalities and alterations in cancerous cells, somatic and/or acquired, are distinct for unique tumour subtypes and may be targets of new treatments. There are multiple mechanisms by which genes or biological pathways can lead to the development of cancer. Most cancer-associated genes are altered at either the chromosome level (e.g. translocations, interstitial chromosome deletions and rearrangements and chromosome

ploidy), the base level (e.g. coding sequence mutations, genomic deletions, rearrangements and amplifications), or at an expression level (e.g. splice site mutations or aberrant methylation of promoter regions). Identifying these molecular markers of disease may provide novel approaches to screening and could enable targeted treatment and/or lead to the design of novel therapies. However, the biological and molecular genetic basis of epithelial ovarian tumour development remains poorly understood.

Comparative genomic hybridisation (CGH) and loss of heterozygosity (LOH) studies have identified multiple, common genomic alterations in cancers (Sakamoto, Sakamoto et al. 1996; Kudoh, Takano et al. 2000; Suehiro, Sakamoto et al. 2000; Bozzetti, Bortesi et al. 2004). CGH is a cytogenetic method of screening a tumour for genetic changes. In a typical CGH experiment, equal amounts of tumour DNA and normal reference DNA are labelled with fluorescent dyes. The samples are then pooled and allowed to competitively hybridise to target DNA, which for conventional CGH would be condensed metaphase chromosomes on a glass slide. The genomic differences are then viewed by microscopy. More recently, genomically mapped DNA fragments (i.e. BAC clones, cDNA, oligonucleotides) immobilized on to a glass slide serve as the target DNA. Laser excitation of the hybridized targets yields emission with characteristic spectra from each dye. The DNA copy number is determined by the ratio of the fluorescence of the test sample over the fluorescence of the reference sample (Fig 1.1.2).

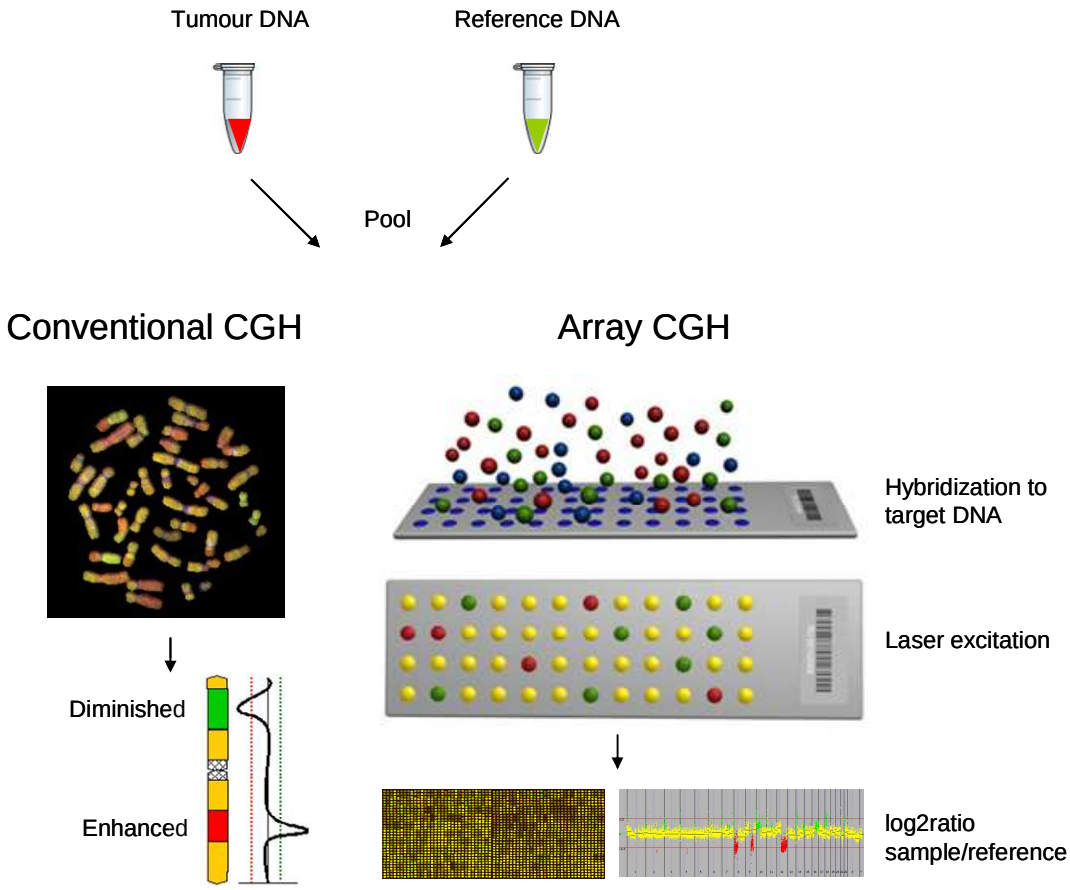

Figure 1.1.2 Conventional and array CGH. An example of the co-hybridization of differentially-labelled test (tumor- red fluorochrome) and reference (normal- green fluorochrome) genomic DNA probes onto metaphase target chromosomes and a BAC array.

In one study, metaphase CGH was used to characterize the deletions and amplifications in 141 ovarian tumours grouped with respect to BRCA1/2 status (Ramus, Pharoah et al. 2003). This showed multiple frequently occurring somatic alterations (Fig 1.1.3). Chromosome deletions are thought to suggest the location of tumour suppressor genes involved in the pathogenesis of the disease and possibly reflect the genetic damage that occurs during tumour progression. Interestingly, they identified molecular genetic

differences between the four tumour types under study, indicating different mechanisms are involved in tumour development which may impact on clinical outcome.

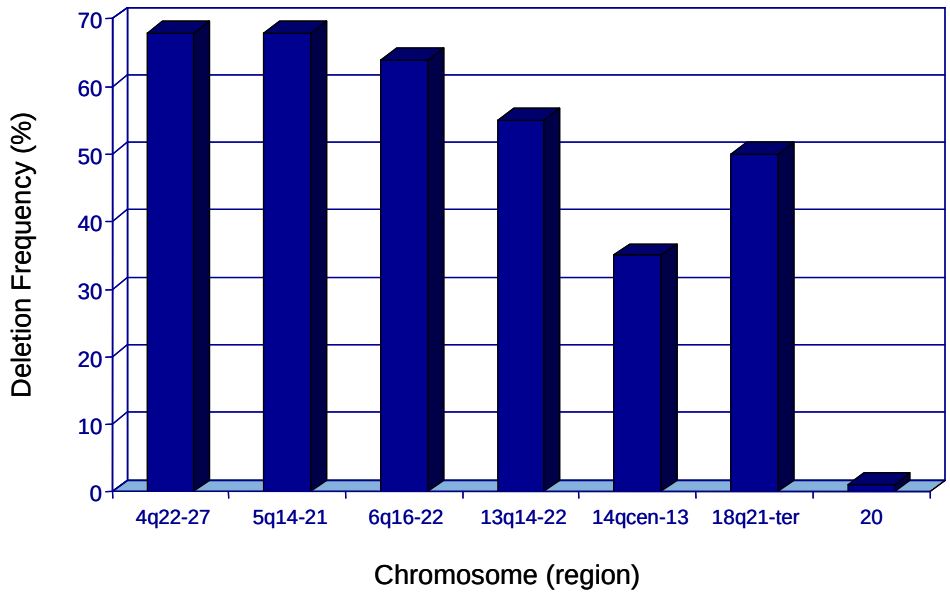

Figure 1.1.3 Metaphase CGH analysis of 141 epithelial ovarian cancers. This graph shows the frequencies of chromosomal deletion identified for each chromosome arm in a cohort of cancers from BRCA1 and BRCA2 mutation carriers, individuals with familial non-BRCA1/2 epithelial ovarian cancer, and women with non-familial ovarian cancer.

CGH studies have revealed that the frequency of deletions increases with grade and stage of ovarian tumours and that low malignant potential/borderline tumours are more similar to benign ovarian cancers than they are to malignant tumours (Wolf, Abdul-Karim et al. 1999).

With the improvements in microarray technology, simultaneous interrogation of thousands of genes in a high-throughput fashion offers unprecedented opportunities to obtain the molecular signatures of cell models or solid tumour samples (Haviv and Campbell 2002). The advantage of microarrays is that you obtain a comprehensive parallel record of genes that are expressed together in a condition-dependent manner (Adib, Henderson et al. 2004).

In a recent study, microcell-mediated chromosome transfer (MMCT) was employed to introduce normal chromosomes into recipient tumour cell lines to induce a suppressive effect on their tumourigenic phenotype. The extent of genomic transfer suspected to carry tumour suppressor genes was characterised by array CGH (Dafou, Ramus et al. 2009). MMCT (Doherty and Fisher 2003) comprises a donor cell (e.g. murine fibroblasts) containing normal human chromosome material tagged with a selectable marker. After prolonged exposure to colcemid, the cell is held in metaphase and forms no functional spindle. The cell eventually leaves mitosis and the nuclear membrane reforms around single chromosomes to produce micronuclei which can be isolated and fused with a recipient cell (Fig 1.1.4).

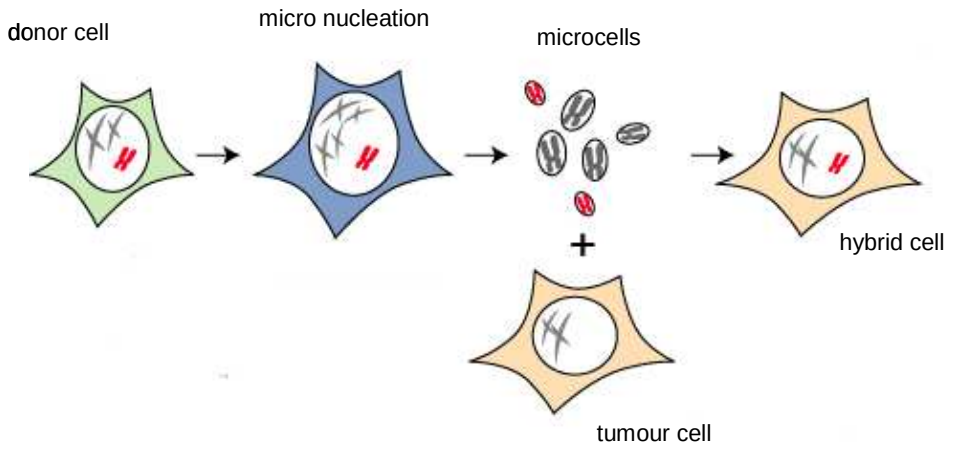

Figure 1.1.4 MMCT. A donor cell containing a chromosome of interest tagged with a selectable marker is treated with colcemid for 48 hours to produce micronuclei. These are isolated and the microcells fused with a recipient tumour cell. The cells containing the chromosome of interest are then selected for.

The study involved the transfer of a number of chromosomes previously identified to be genetically altered in ovarian cancers into two EOC cell lines. Among others, normal chromosome 18 material was transferred into two epithelial ovarian cancer cell lines, TOV-112D and TOV-21G. These ovarian cancer cell lines were originally derived from grade III malignant ovarian tumours. Each was derived from tumours with different histopathologies: a clear cell carcinoma (TOV-21G) and an endometrioid carcinoma (TOV-112D). The TOV-21G cell line grows as a monolayer in tissue culture plates, while the TOV-112D cell line is loosely adherent and the cells have a tendency to grow in compact colonies and form foci (Fig 1.1.5).

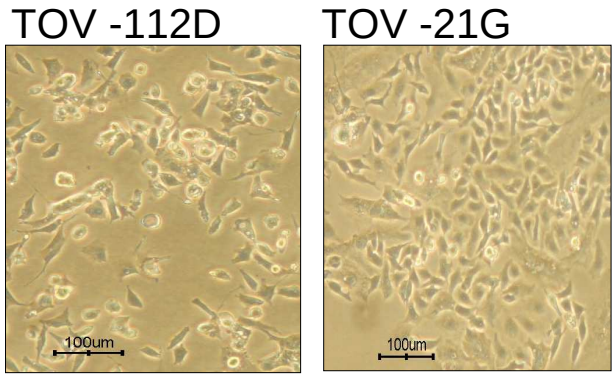

Figure 1.1.5 Morphology of cell lines TOV-112D and TOV-21G. Both cell lines have a rounded morphology characteristic of highly transformed cell lines.

MMCT was used to generate hybrid clones that contained whole or partial chromosome incorporation. Microsatellite analysis, FISH and array CGH revealed a ~10 Mb region (18p11.21-18q11.2) had been transferred into the TOV-112D hybrid cell lines, while a full copy of chromosome 18 was transferred into the TOV-21G hybrid cell lines. In addition, deletion of chromosome 8q and partial deletion of chromosome 9q and 12q was observed in the TOV-112D hybrid cell lines (Fig 1.1.6).

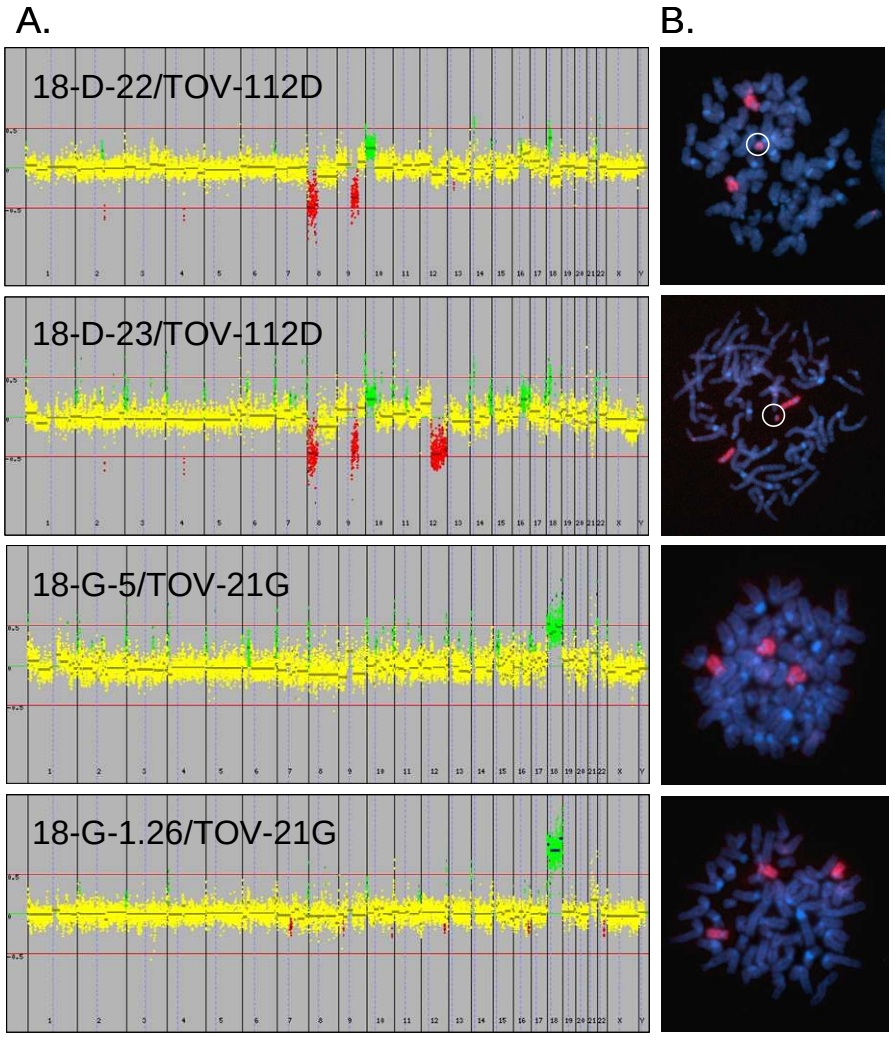

Figure 1.1.6 Genomic analysis of four Chromosome 18 hybrid clones. A) Array CGH analysis of the parental cell line TOV-112D and two hybrid clones, 18-D-22 and 18-D-23 respectively; and the parental cell line TOV-21G and two hybrid clones, 18-G-5 and 18-G-1.26 respectively. CGH profiles are displayed across increasing chromosome number, running from the telomere of the p-arm to the telomere of the q-arm of each chromosome. Yellow spots indicate no change in copy number between the parental cell line and its hybrid clone. Green spots indicate an increase in DNA copy number in the hybrid clone and red spots indicate loss of DNA copy number in the hybrid clone. A red line indicates a threshold of copy number change at +1 and -1. B) Fluorescent in situ hybridization analysis for chromosome 18 in each hybrid clone. The hybrid clones 18-D-22 and 18-D-23 showed only partial incorporation of chromosome 18 (ringed in white), whereas the hybrid clones 18-G-5 and 18-G-1.26, have each received a full copy of chromosome 18.

The hybrid cell lines displayed significantly suppressed tumourigenic phenotype compared to their parental ovarian cancer cell counterparts in a number of assays. To characterise anchorage-independent growth of the ovarian cancer cell lines, their ability to form colonies in soft agar was assessed. The parental line TOV-112D, rapidly formed foci, while TOV-21G showed a more delayed formation of smaller foci. The hybrid clones displayed poor colony forming efficiency (CFE) compared to their parent cell line counterparts (Fig 1.1.7)

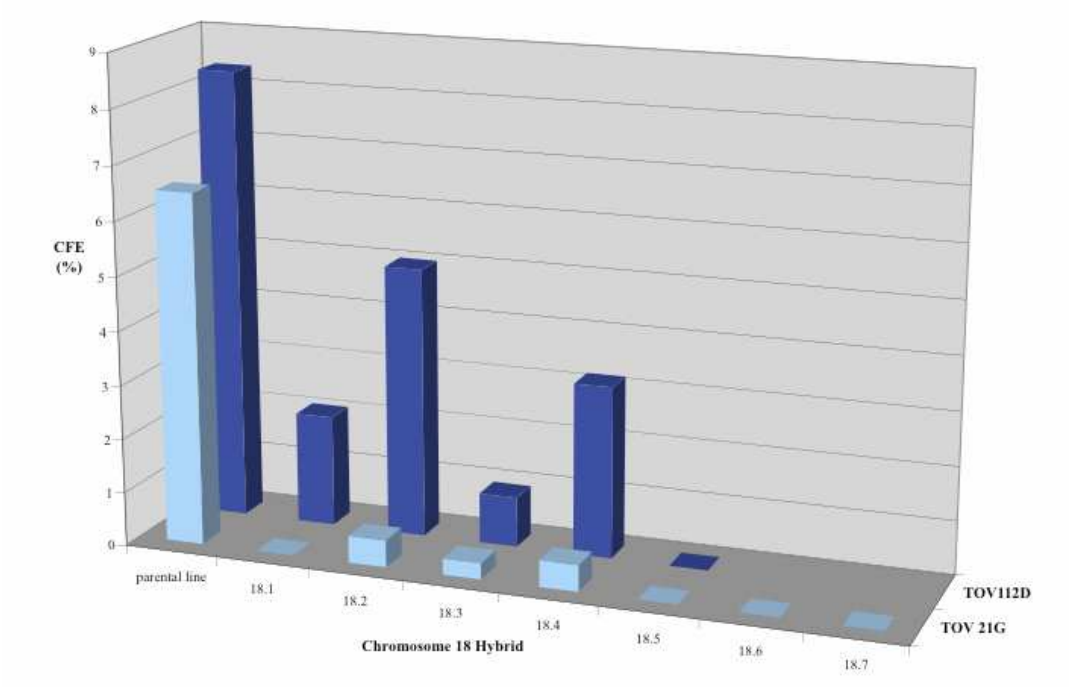

Figure 1.1.7 The colony forming efficiency of ovarian cancer cell lines in soft agar. The parental cell lines, TOV-112D and TOV-21G, rapidly formed distinct foci in soft agar. Seven hybrid clones from each parental cell line examined displayed poor colony forming efficiency in soft agar.

The ovarian cancer cell lines were also tested in *in vivo* assays. Injection of TOV-112D cells into nude mice resulted in the rapid appearance of tumours in four out of four animals tested, with tumours appearing between 2 and 5 weeks. The TOV-21G cell line also produced tumours in all animals although tumours appeared later. Notably, injection of the TOV-21G cell line also resulted in the formation of metastases, characterised by the presence of metastatic deposits in the lungs and ascito. The hybrid clones displayed significant suppression of tumour development in nude mice. In some hybrid clones, no tumours were detected for the duration of the experiment (Fig 1.1.8).

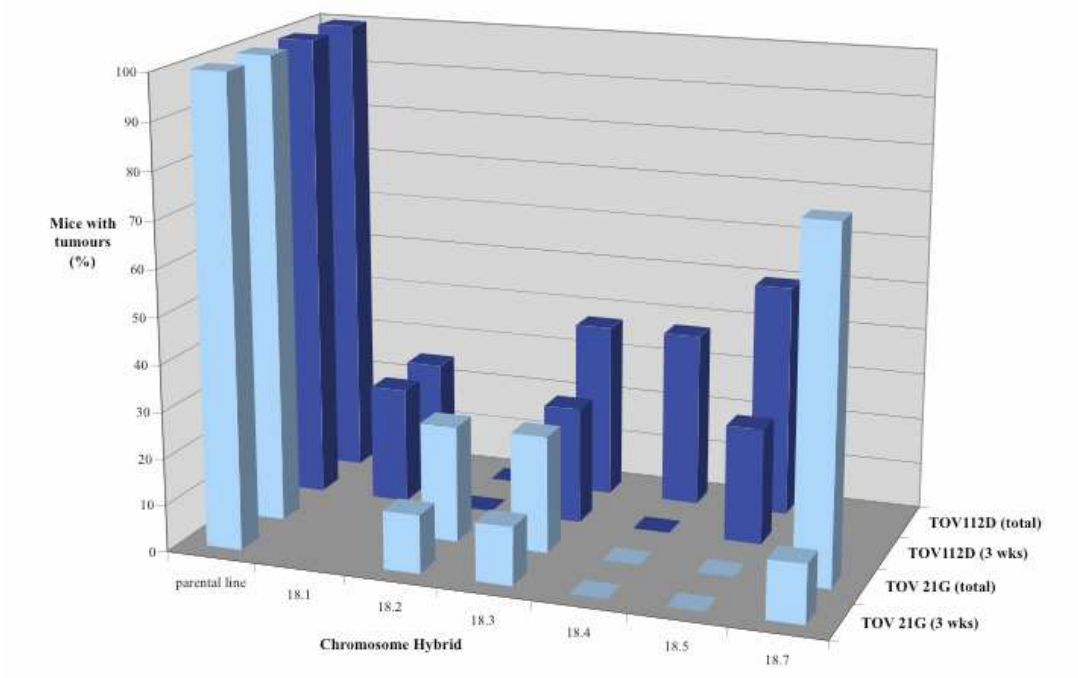

Figure 1.1.8 Tumour growth in vivo of ovarian cancer cell lines. Each parental cell line and their chromosome 18 hybrid clones were injected interperitoneally into nude mice and the natural history of the mice recorded after 3 weeks and 12 weeks. The chromosome 18 hybrid clones display significantly reduced tumour development compared to their parental cell lines.

The introduction of chromosome 18 into two primary ovarian carcinoma cell lines appears to suppress the *in vitro* and *in vivo* neoplastic phenotype suggesting that chromosome 18 harbours tumour suppressor genes for OC. Following on from this work, Dafou et al. employed gene expression microarray profiling to identify 21 candidate tumour suppressor genes located on chromosome 18 that were significantly over-expressed in association with the suppression phenotype reported earlier. Further analysis identified a potential tumour suppressor gene (data not published). These cell models were chosen for proteomic analysis in this study.

Despite the obvious potential of gene-expression profiling, there has been little overlap in the genes that have been identified in different studies as being important in ovarian cancer development or as clinically useful biomarkers. The heterogeneity of EOC, compared with other cancers, makes interpretation of the results extremely difficult and it is probable that multiple independent mechanisms may underlie the same phenotype in different cancer cell lines and tumour samples. In addition, the mRNA changes identified in these studies often do not reflect changes at the protein level, and protein analysis techniques may be more relevant for studying cancer biology and for biomarker discovery (Hernandez, Rosenshein et al. 1984; Jochumsen, Tan et al. 2007; Khalique, Ayhan et al. 2007).

1.2 Proteomics

Proteomics defines the study of the protein complement in a cell, tissue or organism, as genomics defines the DNA & RNA content. Proteomics includes the study of protein expression levels, activities, modifications, localization and the interaction of proteins within complexes and with other biomolecules. Developments in proteomic research have been made possible with the availability of complete sequence data from high-throughput DNA sequencing efforts (Anderson and Anderson 1998; Naaby-Hansen, Waterfield et al. 2001; Patterson and Aebersold 2003; Tyers and Mann 2003). Biological function is not carried out by the static genome, but by the dynamic population of proteins which is determined by the interplay between gene and protein regulation and is dependent on the organism's environment and physiological state. It has been estimated that there are approximately 25 000 genes in the human genome. Taking into account RNA splice variants, post-translational modifications and other post-transcriptional processing events, these genes are estimated to produce between 200 000 and 1 million distinct protein isoforms (Jensen 2004; Tress, Martelli et al. 2007). Proteins encoded by these genes are the true effector molecules and the functional manifestations of genetic information (Fig 1.2.1). The functions of the expressed proteins may be altered by co-translational and post-translational events, biomolecule binding and temporal and spatial signalling within the cell and local microenvironment.

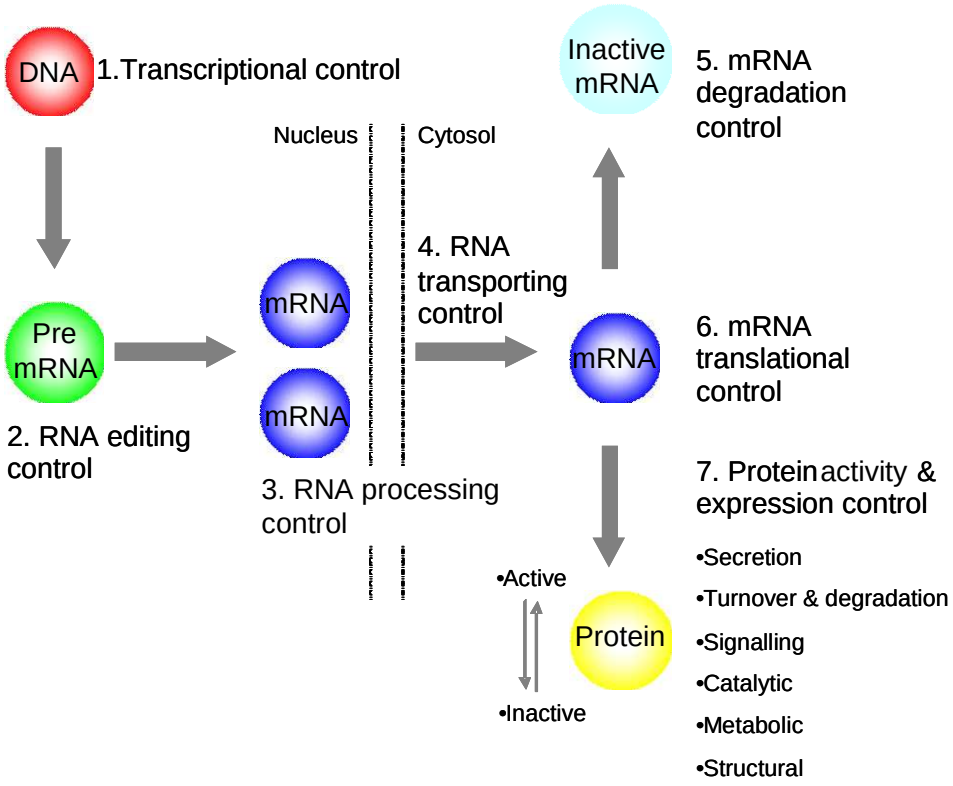

Figure 1.2.1 An overview of the transfer of information from the sequence in genes to the functioning proteins of the cell. A gene is transcribed (step 1) to pre-mRNA, which can be under editing control (step 2), then processed to one mRNA or by alternative splicing to several forms of mRNAs (step 3). The mRNA is then transported (step 4) out of the nucleus into the cytosol. In the cytosol the mRNA can be degraded into inactive forms (step 5) or translated into protein (step 6). Proteins maybe synthesized in an active or inactive form. Control (step 7) by activation or deactivation in a reversible or irreversible manner regulates cellular processes.

1.2.1 Cancer Proteomics

It is widely accepted that tumour development is a multi-step process of cellular transformation driven by somatic genetic alteration. For most cancer types, primary tumour development is associated with an accumulation of genetic changes in the progenitor cell. Successive alterations affecting specific genes are thought to confer an increased growth advantage allowing tumours to develop by clonal expansion and progress from benign to cancerous lesions. Despite these genetic changes the proteins encoded by these genes are the true effector molecules that drive transformation and it is for this reason that proteomic technologies are developing to answer questions about protein expression and function particularly in relation to the changes associated with cancer (Wu, Hu et al. 2002; Hanash 2003; Check 2004; Boyce and Kohn 2005).

The major difficulty in treating ovarian cancer is that it presents at a late clinical stage giving a dismal prognosis (section 1.1). For this reason, there is an urgent need for methods to aid in its successful treatment and for reducing mortality. Biomarkers are typically disease associated proteins that can be detected and quantitatively measured for disease diagnosis, staging and prognosis and treatment monitoring. The development of disease is a multi-step process involving many different biological processes and many proteins will have altered expression or are modified during these processes. These proteins can be detected in tissue, blood, urine, or other body fluids and be used as markers of disease. It is highly desirable for protein markers for use in medical practice to be detected and measured in body fluids. These fluids are highly

complex mixtures of proteins and exhibit a very broad dynamic range of protein abundances (up to 10 orders of magnitude). Because of this, it is believed that many potentially useful biomarkers escape detection using the current proteomics technologies.

In 2002, a serum-based proteomic pattern diagnostic has been developed and applied for differential diagnosis detection in ovarian cancer using a technique known as surface-enhanced laser desorption ionisation-time of flight mass spectrometry (SELDI-TOF MS) (Petricoin and Liotta 2004). SELDI generates protein ions from subsets of protein analytes desorbed from a chemically-modified surfaces or chips. These 'chips' have either a hydrophobic, cationic or anionic chromatographic support surface or are coated with affinity supports such as antibodies and purified proteins such as receptors or ligands. Treated tissue or body fluid can be directly applied to the 'chip' and after washing to remove unbound protein be analysed by TOF-MS. Generated ions extracted into a vacuum chamber migrate towards an oppositely charged detector. The mass-to-charge (*m/z*) value of each ion can be determined from the time it takes for an ion to reach the detector. This is time of flight (TOF). The spectrum acquired in the TOF gives a signature of hundreds of protein ion features that can be used to build a pattern for disease recognition. Detection of potential markers is relatively quick, however, the protein peaks generated are not easily identified since the mass accuracy is relatively poor. Thus, the results cannot provide any information about the relationships and the roles of the proteins of interest to the underlying pathology. Petricoin et al. identified a protein pattern in the serum proteome from non-cancer controls and ovarian cancer

patients (Petricoin, Ardekani et al. 2002). The spectra were used to train a classification algorithm which correctly classified 50/50 of the cancers and 47/50 of the normals in a validation set giving 100% sensitivity and 95% specificity respectively. Independent review of these datasets have revealed discrepancies which suggest the changes observed could be due to artifacts of sample processing, not the underlying biology of cancer. Since this landmark study, pre-analytical handling of samples has been shown to significantly affect protein profiles and the ability to differentiate between disease and control. The transition time, storage conditions, temperature, clotting time, and tube type can all affect serum profiles which is largely driven by proteolytic events and it is therefore essential to handle all case and control samples identically (Timms, Arslan-Low et al. 2007).

The protein levels of most body fluids have substantial intra and inter-individual variability. This distribution should be considered appropriately during experimental design. Clinical proteomics studies, with small sample numbers can be vulnerable to the misinterpretation of signals if not carefully designed and properly interpreted. As alluded to above the dynamic range of protein concentrations in body fluids is also an important concern. For example, 22 high-abundance proteins make up approximately 99% of the total proteins in plasma. There are however approaches that can be used to reduce the dynamic range of protein abundance in body fluids for detection of lower abundance proteins, including affinity depletion and multiple fractionation methods. Care should also be taken to avoid loss of potentially important proteins/peptides that could be bound to high-abundance proteins such as albumin. Indeed, Liotta et al.

proposed that carrier proteins like albumin may accumulate low molecular weight biomarkers and prolong their half-life (Liotta and Petricoin 2006). It is also believed that disease-associated protease activity can result in altered low molecular weight protein/peptide profiles. Villaneuva et al. suggested that many serum peptides, including potential cancer biomarkers, are generated from clotting products ex vivo by unknown cancer-specific exoproteinases leaving a low molecular weight signature with diagnostic potential (Villanueva, Shaffer et al. 2006).

Immuno-affinity depletion of specific high-abundance proteins through the use of targeted polyclonal antibody columns and spin filters has recently emerged as a promising tool for prefractionation. IgY12 columns from Genway use avian polyclonal IgY antibodies to allow highly specific removal of the top 12 highly abundant proteins in human serum/plasma samples. Similarly, the multiple affinity removal system (MARS) column developed by Agilent Technologies, removes the 7 most highly abundant proteins from serum/plasma samples. A fractionation technique that has become a promising alternative to SELDI, is the use of magnetic beads coated with hydrophobic or ionic resins as a purification step. Beads can be added to a sample to bind protein/peptides of interest before thorough washing by manipulation with magnets. This approach is simple, reproducible and offers itself to high-throughput analysis.

Other technologies have been applied for biomarker discovery, including two-dimensional (2DE) gel-electrophoresis, LC-MS, and protein- and antibody-based

microarrays. 2DE provides information about proteins, such as expression volumes, actual pIs and molecular weights and can typically resolve ~2000 protein isoforms from a whole cell lysate. It also gives an insight into intact and fragmented protein species and information regarding post-translational modifications (PTMs). Downstream analysis of excised protein spots by mass spectrometry (MS) results in identification and additional information on PTMs. 2DE has for a long time been the primary tool for biomarker discovery in conventional proteomic analyses. It is uniquely suited for the direct comparisons of protein expression and for the identification of differentially expressed proteins between two or more conditions. For example, Gagne et al. investigated the differential protein expression profile between low malignant potential and highly proliferative human epithelial ovarian cancer cell lines derived from malignant tumours (Gagne, Ethier et al. 2007). Ahmed et al. examined the expression profiles of depleted serum from ovarian cancer patients compared to a control group of healthy women (Ahmed, Oliva et al. 2005). Changes in serum expression of haptoglobin correlated with the change of CA-125 levels before and after chemotherapy. A comparison by 2DE of micro-dissected epithelial cells from two low malignant potential (LMP) ovarian tumours and three invasive cancers by Jones, et al. revealed markers of invasiveness including RHOGD1, glyoxalase-1 and FK506BP (Jones, Krutzsch et al. 2002).

As a technique for biomarker discovery, 2DE suffers from low sensitivity, low dynamic range, difficulties in resolving proteins with extreme masses or isoelectric points, and low-solubility proteins. Improvements can be made, for example the use of

prefractionation techniques to reduce the complexity of the samples for analysis and the use of Cy dye labelling in differential gel-electrophoresis (2D-DIGE) has improved the sensitivity and quantitative performance of this approach.

An emerging technology that requires a complex protein mixture to be digested with a specific protease before 2-dimensional liquid chromatographic separation is multiple dimension protein identification technology (MudPIT). Peptide fragments are separated initially by charge then by hydrophobicity before eluting directly into a mass spectrometer that can be used to identify peptides as they elute. Quantitative differences between two samples can be elucidated from the spectral intensity of the parent ion of a given peptide between each run, or each sample can be labelled differentially (*in vivo* using stable isotopes; or *in vitro* using mass tagging strategies such as ICAT/iTRAQ/TMT) and mixed prior to chromatographic separation and quantification determined from spectral information. This technique has advantages over gel-based techniques in speed, sensitivity, and dynamic range. Limor Grotzak-Uzan et al. examined ovarian cancer ascites in a MudPIT experiment resulting in the identification of over 2500 proteins of which 80 were suggested as potential biomarkers (Gortzak-Uzan, Ignatchenko et al. 2008). Yu et al. used the secreted proteins obtained from SILAC labelled human pancreatic cells as a standard to run with pooled sera of patients with early stage pancreatic cancer or controls using an IEF-2D-LC-MS/MS approach to identify low abundance proteins as biomarker candidates (Yu, Barry et al. 2009). A study by Bouchal et al. has shown the ability of iTRAQ combined with MudPIT to define a protein signature in breast cancer tumour biopsies and to identify

potential biomarkers of metastasis (Bouchal, Roumeliotis et al. 2009). Advances in chromatographic separations and the speed, sensitivity and accuracy of mass spectrometers combined with innovative quantitative labelling strategies have allowed these 'bottom up' proteomic techniques to evolve into an important tool for biomarker discovery.

In recent years, protein and antibody arrays have been developed to allow rapid interrogation of protein activity on a proteomic-wide scale. Recombinant proteins or reagents that interact specifically with proteins (e.g. antibodies, peptides and small molecules) have provided a platform for protein arrays (Nishizuka 2006; Spurrier, Honkanen et al. 2008). High-throughput ELISA microarray technology offers promise for cancer biomarker validation. The advantages of protein microarrays include high sensitivity, good reproducibility, quantitative accuracy and the requirement for small sample volumes e.g. Gunawardana et al. performed parallel protein microarray analysis of ascites fluid, pooled from 30 ovarian cancer patients and a control pool of 30 samples of non-malignant peritoneal fluid to identify tumour associated antigens (Gunawardana, Memari et al. 2009). However, ELISAs suffer from the nonspecificity of protein−antibody interactions, which could result in "false positives". Cell and tissue-based arrays provide a further insight into functional activity (Ouellet, Guyot et al. 2006). A tissue microarray (TMA) is a histological section in which tens to hundreds of specimens are arrayed for analysis. TMAs enable the high-throughput analysis of a large number of tissue samples by immunohistochemical staining that have been collected and archived as formalin fixed paraffin embedded blocks. The

most popular use for TMAs is for the validation of diagnostic and prognostic biomarkers in annotated clinical samples. James et al. have performed immunohistochemical validation of marker proteins on panels of normal ovarian and tumour tissues (Bengtsson, Krogh et al. 2007). They identified statistically valid markers that could distinguish between normal, benign, borderline, and malignant tissue.

Another emerging tool for biomarker validation is the application of peptide multiple reaction monitoring (MRM)-based assays for targeted quantitation of proteins in clinical samples (Mills, Morris et al. 2005). The technology has been employed for over 15 years in the measurement of drugs and metabolites. This MS-based technique solves the challenges to preliminary validation of putative biomarkers for which immune-based reagents are not available and allows detection of low-abundance proteins in complex tissue or biological fluids in addition to high-throughput, high-precision quantification.

A vast amount of research is being focussed on biomarker discovery and hundreds of putative biomarkers are being made available to the scientific community. Despite this, there are very few protein biomarkers in clinical use today and many of the identified biomarkers are abundant serum proteins or non-specific acute-phase proteins, and not proteins directly related to the disease process. Proteomics still has many challenges to overcome in the discovery of tumour biomarkers.

1.3 Proteomic Technologies

In the past, protein analysis was dominated by targeted approaches in which candidates derived from biological knowledge were selectively evaluated for correlation with clinical conditions. However, the recent advances in proteomic tools has allowed for the simultaneous comparison of complex protein profiles and at the same time identification of component proteins in a high throughput manner.

The following sub-sections introduce and discuss the basis of the proteomic methods used in this study and how the combination of these approaches is used quantitatively to characterise proteomes. The two main methods used to separate proteins and peptides were 2D-gel electrophoresis and liquid chromatography (LC). The separated proteins and peptides were then analysed by MS.

3.3.1 Gel Electrophoresis

Electrophoresis describes the process by which a charged molecule migrates in an electric field. Molecules will separate at different velocities depending on their charge state, providing a basis for separation. Typically, electrophoresis of proteins is carried out in a polyacrylamide gel. Polycrylamide gels contain pores, the sizes of which are dependent on the concentration of acrylamide and bis-acrylamide cross-linker present in the gel. A common form of electrophoresis is sodium dodecyl sulphate (SDS) polyacrylamide gel electrophoresis (PAGE). Proteins are reduced and denatured in the

presence of the anionic detergent SDS. SDS binds strongly to the amino acids of the reduced protein, as a result, the intrinsic charge of the protein is masked by the negative charges of the SDS, and thus, proteins of similar molecular weight have the same apparent charge. Therefore, separation by PAGE is mainly related to the size or molecular weight of the protein as it passes through the pores present in the acrylamide gel. Smaller proteins are able to move more rapidly than larger ones through the gel pores as they migrate towards the anode (Chrambach and Rodbard 1971).

Proteins can be separated by another form of electrophoresis, namely isoelectric focussing (IEF) (Bjellqvist, Ek et al. 1982; Choe and Lee 2000). Denatured proteins are separated by IEF in a pH gradient and focus when they acquire a net charge of zero at their isoelectric point (pI). Gels are of high porosity making the effects of sieving negligible.

Two-dimensional gel electrophoresis (2DE) combines the two electrophoretic methods described above. In the first dimension, proteins denatured in urea and DTT/DTE to break disulphide bonds and are separated on the basis of their pI by IEF and in the second dimension by SDS-PAGE according to their molecular weight (Kenrick and Margolis 1970; Rabilloud 1994). The reproducibility of 2DE-based separations has improved with the introduction of gels with immobilized pH gradients (IPG) for the IEF dimension and optimisation of chaotropes (e.g. urea and thiourea) and neutral or zwitterionic detergents (e.g. CHAPS) which prevent precipitation of proteins when they reach their pI during focussing. In the region of 2000 distinct protein spots can be

resolved on a single gel. However, these will largely be abundant proteins and multiple isoforms of the same gene products. Also basic proteins are often poorly resolved due to the inadequate buffering by ampholytes at basic pHs and also because of a loss of reductive capacity and a concentrating effect through electro endo-osmosis resulting in spurious disulphide bond reformation and protein precipitation respectively. Hydrophobic proteins also do not tend to resolve well on 2D gels, again through aggregation, whilst large (>200 kDa) or small proteins (<10 kDa) are also under-represented. Despite these drawbacks, 2DE is still the most widely used protein separation and relative quantitation method used in proteomics. Resolved protein spots can be picked directly from gels for MS-based identification.

There exist a number of strategies for post-electrophoretic protein detection differing in their sensitivities, specificities, linear dynamic ranges and compatibilities with downstream identification by MS. Staining methods include:

- Cooomassie brilliant blue (Meyer and Lamberts 1965; Neuhoff, Arold et al. 1988; Neuhoff, Stamm et al. 1990), a rapid and convenient staining procedure with a detection range of 100-1000 ng and compatible with downstream MS.

- Colloidal Coomassie blue (G-250) (Meyer and Lamberts 1965; Neuhoff, Stamm et al. 1990; Candiano, Bruschi et al. 2004) is relatively simple to use without

the need for destaining, has a detection range of 20-500 ng and is compatible with downstream MS.

- Silver staining (Eschenbruch and Burk 1982; Rabilloud 1990; Rabilloud 1992; Shevchenko, Wilm et al. 1996; Rabilloud 1999) provides excellent sensitivity (typically 1-10 ng) using simple and cheap chemicals. However, classical silver-staining methods can be complex and are often incompatible with MS because of the aldehyde-based cross-linkers used in the sensitisation steps, and because silver ions can interfere with MS analysis. Non-linearity of the dynamic range of detection and preferential staining based on amino acid composition make it less desirable for quantitation of protein expression.

- Fluorescent stains (Patton 2000; Rabilloud, Strub et al. 2001) such as SYPRO Ruby, SYPRO Orange, Deep Purple and ruthenium II-tris bathophenantroline disulfonate (RUBP) bind directly to protein with a sensitivity comparable to silver staining (1 ng), but with a broader linear dynamic range and compatibility with downstream MS. The full potential of these stains can only be realised with a CCD camera or laser scanner-based fluorescence detection. As a result, these stains are not readily compatible with manual spot picking. To take full advantage, a robotic picking system is required.
- Radioactive labelling is an alternative labelling method used prior to electrophoretic separation. This is performed by *in vitro* enzymatic labelling

with radioactive metabolites, or by *in vivo* incorporation (Vuong, Weiss et al. 2000). Radioactive labelling is very sensitive and provides the widest linear dynamic range of any detection method. Proteins in-gel can be detected by exposure to film (autoradiography) or phosphoimaging. The latter is more sensitive and has a wider dynamic range than autoradiography making it more desirable for quantitation. Radioactive labelling is however expensive and great care has to be taken due to its hazardous nature.

- Western blotting requires gel separated proteins to be transferred to a membrane (typically PVDF or nitrocellulose) where they are probed using a primary antibody specific to the target protein. Most commonly, a horseradish peroxidase-linked secondary is used to cleave a chemiluminescent agent, and the reaction product produces proportional luminescence that can be detected by exposure to film. This method is highly specific however, is labour intensive and not high throughput. Specific reagents are not always available.

1.3.2 2D-DIGE

A covalent fluorescence labelling approach for differential protein expression analysis, known as difference gel electrophoresis (DIGE) allows up to three samples to be labelled and combined prior to electrophoretic separation (Unlu, Morgan et al. 1997; Gorg, Obermaier et al. 1999; Tonge, Shaw et al. 2001; Gharbi, Gaffney et al. 2002). Three spectrally distinct dye derivatives (NHS-Cy2/Cy3/Cy5) that are mass and charge

matched are used to covalently label lysine residues (Fig 1.3.1). The ratio of dye to protein used has been optimised to ensure the dyes are limiting in the reaction such that only approximately 3-4% of each protein is labelled on an average of 1 lysine/protein molecule. This 'minimal' labelling limits the generation of multiple protein forms which would separate on 2D gels, adding to the complexity of the sample.

The differentially labelled samples are then mixed in equal amounts and resolved on 2D gels (Fig 1.3.2). Labelled proteins in each sample are then detected at the appropriate excitation and emission wavelengths using a multi-wavelength fluorescence detection device and the signals compared. As well as reducing the number of gels that need to be run, differential labelling and mixing means that samples are subjected to the same handling procedures and microenvironments during 2D separation, raising the confidence with which protein spots can be matched and protein changes quantified. Since fluorescence detection also provides a superior linear dynamic range of detection and sensitivity to many methods, this technology is suited to the analysis of biological samples with their large dynamic ranges of protein abundance. In expression profiling experiments, one dye is often used to label an internal standard which is run on all gels against pairs of test samples labelled with the other two dyes. This allows the direct comparison of ratios of expression across multiple samples and gels, improving the ability to match protein spots and accurately distinguish true biological variation from gel-to-gel variation. In some respects, the advantages in applying 2D-DIGE can be limited by the method of post-staining for spot excision and subsequent identification. CyDyes offer great sensitivity, detecting as little

as 125 pg of protein and giving a linear response to protein concentration of up to four orders of magnitude. In comparison, post-staining detects between 1–500 ng of protein with less than a hundred-fold linear dynamic range. However, it would be unwise to pick from gels using the Cy dye image since the combination of minimal labelling and addition of the Cydye moiety (~500 Da) means that the bulk of the protein does not exactly co-migrate with the labelled portion of the protein, particularly in the lower mass region of the gel.

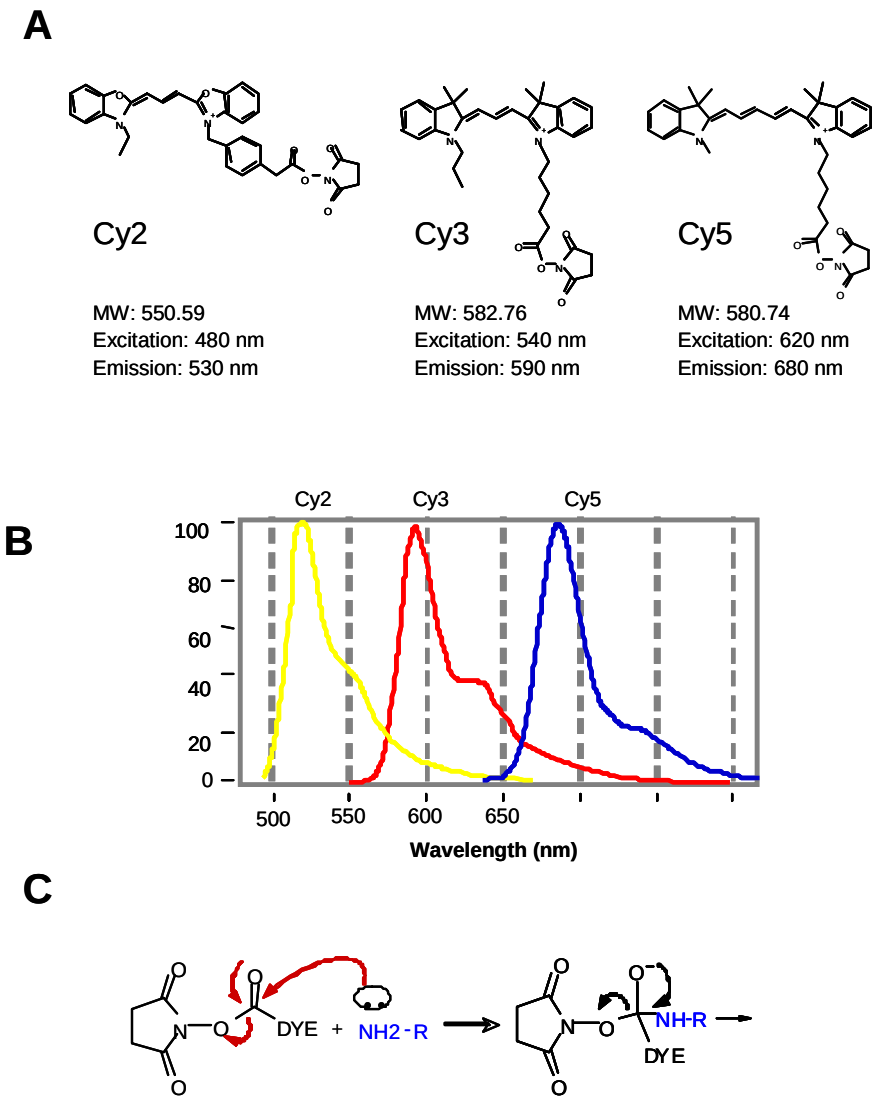

Figure 1.3.1 The chemistry of the NHS-Cy dyes. A) Cy2, 3-(4-carboxymethyl)phenylmethyl)-3'-ethyloxacarbocyanine halide N-hydroxy-succinimidyl ester; Cy3, 1-(5-carboxypentyl)-1'-propylindocarbocyanine halide N-hydroxysuccinimidyl ester; and Cy5, 1-(5-carboxypentyl)-1'-methylindodicarbocyanine halide N-hydroxysuccinimidyl. All are size and charge matched allowing co-separation of different Cy-Dye labelled proteins in the same gel, limiting experimental variation and ensuring accurate within-gel matching. B) Each Cy-dye is spectrally distinct, offering bright and intense colours with narrow excitation and emission band widths. C) The dyes have an N-hydroxysuccinimidyl ester reactive group that covalently interacts with the primary amine groups of lysine residues or the N-terminus of proteins.

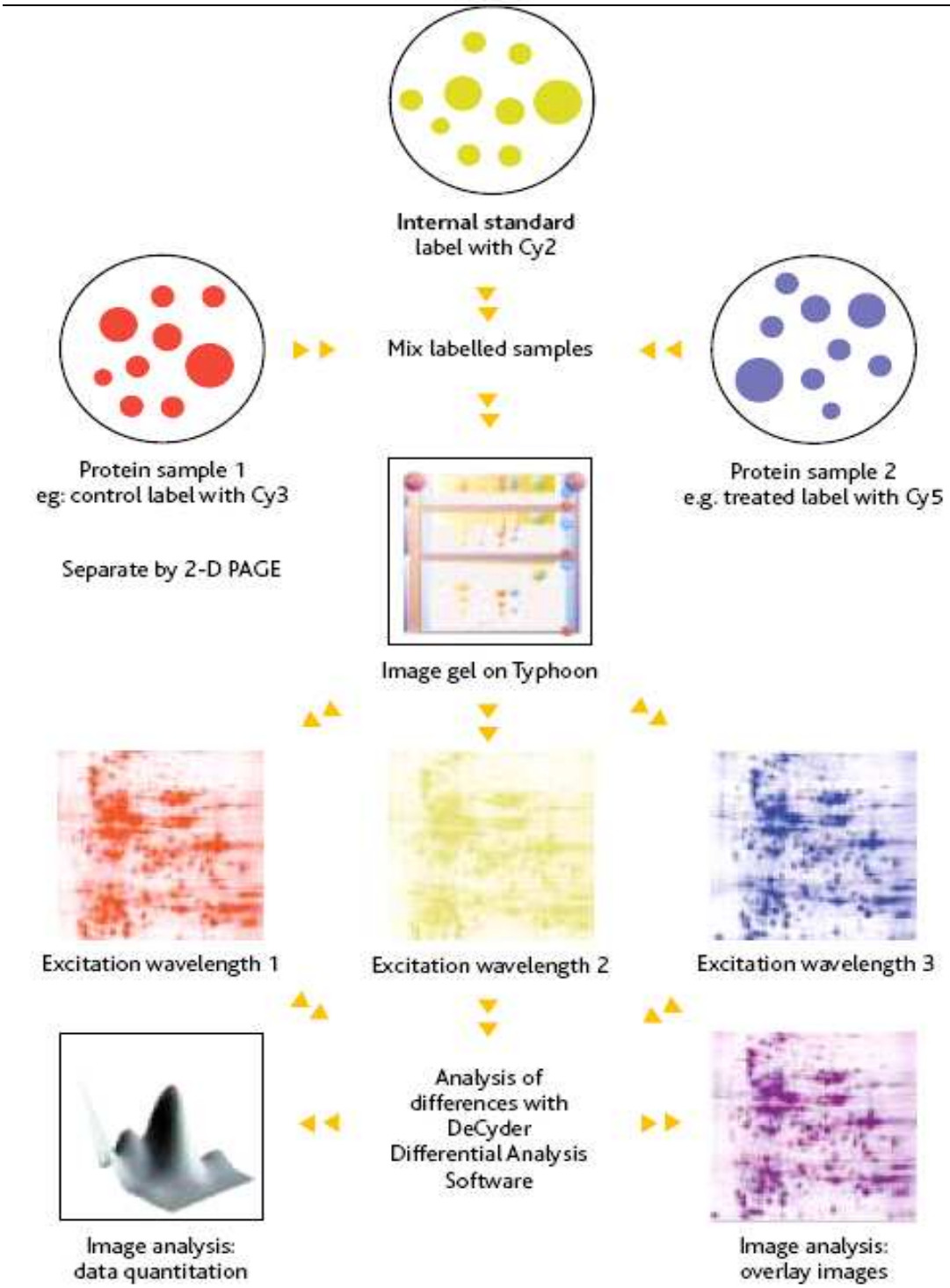

Figure 1.3.2 2D-DIGE work flow (adapted from www.gelifesciences.com, GE Healthcare). Up to 3 labelled protein samples can be run simultaneously on a 2D gel. The internal standard is prepared by pooling aliquots of all biological samples in an experiment. This is run on all the gels in an experiment creating an intrinsic link that once normalised allows the ratio of relative expression of a given protein across all gels to be compared directly.

1.3.3 Liquid chromatography (LC)

Molecules can also be separated on the basis of their differential partition or distribution between two immiscible phases (Peng and Gygi 2001). In column LC, the two phases consist of chromatographic beads of distinct surface chemistry and a liquid phase making up the stationary and mobile phases respectively. Molecules are separated when their distribution coefficients (Kd) are different. Kd is defined as the concentration of a molecule in the stationary phase divided by its concentration in the mobile phase. In this study, high-performance LC (HPLC) was used with reversed-phase (RP) and ion-exchange chromatography. The sample to be analysed is introduced in a small volume to the stream of mobile phase and is retarded by specific chemical or physical interactions with the stationary phase as it traverses the length of the column. The amount of retardation depends on the analyte, stationary phase and mobile phase composition. The time at which a specific analyte elutes is called the retention time and it is considered to be a unique identifying characteristic of the analyte.

1.3.3.1 Reverse phase liquid chromatography (RP-LC)

RP-LC separates proteins or peptides according to their hydrophobicity (Claessens and van Straten 2004). The stationary phase is generally made of hydrophobic alkyl chains (-CH2-CH2-CH2-CH3) that interact with the analyte by hydrophobic and van der Waals interactions. There are three common chain lengths, C4, C8 and C18. C4 is generally used for proteins and C18 is generally used to capture peptides or small

molecules. Proteins and peptides are separated by running a linear gradient of organic solvent in the mobile phase. RP-LC is widely used for the analysis of proteins and peptides due to its high resolution and is often linked on-line to mass spectrometry-based detection.

1.3.3.2 Ion-exchange chromatography

Ion-exchange chromatography retains analyte molecules on the basis of ionic interactions. The stationary phase consists of charged functional groups and separation of molecular species occurs by virtue of their differences in charge. Protein molecules are eluted by adjusting the pH or the ionic concentration of the mobile phase. This type of chromatography is subdivided into two main types of ion exchangers, namely anion exchangers and cation exchangers. The form of ion exchange used in this study was strong cation exchange (SCX). Peptides interact with the negatively charged sulfonic groups linked to the stationary phase with affinities that are proportional to the overall number of positive charges on each peptide. Polypeptide samples were dissolved in a solvent of low pH and ionic strength so that all polypeptides have at least one positive charge. The peptides were eluted by using gradient of increasing salt concentration.

1.3.3.3 Multidimensional protein identification technology (MudPIT)

MudPIT is a non-gel approach for the identification of proteins from complex mixtures. The technique consists of two-dimensional chromatographic separation of peptides following tryptic digestion of protein samples and detection by electrospray-ionisation MS (Liu, Lin et al. 2002). The first dimension is usually strong-cation exchange because of its high loading capacity. The second dimension is reverse-phase chromatography due to its compatibility with electrospray ionisation (ESI). In contrast to 2DE gel-based methods, liquid chromatography can resolve a wide range of proteins encompassing high and low molecular weights and extreme isoelectric points. In addition, large sample volumes can be applied to columns, which overcome the problems of over-loading faced with 2DE gel approaches. This technique is capable of identifying in excess of 5000 proteins which can be increased further by combining with other fractionation strategies. Whilst this improved coverage is highly beneficial it comes at the cost of reduced throughput.

1.4 Mass spectrometry

Mass spectrometry is an analytical tool which allows the determination of the mass of a molecule with high accuracy. This information can be used for identification and chemical characterisation (Gygi and Aebersold 2000; Aebersold and Mann 2003). Mass spectrometers are composed of an ion source where the sample is applied and

transferred as ions into the gas phase, a mass analyser that separates and measures the mass-to-charge ratio (*m/z*) of ionised particles and a detector which measures the intensity of the ions. Mass spectrometry has become an important technique in proteomics for the identification and quantification of proteins and to correlate protein and gene sequences. Genome sequence information has provided a powerful resource for protein identification using data produced by matrix-assisted laser desorption ionization time-of-flight (MALDI-TOF) and electrospray ionisation (ESI) mass spectrometry. These two methods differ in their mode of ionisation of the sample and are described in more detail in the following sections.

1.4.1 Matrix –assisted laser desorption ionization

MALDI generates ions from a solid phase using laser pulses (Hillenkamp and Karas 1990; Hillenkamp, Karas et al. 1991; Griffin, Gygi et al. 2001). The sample is usually applied in a matrix that facilitates the ion formation by absorption of photon energy from the laser beam (Fig 1.4.1). The matrices used are typically acidic compounds with a maximal absorption in the region of the laser wavelength. For the most frequently used laser wavelengths (377 and 355 nm), the most widely used matrices are 2,5-dihydroxybenzoic acid (DHB) and α-cyano-4-hydrocycinnamic acid (CHCA) (Hazama, Nagao et al. 2008). The analyte/matrix mixture is routinely spotted onto a metal surface to crystallise and introduced to a high vacuum and irradiated with the laser beam. DHB crystallises in a crystal rim around the centre of the spot. CHCA forms a homogenous shaped matrix spot, making it more suitable for automated data

acquisition. Protonated analyte ions (MH^+) are formed whose *m/z* values can then be measured using a mass analyser.

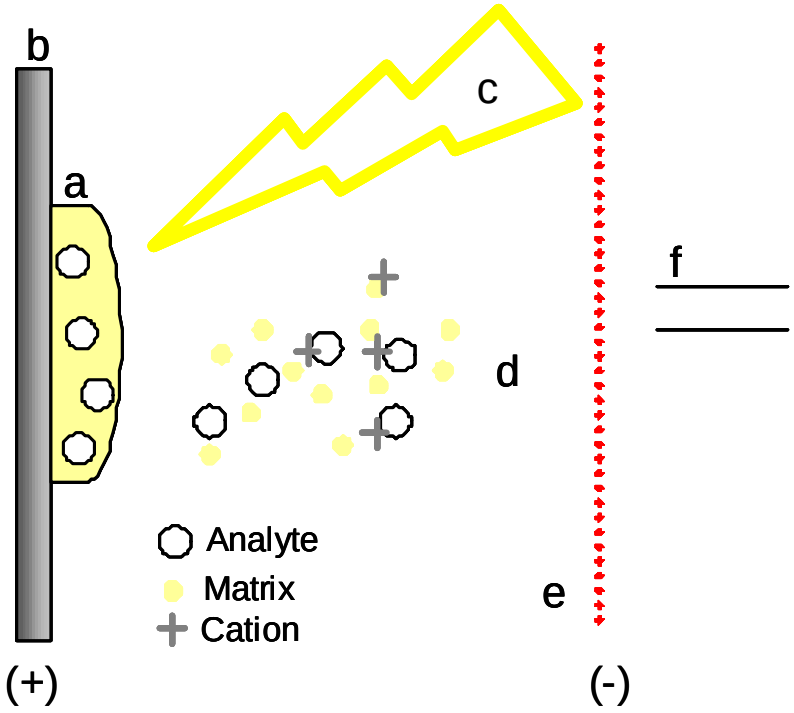

Figure 1.4.1 Ion formation by MALDI. The analyte is co-crystallised with the matrix (a) onto a target plate (b). A pulsed laser (c) is focused onto the target plate by optics. The mixture is desorbed into a plume (d). Protonated analyte ions are extracted by a high potential field (e) into the entrance of the mass spectrometer (f).

1.4.2 Electrospray ionisation

Electrospray ionisation (ESI) creates ions through the application of a potential difference placed between a capillary from which the sample is sprayed and the inlet to the mass spectrometer (Fenn, Mann et al. 1989). The sample is dissolved in an organic solvent, typically methanol or acetonitrile, containing a small concentration of acid

(formic acid, 0.1-1%). The analyte/solvent mixture evaporates upon application of a high voltage and the charged particles enter into the gas phase. Dry gas and heating are used to evaporate solvent from the highly charged drops. As solvent evaporates from drops, the charge density increases until charge-charge repulsion is greater than the surface tension (Raleigh limit) and the drops divide. This process, known as coulomb fission, continues until analyte ions free of solvent are formed. In addition, ion evaporation occurs as charged analyte ions evaporate from the surface of small drops to reduce charge-charge repulsion.

The introduction of the sample into the mass spectrometer can be carried out by a number of methods. In the simplest case, sample is directly infused through a syringe and a narrow transfer capillary. More commonly, it is achieved by the coupling of electrospray directly with reversed-phase chromatography. In this case the capillary end of the chromatographic system is connected to a needle, with typical flow rates of 200 to 500 nl min-1 (nanospray) used (Fig 1.4.2). A feature of ESI is the formation of multiply charged ions. This extends the mass range of analysers (see below). Both ionisation methods can be performed in the positive as well as the negative ion mode but typically, for peptide mass analysis, ionisation scans are performed in the positive ion mode.

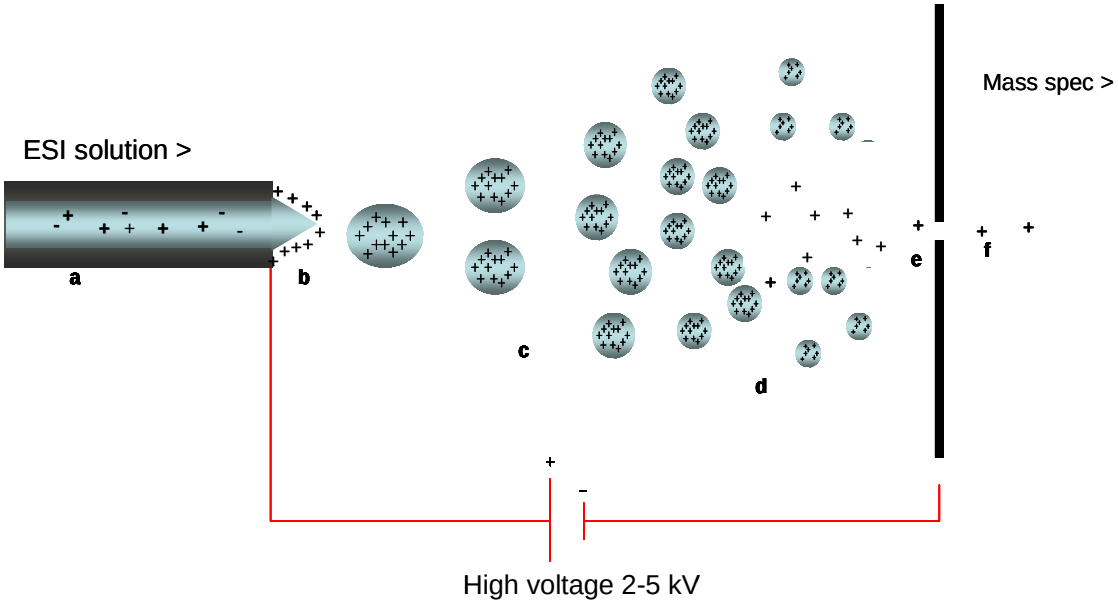

Figure 1.4.2 Electrospray ionization. This figure shows the delivery of sample to the mass spectrometer through a needle with a potential difference applied (a). Charge separation occurs at the tapered end of the needle (b) producing a Taylor cone. Droplets are formed with excess charge on their surface (c). Drops divide by coulomb fission (d). Ions free from solvent are produced by the combined effects of coulomb fission and ion evaporation (e). Multiply charged ions are directed toward the mass spectrometer by an applied electric field (f).

1.4.3 Mass analysers

Mass analysers separate ions according to their mass-to-charge ratios. This is based on the dynamics of charged particles in electric and magnetic fields in vacuum. The preferred analysers used for investigation of biological samples are time-of-flight (TOF), quadrupole (Q), ion trap (IT), fourier transform ion cyclotron resonance (FT-ICR) and the orbitrap.

Whole protein analysis is primarily conducted on TOF and FT-ICR machines because of their high mass range and, in the case of the FT-ICR, its high mass accuracy. Alternatively, enzymatic digestion of whole proteins into smaller peptides with a sequence-specific protease such as trypsin is widely used for peptide mass analysis with the quadrupole and ion trap analysers, which are better suited for the analysis of these lower mass analytes. In addition, peptides are more readily ionized than their larger protein precursors and knowledge of the protease cleavage sites is valuable in providing sequence information for identification.

1.4.3.1 Quadrupole mass analysers

A quadrupole mass analyser is the component of the instrument responsible for filtering sample ions based on their *m/z* ratio and is capable of transmitting only the ion of choice. In essence, a quadrupole mass analyser is composed of four parallel metal rods. Each opposing pair is connected together by direct current (DC) and radio frequency (RF) voltages. One pair of opposite rods has negative DC voltage, while the other pair has positive charge. The DC voltage is superimposed on the RF voltage and at specific voltage settings the trajectory of ions with a defined *m/z* value will be stable and only these reach the detector, while the trajectory of ions with other *m/z* values become unstable and are diverted to the rods. A mass spectrum is obtained by a scanning mechanism that alternates the voltages such that ions with only one *m/z* value are transmitted at a time and the ion signals added together for the whole scan range.

1.4.3.2 Ion traps

Ion trap mass analysers consist of a ring electrode separating two hemispherical electrodes. Ions created by electron impact (EI), electrospray ionisation (ESI) or matrix-assisted laser desorption ionisation (MALDI) are focused using an electrostatic lensing system into the trap. An electrostatic gate pulses open (-V) and closed (+V) to inject ions into the ion trap (ionisation period). The ring electrode RF potential and AC potential of constant frequency but variable amplitude, produces a 3D quadrupolar potential field within the trap. This traps the ions in a stable oscillating trajectory. The exact motion of the ions is dependent on the voltage applied and their individual *m/z* ratios. Structural information is obtained by the application of a low amplitude AC resonance signal across the endcap electrodes causing the ions kinetic energies to increase and leads to ion dissociation due to many collisions with the helium gas in the trap, known as collision-induced dissociation (CID). This causes fragmentation along the peptide backbone and a spectrum is generated by sequentially ejecting fragment ions from low *m/z* to high *m/z* by choosing amplitudes of the ring electrode potential that sequentially make ion trajectories unstable. Ions are ejected through holes in the endcap electrodes and detected using an electron multiplier. The sequential detection of parent ions and their subsequent fragmentation to produce smaller product ions to confer sequence information is known as tandem mass-spectrometry (MS/MS) (see below).

1.4.3.3 Orbitrap

The LTQ Orbitrap XL is a hybrid FT mass spectrometer that combines a linear ion trap and a orbitrap mass analyser. An orbitrap mass analyser is an iontrap, however, neither RF voltages or magnetic fields, as found in conventional traps and FT-ICR instruments respectively, hold ions inside. Instead, an electrostatic field is applied to trap moving ions. In an orbitrap mass analyser, ions are focused by two concentric electrodes. The electrostatic field which is generated, forces ions to move in complex spiral patterns around the central electrode. The axial component of these ion oscillations is measured by a Fourier Transform resulting in an accurate reading of their *m/z*. As a result the device has very high resolution and high mass accuracy (Hu, Noll et al. 2005; Olsen, de Godoy et al. 2005; Makarov, Denisov et al. 2006; Perry, Cooks et al. 2008).

This mass spectrometer features a secondary collision cell to provide additional flexibility to MS/MS experiments. Ions can be selected in the linear ion trap and fragmented either in the ion trap (CID) or in the secondary collision cell. The ions are accumulated in a RF-only quadrupole called a C-trap before being pulsed into the orbitrap. The C-trap stores ions and also carries out higher-energy collision-dissociation (HCD) (Makarov, Denisov et al. 2006; Olsen, Macek et al. 2007). The HCD collision cell offers improved sensitivity, signal-to-noise ratio and fragmentation efficiency ideally suited to isotopic labelling experiments (see below).

1.4.3.4 Time-of-flight analyzers

Ions are separated by TOF on the basis of the time that ions take to travel from the ion source to the detector through a field-free region. Ionised species starting from the same position at the same time, accelerating by means of a constant electric field, have velocities related to their mass-to-charge ratio and their times of arrival at a detector directly indicate their masses. TOF offers an unlimited mass range creating a complex mass spectrum for each ionisation event (Fig 1.4.3).

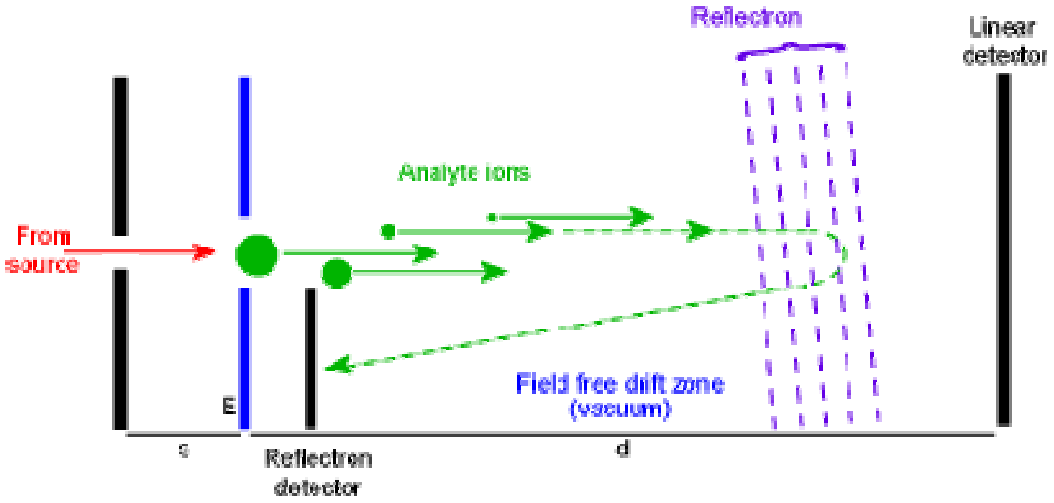

Figure 1.4.3 TOF separation. Ions that are given an initial kinetic energy by an extraction pulse, drift along the field-free drift zone where they are separated according to their *m/z* ratios.

TOF mass analysers are commonly used in conjunction with MALDI because of the pulsed nature of its ionisation (Griffin, Gygi et al. 2001). Ions formed have a varied energy distribution arising from their differences in initial kinetic energies, and because of their spatial and temporal distributions. For these reasons, devices have been incorporated into modern TOF instruments that correct for these energy distributions. Ions are first allowed to expand into a field-free region in the source and after a user defined delay, a voltage pulse is applied to extract ions from the source. This process is known as delayed extraction. In addition, reflectrons (ion mirrors) correct the energy dispersion of ions leaving the source that have the same *m/z* values. The primary structure of peptides can also be obtained through a process called post source decay (PSD). In this mode, an increased internal energy is deposited to the analyte resulting in fragmentation in the field-free region of the TOF analyser. The fragmentation pattern can be used to elucidate the primary structure of the peptide in the same way as for tandem mass spectrometry (described below), however is not always effective.

1.4.3.5 Tandem mass spectrometry (MS/MS)

Tandem mass spectrometry of peptides involves the selection of parent ions for fragmentation to generate smaller product ions with loss of amino acids. Two approaches are commonly used, post-source decay (PSD) in a MALDI-TOF-MS instrument, and collision induced dissociation (CID) in an ESI-MS/MS hybrid instrument such as a Q-TOF. Peptides fragment in a specific manner, that is, the protonated molecules fragment along the peptide backbone, but also show some side-

chain fragmentation with certain instruments. There are three types of bonds that can fragment along the polypeptide backbone, the NH-CH, CH-CO, and CO-NH bonds. Each bond breakage gives rise to two species, one charged and one neutral, only the charged molecules are analysed in the mass spectrometer (Fig 1.4.4).

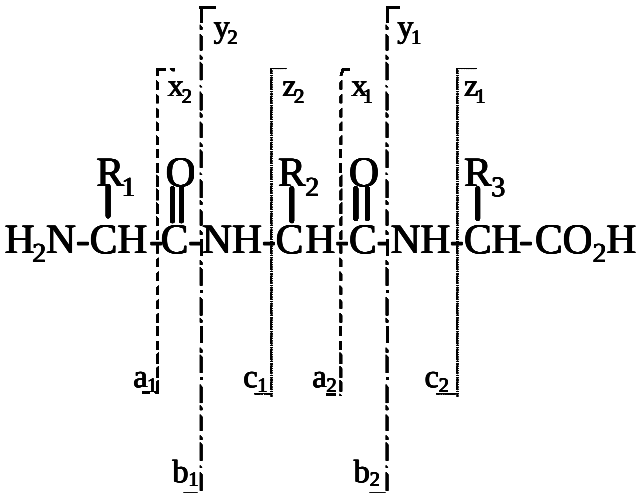

Figure 1.4.4 Nomenclature for the product ions generated in the fragmentation of peptide molecules by tandem mass spectrometry.

Fragment ions generated with the charge retained on their N-terminus are denoted ‘a’, ‘b’, and ‘c’ ions and where the charge is retained on the C-terminal fragment, ‘x’, ‘y’, and ‘z’ ions. The mass difference between ions in an ion series is then indicative of a particular amino acid residue. Analysis of peptide sequence by PSD can be done post peptide mass mapping. A parent ion is selected and further analysed by induced laser energy forcing the peptide to fragment. The advantage of this method is that several

parent ions can be selected from the same aliquot of sample applied onto the target. However, the mass spectra are often harder to interpret due to the complex ion mixtures generated.

The commonly used method for fragmentation in tandem mass spectrometry is by CID. This is carried out in an instrument that contains more than one analyser. Selected ions are introduced into a collision cell, into which an inert gas is admitted to collide with parent ions and bring about their fragmentation before separation and detection in the second mass analyser (Fig 1.4.5). The masses of the fragment ions are measured and then matched against a database of theoretical fragment ions using the parental ion mass as a guide. In addition to accurate information on the sequence of a peptide and thus the identification of a protein, tandem mass spectrometry is also an important tool for the analysis of post-translational modifications, such as glycosylation, phosphorylation and acetylation (Havilio and Wool 2007).

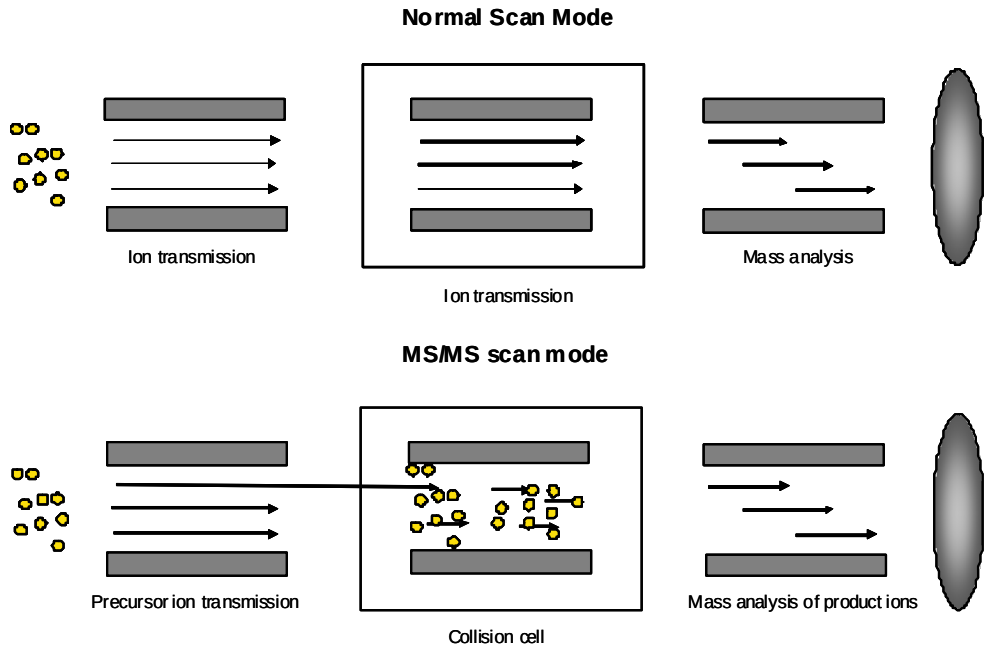

Figure 1.4.5 Tandem mass spectrometry by CID. A tandem mass spectrometer has two mass analysers connected via a collision cell. In normal scan mode, ions with different *m/z* values produced at the source flow through the MS/MS instrument and are separated according to their *m/z* values so that an MS spectrum is recorded. In MS/MS scan mode, the first mass analyser (e.g. quadrupole) isolates a single ion which is then fragmented in the collision cell. The fragmented ions are subsequently separated according to their *m/z* values in the second mass analyser and recorded by a detector.

In conventional electrospray mass spectrometry, peptide mixtures are often pre-separated by high performance liquid chromatography (HPLC) before direct introduction into the mass spectrometer through an electrospray device. This method allows peptides to be resolved according to their retention time on the column during chromatography with subsequent mass analysis. Separation is commonly achieved by reverse-phase chromatography (RP-HPLC) or strong cation-exchange chromatography (SCX-HPLC). These separation methods can also be combined offline to greatly

reduce sample complexity for accurate, efficient and high-coverage protein identification by mass spectrometry. In addition, HPLC is also used to remove excess salts or detergents that can affect the ionisation process and interfere with mass analysis.

1.5 Protein Identification

Protein analysis by mass spectrometry can be carried out by peptide mass mapping or by MS/MS-based peptide fragmentation approaches to generate sequence information. Peptide mass mapping, or peptide mass fingerprinting (PMF) uses the masses of proteolytic peptides obtained from a mass analyser which are searched against a theoretical database of predicted masses that would arise from a digestion of all known proteins (James, Quadroni et al. 1993). Numerous databases can be used, which contain theoretical protein cleavages according to the enzyme of choice and possible post-translational modifications and known chemical modifications (Henzel, Billeci et al. 1993; Mann, Hojrup et al. 1993). A list of potential matches is given and ranked according to a scoring system depending on best probability of a match being real. Confidence in the identification then depends on the species studied, the mass and pI of the protein observed on a gel, the number of peptides matching a particular protein sequence, the mass accuracy of detection, the protein sequence coverage reached, the number of missed cleavages during the proteolysis process and also the type of modifications observed, which can reflect how the sample is processed.

Peptide mass fingerprinting is the method of analysis used with MALDI-TOF-MS instrumentation. The production of singly charged ions $[M^{+}H]^{+}$ creates mass spectra which are simpler to assign. Sample analysis is more tolerant to salts and detergents as the sample crystallisation with the matrix allows a degree of sample purification.

1.5.1 MS-based Peptide & Protein Quantification Methods

Mass spectrometry has largely been used to qualitatively characterise proteins in complex mixtures. The emergence of quantitative mass spectrometry methodologies serves to enhance our understanding of biological processes and facilitating the identification of diagnostic and prognostic markers of disease.

In the past, quantitative proteomics was largely based around 2DE experiments where the staining intensities of matched protein spots from two or more samples were compared and 'up' and 'down-regulated' proteins picked from gels and identified by MS. Protein staining also provides an indication of the amount of protein in a sample. More recently, quantification in 2D gels has become more sophisticated with the development of fluorophores that are covalently attached to proteins before electrophoretic separation (2D-DIGE). These spectrally distinct dye derivatives are mass and charge matched allowing samples to be combined and run together on a single gel and direct comparisons of ratios of expression obtained. As described

previously, 2DE has several limitations; membrane proteins, basic proteins and very large proteins are poorly resolved, the dynamic range of detection often only covers 2-3 orders of magnitude and sensitivity is somewhat limited. Thus only the “well-behaved” and abundant proteins will be detected on gels.

In recent years, with improvements in the accuracy, sensitivity and speed of mass spectrometers efforts have been made to extract quantitative data from mass spectra (Han, Aslanian et al. 2008). Mass spectrometry is not inherently quantitative because proteolytic peptides exhibit a wide range of physiochemical properties such as charge, size and hydrophobicity which lead to differences in mass spectrometric output. Successful detection and identification of protein-specific peptides confirm their presence in a sample. However, failure to identify or detect a peptide does not necessarily confirm absence from a sample as it may be below the detection limits or overlooked by data-dependent acquisition. Database search algorithms score proteins based on numbers of matching sequence fragments rather than their absolute intensities. Therefore, database identification scores are not a reflection of protein abundance although spectral counting has been shown to correlate with abundance. However, peptide quantification has been developed upon the basis that in a MS experiment, the intensity of a signal given by a peptide as it elutes from a chromatographic column can be plotted over time. The area under the curve is known as the extracted ion current (XIC) and for a given peptide and experimental conditions, is linearly related to its amount, although absolute quantitation will depend on ionization efficiency and ion stability as well. If the two proteomes to be compared

have been processed in tandem and analysed in exactly the same way then the intensities of peptides can be compared between the two states to determine their relative abundance. The obvious advantage of this label-free quantification approach is its versatility since it can be applied to any type of sample with reduced processing/ labelling steps and associated costs (Wang, Wu et al. 2006).

The use of stable-isotope labelling in proteomics for quantification has been adopted widely and applications vary in the method of isotope incorporation. Stable isotope atoms impart a mass shift, allowing 'heavy' and 'light' peptides to be distinguished and quantitative ratios to be determined from their signal intensities. This approach eliminates quantification error introduced by experimental procedure because the exact same experimental conditions prevail for both peptide forms.

The chemical synthesis of a stable isotope-labelled peptide analogue and a known quantity 'spiked' into a sample serves as an internal standard in a MS experiment. This results in absolute quantification (AQUA), as the signal intensities are compared for the native peptide and 'heavy' analogue (Gerber, Kettenbach et al. 2007). AQUA has an important role in multiple reaction monitoring (MRM), where a predefined precursor ion and one of its fragments are selected by the two mass filters of a triple quadrupole instrument and monitored over time for precise quantification (Kuhn et al. 2004, Kirkpatrick et al. 2005). The AQUA strategy has also shown use for profiling protein post-translational modifications (Gerber, Rush et al. 2003).

Stable isotopes for quantitation can be also introduced into peptides by the action of a protease. If the digestion is performed in $H_2{}^{18}O$ water, two ^{18}O atoms will be incorporated into the carboxy terminus of each new peptide. The incorporation results in a mass shift of 2 or 4 Da between 'heavy' and 'light' peptides allowing their signal intensities to be differentiated and their quantitative ratios determined (Goshe and Smith 2003).

Another approach to introduce stable-isotope labels is to chemically modify two proteomes of interest with 'heavy' and 'light' chemical labels. In the past, isotope-coded affinity tags (ICAT) were developed consisting of a cysteine reactive moiety, a linker region with eight deuteriums, and a biotin group to facilitate recovery of labelled peptides. A typical ICAT experiment would involve the denaturing and reduction of the two extracted proteomes under study prior to labelling of cysteine residues with either the 'heavy' or 'light' reagent. The proteomes are then mixed, digested and labelled peptides enriched on a streptavidin column. The cysteine containing peptides are eluted from the column and subsequently analysed by MS (Bottari, Aebersold et al. 2004; Yi and Goodlett 2004). This can be advantageous where complex proteomes are being analysed. A disadvantage is the relative abundance of cysteine groups, some proteins contain no cysteine residues and others will have to be quantified on the basis of a single peptide. This approach has not generally been applied.

More recently, the primary amines on peptides have been targeted for labelling. By this approach it should be possible to obtain quantitative data on every peptide

detected. Isobaric tags for relative and absolute quantitation (iTRAQ) uses N-hydroxysuccinimide ester chemistry to add a tag which contains a balance group linked to a reporter group that is only revealed upon MS/MS fragmentation (Gagne, Gagne et al. 2005; Zhang, Wolf-Yadlin et al. 2005; Aggarwal, Choe et al. 2006; Unwin, Smith et al. 2006; Bantscheff, Boesche et al. 2008; Quaglia, Pritchard et al. 2008). Tags have been developed with different reporter ion masses, but through their carbonyl balance group have identical mass. Peptides from proteomes under comparison can be labelled with up to 8 different isobaric tags, combined and analysed by MS. Fragmentation of the tags attached to the peptides generates a low molecular mass reporter ion that is unique to the tag used to label each digested sample. Measurement of the intensity of these reporter ions enables relative quantitation of peptides in each digest and hence protein in the original sample. A major advantage of iTRAQ is multiplexing, allowing for up to 8 labelled pools of protein in a single analysis. Furthermore, it will allow identification of any type of protein, including high molecular weight proteins, acidic protein, and basic proteins, all of which are problematic when using alternative methods such as 2D-DIGE. Furthermore, 2D-DIGE is not particularly useful for resolving insoluble proteins such as membrane proteins, but coupling the iTRAQ labelling system and MS can at least partially solve this problem.

Recently, Tandem Mass Tags (TMT) have become commercially available, taking advantage of the principle described above (Fig 1.5.1).

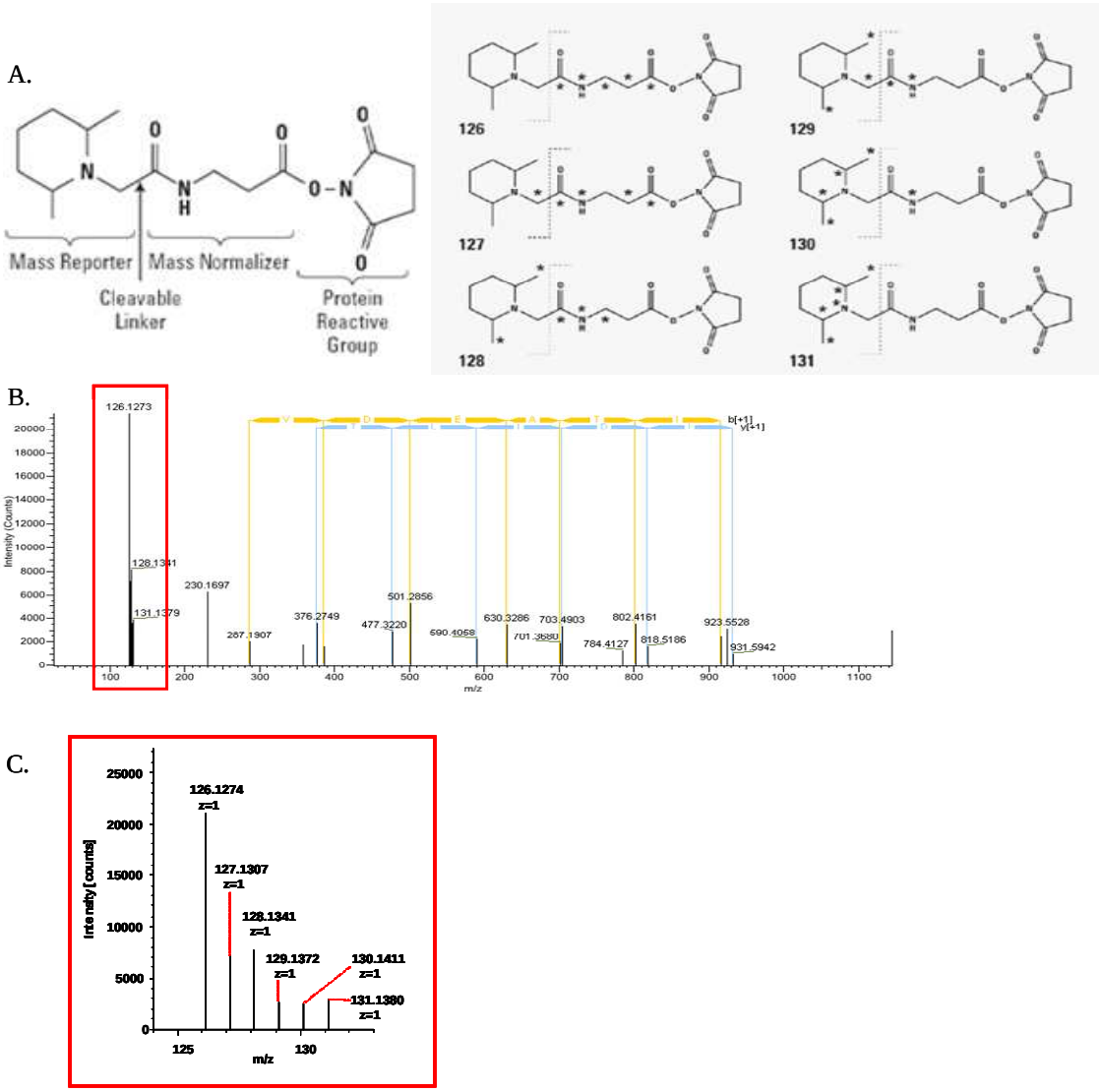

Figure 1.5.1 TMT quantitative protein expression profiling. A) Structural design of TMT tags. The mass reporter is released from the cleavable linker under MS/MS fragmentation conditions. Each tag has a unique mass normalizer that balances the mass reporter, ensuring the same overall mass for all tags in a set. The protein reactive group is an NHS ester that reacts with primary amino groups. B) Analysis of a TMT-6 labelled peptide by HCD. MS/MS fragmentation spectra with reporter ions highlighted in red. C) Close-up of reporter ion region. Individual ion intensities for the 6 reporter ion masses.

Like iTRAQ, these are amino-group labelling isobaric tags and labelled peptides will co-migrate in chromatographic separations (Dayon, Hainard et al. 2008). These mass tags are currently available in 2, 4 and 6-plex forms and were used in the project described here.

Tandem Mass Tags (TMT) comprise a 'reactive group' with a primary amine reactive N-hydroxysuccinimide ester (NHS-ester); a 'mass normalization' group that ensures that each tag shares the same overall mass and a fragmentation susceptible reporter group with a specific mass-to-charge ratio. Their chemical structure is composed of a combination of five heavy isotopes (^{13}C or ^{15}N) in the reporter group and five heavy isotopes (^{13}C or ^{15}N) in the mass normaliser group to produce 6 isobaric tags for the comparison of up to 6 different protein extracts in a single run. Quantification relies on CID/HCD to release the reporter ions from labelled peptides, which are detected in the low mass range and used to report relative peptide expression levels following fragmentation. The 6-plex tags contain unique reporter ion masses in the range *m/z* 126.1 to 131.1.

To handle and interrogate the very large datasets produced during quantitative mass spectrometry-based experiments several software solutions are available. ThermoFisher offer Bioworks 3.3 to handle all the major quantitative labelling techniques including iTRAQ, TMT, SILAC and ICAT. Relative expression ratios are reported for the peptides of a given protein. Bioworks uses the Sequest algorithm for identification of peptides and proteins. More recently, ThermoFisher has developed Proteome

Discoverer to handle iTRAQ and TMT labelling techniques using the Sequest and Mascot algorithms for peptide and protein identification. In addition it can determine false discovery rates for validation of protein identifications. Mascot 2.2 by Matrix Science offers reporter, multiplex and exponentially modified protein abundance index (emPAI) quantitative methodologies. Reporter quantitation is based on the relative intensities of fragment peaks at fixed *m/z* values within a MS/MS spectrum, e.g. 114 and 115 for iTRAQ. Multiplex quantitation relies on the relative intensities of sequence ion fragment peaks within an MS/MS spectrum. EmPAI is a label-free quantitation method based on protein coverage by the peptide matches in a database search result. Peptide and protein identifications are assigned using the Masocot algorithm. False discovery values are calculated for all database searches.

Finally, a widely used method of stable-isotope incorporation is by metabolic labelling *in vivo*. A whole proteome can be stable-isotope labelled before an MS experiment. This is achieved by introducing isotopic metabolic precursors into the growth media of living cells. During cell growth and protein turnover the isotope labelled precursors are incorporated into all cellular proteins. Stable isotope labelling by amino acids in cell culture (SILAC) is emerging as a very effective approach for quantitative MS experiments (Ong, Blagoev et al. 2002; Everley, Krijgsveld et al. 2004; Amanchy, Kalume et al. 2005; Uitto, Lance et al. 2007). The amino acids arginine and lysine in the labelling media contain ^{13}C to ensure that each tryptic cleavage product contains at least one heavy amino acid after tryptic cleavage that confers a mass shift to distinguish between the ‘heavy’ and ‘light’ labelled cell populations. Typically, after several cell

population doublings, the cellular proteome will incorporate the ‘heavy’ amino acids to >90%. The two cell populations grown in either ‘heavy’ or ‘light’ media can then be combined at the earliest stage of any fractionation and digestion procedure for more accurate quantitative MS (Fig 1.5.2).

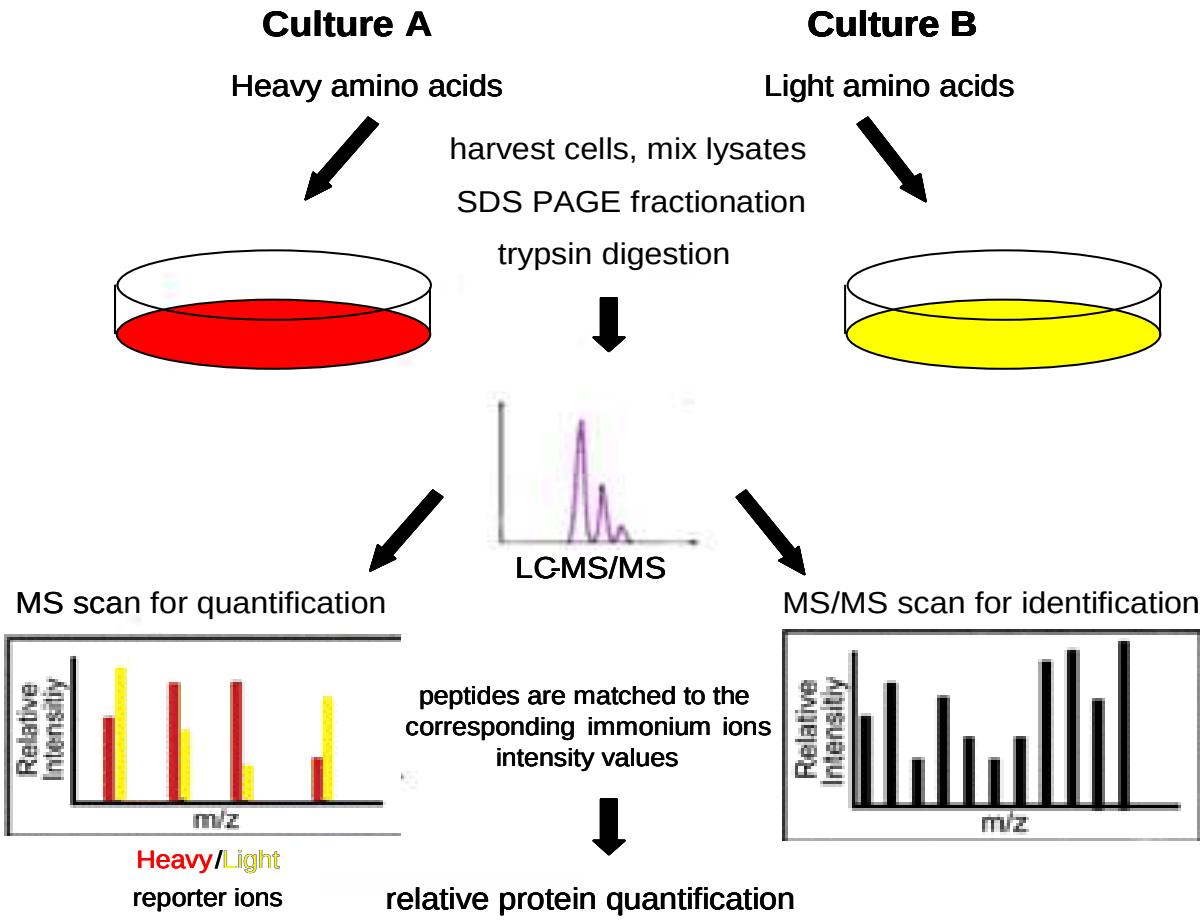

Figure 1.5.2 SILAC experimental workflow. Two groups of cells are grown in culture media that are identical except in one respect; one media contains the ‘light’ and the other a ‘heavy’ form of a particular amino acid e.g. leucine or lysine. Cell passaging results in the incorporation of > 90 % of the ‘heavy’ or ‘light’ form of the amino acid. The cells are harvested, mixed and digested with trypsin. Quantitative information is extracted from the ‘heavy’ and ‘light’ parent ions for a given peptide.

More recently, ^{15}N labelling of simple organisms through the use of ^{15}N-ammonium salts results in the complete labelling of amino acids within the cells. In turn, these micorooganisms such as ^{15}N-labelled algae can be fed to small mammals. Kruger M. et al. have fed mice with a $^{13}C_6$-lysine diet. No adverse effects have been observed on feeding and growth, fertility or activity, or development and physiology over several generations of SILAC labelling (Kruger, Moser et al. 2008). Stable-isotope labelled mice have been produced with complete incorporation. The limiting factor to this approach is currently the high costs involved.

1.6 Aims

Epithelial ovarian cancer is the most lethal form of gynaecological malignancy in the western world. At present there is no reliable and specific method of early detection and robust biomarkers for the disease are urgently required. In addition, the molecular changes associated with ovarian cancer development and progression are poorly understood. The major aim of this project was to identify the protein changes associated with suppression of the tumourigenic phenotype in epithelial ovarian cancer cell models. This work would hopefully not only identify candidate biomarkers of ovarian cancer, but also increase our understanding of the protein changes associated with reconstitution of normal human chromosome 18 material that contain putative tumour suppressor genes.

The cellular, secreted and surface proteomes will be probed in order to gain a comprehensive coverage of protein changes. Cell surface and secreted proteins are important not only in normal cell physiology (e.g. cell-cell signalling, cellular adhesion, migration, morphogenesis and ionic conductance) but also in cancer (e.g. controlling many characteristics of malignancy including proliferation, angiogenesis, tissue invasion, and metastasis). These proteins may be important cancer biomarkers for diagnostic blood screening tests and targets for small molecule inhibitors and monoclonal antibody therapies.

The project involves a detailed quantitative proteomic comparison of two parental ovarian cancer cell lines derived from primary endometrioid and clear cell carcinomas and their MMCT Ch18 hybrids (see section 1.3) (Dafou, Ramus et al. 2009). These cell lines have been well characterised with regards to their tumourigenic phenotype. The parental cell lines displayed the characteristic of transformed cell lines whilst their hybrid clones displayed significant suppression of this phenotype in a number of assays. Firstly, the cellular and secreted proteomes were examined by 2D-DIGE and differentially expressed proteins identified by (MS) directly from gels. The same fractions were also analysed using multiple dimensional LC combined with MS/MS and Tandem Mass Tagging (TMT) for quantification. TMT has only recently become commercially available and enables protein expression levels to be determined in up to 6 samples simultaneously from peptide-specific reporter ion intensities produced during fragmentation, as with the iTRAQ technology. The cell surface proteome was also examined by NHS-biotin surface labelling and streptavidin enrichment linked to 1D-SDS-PAGE, 2D-LC and TMT-based identification and quantitation. For confirmation of changes and assessment of strategy, altered proteins will be analysed by western blotting and ELISA. To summarise, the aims of this research project are:

- To identify the protein changes associated with tumour suppression in epithelial ovarian cancer Chromosome 18 MMCT cell models. The cellular, secreted and surface proteomes were probed in order to gain a comprehensive coverage of the protein altered. Enrichment strategies for the ‘secreted’ and ‘surface’

proteome were developed, optimized and coupled to a quantitative proteomic technique for protein expression profiling.

- To evaluate the similarities and differences between the different proteomic technologies used within the context of the biological questions that the project aims to answer.

- To validate expression changes of proteins of interest by western blot analysis of the parental cell lines, and their Ch18 hybrids and revertant cell lines, where the selection conditions are no longer applied and transferred Ch18 material is lost from cells. To address the potential of candidates as biomarkers of ovarian cancer by examining expression in other ovarian cancer cell lines and normal ovarian surface epithelial cells and in serum from malignant and benign cases of ovarian cancer and healthy controls.

Chapter 2 Materials & Methods

2.1 Cell Lines

The ovarian cancer cell lines, TOV-112D and TOV-21G (American Tissue Culture Collection, LGC Standards, Middlesex, UK) were fused with monochromosome hybrids (chromosome 18 tagged with hygromycin phosphotransferase selectable marker) in mouse A9 cells. Micronucleation was achieved by exposure to colcemid for 48 hours. Post-fusion, hybrid clones were isolated and expanded in complete culture medium containing 400U/ml hygromycin B to maintain the transferred Ch18 material (Gynaecological Cancer Research Laboratory, IFWH, UCL (Dafou, Ramus et al. 2009)). Revertant cell lines were isolated by culturing hybrid clones in the presence of ganciclovir. Ganciclovir-resistant clones with the loss of transferred Ch18 were selected. A panel of ovarian cancer cell lines including Cov413b, PE014, Intov2, Jaue 2, OvP1, OvcaX, Skov3, IgOV, Ovca3, Cov624, PxN94, 847AD, 41D, Cov318, LK2, OAW42M, 1847, Cov664, OAW41M and NOSE cell lines including NOSE4p5 and NOSE11p5 were obtained from the ATCC and cultured under recommended conditions.

2.2 Tissue Culture

Parental ovarian cancer epithelial cell lines TOV-112D and TOV-21G were maintained in MCB105 and 199 media (Sigma, St Louis, MO) at 1:1 ratio containing 15% (v/v) foetal calf serum (FCS), supplemented with 2 mM L-glutamine, 100 mg/ml streptomycin and 100 unit/ml penicillin (Invitrogen, Paisley) in tissue culture dishes at 37°C in a 5% CO2 humidified incubator. The hybrid cell lines, 18-G-5, 18-G-1-26, 18-D-22 and 18-D-23 were cultured under the same conditions with an additional 400 U/ml of hygromycin to maintain clonal selection. Cells were passaged when they reached 70-80% confluence by trypsinisation according to standard procedures. Stocks of epithelial cells were stored in 10% DMSO and 90% FCS, frozen slowly overnight and submerged in liquid nitrogen for long-term storage.

2.3 Extraction of total cell proteins

Cells at 80% confluency were washed twice with phosphate buffered saline (PBS), drained well and cells lysed in 2D lysis buffer (4% (w/v) CHAPS, 0.5% NP40, 8 M urea, 2 M thiourea, 10 mM Tris-HCl (pH 8.3), 1 mM EDTA) and scraped. Samples were homogenized by passage through a 25-gauge needle (4 times) and insoluble material removed by centrifugation (13,000 rpm/10 min/4°C). Protein concentrations were determined using a Bradford microtitre plate assay (Pierce). Standard curves were determined using dilutions of bovine serum albumin (BSA) and samples were assayed in triplicate.

2.4 Preparation of secreted proteins

For preparation of the secretome, cells at 80% confluence were washed twice in PBS and further incubated for 24 hours in serum-free medium. The medium was then replaced with 10 ml of fresh serum-free medium which was collected after a further 24 hours and chilled on ice. Floating cells and cellular debris were removed by centrifugation (2000 g, 10 min). Protease inhibitors were added (100 μg/ml AEBSF, 17 μg/ml aprotinin, 1 μg/ml leupeptin and 1 μg/ml pepstatin) and the sample concentrated (25-fold) and desalted by ultrafiltration through centriplus YM-3 filters (MWCO 3kDa). The samples were dried down in a speed vac and resuspended in 100 μl of 2D lysis buffer. Protein concentrations were determined as above.

2.5 Crude membrane preparation

Cells were harvested in 1 ml of hypotonic buffer (10 mM HEPES pH 7.4, 5 mM KCl, 5 mM $MgCl_2$) prior to homogenisation with a Dounce homogeniser (at least 25 strokes). A crude nuclear fraction was prepared by centrifugation for 5 min at 800 g using a bench top centrifuge. The supernatant was centrifuged at 100,000 g using an Optima ultracentrifuge (Beckman Coulter, Inc., USA) for 60 min enabling the separation of a cytosolic supernatant fraction (S100) and a crude membrane fraction (P100). P100 was washed in hypotonic buffer and the final pellet was resuspended in 1 mL RIPA buffer (150 mM NaCl, 10 mM Tris (pH 7.4), 0.1% SDS, 1% NP40, 0.5% sodium deoxycholate, 5 mM EDTA with protease and phosphatase inhibitors (100μg/mL

AEBSF, 17µg/mL aprotinin, 1 µg/mL leupeptin, 1 µg/mL pepstatin, 5µM BpVphen, 5µM fenvalerate, 1 µM okadaic acid).

2.6 Biotinylation of EOC Cell Surface Proteins

Cells in four 15 cm tissue culture dishes at 80% confluency were washed twice in PBS and incubated for a further 24 hours in serum-free media. The media was removed and the cells washed twice with PBS before labelling with 0.3 mg/mL Sulfo-NHS-SS-Biotin (Pierce) in PBS for 30 minutes on ice. Excess label was removed by three washes in PBS. Cells were gently scraped into solution and washed in Tris buffered saline (TBS) 3 times to remove cellular material from damaged cells before a final centrifugation at 500 x g for 3 minutes. The cell pellet was lysed in 1 mL RIPA buffer (150 mM NaCl, 10 mM Tris (pH 7.4), 0.1% SDS, 1% NP40, 0.5% sodium deoxycholate, 5 mM EDTA with protease and phosphatase inhibitors (100µg/mL AEBSF, 17µg/mL aprotinin, 1 µg/mL leupeptin, 1 µg/mL pepstatin, 5µM BpVphen, 5µM fenvalerate, 1 µM okadaic acid). Samples were homogenized by passage through a 25-gauge needle (4 times) and insoluble material removed by centrifugation (13,000 rpm/10 min/4°C). Protein concentrations were determined with a BCA microtitre plate assay (Pierce) using BSA as a standard. Yields were less than expected because of cell loss during the washing stages. Streptavidin-agarose slurry (100 µL of 50% slurry) washed in RIPA buffer was incubated for 2 hours at 4ºC then washed 5 times with RIPA buffer and then twice with PBS. Captured proteins were eluted with Laemmli sample buffer (50 mM Tris pH 6.8, 10% (v/v) glycerol, 2% SDS (w/v), 2% β-

mercaptoethanol, 0.1% (w/v) bromophenol blue) by heating for 5 min at 100°C and the eluate collected. Elution by cleavage with DTT of the disulphide bond linking the biotin moiety and the protein with the cleavable reagent was investigated by 1D-gel analysis but found to result in poor yields compared to elution in Laemmli sample buffer.

2.7 Protein labelling with Cy Dyes for 2D-DIGE

Samples (typically 100 µg protein) in 2D lysis buffer were labelled with NHS-Cyanine (Cy) dyes, at a dye to protein ratio of 4 pmol of dye/µg of protein on ice for 30 minutes in the dark (Cy2 dye was obtained from GE Healthcare, Cy3 and Cy5 were synthesized in-house, as outlined by Chan et al. 2005). A standard pool was prepared by mixing equal amounts of protein from each condition and labelled with Cy2. Reactions were quenched by adding a 20-fold molar excess of L-lysine to dye and incubating on ice for 10 min in the dark. Equal protein amounts from pairs of differentially labelled samples and Cy2 labelled standard were mixed appropriately and reduced by addition of dithiothreitol (DTT) to 65 mM. Carrier ampholines and pharmalyte mix (1:1) was added to a final concentration of 2% (v/v) and bromophenol blue to 0.001% (v/v). The final volume was made up to 450 µL with 2D lysis buffer plus DTT for rehydration of Immobiline (IPG) dry strip (IEF) gels (GE Healthcare).

2.8 Protein separation by 2D gel electrophoresis and gel imaging

The IPG strips (24 cm Non Linear pH 3-10, GE Heathcare) were rehydrated with labelled samples in the dark overnight according to the manufacturer's guidelines. Isoelectric focussing was performed using a Multiphore II apparatus (GE Healthcare) for a total of 80 kVh at 16°C. Strips were equilibrated for 15 min in equilibration buffer (6 M urea, 30% (v/v) glycerol, 50 mM Tris-HCl pH 6.8, 2% (w/v) SDS) containing 65 mM DTT and then for 15 min in the same buffer containing 240 mM iodoacetamide. Equilibrated strips were transferred to 12% uniform polyacrylamide gels cast between 20 x 24 cm low-fluorescence glass plates. Gels were bonded to the inner plate at casting using bind saline (PlusOne) according to the manufacturer's guidelines. Strips were overlaid with 0.5% (w/v) low melting point agarose in running buffer containing bromophenol blue. Gels were run in an Ettan Dalt 12 gel tank at 16°C and 2.2 W until the dye front had run off the bottom of the gels.

Gels were scanned on a Typhoon^{TM} 9400 multi-wavelength fluorescence imager (GE Healthcare). The photomultiplier tube voltage was adjusted on each channel (Cy2, 3 and 5) for preliminary low resolution scans (1000 mm) to give maximum pixel values within 10% for each channel but below saturation level. A final high-resolution scan (100 mm) was performed and the images cropped in ImageQuant software and exported into DeCyder software for image analysis.

2.9 Image analysis

Images were curated and analysed using Decyder software (GE Healthcare). This consists of two modules, the differential in gel analysis (DIA) module and the biological variance analysis (BVA) module. DIA performs spot detection and calculates spot volumes/abundances for the three images (Cy2, 3 and 5) from a single gel and performs normalisation. In BVA, spots are manually matched between multiple samples across all the gel images in an experiment. This allows statistical analysis of changes in abundance across samples. The internal standard was employed here to facilitate spot matching and allow a spot by spot standardisation for improved reproducibility and accurate quantitation of protein abundance changes across the samples. A student *t*-test was performed whereby average standardised abundances from replicate samples were compared across the different conditions being tested. Spots displaying significant changes in abundance were then filtered by specifying a threshold of average-fold change with P values of <0.05. Pick lists for spots of interest were created from colloidal coomassie blue post-stained images of the same gels which were matched with the Cy Dye images in Decyder where peak lists were created and exported to an Ettan spot picking robot (GE Healthcare).

2.10 Colloidal Coomassie Blue staining

Bonded gels were fixed in 35% (v/v) ethanol with 2% (v/v) phosphoric acid overnight and then washed three times for 30 min in ddH_2O. The gels were then incubated in 34% (v/v) methanol with 17% (w/v) ammonium sulphate and 3% (v/v) phosphoric acid

for 1 hour prior to the addition of 0.5g/L Coomassie G-250 (Merck), and left to stain for 2-3 days. Stained gels were scanned on the Typhoon 9400 scanner using the red laser with no emission filter. A similar procedure was followed for unbonded 1D gels, except that the washing and staining times were reduced.

2.11 SYPRO Ruby fluorescence staining

SYPRO Ruby fluorescent protein stain (Molecular Probes, USA) was used as an alternative post-staining technique with 2D-gels for its increased sensitivity where protein loads were less. Following electrophoresis, gels were fixed for at least 3 hours in fixing solution (30% (v/v) methanol, 7.5% (v/v) acetic acid, in ddH_2O). Lower concentrations of methanol and acetic acid were used in order to avoid shrinkage and cracking of bonded gels. Gels were washed twice in water and then incubated in SYPRO Ruby staining solution for a minimum of 3 hours in the dark. Gels were then washed briefly in water to remove excess dye. Gels were then scanned on the Typhoon^{TM} 9400 scanner

2.12 Spot Picking and Trypsin Digestion

Spots were excised from gels using an Ettan spot picker (GE Healthcare) with a 2 mm picking head. For in-gel digestion, gel pieces were washed three times in 50% (v/v) acetonitrile (ACN), dried in a SpeedVac for 10 min, reduced in 10 mM dithiothreitol in 5 mM ammonium bicarbonate (AmBic) pH 8.0 for 45 min at 50°C and then alkylated

with 50 mM iodoacetamide in AmBic for 1 h at room temperature in the dark. Gel pieces were then washed twice in 50% ACN and vacuum dried. 50 ng of sequencing grade modified trypsin (Promega, Southampton, UK) in 5 mM AmBic was added to each dried gel piece and pieces were allowed to re-swell for 5 min. 5 mL of 5 mM AmBic was then overlaid onto the gel pieces and the samples incubated at 37°C for at least 18 hours. Tryptic peptides were then extracted three times with 50% (v/v) ACN plus 5% (v/v) trifluoroacetic acid, the extracts pooled and vacuum centrifuged to dryness. Peptides were finally resuspended in 5 mL of 0.1% (v/v) formic acid and stored at –20°C prior to mass spectrometric analysis.

2.13 MALDI-TOF MS and Peptide Mass Fingerprinting

Routinely, 0.5 mL of tryptic digest was mixed with 1 µL of matrix solution (saturated aqueous 2,5-dihydroxybenzoic acid (DHB)) and spotted onto a target plate and left to dry. MALDI-TOF mass spectra were acquired using an Ultraflex mass spectrometer (Bruker Daltonik, Bremen, Germany) in the reflector mode. The mass spectrometer was calibrated with external standards using a standard mixture of peptides prior to aquisition. Internal calibration was carried out using trypsin autolysis peaks at *m/z* 842.51 and *m/z* 2211.10. Spectra were collected in the *m/z* range 500-4000 to generate a peptide mass fingerprint. Spectra were processed using FlexAnalysis software (BrukerDaltronics). The mass lists were extracted from Ultraflex data files using a Pearl script written in-house, UltraMass List, (http://www.ludwig.ucl.ac.uk/bachem_html/software.html). Mascot search engine,

version 2.0.02 (Matrix Science, UK) was used for database searching. For search criteria, carbamidomethylation of cysteines was selected as a fixed modification, while oxidation on methionine, N-acetylation and pyro-glutamate were selected as variable modifications. A positive identification was accepted when ≥6 peptides masses matched a particular protein (mass error of ±50 ppm, allowing 2 missed cleavage), sequence coverage was >25%, MOWSE scores were higher than a threshold value where p=0.05 and predicted protein mass matched the gel-based location.

2.14 TMT labelling

An equal amount of protein (25-100 µg) from each cell line was resuspended in 90 mM triethylammoniumbicarbonate (TEAB) and then reduced, alkylated, digested and labelled according to the standard protocol supplied by the manufacturer (TMT 6plex Label Reagent, Thermo Scientific). Briefly, the protein sample was solubilised in 90 mM TEAB and 0.5% SDS before reducing with 9.5 mM tris(2-carboxyethyl)phosphine (TCEP) for 1 hour at 55ºC and then alkylated with 17 mM iodoacetamide (IAM) for 30 minutes in the dark. The sample was digested with trypsin (2.5 µg/100 µg protein) overnight at 37ºC. The TMT labels were reconstituted prior to labelling with 41 µl of ACN and added to the appropriate sample for labelling over 1 hour at room temperature. TMT results were generated from the analysis of isobaric tag combinations. The parental cell line TOV-112D was labelled with reagent 126 and its hybrid cell lines, 18-D-22 and 18-D-23, labelled with reagents 127 and 128 respectively. The parental cell line TOV-21G was labelled with reagent 129 and its

hybrid cell lines, 18-G-5 and 18-G-1.26, labelled with reagents 130 and 131 respectively.

2.15 SCX Chromatography

Tryptic peptides were fractionated by strong cation exchange (SCX). TMT-labelled digests were combined and dried down in a Speedvac, resuspended in buffer A (95%/5% water/ACN, 5 mM NaH_2PO_4 buffer pH=3) and acidified (pH 2) before injection (50 µg) onto a Polysulfoethyl column (1 mm I.D x 15 cm, 5 µm, 300Å) (PolyLC, Columbia, MD) using an Ultimate 3000 LC system. The column was allowed to equilibrate for 25 min in buffer A before injection. A gradient was applied of 5-55 % B (mobile phase A + 1M NaCl) at 50 µl/min in 30 minutes using the loading pump and fractions of 150 µl were collected every 3 minutes.

2.16 Sample clean-up using C18 pre-packed tips

Samples were de-salted after SCX using the 'ZipTip' protocol. The clean-up is based on reverse phase LC using ZipTips (Millipore). The C18 packing material was wetted 3 times with 10 µL of 50 % ACN using a standard 10 µL Gilson pipette. The C18 tip was then washed 3 times with 0.5 % TFA. The sample solution was then passed over the packing material a minimum of 10 times by aspirating and dispensing with care not to create air bubbles. The C18 tip was then washed 3 times with 0.5 % TFA. Finally, the

sample was eluted from the packing material by aspirating and dispensing 10 µL of 50% ACN/0.5% TFA 10 times before collection in a siliconised tube for drying down.

2.17 Liquid Chromatography Tandem MS (LC-MS/MS)

Tandem MS analyses of WCL proteins isolated from DIGE gels were performed by nanoflow capillary reversed-phase liquid chromatography coupled on-line to electrospray quadrupole time-of-flight tandem mass spectrometry (ESI Q-TOF MS/MS) using a Q-Tof (MicroMass, Manchester, UK) or a QSTAR (Applied Biosystems) instrument. Typically, 5 µl of sample was injected via a Famos system (Dionex) on to a 300 µm i.d x 5mm C18 PepMap guard column (5µm, 100A, LC Packings, Netherlands) and washed for 3 min with 95% solvent A (water + 0.1% FA) at a flow rate of 250 nl/min. Reversed-phase chromatographic separation was carried out using an Ultimate system (Dionex) on a 75mm i.d x 150mm column C18 PepMap Nano LC column (3µm, 100A, LC Packings, Netherlands) with a linear gradient of 5-50% solvent B (water/ACN 20%:80% v/v + 0.1% FA). ESI MS/MS tandem spectra were recorded in the automated MS to MS/MS switching mode, with an *m/z* dependent set of collision offset values. Singly to triply charged ions were selected and fragmented, with argon (Q-TOF) or a second reservoir of nitrogen (Q-Star) as the collision gas. Acquired spectra were processed using ProteinLynx (Q-Tof) or Analyst QS (Q-Star) software and submitted to Mascot database search routines including +2 and +3 peptide charge, and mass tolerance ±50ppm. Positive identifications were

accepted when at least two peptide sequences matched an entry with MOWSE scores above the p=0.05 threshold value.

Tandem MS for 2D-LC with TMT labels work was performed on a Ultimate 3000 system linked to a Orbitrap XL mass spectrometer (Thermo). Reverse-phase chromatography was performed under the conditions described above. The mass spectrometer was operated in the data-dependent mode to automatically switch between Orbitrap MS and MS/MS acquisition. Survey full scan MS spectra (from *m/z* 400-2000) were acquired in the Orbitrap with resolution r = 60,000 at *m/z* 400. The most intense ions (typically top 3-5 ions/scan) were sequentially isolated for fragmentation. Ions were selected in either the linear ion trap (LTQ) and fragmented by CID or in the collision cell and further measured in the Orbitrap mass analyser. Ions are passed to the collision cell through the C-trap for Higher Energy Collisional Dissociation (HCD) fragmentation. 1 x 10^6 ions were accumulated in the C-trap for HCD spectra. HCD normalized collision energy was set to 40% and fragmentation ions were detected in the Orbitrap at a resolution r = 7500. Due to the higher ion accumulation and ion transfer times required for HCD only, up to three of the most intense ions were acquired following each full scan. Target ions that had been selected for MS^2 were dynamically excluded for 30 seconds. For accurate mass measurements the lock mass option was enabled. The polydimethylcyclosiloxane (PCM) ion *m/z* 455.120025 was used as an internal calibrant.

For peptide identification, data files were processed in Proteome Discoverer (Thermo Scientific) and Mascot Daemon using the IPI human database and the following parameters for database searching. The MS tolerance was ±10 ppm and MS/MS tolerance 0.1 Da, one missed cleavage and carbamidomethylation of cysteines set as a fixed modification. Where TMT-mass tagging was used, searches were carried out using carbamidomethylation of cysteine residues set as a fixed modification. In addition, TMT modification of peptide N-termini and lysine residues were set as fixed modifications. Methionine oxidation and N-terminal acetylation were set as variable modifications. Search filters were selected as follows, Mudpit scoring, Mascot significance threshold $p>0.05$, score > 20, requires bold red (matches that are red and bold are statistically strongest assignments) and quantitation requires at least homology. Peptides with a ratio above 2 and below 0.5 are significantly different from the average to be considered as a potential change in protein expression.

2.18 Western Blotting

Cell extracts were separated by 1D electrophoresis and electro-blotted onto polyvinylidene fluoride (PVDF) membrane (Immobilon P, Millipore) using a wet transfer tank in transfer buffer (195 mM glycine, 25 mM Tris, 20% (v/v) methanol). Membranes were blocked for 1h with 5% BSA (w/v) in Tris buffered saline with tween 20 (TBS-T) (50 mM Tris pH 8, 150 mM NaCl, 0.1 % tween 20). Membranes were then incubated for a minimum of 1h in a primary antibody solution in TBS-T. Membranes were washed in TBS-T (three times 15 min) and then probed with the appropriate

horseradish peroxidase (HRP)-coupled secondary antibody (Amersham Biosciences, UK). After further washes in TBS-T, immunoprobed proteins were visualised using the enhanced chemiluminescence (ECL) method (NEN-Life Science Products, Inc., USA). All antibodies used in the present study are shown in Table 2.1.

Antibody	Company	Mon/polyclonal	Dilution
Actin beta (clone AC-15)	Sigma	mo mAb	1:25000
Akt	Cell Signaling Technology	rab pAb	1:2000
Akt anti-pSer473	Cell Signaling Technology	rab pAb	1:2000
ErbB1/EGFR (1005)	Santa Cruz	rab pAb	1:2000
ERK1/2	Promega	rab pAb	1:5000
ERK1/2 activate (pT183/pY185-ERK2)	Promega	rab pAb	1:5000
Fascin1	Insight Biotech	mo mAb	1:2000
PDLIM1	Abcam	rab pAb	1:2000
Pigment derived epithelium-derived factor precursor (PEDF)	Abcam	rab pAb	1:2000
PIG3	Santa Cruz	goat pAb	1:2000
Prohibitin	Lab Vision	mo mAb	1:5000
PTEN Affinity Purified	Ben Neel	rab pAb	1:2000
Prolactin (M-19)	Santa Cruz	goat pAb	1:2000

Table 2.1 List of antibodies used for western blotting in the present study

2.19 ELISA

The MMP10 immunoassay (Quantikine) is a sandwich enzyme immunoassay technique. A monoclonal antibody specific for MMP10 is precoated onto the wells of a microplate. Standards and samples are pipetted into the wells and any MMP10 binds. Serum samples were diluted 2-fold with calibrator diluent solution and standards prepared according to the manufacturer's guidelines. After washing, an enzyme-linked monoclonal antibody specific for MMP10 is added to the wells. After repeated washing, a substrate solution is added and colour develops in proportion to the amount of total MMP10 bound in the initial step.

Chapter 3 Proteomic profiling of Ch18 MMCT models of tumour suppression by 2D-DIGE

Introduction

The transfer of chromosome 18 by MMCT into two recipient tumour cell lines, TOV-112D and TOV-21G, induced a suppressive effect on their tumourigenic phenotype. The aim of this project was to identify the protein changes associated with this suppression and candidate biomarkers of ovarian cancer. To investigate the protein changes associated with tumour suppression in the Ch18 MMCT models, 2D-DIGE was carried out and the identification of differentially expressed proteins was performed by MALDI-TOF-MS and LC-MS/MS analysis.

Firstly, 2D-DIGE was applied to compare the whole cell proteomes of each parental cell line and a pool of 5 hybrid clones derived from each. The hybrid clones were selected for their potency of suppression (Chapter 1). Pooling of a number of hybrid clones was chosen for this preliminary experiment to test the system and to reduce costs and facilitate the identification of common changes. However, the major caveat of this approach is that single clones may bias the results and clonal variation is thus masked (see later). Whole cell lysates from each parental cell line and five chromosome 18 MMCT hybrids from each were prepared, protein concentrations equalised and the five clones pooled. Each parent and hybrid pool were labelled with

Cy3 or Cy5 in triplicate. A pool of all samples was also prepared as an internal standard and labelled with Cy2 to be run on all gels. Samples were mixed appropriately (Table 3.1) and proteins separated by 2D electrophoresis and images analysed as described in Materials and Methods.

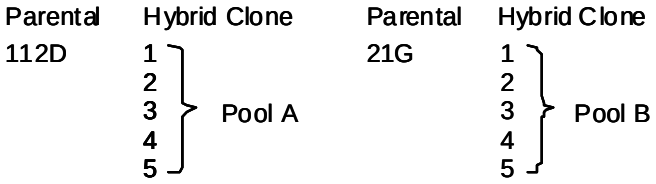

Gel	Cy3	Cy5	Cy2
1	A-1	B-1	Pool
2	112D-1	21G-1	Pool
3	A-2	112D-2	Pool
4	21G-2	B-2	Pool
5	21G-3	A-3	Pool
6	B-3	112D-3	Pool

Table 3.1 Experimental strategy for the 2D-DIGE comparison of two parental EOC cell lines and their pooled hybrid clones. Whole cell lysates from the parental cell lines and 5 chromosome 18 MMCT hybrids for each were harvested. The 5 clones were pooled. Total protein (150µg) for each parent and the hybrid pool was labelled appropriately in triplicate and separated on large format 2D gels prior to image analysis and differential protein expression analysis. A pool of equal amounts of the parent and hybrid pool lysates were labelled with Cy2 as an internal standard.

The 2D-DIGE comparison of parental and hybrid pools revealed a total of 318 spots displaying a change in average abundance of ≥ 2-fold where $p \leq 0.05$; this from gel images with around 1300 matched spots (Fig 3.1). Direct comparison of TOV-112D and its hybrid pool cell lysates revealed 118 spots displaying differential expression, of which 63 were up-regulated and 85 down-regulated. Comparison of TOV-21G and its hybrid pool cell lysates revealed a total of 255 spots showing differential expression, of which 157 were up-regulated and 98 down-regulated. 82 of these gel features were common in the two comparisons. Post-staining of the gels with colloidal coomassie blue and matching of the images to a master Cydye image (Gel 01; Cy2) resulted in 143 well-defined, coomassie-detectable protein spots which were picked for downstream MS-based identification. The lower number of spots for picking arose since fewer spots were detected by CCB staining verses Cydye differential labelling and because only well-resolved spots were chosen rather than spot shoulders or labelled areas between closely migrating spots. It is also unlikely that non-staining spots can be identified with confidence in some MS instuments due to their low abundance.

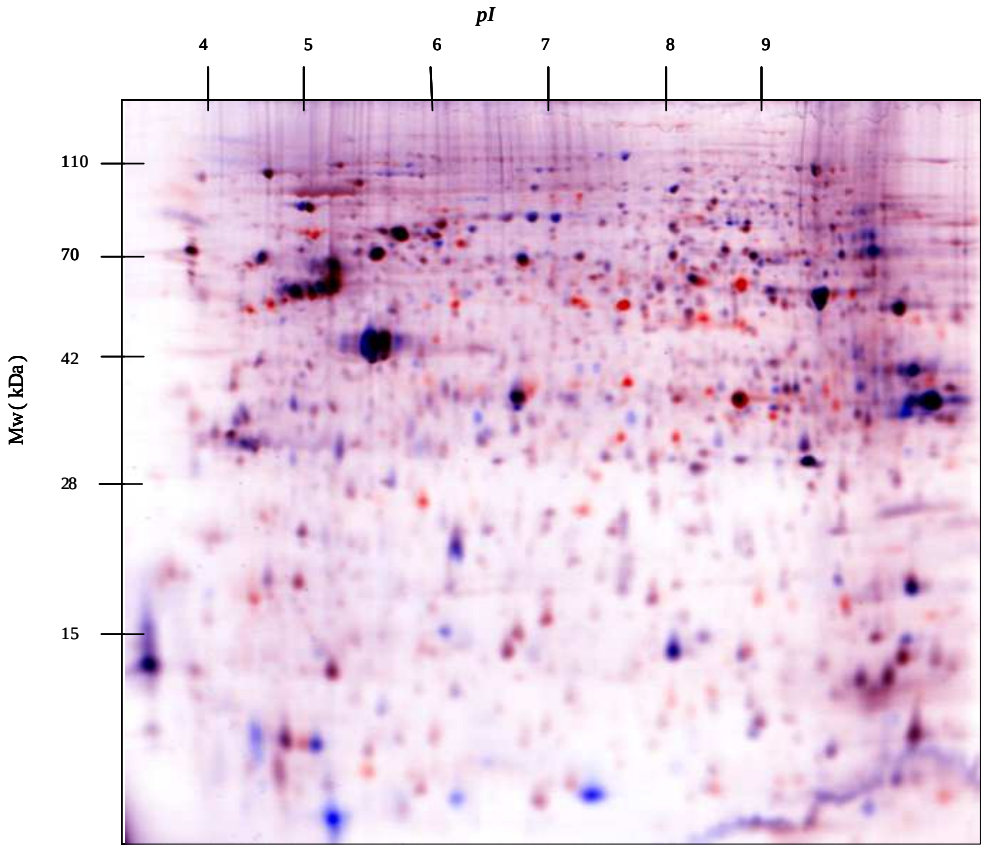

Figure 3.1 Merged 2D gel images of differential protein expression in the 112D cell line and its MMCT-derived hybrid pool. 150µg of total cell lysate from TOV-112D and its hybrid pool (Pool A) were labelled with Cy3 and Cy5 respectively, mixed and loaded with an equal amount of internal standard labelled with Cy2. Differences between Cy3 and Cy5 labelled samples can be linked through the internal standard labelled with Cy2 as ratios Cy3/Cy2 compared to Cy5/Cy2 across all gels. This image, created in Adobe Photoshop, shows differentially expressed proteins in red and blue (up and down-regulated in Pool A vs. TOV-112D respectively). A total of 2,327 protein features were defined and 1300 spots matched using the DeCyder image analysis software.

3.1.1 Identification of differentially expressed proteins

All 143 spots picked from CCB stained gels, were digested and in some cases identified largely by MALDI-TOF-MS peptide mass fingerprinting (see Chapters 1 & 2). Mass lists generated from spectra were compared against theoretically expected tryptic peptide masses in the NCBI and IPI databases searched using Mascot. The identifications were scored according to algorithms that take into account mass accuracy and peptide coverage. The search criteria used allowed +/- 50 ppm mass error and up to 2 missed cleavages. The identified proteins were also verified by comparison of their theoretical molecular weights and pIs with gel position on the master gel.

In total, 92 protein isoforms were identified with high confidence (Table 3.2). The expression changes for some parent: hybrid pool protein spot comparisons were as high as 24-fold and a number of the identified proteins have been previously implicated as putative markers of ovarian cancer in the literature. Notably, none of the proteins identified were chromosome 18 gene products.

Common changes detected included a significant up-regulation of cofilin in both the TOV-112D (3.1 fold) and TOV-21G hybrid pools (1.69 fold). A number of nuclear proteins were detected displaying the same expression profile in the hybrid pools. ATP-dependent DNA helicase II was down-regulated in the TOV-112D (-7.93 fold) and TOV-21G hybrid pools (-5.05 fold). This nuclear protein plays a role in chromosome translocation. Fizzy-related protein homolog displayed up-regulation in the TOV-112D

(2.51 fold) and TOV-21G hybrid pools (2.91 fold). This protein regulates the ubiquitin ligase activity of the anaphase promoting complex/cyclosome (APC/C) and may confer substrate specificity upon the complex. Exosome complex exonuclease RRP41 was significantly down-regulated in the TOV-112D (-19.71 fold) and TOV-21G hybrid pools (-10.13 fold).

Despite these common changes there was little overlap between the two cell systems in terms of the proteins identified and surprisingly 38 of the common proteins displayed opposite regulation between the cell line-hybrid pairs. For example stathmin (Gagne, Gagne et al. 2005), a conserved cytosolic phosphoprotein that regulates microtubule dynamics, was down-regulated (-2.05 fold) in the TOV-112D hybrid pool, but up-regulated (3.03 fold) in the TOV-21G hybrid pool. WD-repeat protein 1 displayed significant up-regulation in the TOV-112D hybrid pool (3.83 fold) and down-regulation in the TOV-21G hybrid pool (-3.94 fold). T-complex protein 1 (epsilon subunit) was identified in two protein spots. Expression was significantly up-regulated for one hybrid pool and significantly down-regulated for the other hybrid pool in one spot and vice-versa in the other spot suggesting differential PTMs. Hsp70 and hsp27 were down-regulated in the TOV-112D hybrid pool but displayed up-regulation in the TOV-21G hybrid pool. The phospholipid and Ca^{2+}-binding protein annexin A1 was down-regulated (-2.25 fold) in the TOV-112D hybrid pool and conversely up-regulated (2.75 fold) in the TOV-21G hybrid pool. The phosphoprotein ezrin, a member of the ezrin/radixin/moesin family of membrane-actin cross-linking proteins that transduces signals by growth factors to the cytoskeleton was up-regulated (2.17 fold) in the TOV-

112D hybrid pool. In contrast, its expression was moderately down-regulated (-1.31 fold) in the TOV-21G hybrid pool. Galectin-1, a secreted protein was significantly up-regulated in the TOV-112D hybrid pool (4.93 fold) and significantly down-regulated (-4.32) in the TOV-21G hybrid pool. Valosine-containing protein (VCP) was significantly up-regulated (4.62 fold) in the TOV-21G hybrid pool and down-regulated (-1.69 fold) in the TOV-112D hybrid pool. VCP is a member of the ATPase superfamily associated with a variety of cellular activities. Peroxiredoxin 2, part of the antioxidant family of thioredoxin-dependent peroxidases, was potently up-regulated (5.71 fold) in the TOV-112D hybrid pool, but down-regulated (-4.75 fold) in the TOV-21G hybrid pool compared to their respective parental cell lines. Finally, the largest contrast in expression observed between the cell models was aldehyde dehydrogenase 1A1. Significant down-regulation by -24.65 fold was observed in the TOV-112D hybrid pool and conversely an up-regulation of 15.01 fold was observed in the TOV-21G hybrid pool. These data suggest considerable heterogeneity between the cell models, which may reflect their different origins; TOV-112D from clear cell and TOV-21G from endometrioid carcinoma. It also shows that these proteins are not involved in the observed tumour suppression displayed by the Ch18 MMCT hybrid clones.

Other proteins of interest; were growth factor receptor bound-2 (Grb2) (significantly up-regulated 3.21 fold in the TOV-21G hybrid pool), an adaptor protein responsible for recruitment of Ras and the activation of the mitogen-activated protein kinase (MAPK) cascade in response to growth factor receptor activation (see Introduction) and Ras-

related protein (Rab2A) (up-regulated in the TOV-21G hybrid pool), which is required for protein transport from the endoplasmic reticulum to the Golgi complex.

Spot No.	Name	IPI No.	HGNC Symbol	Chr	112D hybrid pool / 112D parental Av. Ratio	112D hybrid pool / 112D parental T-test	21G hybrid pool / 21G parental Av. Ratio	21G hybrid pool / 21G parental T-test	pI (gel)	Mw (gel)	pI (pred)	Mw (pred)	Score	%Cov	Molecular and Bilological Function	Localisation
1483	ACETYL-COA ACETYLTRANSFERASE, CYTOSOLIC	IPI00291419	ACAT2	6	-2.4	0.00013	1.43	*0.29*	7.65	43338	6.47	41838	141	71	Lipid metabolism. 2 acetyl-CoA = CoA + acetoacetyl-CoA.	Cytoplasmic
1357	ADENOSYLHOMOCYSTEINASE	IPI00012007	AHCY	20	-1.9	0.021	4.97	0.00017	6.84	47275	5.92	48255	200	54	Adenosylhomocysteine is a competitive inhibitor of S- adenosyl-L-methionine-dependent methyl transferase reactions; therefore adenosylhomocysteinase may play a key role in the control of methylations via regulation of the intracellular concentration of adenosylhomocysteine.	Cytoplasmic
1184	ALDEHYDE DEHYDROGENASE 1A1	IPI00218914	ALDH1A1	9	-24.65	0.0015	15.01	2.60E-06	7.55	52770	6.3	55454	174	55	Binds free retinal and cellular retinol-binding protein- bound retinal. Can convert/oxidize retinaldehyde to retinoic acid (By similarity).	Cytoplasmic
1694	ANNEXIN A1	IPI00218918	ANXA1	9	-2.25	0.00071	2.75	0.00018	7.14	37126	6.57	38918	78	55	Calcium/phospholipid-binding protein which promotes membrane fusion. Involved in exocytosis and regulates phospholipase A2 activity. Binds from two to four calcium ions with high affinity.	Plasma Membrane
1805	ANNEXIN A3	IPI00024095	ANXA3	4	7.44	0.0034	-5.29	0.0097	5.7	33645	5.63	36524	192	74	Inhibitor of phospholipase A2, also possesses anti- coagulant properties. Also cleaves the cyclic bond of inositol 1,2-cyclic phosphate to form inositol 1-phosphate	Cytoplasm
779	ATP-DEPENDENT DNA HELICASE II, 70 KDA SUBUNIT; KU70	IPI00465430	XRCC6	22	-7.93	0.016	-5.05	0.016	7.3	64008	6.23	70114	88	41	Has a role in chromosome translocation. Involved in DNA nonhomologous end joining (NHEJ) required for double-strand break repair and V(D)J recombination.	Nuclear
605	ATP-DEPENDENT DNA HELICASE II, 80 KDA SUBUNIT; KU80	IPI00220834	XRCC5	2	1.6	*0.095*	-2.88	0.0026	5.75	68234	5.55	83222	67	24	Chromosome translocation	Nuclear
1856	CATHEPSIN D PRECURSOR	IPI00011229	CTSD	11	2.81	0.00017	-2.06	0.0014	5.76	32421	6.1	45037	74	42	Acid protease active in intracellular protein breakdown. Involved in the pathogenesis of several diseases such as breast cancer and possibly Alzheimer's disease.	Lysosomal
2156	COFILIN 1 (NON-MUSCLE)	IPI00012011	CFL1	11	3.1	1.70E-05	1.69	0.00066	7.07	16718	8.22	18719	89	81	Controls reversibly actin polymerization and depolymerization in a pH-sensitive manner. It has the ability to bind G- and F-actin in a 1:1 ratio of cofilin to actin. It is the major component of intranuclear and cytoplasmic actin rods.	Intranuclear and cytoplasmic; almost completely in nucleus in cells exposed to heat shock or 10% dimethyl sulfoxide
1003	D-3-PHOSPHOGLYCERATE DEHYDROGENASE.	IPI00011200	PHGDH	1	-1.6	0.00031	2.66	9.20E-05	7.59	57564	6.29	57356	91	40	Serine biosynthesis; first step. 3-phosphoglycerate + NAD(+) = 3-phosphohydroxypyruvate + NADH.	Cytoplasmic
2103	DJ-1; PARK7	IPI00298547	PARK7	1	-1.18	0.031	3.22	3.40E-05	6.92	19490	6.33	20063	160	78	Acts as positive regulator of androgen receptor- dependent transcription.	Nuclear and cytoplasmic
1422	DNAJ HOMOLOG SUBFAMILY B MEMBER 11 PRECURSOR	IPI00008454	DNAJB11	3	-1.46	*0.12*	2.59	0.0012	6.87	45033	5.81	40774	79	41	Protein folding - endoplasmic reticulum - chaperone activity	Endoplasmic reticulum lumen
1937	ENDOPLASMIC RETICULUM PROTEIN ERP29 PRECURSOR	IPI00024911	ERP29	12	-1.46	0.00074	3.42	0.00024	6.87	30027	6.77	29032	57	52	Plays an important role in the processing of secretory proteins within the endoplasmic reticulum (ER), possibly by participating to the folding of proteins in the ER. Does not seem to be a disulfide isomerase.	Endoplasmic reticulum lumen
1258	ENOLASE ALPHA	IPI00465248	ENO1	1	1.04	*0.75*	2.12	9.80E-05	7.18	50784	6.99	47350	82	49	Multifunctional enzyme that, as well as its role in glycolysis, plays a part in various processes such as growth control, hypoxia tolerance and allergic resonses. May also function in the intravascular and pericellular fibrinolytic system due to its ability to serve as a receptor and activator of plasminogen on the cell surface of several cell-types such as leukocytes and neurones.	Cytoplasmic
1250	ENOLASE ALPHA	IPI00465248	ENO1	1	1.78	0.00017	1.25	*0.11*	7.77	50914	7.57	47405	184	64	Multifunctional enzyme that, as well as its role in glycolysis, plays a part in various processes such as growth control, hypoxia tolerance and allergic resonses. May also function in the intravascular and pericellular fibrinolytic system due to its ability to serve as a receptor and activator of plasminogen on the cell surface of several cell-types such as leukocytes and neurones.	Cytoplasmic
1254	ENOLASE ALPHA	IPI00465248	ENO1	1	2.21	0.0012	1.15	*0.34*	7.11	50784	7.57	47405	90	45	Multifunctional enzyme that, as well as its role in glycolysis, plays a part in various processes such as growth control, hypoxia tolerance and allergic resonses. May also function in the intravascular and pericellular fibrinolytic system due to its ability to serve as a receptor and activator of plasminogen on the cell surface of several cell-types such as leukocytes and neurones.	Cytoplasmic
1187	EUKARYOTIC TRANSLATION ELONGATION FACTOR 1 GAMMA	IPI00000875	EEF1G	11	-1.61	0.029	3.98	8.90E-05	7.28	52501	6.25	50429	210	61	Probably plays a role in anchoring the complex to other cellular components.	Cytoplasm
1873	EXOSOME COMPLEX EXONUCLEASE RRP41	IPI00218310	EXOSC4	8	-19.71	3.80E-05	-10.13	0.00078	7.07	32009	6.14	27905	56	43	Component of the exosome 3'->5' exoribonuclease complex. Required for the 3'processing of the 7S pre-RNA to the mature 5.8S rRNA. Has a 3'-5' exonuclease activity.	Cytoplasm. Nucleus; nucleolus
559	EZRIN	IPI00479359	VIL2	6	2.17	0.0022	-1.31	*0.13*	6.85	69378	5.94	69313	122	48	Probably involved in connections of major cytoskeletal structures to the plasma membrane.	Microvillar peripheral membrane protein (cytoplasmic side)
1980	F-ACTIN CAPPING PROTEIN BETA SUBUNIT	IPI00218782	CAPZB	1	1.05	*0.18*	3.22	0.0014	4.84	27176	5.69	30952	129	61	F-actin capping proteins bind in a Ca(2+)-independent manner to the fast growing ends of actin filaments (barbed end) thereby blocking the exchange of subunits at these ends.	Cytoskeleton
1055	FASCIN 1	IPI00163187	FSCN1	7	1.88	8.00E-05	-2.67	0.00013	8	56182	6.83	55729	120	54	Organizes filamentous actin into bundles with a minimum of 4.1:1 actin/fascin ratio. Probably involved in the assembly of actin filament bundles present in microspikes, membrane ruffles, and stress fibers.	Cytoskeleton
1972	FIZZY-RELATED PROTEIN HOMOLOG, SPLICE ISOFORM 1	IPI00383919	FZR1	19	2.51	0.0004	2.91	2.60E-05	5.11	27952	9.4	55544	54	27	Regulates ubiquitin ligase activity of the anaphase promoting complex/cyclosome (APC/C) and may confer substrate specifity upon the complex. The APC/C-Cdh1 dimeric complex is activated during anaphase and telophase and remains active in degrading substrates until onset of the next S phase.	Nuclear (isoform 2) and cytoplasmic (isoform 3)
1348	FUMARYLACETOACETASE	IPI00031708	FAH	15	1.3	0.0034	-3.83	2.40E-06	7.72	47275	6.46	46743	82	51	Hydrolase activity 4-fumarylacetoacetate + H(2)O = acetoacetate + fumarate.	Cytoplasm
2230	GALECTIN-1	IPI00219219	LGALS1	22	4.93	3.20E-05	-4.32	0.0016	4.67	12190	5.34	15048	96	95	May regulate cell apoptosis and cell differentiation. Binds beta-galactoside. Binds CD45, CD3 and CD4. Inhibits CD45 protein phosphatase activity and therefore the dephosphorylation of Lyn kinase.	Extracellular+nucleus+cytoplasm+plasma membrane
1141	GLUTAMATE DEHYDROGENASE 1, MITOCHONDRIAL PRECURSOR	IPI00016801	GLUD1	10	1.88	0.0012	-2.46	0.0024	8.13	54068	7.66	61701	133	48	May be involved in learning and memory reactions by increasing the turnover of the excitatory neurotransmitter glutamate (By similarity).	Mitochondrial matrix

726	GLYCEROL-3-PHOSPHATE DEHYDROGENASE, MITOCHONDRIAL PRECURSOR	IPI00017895	GPD2	2	2.17	0.00075	-1.51	0.00016	7.71	65331	6.98	81277	84	31	Oxidoreductase activity, Sn-glycerol 3-phosphate + acceptor = glycerone phosphate + reduced acceptor.	Mitochondrial
2064	GROWTH FACTOR RECEPTOR-BOUND PROTEIN 2; GRB2	IPI00021327	GRB2	17	-1.02	*0.83*	3.21	3.20E-05	6.38	21867	5.89	25304	93	64	Associates with activated EGF and PDGF receptors via SH2 domain. GRB2 also associates to other cellular Tyr-phosphorylated proteins such as IRS1, SHC and LNK; Binds to and translocates the guanine nucleotide exchange factors SOS (By similarity).	Cytoplasmic
852	HEAT SHOCK COGNATE 71 KDA PROTEIN, SPLICE ISOFORM 1	IPI00003865	HSPA8	11	-1.12	*0.055*	3.44	5.60E-05	5.16	61995	5.37	71082	[1339]	[49]	Chaperone. Isoform 2 may function as an endogenous inhibitory regulator of HSC70 by competing the cochaperones.	Translocates to nuclei, upon heat shock
865	HEAT SHOCK COGNATE 71 KDA PROTEIN, SPLICE ISOFORM 1	IPI00003865/IPI00037070	HSPA8	11	-1.05	*0.5*	2.31	5.80E-05	5.05	61836	5.37	71082	189	57	Chaperone. Isoform 2 may function as an endogenous inhibitory regulator of HSC70 by competing the cochaperones.	Translocates to nuclei, upon heat shock
937	HEAT SHOCK COGNATE 71 KDA PROTEIN, SPLICE ISOFORM 1	IPI00003865/IPI00037070	HSPA8	11	-1.02	*0.98*	2.42	0.0024	5.22	59206	5.37	71082	89	43	Chaperone. Isoform 2 may function as an endogenous inhibitory regulator of HSC70 by competing the cochaperones.	Translocates to nuclei, upon heat shock
997	HEAT SHOCK PROTEIN 60, MITOCHONDRIAL PRECURSOR	IPI00472102	HSPD1	2	-1.02	*0.69*	4.15	1.20E-05	5	57343	5.7	61346	210	67	Mitochondrial protein import and macromolecular assembly. May also prevent misfolding and promote the refolding and proper assembly of unfolded polypeptides generated under stress conditions in the mitochondrial matrix.	Mitochondrial matrix
1006	HEAT SHOCK PROTEIN 60, MITOCHONDRIAL PRECURSOR	IPI00472102	HSPD1	2	1.01	*0.99*	3.06	0.0014	4.88	57490	5.7	61346	186	65	Implicated in mitochondrial protein import and macromolecular assembly. May also prevent misfolding and promote the refolding and proper assembly of unfolded polypeptides generated under stress conditions in the mitochondrial matrix.	Mitochondrial matrix
882	HEAT SHOCK PROTEIN 70KDA 1	IPI00304925	HSPA1A	6	-1.71	0.022	6.3	0.00085	5.39	61207	5.48	70280	161	49	In cooperation with other chaperones, Hsp70s stabilize preexistent proteins against aggregation and mediate folding of newly translated polypeptides in the cytosol as well as within organelles.	Cytoplasmic
2026	HEAT-SHOCK PROTEIN BETA-1; HSP27	IPI00025512	HSPB1	7	-1.69	0.0036	5.33	0.0009	6.62	24099	5.98	22826	62	50	Involved in stress resistance and actin organization.	Cytoplasmic in interphase cells. Colocalizes with mitotic spindles. Translocates to nucleus during heat shock
2118	HEME BINDING PROTEIN 1	IPI00148063	HEBP1	12	-1.43	0.0048	3.28	2.10E-05	5.36	18661	5.71	21198	80	82	Heme binding	Secreted
1166	HETEROGENEOUS NUCLEAR RIBONUCLEOPROTEIN H	IPI00026230	HNRPH2	X	-1.61	4.90E-05	2.52	0.0068	6.54	52973	5.89	49517	99	52	This protein is a component of the heterogenous nuclear ribonucleoprotein (hnRNP) complexes which provide the substrate for the processing events that pre-mRNAs undergo before becoming functional, translatable mRNAs in the cytoplasm. Binds poly(RG).	Nuclear; nucleoplasm
917	HETEROGENEOUS NUCLEAR RIBONUCLEOPROTEIN K, SPLICE ISOFORM 2	IPI00216746	HNRPK	9	-1.26	*0.14*	2.65	8.40E-05	4.91	60121	5.19	51281	182	64	One of the major pre-mRNA-binding proteins. Binds tenaciously to poly(C) sequences. Likely to play a role in the nuclear metabolism of hnRNAs.	Cytoplasmic and nuclear; nucleoplasm.
1301	ISOCITRATE DEHYDROGENASE [NADP] CYTOPLASMIC	IPI00027223	IDH1	2	-1.31	0.011	2.27	0.0011	7.86	49187	6.53	46915	139	64	Isocitrate + NADP(+) = 2-oxoglutarate + CO(2) + NADPH.	Cytoplasmic and peroxisomal
2089	LACTOYLGLUTATHIONE LYASE.	IPI00220766	GLO1	6	-1.81	2.00E-05	2.81	4.60E-05	4.54	20487	5.24	20934	98	72	Catalyzes the conversion of hemimercaptal, formed from methylglyoxal and glutathione, to S-lactoylglutathione.	Cytoplasmic
822	LAMIN A/C, SPLICE ISOFORM 2	IPI00216952	LMNA	1	2.48	7.70E-05	-1.31	*0.059*	7.89	62712	6.4	65153	[225]	[22]	Structural component of nuclear envelope and may also interact with chromatin	Nuclear
1273	LUPUS LA PROTEIN	IPI00009032	SSB	2	-1.53	0.038	2.37	0.006	7.51	50203	6.68	46979	102	50	Plays a role in the transcription of RNA polymerase III most probably as a transcription termination factor.	Nuclear (Probable)
1258	LUPUS LA PROTEIN	IPI00009032	SSB	2	1.04	*0.75*	2.12	9.80E-05	7.18	50784	6.68	46979	155	61	Plays a role in the transcription of RNA polymerase III most probably as a transcription termination factor.	Nuclear (Probable)
940	MYO-INOSITOL 1-PHOSPHATE SYNTHASE A1.	IPI00301189		19	5.91	0.00045	-2.37	0.01	5.41	59206	5.44	61528	98	46	Inositol-3-phosphate synthase activity	Cytoplasmic
1376	ORNITHINE AMINOTRANSFERASE, MITOCHONDRIAL PRECURSOR	IPI00022334	OAT	10	-1.43	0.047	-2.07	0.002	6.98	46318	6.57	48846	101	48	Transferase activity. L-ornithine + a 2-oxo acid = L-glutamate 5- semialdehyde + an L-amino acid.	Mitochondrial matrix
1688	PDZ AND LIM DOMAIN PROTEIN 1; ELFIN	IPI00010414	PDLIM1	10	2.36	0.00056	-2.27	0.0032	7.81	37317	6.56	36505	124	63	Protein binding - response to oxidative stress	Cytoplasmic
2141	PEROXIREDOXIN 2	IPI00027350	PRDX2	19	5.71	0.00014	-4.25	0.00012	5.49	17394	5.66	22049	109	63	Electron transporter activity-antioxidant activity-oxidoreductase activity	Cytoplasmic
726	PHENYLALANYL-TRNA SYNTHETASE BETA CHAIN	IPI00300074	FARSLB	2	2.17	0.00075	-1.51	0.00016	7.71	65331	6.4	66715	58	26	Ligase activity, ATP + L-phenylalanine + tRNA(Phe) = AMP + diphosphate + L-phenylalanyl-tRNA(Phe).	Cytoplasmic (By similarity)
1134	PRE-B CELL ENHANCING FACTOR PRECURSOR	IPI00018873	PBEF1	7	2.02	0.0042	-2.21	0.0012	8.07	54694	6.69	55772	79	37	It is the rate limiting component in the mammalian NAD biosynthesis pathway (By similarity). Nicotinamide D-ribonucleotide + diphosphate = nicotinamide + 5-phospho-alpha-D-ribose 1-diphosphate.	Secreted
1359	PROLIFERATION-ASSOCIATED PROTEIN 2G4	IPI00299000	PA2G4	12	-1.1	*0.39*	2.48	0.0012	7.2	46914	6.13	44101	167	73	Hydrolase activity	Cytoplasm. Nucleus; nucleolus.
1846	PROTEASOME ACTIVATOR COMPLEX SUBUNIT 1	IPI00030154	PSME1	14	2.03	5.90E-05	-1.81	0.00077	5.94	32462	5.78	28876	92	61	Proteasome activator complex subunit 1 (Proteasome activator 28-alpha subunit) (PA28alpha) (PA28a) (Activator of multicatalytic protease subunit 1) (11S regulator complex alpha subunit) (REG-alpha) (Interferon gamma up-regulated I-5111 protein) (IGUP I-5111).	Cytoplasmic
1100	PROTEIN DISULFIDE-ISOMERASE A3 PRECURSOR	IPI00025252	PDIA3	15	-1.12	0.0035	2.71	4.30E-05	5.97	55610	5.98	57146	241	58	Electron transporter activity/isomerase activity/hydrolase activity. Catalyzes the rearrangement of -S-S- bonds in proteins.	Endoplasmic reticulum lumen (By similarity)
1068	PROTEIN DISULFIDE-ISOMERASE A3 PRECURSOR	IPI00025252	PDIA3	15	1.09	*0.2*	2.01	0.0033	5.75	55753	5.98	57146	[58]	[8]	Electron transporter activity/isomerase activity/hydrolase activity. Catalyzes the rearrangement of -S-S- bonds in proteins.	Endoplasmic reticulum lumen (By similarity)
1147	PRP19/PSO4 HOMOLOG.	IPI00004968	PRPF19	11	-2.08	0.00068	1.57	*0.057*	7.28	53930	6.14	55603	62	34	Plays a role in DNA double-strand break (DSB) repair. Acts as a structural component of the nuclear framework. May also serve as a support for spliceosome binding and activity.	Nucleoplasmic in interphase cells
1802	PURINE NUCLEOSIDE PHOSPHORYLASE	IPI00017672	NP	14	-2.79	7.00E-05	-1.03	*0.76*	7.49	34035	6.71	32758	57	52	Transferase activity	Cytoplasmic
2103	RAS-RELATED PROTEIN RAB-2A	IPI00031169	RAB2	8	-1.18	0.031	3.22	3.40E-05	6.92	19490	6.08	23702	71	64	Required for protein transport from the endoplasmic reticulum to the Golgi complex.	Intermediate compartment between ER and Golgi apparatus
1104	RUVB-LIKE 1	IPI00021187	RUVBL1	3	-1.29	0.038	2.59	4.80E-06	7.38	55327	6.02	50538	100	59	Single-stranded DNA-stimulated ATPase and ATP- dependent DNA helicase (3' to 5'). Component of NuA4 histone acetyltransferase complex involved in transcriptional activation associated with oncogene mediated growth induction, tumor suppressor mediated growth arrest and replicative senescence, apoptosis, and DNA repair.	Nuclear

801	SERUM ALBUMIN PRECURSOR	IPI00022434	ALB	4	2.15	5.60E-05	-1.89	1.50E-05	6	68000	5.92	71317	[108]	[7]	Regulation of the colloidal osmotic pressure of blood.good binding capacity for water, Ca(2+), Na(+), K(+), fatty acids, hormones, bilirubin and drugs.	Secreted
803	SERUM ALBUMIN PRECURSOR	IPI00022434	ALB	4	3.16	0.00021	-1.94	1.40E-05	6.22	63682	5.92	71317	[63]	[7]	regulation of the colloidal osmotic pressure of blood.good binding capacity for water, Ca(2+), Na(+), K(+), fatty acids, hormones, bilirubin and drugs.	Secreted
779	SIMILAR TO ATP-DEPENDENT DNA HELICASE II, 70 KDA SUBUNIT; KU70	IPI00412259	XRCC6	X	-7.93	0.016	-5.05	0.016	7.3	64008	7.31	65656	52	34	Has a role in chromosome translocation. Involved in DNA nonhomologous end joining (NHEJ) required for double-strand break repair and V(D)J recombination.	Nuclear
1134	SIMILAR TO PRE-B CELL ENHANCING FACTOR	IPI00472879	PEBF	10	2.02	0.0042	-2.21	0.0012	8.07	54694	7.72	53773	64	31	It is the rate limiting component in the mammalian NAD biosynthesis pathway (By similarity). Nicotinamide D-ribonucleotide + diphosphate = nicotinamide + 5-phospho-alpha-D-ribose 1-diphosphate.	Secreted
2159	STATHMIN	IPI00479997	STMN1	1	-2.05	0.00028	3.03	0.00028	5.31	16527	5.76	17326	51	48	Involved in the regulation of the microtubule (MT) filament system by destabilizing microtubules. It prevents assembly and promotes disassembly of microtubules.	Cytoplasmic
814	STRESS-70 PROTEIN, MITOCHONDRIAL PRECURSOR; GRP75	IPI00007765	HSPA9B	5	-1.63	7.40E-05	3.45	4.60E-05	5.41	62873	6.04	74093	142	53	Implicated in the control of cell proliferation and cellular aging. May also act as a chaperone.	Mitochondrial
1037	STRESS-INDUCED-PHOSPHOPROTEIN 1	IPI00013894	STIP1	11	1.17	0.024	2.45	3.70E-06	7.42	56978	6.4	63227	125	50	Mediates the association of the molecular chaperones HSC70 and HSP90 (HSPCA and HSPCB).	Nuclear and cytoplasmic (By similarity)
1061	T-COMPLEX PROTEIN 1, BETA SUBUNIT	IPI00297779	CCT2	12	-1.08	*0.18*	2.43	0.0015	7.07	56182	5.91	59929	265	70	Molecular chaperone; assist the folding of proteins upon ATP hydrolysis. Known to play a role, in vitro, in the folding of actin and tubulin.	Cytoplasmic
949	T-COMPLEX PROTEIN 1, EPSILON SUBUNIT	IPI00010720	CCT5	5	-5.19	0.00012	6.85	3.30E-06	5.57	59130	5.45	60089	182	61	Molecular chaperone; assist the folding of proteins upon ATP hydrolysis. Known to play a role, in vitro, in the folding of actin and tubulin.	Cytoplasmic
940	T-COMPLEX PROTEIN 1, EPSILON SUBUNIT	IPI00010720	CCT5	5	5.91	0.00045	-2.37	0.01	5.41	59206	5.45	60089	85	47	Molecular chaperone; assist the folding of proteins upon ATP hydrolysis. Known to play a role, in vitro, in the folding of actin and tubulin.	Cytoplasmic
2226	THIOREDOXIN	IPI00216298	TXN	9	1.24	*0.12*	3.27	0.00011	4.4	15000	4.82	12015	49	78	Participates in various redox reactions through the reversible oxidation of its active center dithiol to a disulfide and catalyzes dithiol-disulfide exchange reactions.	Cytoplasmic
471	TRANSITIONAL ENDOPLASMIC RETICULUM ATPASE; VALOSIN-CONTAINING PROTEIN	IPI00022774	VCP	9	-1.69	8.60E-05	4.62	7.50E-05	4.91	71540	5.14	89950	331	74	Necessary for the fragmentation of Golgi stacks during mitosis and for their reassembly after mitosis. Involved in the formation of the transitional endoplasmic reticulum (tER).	Nuclear and cytoplasmic
1285	TRANSLATION ELONGATION FACTOR TU, MITOCHONDRIAL	IPI00027107	TUFM	16	-1.13	0.04	2.52	1.50E-05	7.78	49692	7.26	50185	168	54	This protein promotes the GTP-dependent binding of aminoacyl-tRNA to the A-site of ribosomes during protein biosynthesis.	Mitochondrial
1932	TRIOSEPHOSPHATE ISOMERASE 1	IPI00465028	TPI1	12	1.92	0.00017	1.38	0.0049	8	28000	6.45	26910	142	76	Plays an important role in several metabolic pathways.D-glyceraldehyde 3-phosphate = glycerone phosphate.	Cytoplasmic
1935	TRIOSEPHOSPHATE ISOMERASE 1	IPI00465028	TPI1	12	2.66	0.0013	1.24	*0.13*	7.05	30027	6.45	26910	121	80	Plays an important role in several metabolic pathways.D-glyceraldehyde 3-phosphate = glycerone phosphate.	Cytoplasmic
1780	TROPOMYOSIN 4 .	IPI00010779	TPM4	19	1.23	*0.36*	2.46	0.0078	4.21	34694	4.67	28619	94	52	Binds to actin filaments in muscle and nonmuscle cells. Plays a central role, in association with the troponin complex, in the calcium dependent regulation of vertebrate striated muscle contraction.	Cytoplasmic
1807	TROPOMYOSIN ALPHA 3 CHAIN, SPLICE ISOFORM 2	IPI00218319	TPM3	1	1.45	0.0014	2.3	0.0014	4.3	30000	4.75	29243	157	72	Binds to actin filaments in muscle and nonmuscle cells	Cytoplasmic
1988	UBIQUITIN CARBOXYL-TERMINAL HYDROLASE ISOZYME L1	IPI00018352	UCHL1	4	-7.76	1.80E-07	8.37	0.0011	5.29	26456	5.33	25151	54	53	Ubiquitin-protein hydrolase involved both in the processing of ubiquitin precursors and of ubiquinated proteins. This enzyme is a thiol protease that recognizes and hydrolyzes a peptide bond at the C-terminal glycine of ubiquitin. Also binds to free monoubiquitin and may prevent its degradation in lysosomes. The homodimer may have ATP-independent ubiquitin ligase activity.	Cytoplasmic
1300	VIMENTIN	IPI00418471	VIM	10	-3.93	0.0011	1.73	0.00091	4.42	49313	5.09	53604	237	72	Class-III intermediate filaments found in various non-epithelial cells, especially mesenchymal cells.	Cytoplasm
1333	VIMENTIN	IPI00418471	VIM	10	-5.45	0.00021	1.58	0.013	4.27	48191	5.09	53604	172	61	Class-III intermediate filaments found in various non-epithelial cells, especially mesenchymal cells.	Cytoplasm
821	WD-REPEAT PROTEIN 1, SPLICE ISOFORM 2	IPI00216256	WDR1	4	3.83	9.80E-05	-3.94	0.0007	7.52	62632	6.41	58593	225	68	Induces disassembly of actin filaments in conjunction with ADF/cofilin family proteins (By similarity).	Cytoplasmic

Table 3.2 Differentially expressed proteins identified from a comparison between the two MMCT hybrid cell line pools and their respective parental cell lines. Protein features that were matched across all gels with a fold change ≥ 2 fold where $p \leq 0.05$ were identified. Ratios are shown with T-test P values for the TOV-112D hybrid pool/TOV-112D parental and the TOV-21G hybrid pool/TOV-21G parental. Orange shading indicates a ≥2-fold increase in expression and green indicates a ≥ 2-fold decrease in expression. Yellow shading indicates multiple identifications from a single gel spot. Protein identification by LC-MS/MS is indicated in the 'Score' column by square brackets, all other identifications were performed by MALDI-TOF MS peptide mass finger printing. The identifications were scored according to algorithms that take into account mass accuracy and peptide coverage. The search criteria used allowed +/- 50 ppm mass error and up to 2 missed cleavages. The identified proteins were also verified by comparison of their theoretical molecular weights and pIs with gel position on the master gel.

In summary there were a few proteins that displayed concordant changes in expression in both cell models. Notable among these was cofilin, a protein responsible for rapid recycling of the actin cytoskeleton associated with membrane ruffling, motility and cytokinesis. It is also required for controlled changes in cell shape, organelle and ion transport and receptor-mediated responses to external stimuli (Bailly and Jones 2003). Cofilin has been reported as a potential marker of ovarian cancer associated with proliferation and differentiation (Martoglio, Tom et al. 2000).

Despite the obvious heterogeneity between the cell models many of the proteins identified have been implicated in human cancers. Annexin A1 and A3 belong to the annexin family of calcium-dependent phospholipid binding proteins that are involved in a diverse range of cellular functions that include cell division, apoptosis, vesicle trafficking, calcium signalling and growth regulation. Differential expression of the annexins has been commonly found in a host of human cancers (Sinha, Hutter et al. 1998; Xia, Hu et al. 2002; Garcia Pedrero, Fernandez et al. 2004; Pedrero, Fernandez et al. 2005; Wang, Wu et al. 2006; Xue, Teng et al. 2007; Inokuchi, Lau et al. 2009). Aldehyde dehydrogenase 1A1 (ADH1A1) displayed the most extreme change in expression between the cell models. This protein belongs to the aldehyde dehydrogenase family of proteins which are involved in the conversion of aldehydes to their corresponding acids through $NAD(P)^+$-dependent reactions. Recently, ADH1A1 was reported to strongly promote cell invasion in pancreatic cancer cell lines (Walsh, Dowling et al. 2008). Adenosylhomocysteinase is an important regulator of methylation and it is known that expression of some tumour suppressor genes can be blocked by methylation of their

promoter regions (Garinis, Patrinos et al. 2002; Kloor and Osswald 2004; Esteller 2005; Christoph, Kempkensteffen et al. 2006; Ha and Califano 2006; Soufir, Queille et al. 2007). GRB2 overexpression has been reported in human breast, bladder and prostate cancer (Daly, Binder et al. 1994; Watanabe, Shinohara et al. 2000; Dankort, Maslikowski et al. 2001; Gril, Vidal et al. 2007). Galectin-1 may regulate apoptosis, cell proliferation and cell differentiation and has been identified as a counter receptor for the ovarian cancer antigen, CA125 (Seelenmeyer, Wegehingel et al. 2003). T-complex protein 1 epsilon subunit is a cytosolic chaperonin and its over-expression has been observed in colon cancer cells (Coghlin, Carpenter et al. 2006). This protein was identified from two protein spots, each displaying contrasting expression between the two cell models. This may be attributed to a post-translational modification on one of the isoforms. However, one spot contains another protein, myo-inostitol 1-phosphatase synthase A1, which may reflect the change in expression. Gel features containing multiple protein identifications are a drawback of 2D-DIGE since it is difficult to know which protein is responsible for the change in signal. Few chromosome 18 gene products were also found. This is likely to reflect the complexity of the proteome versus the genome and the measurement of secondary effects of tumour suppression effected through chromosome 18 gene expression, the products of which were not detected or identified due to their low abundance or poor resolution on 2D gels.

3.2 2D-DIGE analysis of Parent:Single Hybrid clones

The lack of common trends between the two cell line systems and large changes in abundance recorded in the previous experiment raised concerns that variation between individual clones within each pool had biased the results. To further examine this, a direct comparison by 2D-DIGE was applied to each parental cell line and two hybrids from each pool. The hybrid cell lines were chosen based on their potent tumour suppression in nude mice. Hybrid cell lines 18-D-22, 18-D-23 and 18-G-5, 18-G-1.26 were selected from hybrid pool 'A' and 'B' respectively. The samples were labelled and run in the same manner as before in two experiments. 2D gel images were curated, matched and statistical analysis carried out and protein features displaying reproducible changes were selected. This time, protein features displaying a change in average abundance ≥ 1.5 fold (n=3, p value <0.05) were selected for identification as fewer changes overall were observed.

3.2.1 Identification of differentially expressed proteins in single clone comparisons

In the first experiment, the parental cell lines were compared to the hybrid clones 18-D-22 and 18-G-5. A total of 2088 protein spots were detected and matched. Direct comparison of the TOV-112D and 18-D-22 cell lysates resulted in a total of 28 differentially expressed protein spots with 19 up-regulated and 9 down-regulated. Direct comparison between the TOV-21G and 18-G-5 cell lysates resulted in a total of 8 spots

changing, of which 5 were up-regulated and 3 down-regulated. In the second experiment the parental cell lines were compared to the hybrid clones 18-D-23 and 18-G-1.26. A total of 2089 protein features were detected. The direct comparison of the TOV-112D and 18-D-23 cell lysates resulted in a total of 28 differentially expressed protein spots with 11 up-regulated and 17 down-regulated. Direct comparison between the TOV-21G and 18-G-1.26 cell lysates resulted in a total of 214 protein spots changing with 78 up-regulated and 136 down-regulated. Again, there was little overlap in differential expression between the two cell models with only 1 common feature displaying contrasting expression. The analysis of the two cell models were treated separately from this point on. The protein features displaying a change in abundance $\geq$ 1.5 fold (n=3, p value $\leq$ 0.05) were selected. The spots were matched to a CCB stained gel image and spots excised and digested with trypsin for identification by mass spectrometry. A total of 30 spots were picked in the first experiment. Of these, 28 were identified by LC-MS/MS with high confidence (Fig 3.2 and Table 3.3A). A total of 189 spots were picked in the second experiment and of these, 137 were identified by LC-MS/MS with a high degree of confidence (Fig 3.3 and Table 3.3B).

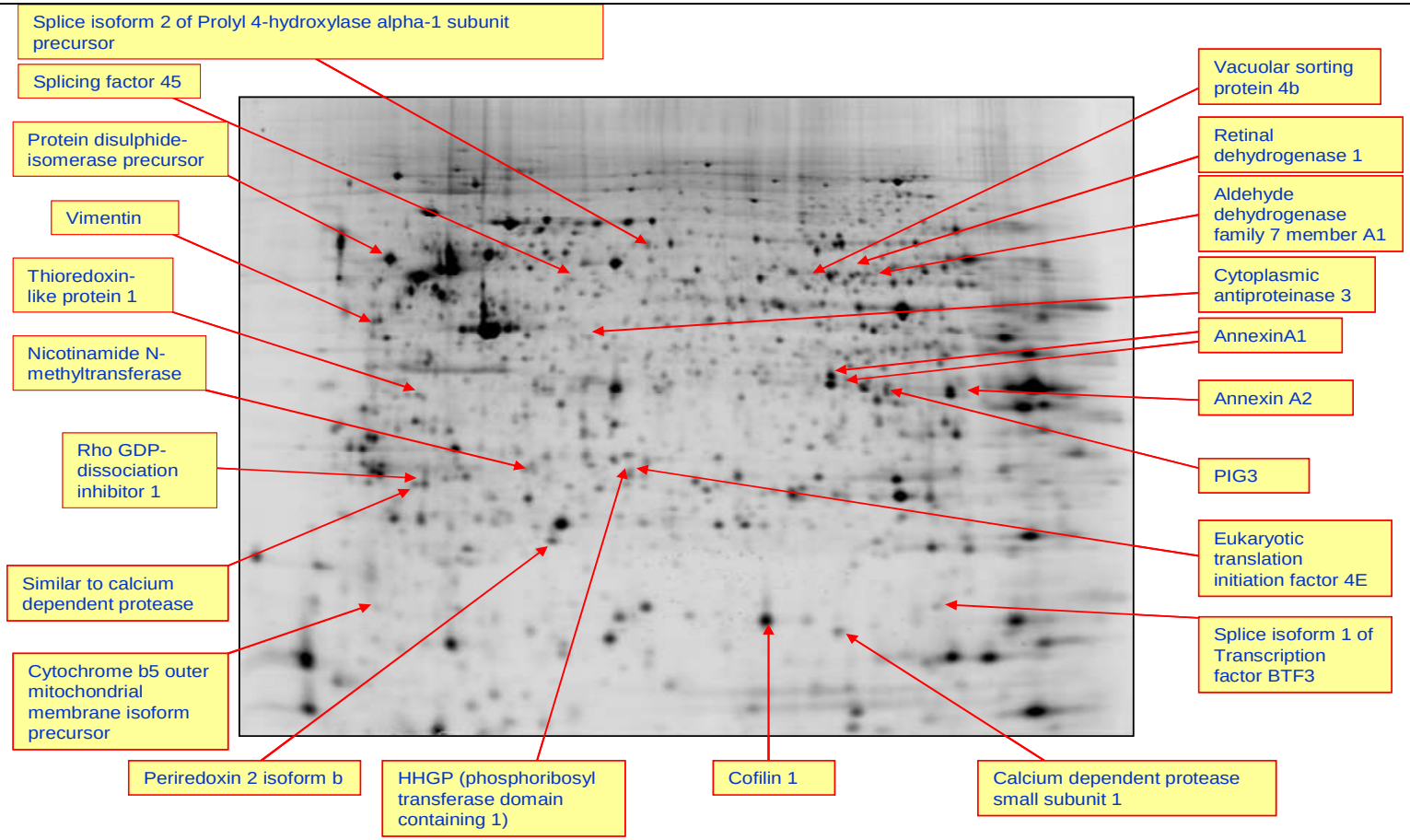

Figure 3.2 Annotated master gel image of identified proteins in the first single hybrid clone: parental comparison experiment. The gel pieces were digested with trypsin and MS/MS peak lists were compared against theoretically expected tryptic peptide fragment masses in the NCBI and IPI databases using the Mascot search engine including +2 and +3 peptide charge, and a mass tolerance of ±50ppm. The identifications were accepted when at least two peptide sequences matched an entry with MOWSE scores above the p=0.05 threshold value. The identified proteins were also verified by comparison of their theoretical molecular weights and pIs with gel position on the master gel.

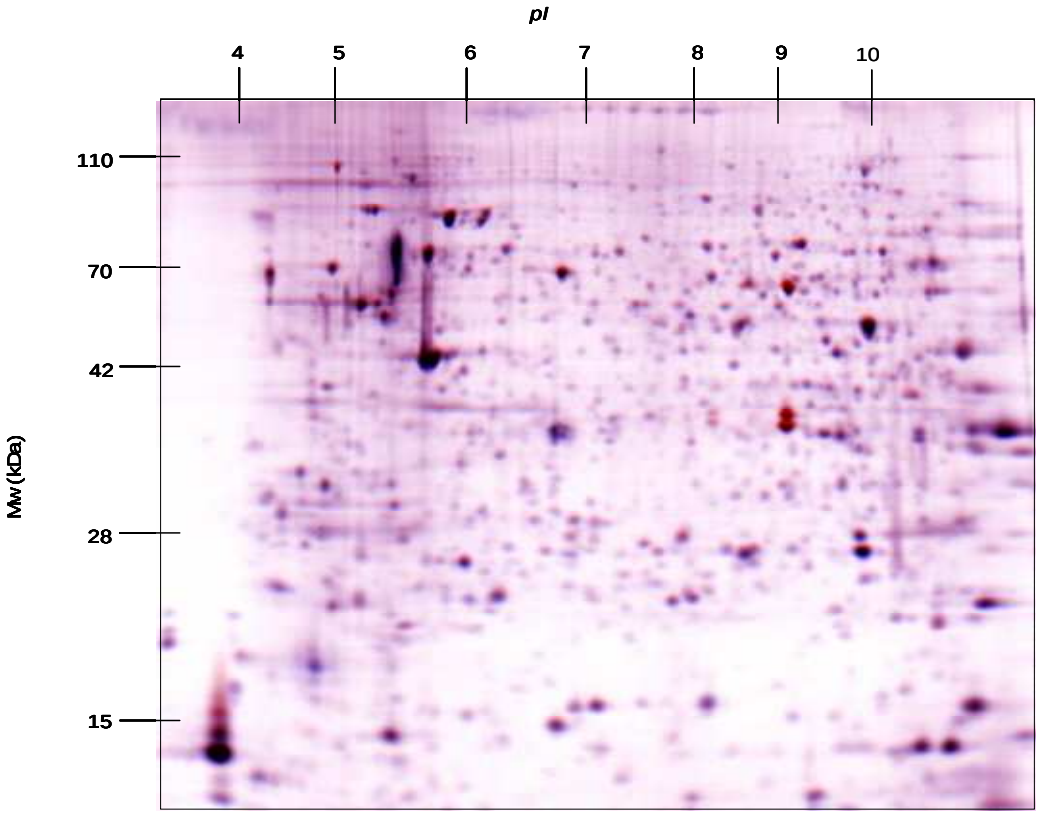

Figure 3.3 Representative 2D gel image of differential protein expression in TOV-112D cell line and its hybrid cell line 18-D-23. 150µg of total cell lysate from TOV-112D and 18-D-23 were labelled with Cy3 and Cy5 respectively, mixed and loaded with an equal amount of internal standard labelled with Cy2. This superimposed image was created in Adobe Photoshop and shows TOV-112D in red and 18-D-22 in blue

Master No.	Name	IPI No.	Gene Symbol	Chr.	18-D-22 clone/112D parental Av. Ratio	18-D-22 clone/112D parental T-test	18-G-5 clone/21G parental Av. Ratio	18-G-5 clone/21G parental T-test	pI (gel)	Mw (gel)	pI (pred)	Mw (pred)	Score	% Cov	Peptides Matched	Function	Localisation
511	No ID				1.31	0.43	-2.17	0.021	5	95000							
653	No ID				-1.52	0.032	1.53	*0.064*	6.63	85427							
1029	No ID				1.51	0.00037	-1.11	*0.65*	6.43	61762							
1345	No ID				1.5	0.023	-1.39	0.021	4.46	44307							
1492	Unpickable				-2.67	0.032	1	*0.96*	6.25	38078							
1497	Unpickable				-1.53	0.0046	-1.11	*0.31*	6.39	37710							
1910	Unpickable				1.96	0.006	-1.03	*0.76*	4.35	18308							
1919	Unpickable				1.29	*0.28*	1.9	0.023	5.79	18026							
1959	Unpickable				1.61	*0.11*	1.8	0.018	4.34	15857							
1230	Adenosylhomocysteinase	IPI00012007	AHCY	20	1.52	0.017	1.19	0.024	6.07	50367	5.92	48124	779	40	21	Control of S-adenosyl-L-methionine-dependent methylation via regulation of adenosylhomocysteine concentrations	Cytoplasm
1042	Aldehyde dehydrogenase family 7 member A1	IPI00221234	ALDH7A1	5	1.74	0.037	1.05	*0.72*	6.77	61046	6.24	55714	659	34	19	Oxidoreductase activity. An aldehyde + NAD(+) + H(2)O = an acid + NADH.	Cytoplasm
1505	Annexin A1	IPI00218918	ANXA1	9	-2.83	0.0059	-1.02	*0.75*	6.56	37418	6.64	38787	1329	74	53	Inflammatory response, phospholipase A2 inhibitor activity, calcium-dependent phospholipid binding	Cytoplasm
1542	Annexin A1	IPI00218918	ANXA1	9	-3.05	0.0043	-1.15	*0.051*	6.8	40000	6.64	38787	1329	74	53	Inflammatory response, phospholipase A2 inhibitor activity, calcium-dependent phospholipid binding	Cytoplasm
1573	Annexin A1	IPI00218918	ANXA1	9	-1.06	*0.68*	1.59	0.0051	4.68	34353	6.64	38787	258	20	11	Inflammatory response, phospholipase A2 inhibitor activity, calcium-dependent phospholipid binding	Cytoplasm
1562	Annexin A2	IPI00455315	ANXA2	15	1.67	0.0026	1.09	*0.17*	7.11	35095	7.56	38677	1511	71	50	Cytoskeletal protein binding, calcium-dependent phospholipid binding, phospholipase inhibitor activity, skeletal development	Cytoplasm
1584	Annexin A2	IPI00455315	ANXA2	15	1.68	0.0022	1.06	*0.45*	7.11	33889	7.56	38677	1511	71	50	Cytoskeletal protein binding, calcium-dependent phospholipid binding, phospholipase inhibitor activity, skeletal development	Cytoplasm
1835	Annexin A2	IPI00455315	ANXA2	15	1.62	0.0099	1.29	*0.23*	4.64	21721	7.56	38677	871	59	22	Cytoskeletal protein binding, calcium-dependent phospholipid binding, phospholipase inhibitor activity, skeletal development	Cytoplasm
1003	Aspartyl-tRNA synthetase	IPI00216951	DARS	2	-1.54	0.0033	1.31	*0.052*	6.53	62973	6.11	57499	[124]	37	21	Belongs to the class-II aminoacyl-tRNA synthetase family.	Cytoplasm
1835	Calpain, small subunit 1	IPI00025084	CAPNS1	19	1.62	0.0099	1.29	*0.23*	4.64	21721	5.82	34050	545	45	19	Calcium-regulated thiol-protease. Proteolysis of substrates involved in cytoskeletal remodelling and signal transduction	Cytoplasm; PM on calcium binding
2036	Calpain, small subunit 1	IPI00025084	CAPNS1	19	1.78	0.043	1.01	*0.93*	6.57	9776	5.05	28453	[62]	57	12	Calcium-regulated thiol-protease. Proteolysis of substrates involved in cytoskeletal remodelling and signal transduction	Cytoplasm; PM on calcium binding
2026	Cofilin-1	IPI00012011	CFL1	11	1.87	0.018	-1.09	*0.56*	6	10000	8.26	18588	515	72	19	Actin binding protein. Controls reversible actin polymerization. Major component of intranuclear and cytoplasmic actin rods	Intranuclear and cytoplasmic
1990	Cytochrome b5 outer mitochondrial membrane isoform precursor	IPI00303954	CYB5B	16	2.53	0.026	1.31	*0.24*	4.45	14003	4.88	16798	217	62	7	Electron carrier for several membrane bound oxygenases	Mitochondrial outer membrane
1304	Cytoplasmic antiproteinase 3; SerpinB9	IPI00032139	SERPINB9	6	1.64	0.041	-1.36	0.014	5.43	47056	5.61	43004	459	28	12	Serine endopeptidase inhibitor activity. Tumour antigen	Cytoplasm
1844	Eukaryotic translation initiation factor 4E	IPI00027485	EIF4E	4	1.86	0.0058	1.41	*0.43*	5.66	21386	5.79	25310	251	30	6	RNA binding. Protein biosynthesis	Cytoplasm
1781	Nicotinamide N-methyltransferase	IPI00027681	NNMT	11	1.74	0.017	-1.12	*0.54*	5.14	23476	5.56	30011	345	31	10	Nicotinamide N-methyltransferase activity	Cytoplasm
1953	Peroxiredoxin 2, isoform b	IPI00027350	PRDX2	19	1.51	0.033	1	*0.97*	5.25	16199	6.13	16036	92	78	17	Protection from redox stress	Cytoplasm
1838	Phosphoribosyl transferase domain containing 1 (PRTFDC1), similar to hypoxanthine phosphoribosyl transferase	IPI00024644	PRTFDC1	10	1.51	0.022	1.02	*0.91*	5.59	21637	5.76	25828	257	37	9	Nucleoside metabolism. Phosphoribosyl transferase activity	Cytoplasm
800	Prolyl 4-hydroxylase alpha-1 subunit precursor, splice isoform 2	IPI00218682	P4HA1	10	1.11	*0.65*	-1.68	0.042	5.69	75295	5.7	61214	809	38	23	Catalyzes the posttranslational formation of 4-hydroxyproline in -Xaa-Pro-Gly- sequences in collagens and other proteins.	ER lumen
845	Protein disulfide-isomerase precursor	IPI00010796	P4HB	17	1.53	0.024	-1.29	*0.13*	4.52	70895	4.76	57480	1515	55	45	Catalyzes the rearrangement of -S-S- bonds in proteins.	ER lumen
959	Retinal dehydrogenase 1	IPI00218914	ALDH1A1	9	-1.34	0.026	1.55	0.024	6.5	64584	6.29	55323	212	12	6	Binds free retinal and retinol-binding protein-bound retinal. Can oxidize retinaldehyde to retinoic acid	Cytoplasm
985	Retinal dehydrogenase 1	IPI00218914	ALDH1A1	9	-2.63	0.0037	-1.2	*0.36*	6.57	63588	6.29	55323	771	54	25	Binds free retinal and retinol-binding protein-bound retinal. Can oxidize retinaldehyde to retinoic acid	Cytoplasm
1830	Rho GDP-dissociation inhibitor 1	IPI00003815	ARHGDIA	17	1.08	*0.29*	-1.52	0.00065	4.69	21805	5.02	23250	403	51	14	GTPase activator activity. RhoGDP-dissociation inhibitor activity. Rho protein signal transduction.	Cytoplasm

980	Splicing factor 45	IPI00176706	RBM17	10	-1.42	*0.38*	1.52	0.04	5.6	60000	5.76	45162	141	14	5	Involved in the regulation of alternative splicing and the utilization of cryptic splice sites.	Nuclear
1573	Thioredoxin-like protein 1	IPI00305692	TXNL1	18	-1.06	*0.68*	1.59	0.0051	4.68	34353	4.84	32499	329	44	11	Signal transduction, electron transporter activity, apoptosis, transport, thiol-disulfide exchange activity	Cytoplasm
2015	Transcription factor BTF3, isoform 1	IPI00221035	BTF3	5	-1.55	0.023	1.23	*0.33*	7.02	11092	9.41	22211	116	24	5	Transcription regulator activity	Nuclear
1577	Tumor protein p53 inducible protein 3 (PIG3)	IPI00472656	TP53I3	2	1.67	0.0097	1.21	*0.2*	6.85	34553	7.05	34601	569	45	14	Oxidoreductase activity. Gene contains a microsatellite polymorphism that may be associated with cancer susceptibility	Cytoplasmic
959	Vacuolar sorting protein 4b	IPI00182728	VPS4B	18	-1.34	0.026	1.55	0.024	6.5	64584	6.75	49443	625	45	20	Intracellular protein transport	Cytoplasmic and prevacuolar endosomes
1162	Vimentin	IPI00418471	VIM	10	3.5	0.021	-2	*0.21*	4.57	53597	5.06	53545	[65]	37	21	Class-III intermediate filament protein. Structural constituent of cytoskeleton found in non-epithelial cells	Cytoplasm
1248	Vimentin	IPI00418471	VIM	10	1.78	0.002	-1.2	0.016	4.6	50000	5.06	53545	892	46	25	Class-III intermediate filament protein. Structural constituent of cytoskeleton found in non-epithelial cells	Cytoplasm

Table 3.3A Proteins differentially expressed in the two epithelial ovarian cancer cell models identified by LC-MS/MS and MALDI-TOF MS PMF. Protein features that were matched across all gels with a fold change $\geq$ 1.5 fold where $p \leq 0.05$ are identified. Ratios are shown for 18-D-22 vs. TOV-112D parental and 18-G-5 clone vs. TOV-21G parental. Orange shading indicates an increase in expression and green indicates a decrease. Yellow shading indicates multiple identifications from a single gel spot. Protein identifications were made by database searching of peptide ion fragments from LC-MS/MS or by MALDI-TOF MS PMF, the latter indicated by [ ] in the 'Score' column. The identifications were scored according to algorithms that take into account mass accuracy and peptide coverage. The search criteria used allowed +/- 50 ppm mass error and up to 2 missed cleavages. The identified proteins were also partly verified by comparison of their theoretical molecular weights and pIs with gel position on the master gel.

Master No.	Protein Name	HGNC	IPI	Chr.	18D23/112D Av. Ratio	18D23/112D T-test	18G1.26/21G Av. Ratio	18G1.26/21G T-test	Gel Mwt	Gel pI	Pred Mwt	Pred pI	Score	%Cov	No. of Pep's	Function	Localisation
1731	14-3-3 protein zeta/delta	YWHAZ	IPI00021263	8	1.3	*0.13*	1.72	0.022	27190	4.52	27899	4.73	114	12	3	Adapter protein implicated in the regulation of a large spectrum of both general and specialized signaling pathway. Binds to a large number of partners, usually by recognition of a phosphoserine or phosphothreonine motif. Binding generally results in the modulation of the activity of the binding partner.	Cytoplasm. Melanosome
1163	26S protease regulatory subunit 6B, isoform 1	PSMC4	IPI00020042	19	1.02	*0.87*	-1.89	0.0019	58218	5.08	47451	5.09	[231]	54	26	The 26S protease is involved in the ATP-dependent degradation of ubiquitinated proteins. The regulatory (or ATPase) complex confers ATP dependency and substrate specificity to the 26S complex.	Cytoplasm. Nucleus
876	60 kDa heat shock protein, mitochondrial precursor	HSPD1	IPI00784154	2	1.06	*0.5*	-2.54	0.0025	72203	5.41	61187	5.7	1314	49	29	Implicated in mitochondrial protein import and macromolecular assembly. May facilitate the correct folding of imported proteins. May also prevent misfolding and promote the refolding and proper assembly of unfolded polypeptides generated under stress conditions in the mitochondrial matrix.	Mitochondrion; mitochondrial matrix
1496	60S acidic ribosomal protein P0	RPLP0	IPI00008530	12	1.4	*0.26*	2.14	0.0085	39335	6.45	34423	5.71	62	6	1	Ribosomal protein P0 is the functional equivalent of E.coli protein L10.	Cytoplasm
1289	Actin, aortic smooth muscle	ACTA2	IPI00008603	10	1.13	*0.14*	1.61	0.016	51207	6.14	42381	5.23	181	12	4	Actins are highly conserved proteins that are involved in various types of cell motility and are ubiquitously expressed in all eukaryotic cells.	Cytoplasm
1157	Actin, cytoplasmic 1	ACTB	IPI00021439	7	1.13	*0.48*	-1.71	0.022	58635	5.53	42052	5.29	203	10	4	Actins are highly conserved proteins that are involved in various types of cell motility and are ubiquitously expressed in all eukaryotic cells.	Cytoplasm
1270	Actin, cytoplasmic 1	ACTB	IPI00021439	7	1.07	*0.77*	1.97	0.0031	51500	5.82	42052	5.29	881	44	19	Actins are highly conserved proteins that are involved in various types of cell motility and are ubiquitously expressed in all eukaryotic cells.	Cytoplasm
1287	Actin, cytoplasmic 1	ACTB	IPI00021439	7	1.12	0.031	1.65	0.00066	51281	6.03	42052	5.29	565	32	11	Actins are highly conserved proteins that are involved in various types of cell motility and are ubiquitously expressed in all eukaryotic cells.	Cytoplasm
1296	Actin, cytoplasmic 1	ACTB	IPI00021439	7	-1.03	*0.83*	1.52	0.031	50555	5.11	42052	5.29	591	26	13	Actins are highly conserved proteins that are involved in various types of cell motility and are ubiquitously expressed in all eukaryotic cells.	Cytoplasm
1297	Actin, cytoplasmic 1	ACTB	IPI00021439	7	1	*0.97*	1.83	0.00062	50627	5.25	42052	5.29	539	23	12	Actins are highly conserved proteins that are involved in various types of cell motility and are ubiquitously expressed in all eukaryotic cells.	Cytoplasm
1308	Actin, cytoplasmic 1	ACTB	IPI00021439	7	1.05	*0.59*	1.73	0.042	49697	5.45	42052	5.29	861	36	22	Actins are highly conserved proteins that are involved in various types of cell motility and are ubiquitously expressed in all eukaryotic cells.	Cytoplasm
1894	Adenine phosphoribosyltransferase	APRT	IPI00218693	16	1.19	0.0014	-1.65	0.008	19983	5.13	19766	5.78	109	11	2	Catalyzes a salvage reaction resulting in the formation of AMP, that is energically less costly than de novo synthesis.	Cytoplasm
1309	Adenosine kinase, short isoform	ADK	IPI00234368	10	-1.11	0.04	1.71	0.0027	50053	8.12	39078	6.23	[91]	32	11	ATP dependent phosphorylation of adenosine and other related nucleoside analogs to monophosphate derivatives. Serves as a potential regulator of concentrations of extracellular adenosine and intracellular adenine nucleotides.	Cytoplasm
1489	AIP AH receptor-interacting protein	AIP	IPI00010460	11	-1.83	0.0012	-1.19	*0.25*	39504	7.84	38096	6.09	216	14	4	May play a positive role in AHR-mediated (aromatic hydrocarbon receptor) signaling, possibly by influencing its receptivity for ligand and/or its nuclear targeting.	Cytoplasm

861	Alpha-internexin	INA	IPI00001453	10	1.26	*0.61*	-2.33	0.0034	72616	5.61	55528	5.34	[96]	30	19	Class-IV neuronal intermediate filament able to self-assemble. Involved in the morphogenesis of neurons. May form an independent structural network without involvement of other neurofilaments or may cooperate with NF-L to form the filamentous backbone to which NF-M and NF-H attach to form the cross-bridges.	Cyto
1494	Annexin A1	ANXA1	IPI00218918	9	-2.37	0.00064	-1.07	*0.61*	39448	8.07	38918	6.57	764	45	12	Calcium/phospholipid-binding protein which promotes membrane fusion and is involved in exocytosis. This protein regulates phospholipase A2 activity. It seems to bind from two to four calcium ions with high affinity.	Cyto
1592	Annexin A3	ANXA3	IPI00024095	4	1.09	*0.63*	1.67	0.038	34796	6.12	36524	5.63	319	18	4	Inhibitor of phospholipase A2, also possesses anti-coagulant properties. Also cleaves the cyclic bond of inositol 1,2-cyclic phosphate to form inositol 1-phosphate.	Cyto
1599	Annexin A4 protein	ANXA4	IPI00555692	2	1.09	*0.13*	-2.38	0.0053	34109	6.32	33759	5.64	237	19	6	Calcium ion binding	Cyto
959	Calreticulin precursor	CALR	IPI00020599	19	-1.12	*0.096*	-1.65	0.0012	68201	4.22	48283	4.29	162	12	11	Molecular calcium binding chaperone promoting folding, oligomeric assembly and quality control in the ER via the calreticulin/calnexin cycle. This lectin interacts transiently with almost all of the monoglucosylated glycoproteins that are synthesized in the ER. Interacts with the DNA-binding domain of NR3C1 and mediates its nuclear export.	Endo endo lume Secr extra extra surfa
1006	Calreticulin precursor	CALR	IPI00020599	19	-1.14	0.028	-2.06	0.00036	66001	4.22	48283	4.29	687	23	15	Molecular calcium binding chaperone promoting folding, oligomeric assembly and quality control in the ER via the calreticulin/calnexin cycle. This lectin interacts transiently with almost all of the monoglucosylated glycoproteins that are synthesized in the ER. Interacts with the DNA-binding domain of NR3C1 and mediates its nuclear export.	Endo endo lume Secr extra extra surfa
1979	Cofilin-1	CFL1	IPI00012011	11	1.15	*0.4*	-2.35	0.02	15372	3.95	18719	8.22	299	37	6	Controls reversibly actin polymerization and depolymerization in a pH-sensitive manner. It has the ability to bind G- and F-actin in a 1:1 ratio of cofilin to actin. It is the major component of intranuclear and cytoplasmic actin rods.	Nucl
2000	Cofilin-1	CFL1	IPI00012011	11	1.39	0.00022	-1.63	8.30E-05	14499	7.52	18719	8.22	143	15	2	Controls reversibly actin polymerization and depolymerization in a pH-sensitive manner. It has the ability to bind G- and F-actin in a 1:1 ratio of cofilin to actin. It is the major component of intranuclear and cytoplasmic actin rods.	Nucl
1890	Cytidylate kinase	CMPK	IPI00219953	1	1.49	0.004	-1.74	0.0017	22000	6.2	26180	8.17	196	15	10	Catalyzes specific phosphoryl transfer from ATP to UMP and CMP.	Nucl Note
2002	Destrin	DSTN	IPI00473014	20	1.03	*0.42*	-3.4	1.20E-05	14335	6.52	18950	8.06	222	19	4	Actin-depolymerizing protein. Severs actin filaments (F- actin) and binds to actin monomers (G-actin). Acts in a pH- independent manner.	Cyto
2011	Destrin	DSTN	IPI00473014	20	1.66	0.0055	-1.02	*0.96*	13000	8	18950	8.06	78	44	12	Actin-depolymerizing protein. Severs actin filaments (F- actin) and binds to actin monomers (G-actin). Acts in a pH- independent manner.	Cyto
1599	DnaJ homolog subfamily C member 9	DNAJC9/MRPS16	IPI00154975	10	1.09	*0.13*	-2.38	0.0053	34109	6.32	30062	5.58	127	11	3	Chaperone activity.	Cyto

1128	Dynactin 2	DCTN2	IPI00220503	12	1.11	*0.32*	-1.62	0.024	59902	5.16	44906	5.06	138	4	3	Modulates cytoplasmic dynein binding to an organelle, and plays a role in prometaphase chromosome alignment and spindle organization during mitosis.	Cytoplasm. Membrane; peripheral membrane protein.
1702	Elongation factor 1-beta	EEF1B2	IPI00178440	2	1.08	*0.092*	-1.78	0.0015	28541	4.31	24788	4.5	94	18	9	EF-1-beta and EF-1-delta stimulate the exchange of GDP bound to EF-1-alpha to GTP.	Nucleus
1758	Endoplasmic reticulum protein ERp29 precursor	ERP29	IPI00024911	12	-1.31	9.70E-05	-1.67	1.20E-05	26313	7.32	29032	6.77	176	11	3	Does not seem to be a disulfide isomerase. Plays an important role in the processing of secretory proteins within the ER, possibly by participating in the folding of proteins in the ER.	Endoplasmic reticulum; endoplasmic reticulum lumen.
1759	Endoplasmic reticulum protein ERp29 precursor	ERP29	IPI00024911	12	-1.62	0.00025	-1.65	0.0016	26351	6.48	29032	6.77	126	14	3	Does not seem to be a disulfide isomerase. Plays an important role in the processing of secretory proteins within the ER, possibly by participating in the folding of proteins in the ER.	Endoplasmic reticulum; endoplasmic reticulum lumen.
1768	Enoyl-CoA hydratase, mitochondrial precursor	ECHS1	IPI00024993	10	1.06	0.0024	-1.55	0.00011	25793	7.04	31823	8.34	496	40	9	Straight-chain enoyl-CoA thioesters from C4 up to at least C16 are processed, although with decreasing catalytic rate.	Mitochondrion; mitochondrial matrix.
2017	Eukaryotic translation initiation factor 5A-1, isoform 2	EIF5A	IPI00376005	17	1.07	*0.11*	-5.4	2.60E-06	13368	6.38	20442	6.52	207	21	4	The precise role of eIF-5A in protein biosynthesis is not known but it functions by promoting the formation of the first peptide bond.	Nucleus
1635	F-actin capping protein subunit beta, , isoform 1	CAPZB	IPI00026185	1	1.09	*0.27*	1.54	0.0081	32172	6.14	31616	5.36	344	21	7	F-actin capping proteins bind in a Ca(2+)-independent manner to the fast growing ends of actin filaments (barbed end) thereby blocking the exchange of subunits at these ends. Unlike other capping proteins (such as gelsolin and severin), these proteins do not sever actin filaments.	Cytoplasm
1068	Fascin	FSCN1	IPI00163187	7	1.21	*0.12*	1.97	0.0016	63057	8.41	55123	6.84	176	6	4	Organizes filamentous actin into bundles with a minimum of 4.1:1 actin/fascin ratio. Probably involved in the assembly of actin filament bundles present in microspikes, membrane ruffles, and stress fibers.	Cytoplasm
1848	FLJ25678, highly similar to purine nucleoside P	NP	IPI00017672	14	1.2	*0.12*	-1.93	0.00063	22270	7.13	32758	6.71	146	13	3	Belongs to the PNP/MTAP phosphorylase family.	Cytoplasm
428	Full-length cDNA clone CS0CAP007YF18 of Thymus of Homo sapiens	HSP90AA1	IPI00796844	14	1.02	*0.91*	1.63	0.0019	95074	5.75	49669	5.33	[85]	28	15	Molecular chaperone. Has ATPase activity (By similarity).	Cytoplasm (By similarity).
1304	Fumarylacetoacetase	FAH	IPI00031708	15	1.11	*0.12*	1.75	0.0045	49910	8.34	46743	6.46	[64]	23	11	Amino-acid degradation; L-phenylalanine degradation; acetoacetate and fumarate from L-phenylalanine: step 6 [final step].	Cytoplasm
1067	Glutamate dehydrogenase 1	GLUD1	IPI00016801	10	1.23	0.011	1.57	0.00045	63418	8.79	61701	7.66	[98]	35	19	Belongs to the Glu/Leu/Phe/Val dehydrogenases family	Mitochondrion; mitochondrial matrix.
1090	Glutathione synthetase	GSS	IPI00010706	20	1.18	*0.068*	1.5	9.70E-05	62253	6.13	52523	5.67	[141]	34	22	Sulfur metabolism; glutathione biosynthesis; glutathione from L-cysteine and L-glutamate: step 2 [final step].	Cytoplasm
837	Heat shock protein 60 kDa , mitochondrial precursor	HSPD1	IPI00784154	2	1.11	*0.55*	-2.16	0.01	74080	5.42	61187	5.7	177	52	25	Implicated in mitochondrial protein import and macromolecular assembly. May facilitate the correct folding of imported proteins. May also prevent misfolding and promote the refolding and proper assembly of unfolded polypeptides generated under stress conditions in the mitochondrial matrix.	Mitochondrion; mitochondrial matrix.

839	Heat shock protein 60 kDa, mitochondrial precursor	HSPD1	IPI00784154	2	1.32	*0.45*	-1.8	0.0013	74292	5.29	61187	5.7	1403	42	23	Implicated in mitochondrial protein import and macromolecular assembly. May facilitate the correct folding of imported proteins. May also prevent misfolding and promote the refolding and proper assembly of unfolded polypeptides generated under stress conditions in the mitochondrial matrix.	Mitochondrion; mitochondrial matrix.
1772	Heat-shock protein beta-1	HSPB1	IPI00025512	7	1.72	0.00049	2.65	0.00014	25501	6.01	22826	5.98	324	30	6	Involved in stress resistance and actin organization.	Cytoplasm. Nucleus. Cytoplasmic in interphase cells. Colocalizes with mitotic spindles in mitotic cells. Translocates to the nucleus during heat shock.
1467	Hepatoma-derived growth factor	HDGF	IPI00020956	1	-1.02	*0.61*	-3.06	0.024	40705	4.56	26886	4.7	[76]	37	10	Heparin-binding protein, with mitogenic activity for fibroblasts.	Cytoplasm
1364	Heterogeneous nuclear ribonucleoprotein A/B, isoform 2	HNRPAB	IPI00334587	5	-1.04	*0.18*	-1.63	0.011	45688	8.17	36059	6.49	240	13	4	Binds single-stranded RNA. Has a high affinity for G- rich and U-rich regions of hnRNA. Also binds to APOB mRNA transcripts around the RNA editing site.	Nucleus
1346	Heterogeneous nuclear ribonucleoprotein D0, isoform 1	HNRPD	IPI00028888	4	-1	*0.96*	-1.77	0.0026	46942	8.91	38581	7.62	446	22	8	Binds with high affinity to RNA molecules that contain AU-rich elements (AREs) found within the 3'-UTR of many proto- oncogenes and cytokine mRNAs. Also binds to double- and single-stranded DNA sequences in a specific manner and functions a transcription factor.	Nucleus.Component of ribonucleosomes.
1346	Heterogeneous nuclear ribonucleoprotein D0, isoform 3	HNRPD	IPI00220684	4	-1	*0.96*	-1.77	0.0026	46942	8.91	32985	8.23	82	33	8	Binds with high affinity to RNA molecules that contain AU-rich elements (AREs) found within the 3-prime untranslated regions of many protooncogenes and cytokine mRNAs. Also binds to double- and single-stranded DNA sequences in a specific manner and functions a transcription factor.	Nucleus
1524	Heterogeneous nuclear ribonucleoprotein D-like, isoform 3	HNRPDL	IPI00045498	4	1.16	0.0011	-2.26	0.00031	38339	8.4	27346	8.76	98	10	2	Acts as a transcriptional regulator. Promotes transcription repression. Promotes transcription activation in differentiated myotubes (By similarity). Binds to double- and single-stranded DNA sequences. Binds to the transcription suppressor CATR sequence of the COX5B promoter (By similarity). Binds with high affinity to RNA molecules that contain AU-rich elements (AREs) found within the 3'-UTR of many proto-oncogenes and cytokine mRNAs.	Nucleus. Cytoplasm.
1111	Heterogeneous nuclear ribonucleoprotein H1	HNRPH1	IPI00013881	5	1.02	*0.79*	-1.83	0.038	61023	6.98	49484	5.89	[110]	42	21	Involved in the splicing process and participates in early heat shock-induced splicing arrest. Due to their great structural variations the different isoforms may possess different functions in the splicing reaction.	Nucleus
1524	Heterogeneous nuclear ribonucleoprotein H3, isoform 1	HNRPH3	IPI00013877	10	1.16	0.0011	-2.26	0.00031	38339	8.4	36960	6.37	81	9	2	Involved in the splicing process and participates in early heat shock-induced splicing arrest. Due to their great structural variations the different isoforms may possess different functions in the splicing reaction.	Nucleus
866	Heterogeneous nuclear ribonucleoprotein K	HNRPK	IPI00647717	9	1.18	*0.43*	-1.95	0.042	72513	5.31	42009	5.43	638	32	13	One of the major pre-mRNA-binding proteins. Binds tenaciously to poly(C) sequences. Likely to play a role in the nuclear metabolism of hnRNAs, particularly for pre-mRNAs that contain cytidine-rich sequences. Can also bind poly(C) single-stranded DNA (By similarity).	Nucleus
624	HSPA5 protein	HSPA5	IPI00003362	9	1.05	*0.81*	-2.83	0.0022	86659	4.85	72492	5.07	[145]	40	24	Probably plays a role in facilitating the assembly of multimeric protein complexes inside the ER.	Endoplasmic reticulum; endoplasmic reticulum lumen.
969	HSPA5 protein	HSPA5	IPI00003362	9	1.42	*0.34*	-2.42	0.022	68007	5.85	72492	5.07	821	29	14	Probably plays a role in facilitating the assembly of multimeric protein complexes inside the ER.	Endoplasmic reticulum; endoplasmic reticulum lumen.
635	HSPA5 protein	HSPA5	IPI00003362	9	-1.18	*0.2*	-2.57	0.016	86043	4.95	72492	5.07	[151]	40	32	Probably plays a role in facilitating the assembly of multimeric protein complexes inside the ER.	Endoplasmic reticulum; endoplasmic reticulum lumen.

1270	Hypothetical protein LOC345651		IPI00003269	5	1.07	*0.77*	1.97	0.0031	51500	5.82	42318	5.39	[224]	15	11	Unknown	Cytoplasm
1287	Hypothetical protein LOC345651		IPI00003269	5	1.12	0.031	1.65	0.00066	51281	6.03	42318	5.39	[235]	17	13	Unknown	Cytoplasm
1408	Isocitrate dehydrogenase [NAD] subunit alpha, isoform 2	IDH3A	IPI00607898	15	-1.1	*0.25*	-3.06	0.0015	43278	6.7	34940	6.02	[90]	30	11	Isocitrate + NAD(+) = 2-oxoglutarate + CO(2) + NADH.	Mitochondrion.
1061	Keratin, type II cytoskeletal 8	KRT8	IPI00793917	12	1	*0.94*	1.86	0.011	63147	6.29	26765	4.66	[91]	48	12	Intermediate filament protein	Cytoplasm
294	KIAA1187 protein	MAP7D1	IPI00645814	1	-1.56	0.037	-1.26	*0.2*	101518	6.45	88958	10.06	[72]	21	19	Hypothetical protein DKFZp761F19121 (Fragment).	Cytoplasm
1496	Lactate dehydrogenase B chain	LDHB	IPI00219217	12	1.4	*0.26*	2.14	0.0085	39335	6.45	36900	5.71	101	10	3	Anaerobic glycolysis; final step.S)-lactate + NAD(+) = pyruvate + NADH.	Cytoplasm
1119	Lupus La protein	SSB	IPI00009032	2	1.09	*0.28*	-1.92	0.015	60676	8.05	46979	6.68	[67]	9	12	La protein plays a role in the transcription of RNA polymerase III. It is most probably a transcription termination factor. Binds to the 3' termini of virtually all nascent polymerase III transcripts. It is associated with precursor forms of RNA polymerase III transcripts including tRNA and 4.5S, 5S, 7S, and 7-2 RNAs.	Nucleus (Probable).
1121	Lupus La protein	SSB	IPI00009032	2	1.02	*0.83*	-2.85	0.0021	60590	7.65	46979	6.68	[115]	47	25	La protein plays a role in the transcription of RNA polymerase III. It is most probably a transcription termination factor. Binds to the 3' termini of virtually all nascent polymerase III transcripts. It is associated with precursor forms of RNA polymerase III transcripts including tRNA and 4.5S, 5S, 7S, and 7-2 RNAs.	Nucleus (Probable).
1353	Macrophage capping protein	CAPG	IPI00027341	2	1.1	*0.87*	-2.24	0.00027	46146	7.01	38779	5.88	77	28	13	Calcium-sensitive protein which reversibly blocks the barbed ends of actin filaments but does not sever preformed actin filaments. May play an important role in macrophage function. May play a role in regulating cytoplasmic and/or nuclear structures through potential interactions with actin. May bind DNA.	Cytoplasm. Nucleus.
1770	Membrane-associated progesterone receptor component 2	PGRMC2	IPI00005202	4	1.15	*0.19*	3.49	0.00012	29000	4.3	26211	5.2	105	7	1	Membrane-associated progesterone receptor component 2 (Progesterone membrane-binding protein) (Steroid receptor protein DG6).	Cytoplasm. Memebrane.
1659	Nuclear protein Hcc-1	CIP29	IPI00014938	12	1.01	*0.81*	-3.22	0.00091	30737	7.73	23713	6.1	400	32	8	May have nucleic acid binding capability that may participate in important transcriptional or translational control of cell growth, metabolism and carcinogenesis.	Nucleus
1426	Nucleophosmin, isoform 2	NPM1	IPI00220740	5	-1.05	*0.51*	-4.7	0.0045	42605	5.35	29617	4.47	101	6	3	Associated with nucleolar ribonucleoprotein structures and bind single-stranded nucleic acids. It may function in the assembly and/or transport of ribosome.	Nucleus
1443	Nucleophosmin, isoform 2	NPM1	IPI00220740	5	1.15	*0.21*	-2.6	0.0017	41942	5.83	29617	4.47	86	5	2	Associated with nucleolar ribonucleoprotein structures and bind single-stranded nucleic acids. It may function in the assembly and/or transport of ribosome.	Nucleus
1960	Parathymosin	PTMS	IPI00550020	12	2.21	0.00022	1.31	*0.21*	16674	4.56	11523	4.14	59	10	1	Parathymosin may mediate immune function by blocking the effect of prothymosin alpha which confers resistance to certain opportunistic infections.	Cytoplasm
1484	PDZ and LIM domain protein 1	PDLIM1	IPI00010414	10	-1.09	*0.59*	-2.5	0.00083	39448	8.43	36505	6.56	[119]	45	14	Cytoskeletal protein that may act as an adapter that brings other proteins (like kinases) to the cytoskeleton.	Cytoplasm, Cytoplasm; cytoskeleton (By similarity). Associates with actin stress fibers (By similarity)

1890	Peroxiredoxin-2	PRDX2	IPI00027350	19	1.49	0.004	-1.74	0.0017	22000	6.2	22049	5.66	369	31	7	Involved in redox regulation of the cell. Reduces peroxides with reducing equivalents provided through the thioredoxin system. It is not able to receive electrons from glutaredoxin. May play an important role in eliminating peroxides generated during metabolism. Might participate in the signaling cascades of growth factors and tumor necrosis factor-alpha by regulating the intracellular concentrations of H(2)O(2).	Cytoplasm
1797	Peroxiredoxin-6	PRDX6	IPI00220301	1	1.26	0.039	-2.14	0.00022	24854	7.79	25133	6	410	38	8	Involved in redox regulation of the cell. Can reduce H(2)O(2) and short chain organic, fatty acid, and phospholipid hydroperoxides. May play a role in the regulation of phospholipid turnover as well as in protection against oxidative injury.	Cytoplasm, Lysosome, Cytoplasmic vesicle (By similarity).
748	Phenylalaninyl-tRNA synthetase beta chain	FARSB	IPI00300074	2	1.22	*0.14*	-1.91	0.033	79667	8.51	66715	6.4	[71]	23	13	ATP + L-phenylalanine + tRNA(Phe) = AMP + diphosphate + L-phenylalanyl-tRNA(Phe).	Cytoplasm (by simularity)
1694	Prohibitin	PHB	IPI00017334	17	1.27	0.011	1.5	0.0025	28868	5.82	29843	5.57	273	18	5	Prohibitin inhibits DNA synthesis. It has a role in regulating proliferation. As yet it is unclear if the protein or the mRNA exhibits this effect. May play a role in regulating mitochondrial respiration activity and in aging.	Mitochondrion; mitochondrial inner membrane (By similarity).
1695	Prohibitin	PHB	IPI00017334	17	1.06	*0.55*	-2.44	0.00023	28951	6.37	29843	5.57	126	55	5	Prohibitin inhibits DNA synthesis. It has a role in regulating proliferation. As yet it is unclear if the protein or the mRNA exhibits this effect. May play a role in regulating mitochondrial respiration activity and in aging.	Mitochondrion; mitochondrial inner membrane (By similarity).
1609	Proliferating cell nuclear antigen	PCNA	IPI00021700	20	1.24	*0.054*	1.85	0.0055	33387	4.45	29092	4.57	497	42	11	This protein is an auxiliary protein of DNA polymerase delta and is involved in the control of eukaryotic DNA replication by increasing the polymerase's processibility during elongation of the leading strand.	Nucleus
1657	Proteasome subunit alpha type 1, short isoform	PSMA1	IPI00016832	11	1.16	0.046	1.55	0.0079	30693	7.95	29822	6.15	207	22	5	Ubiquitin- and ATP-dependent proteasomal degradation	Cytoplasm. Nucleus.
1840	Proteasome subunit alpha type 2	PSMA2	IPI00219622	7	1.15	*0.083*	1.6	0.0092	22719	8.7	25996	6.92	180	17	4	Ubiquitin- and ATP-dependent proteasomal degradation	Cytoplasm. Nucleus.
1770	Proteasome subunit alpha type 5	PSMA5	IPI00291922	1	1.15	*0.19*	3.49	0.00012	29000	4.3	26565	4.74	219	26	5	Ubiquitin- and ATP-dependent proteasomal degradation	Cytoplasm. Nucleus.
953	Protein disulfide-isomerase A3 precursor	PDIA3	IPI00025252	15	-1.05	*0.67*	-1.76	0.00077	68493	6.49	57146	5.98	98	35	10	Catalyzes the rearrangement of -S-S- bonds in proteins.	Endoplasmic reticulum; endoplasmic reticulum lumen (By similarity).
909	Protein disulfide-isomerase precursor	P4HB	IPI00010796	17	-1.1	*0.11*	-2.2	0.0021	70074	4.52	57480	4.76	113	24	10	This multifunctional protein catalyzes the formation, breakage and rearrangement of disulfide bonds.	Endoplasmic reticulum lumen. Melanosome. May also be secreted or associated with plasma membrane
926	Protein disulphide-isomerase precursor	P4HB	IPI00010796	17	-1.05	*0.49*	-3.68	5.70E-06	69576	4.7	57480	4.76	[163]	42	26	This multifunctional protein catalyzes the formation, breakage and rearrangement of disulfide bonds.	Endoplasmic reticulum lumen. Melanosome. May also be secreted or associated with plasma membrane
939	Protein disulphide-isomerase precursor	P4HB	IPI00010796	17	-1.29	*0.26*	-2.27	0.022	69477	6.21	57146	5.98	70	6	2	This multifunctional protein catalyzes the formation, breakage and rearrangement of disulfide bonds.	Endoplasmic reticulum lumen. Melanosome. May also be secreted or associated with plasma membrane

957	Protein disulphide-isomerase precursor	P4HB	IPI00010796	17	-1.16	0.00086	-2.04	3.50E-05	68396	6.42	57146	5.98	[102]	37	28	This multifunctional protein catalyzes the formation, breakage and rearrangement of disulfide bonds.	Endoplasmic reticulum lumen. Melanosome. May also be secreted or associated with plasma membrane
1872	Protein DJ-1	PARK7	IPI00298547	1	1.08	*0.28*	-2.63	0.0002	21338	7.39	20050	6.33	279	32	6	Acts as a positive regulator of androgen receptor-dependent transcription. May function as a redox-sensitive chaperone and as a sensor for oxidative stress. Prevents aggregation of SNCA. Protects neurons against oxidative stress and cell death. Plays a role in fertilization. Has no proteolytic activity. Has cell-growth promoting activity and transforming activity.	Nucleus. Cytoplasm. Associated with mitochondria in some cells, particularly after oxidative stress. Detected in tau inclusions in brains from neurodegenerative disease patients.
1029	Retinal dehydrogenase 1	ALDH1A1	IPI00218914	9	-2.04	0.0068	-1.01	*0.93*	65159	8.1	55323	6.29	[144]	31	11	Binds free retinal and cellular retinol-binding protein- bound retinal. Can convert/oxidize retinaldehyde to retinoic acid (By similarity).	Cytoplasm
1577	Ribose-phosphate pyrophosphokinase I	PRPS1	IPI00219616	X	1.08	*0.54*	-1.52	0.014	35956	8.73	35194	6.56	84	12	2	ATP + D-ribose 5-phosphate = AMP + 5-phospho-alpha-D-ribose 1-diphosphate.	Cytoplasm
1372	RNA-binding protein 4, isoform 1	RBM4	IPI00003704	11	1.17	*0.12*	-1.77	0.047	45493	8.36	40688	6.61	102	35	3	May play a role in alternative splice site selection during pre-mRNA processing.	Nucleus. Nucleus; nucleolus. Cytoplasm. Note=May undergo continuous nucleocytoplasmic shuttling.
1929	RNA-binding protein 8A, isoform 2	RBM8A	IPI00216659	1	1.1	*0.36*	-3.96	6.20E-05	18241	5.2	19805	5.64		10	12	Part of a post-splicing multiprotein complex involved in both mRNA nuclear export and mRNA surveillance. Involved in nonsense-mediated decay (NMD) of mRNAs containing premature stop codons. Associates preferentially with mRNAs produced by splicing. Does not interact with pre-mRNAs, introns, or mRNAs produced from intronless cDNAs. Associates with both nuclear mRNAs and newly exported cytoplasmic mRNAs. Complex with MAGOH is a component of the nonsense mediated decay (NMD) pathway.	Cytoplasm. Nucleus.
1089	RuvB-like2	RUVBL2	IPI00009104	19	-1.03	*0.62*	1.68	0.013	62253	5.93	51165	5.49	64	31	14	Possesses single-stranded DNA-stimulated ATPase and ATP- dependent DNA helicase (5' to 3') activity. Component of the NuA4 histone acetyltransferase complex which is involved in transcriptional activation of select genes principally by acetylation of nucleosomal histone H4 and H2A. This modification may both alter nucleosome - DNA interactions and promote interaction of the modified histones with other proteins which positively regulate transcription. This complex may be required for the activation of transcriptional programs associated with oncogene and proto-oncogene mediated growth induction, tumor suppressor mediated growth arrest and replicative senescence, apoptosis, and DNA repair.	Nucleus; nuclear matrix. Nucleus; nucleoplasm. Cytoplasm. Membrane.
1057	Selenium binding protein 1	SELENBP1	IPI00745729	1	1.05	*0.76*	1.56	0.032	63690	7.23	53598	6.03	[132]	36	15	Selenium-binding protein which may be involved in the sensing of reactive xenobiotics in the cytoplasm. May be involved in intra-Golgi protein transport (By similarity).	Nucleus. Cytoplasm, cytosol. Cytoplasm; Peripheral membrane protein (By similarity).
1314	Septin-2	Sep-02	IPI00014177	2	1.32	*0.077*	1.65	0.0076	49133	7.71	41689	6.15	340	18	5	Involved in cytokinesis (Potential).	Cytoplasm
1394	Serine-threonine kinase receptor-associated protein	STRAP	IPI00294536	12	1.17	*0.077*	1.75	0.015	44277	4.99	38756	4.98	231	18	20	The SMN complex plays an essential role in spliceosomal snRNP assembly in the cytoplasm and is required for pre-mRNA splicing in the nucleus. STRAP may play a role in the cellular distribution of the SMN complex.	Cytoplasm. Nucleus.

1157	Similar to Polyprotein	DNAJC14	IPI00783777	12	1.13	*0.48*	-1.71	0.022			23916	5.69	61	27	10	Regulation of transport of the dopamine D1 receptor by a new membrane-associated ER protein.	Cytoplasm
1942	Sorcin	SRI	IPI00027175	7	1.24	*0.054*	-3.36	7.30E-05	17577	5.08	21947	5.32	108	22	9	This protein has been shown to bind calcium with high affinity.	Cytoplasm
877	Splicing factor U2AF 65 kDa subunit	U2AF2	IPI00031556	19	-1.01	*0.95*	-1.55	0.04	71690	7.23	53809	9.19	66	20	4	Necessary for the splicing of pre-mRNA. Binds to the polypyrimidine tract of introns early during spliceosome assembly. Required for the export of mRNA out of the nucleus, even if the mRNA is encoded by an intron-less gene.	Nucleus
2011	Stathmin	STMN1	IPI00479997	1	1.66	0.0055	-1.02	*0.96*	13000	8	17292	5.76	254	44	6	Involved in the regulation of the microtubule (MT) filament system by destabilizing microtubules. Prevents assembly and promotes disassembly of microtubules.	Cytoplasm
2017	Stathmin 1 variant (Fragment)	STMN1	IPI00744618	1	1.07	*0.11*	-5.4	2.60E-06	13368	6.38	15264	8.47	123	26	9	Involved in the regulation of the microtubule (MT) filament system by destabilizing microtubules. Prevents assembly and promotes disassembly of microtubules.	Cytoplasm
661	Stress-70 protein, mitochondrial precursor	HSPA9	IPI00007765	5	-1.27	0.0024	-1.82	0.00032	84825	5.84	73920	5.87	[221]	50	41	Implicated in the control of cell proliferation and cellular aging. May also act as a chaperone.	Mitochondrion.
1465	SUGT1 32 kDa protein	SUGT1	IPI00009149	13	1.16	*0.12*	-2	0.038	40589	5.01	32347	5.28	140	11	2	Involved in kinetochore function and required for th	Nucleus.
2000	Superoxide dismutase 1	SOD1	IPI00218733	21	1.39	0.00022	-1.63	8.30E-05	14499	7.52	16340	5.87	195	16	2	Important antioxidant catalyzes the dismutation of superoxide into oxygen and hydrogen peroxide.	Cytoplasm.
1879	Thioredoxin-dependent peroxide reductase	PRDX3	IPI00024919	10	1.21	*0.38*	-1.54	0.014	20946	4.9	28017	7.67	267	28	33	Involved in redox regulation of the cell. Protects radical-sensitive enzymes from oxidative damage by a radical- generating system. Acts synergistically with MAP3K13 to regulate the activation of NF-kappa-B in the cytosol.	Mitochondrion.
1878	Thioredoxin-dependent peroxide reductase	PRDX3	IPI00024919	10	-1.02	*0.75*	-1.73	0.00043	21006	7.26	28017	7.67	324	27	6	Involved in redox regulation of the cell. Protects radical-sensitive enzymes from oxidative damage by a radical- generating system. Acts synergistically with MAP3K13 to regulate the activation of NF-kappa-B in the cytosol.	Mitochondrion.
1778	Triosephosphate isomerase 1 variant	TPI1	IPI00465028	12	1.28	0.046	-1.75	5.40E-05	25283	8.16	31057	5.65	457	35	8	Glycolytic pathway	Cytoplasm
1809	Triosephosphate isomerase 1 variant	TPI1	IPI00465028	12	-1.17	*0.28*	-1.55	0.04	24121	7.39	31057	5.65	423	34	7	Glycolytic pathway	Cytoplasm
1638	Tropomyosin alpha-4 chain, isoform 1	TPM4	IPI00010779	19	1.17	0.011	-2.05	0.00044	31807	4.64	28619	4.67	357	18	7	Implicated in stabilizing cytoskeleton actin filaments.	Cytoplasm
1412	Tropomyosin isoform	TPM1	IPI00018853	15	1.26	*0.07*	-2.16	0.041	43155	4.65	28517	4.89	132	11	3	Implicated in stabilizing cytoskeleton actin filaments.	Cytoplasm
1040	Tubulin 46 kDa protein	TUBA1B	IPI00792677	12	1.32	*0.24*	1.69	0.027	64054	5.39	46797	4.96	[89]	36	12	Constituent of microtubules	Cytoplasm
1057	Tubulin 46 kDa protein	TUBA1B	IPI00792677	12	1.05	*0.76*	1.56	0.032	63690	7.23	46797	4.96	[73]	29	11	Constituent of microtubules	Cytoplasm
1030	Tubulin alpha-3 chain	TUBA1A	IPI00180675	12	1.07	*0.84*	1.6	0.01	64881	5.56	50788	4.94	385	25	8	Major constituent of microtubules	Cytoplasm
1627	Tubulin folding cofactor B	TBCB	IPI00293126	19	1.06	*0.41*	-2.11	0.02	31989	4.91	27594	5.06	345	26	6	Binds to alpha-tubulin folding intermediates after their interaction with cytosolic chaperonin in the pathway leading from newly synthesized tubulin to properly folded heterodimer. Involved in regulation of tubulin heterodimer dissociation. May function as a negative regulator of axonal growth.	Cytoplasm
1083	Tubulin, beta polypeptide	TUBB	IPI00645452	6	-1.17	*0.39*	1.62	0.011	62342	5.8	48135	4.7	[91]	27	15	Major constituent of microtubules	Cytoplasm
1125	Tubulin, beta polypeptide	TUBB	IPI00645452	6	1.15	*0.41*	1.6	0.033	58000	5	48135	4.7	120	33	14	Major constituent of microtubules	Cytoplasm
1372	Twinfilin-2	TWF2	IPI00550917	3	1.17	*0.12*	-1.77	0.047	45493	8.36	39751	6.37	162	9	5	Actin-binding protein involved in motile and morphological processes. Inhibits actin polymerization, likely by sequestering G-actin. By capping the barbed ends of filaments, it also regulates motility. Seems to play an important role in clathrin-mediated endocytosis and distribution of endocytic organelles (By similarity).	Cytoplasm. Cytoplasm; perinuclear region. Note=Perinuclear and G-actin-rich cortical actin structures sublocalization.

2021	Ubiquitin-conjugating enzyme E2 N	UBE2N	IPI00003949	12	1.06	*0.4*	-1.89	0.003	13000	5.2	17184	6.13	157	26	4	Mediates transcriptional activation of target genes. Plays a role in the control of progress through the cell cycle and differentiation. Plays a role in the error-free DNA repair pathway and contributes to the survival of cells after DNA damage.	Cytoplasm
1835	Ubiquitin-conjugating enzyme E2-25 kDa, isoform 1	HIP2	IPI00021370	4	-1.52	0.013	1.94	0.00015	22947	5.23	22507	5.33	290	30	6	Catalyzes the covalent attachment of ubiquitin to other proteins. Mediates the selective degradation of short-lived and abnormal proteins. Ubiquitinates huntingtin. May mediate foam cell formation by the suppression of apoptosis of lipid-bearing macrophages through ubiquitination and subsequence degradation of p53.	Cytoplasm (By similarity).
1017	UV excision repair protein RAD23 homolog B	RAD23B	IPI00008223	9	1.56	0.013	1.38	*0.084*	65252	4.73	43202	4.79	69	20	6	Plays a central role both in proteosomal degradation of misfolded proteins and DNA repair. Central component of a complex required to couple deglycosylation and proteasome-mediated degradation of misfolded proteins in the endoplasmic reticulum that are retrotranslocated in the cytosol. Involved in DNA excision repair by stabilizing XPC protein. May play a part in DNA damage recognition and/or in altering chromatin structure to allow access by damage-processing enzymes.	Nucleus. Cytoplasm (By similarity).
570	Villin 2 (Ezrin)	VIL2	IPI00746388	6	1.02	*0.65*	-1.55	0.0038	89420	7.51	69816	5.94	[284]	45	42	Probably involved in connections of major cytoskeletal structures to the plasma membrane.	Membrane
727	Vimentin	VIM	IPI00418471	10	-1.03	*0.48*	-1.54	0.0043	80811	6.07	53545	5.06	[105]	36	20	Vimentins are class-III intermediate filaments found in various non-epithelial cells	Cytoplasm
786	Vimentin	VIM	IPI00418471	10	1.45	0.041	-2.48	0.00091	76768	5.18	53545	5.06	181	22	32	Vimentins are class-III intermediate filaments found in various non-epithelial cells	Cytoplasm
821	Vimentin	VIM	IPI00418471	10	1.11	*0.85*	-2.56	0.0085	74930	5.63	53545	5.06	[208]	59	36	Vimentins are class-III intermediate filaments found in various non-epithelial cells	Cytoplasm
837	Vimentin	VIM	IPI00418471	10	1.11	*0.55*	-2.16	0.01	74080	5.42	53676	5.06	114	38	16	Vimentins are class-III intermediate filaments found in various non-epithelial cells	Cytoplasm
839	Vimentin	VIM	IPI00418471	10	1.32	*0.45*	-1.8	0.0013	74292	5.29	53676	5.06	803	32	17	Vimentins are class-III intermediate filaments found in various non-epithelial cells	Cytoplasm
851	Vimentin	VIM	IPI00418471	10	-1.15	*0.64*	-1.94	0.046	73449	4.93	53676	5.06	165	8	4	Vimentins are class-III intermediate filaments found in various non-epithelial cells	Cytoplasm
857	Vimentin	VIM	IPI00418471	10	1.23	*0.27*	-2.07	0.0037	73659	5.18	53545	5.06	105	14	16	Vimentins are class-III intermediate filaments found in various non-epithelial cells	Cytoplasm
861	Vimentin	VIM	IPI00418471	10	1.26	*0.61*	-2.33	0.0034	72616	5.61	53676	5.06	303	74	23	Vimentins are class-III intermediate filaments found in various non-epithelial cells	Cytoplasm
866	Vimentin	VIM	IPI00418471	10	1.18	*0.43*	-1.95	0.042	72513	5.31	53676	5.06	296	14	6	Vimentins are class-III intermediate filaments found in various non-epithelial cells	Cytoplasm
903	Vimentin	VIM	IPI00418471	10	1.67	0.0025	-1.52	*0.16*	70374	5.18	53676	5.06	576	27	13	Vimentins are class-III intermediate filaments found in various non-epithelial cells	Cytoplasm
924	Vimentin	VIM	IPI00418471	10	-1.04	*0.74*	-1.76	0.043	69675	5.84	53676	5.06	864	35	17	Vimentins are class-III intermediate filaments found in various non-epithelial cells	Cytoplasm
927	Vimentin	VIM	IPI00418471	10	1.14	*0.63*	-1.68	0.0083	69774	5.59	53545	5.06	[94]	28	20	Vimentins are class-III intermediate filaments found in various non-epithelial cells	Cytoplasm
1093	Vimentin	VIM	IPI00418471	10	-1.04	*0.5*	1.57	0.023	61988	5.21	53545	5.06	146	47	24	Vimentins are class-III intermediate filaments found in various non-epithelial cells	Cytoplasm
1137	Vimentin	VIM	IPI00418471	10	1.2	*0.4*	2.28	0.022	58551	4.65	53676	5.06	578	21	11	Vimentins are class-III intermediate filaments found in various non-epithelial cells	Cytoplasm

969	Vimentin 50 kDa protein	VIM	IPI00827679	10	1.42	*0.34*	-2.42	0.022	68007	5.85	49680	5.19	[111]	34	28	Vimentins are class-III intermediate filaments found in various non-epithelial cells	Cytoplasm
560	Vinculin isoform	VCL	IPI00291175	10	1.02	*0.92*	-1.65	0.0053	89931	7.15	117220	5.83	[106]	24	26	Involved in cell adhesion. May be involved in attachment of actin-based microfilaments to the plasma membrane.	Cytoplasm, cytoskeleton.
213	Vinculin isoform meta-VCL	VCL	IPI00307162	10	1.29	*0.064*	-1.77	4.10E-05	106712	7.16	124292	5.5	97	5	2	Involved in cell adhesion. May be involved in attachment of actin-based microfilaments to the plasma membrane.	Cytoplasm, cytoskeleton.
1858	Von Hippel-Lindau binding protein 1	VBP1	IPI00334159	X	-1.21	*0.083*	-2.26	0.011	21799	7.51	26690	9.1	123	12	3	Binds specifically to cytosolic chaperonin (c-CPN) and transfers target proteins to it. Binds to nascent polypeptide chain and promotes folding in an environment in which there are many competing pathways for nonnative proteins.	Cytoplasm. Nucleus.

Table 3.3B Differentially expressed proteins identified from a comparison between the whole cell lysates of hybrid clones 18-D-23 and 18-G-1.26 and their respective parental cell lines. Protein features that were matched across all gels with a fold-change ≥1.5-fold where $p \leq 0.05$ are identified. Orange shading indicates an increase in expression and green indicates a decrease in expression. Yellow shading indicates a protein feature with two distinct protein identifications. Protein identifications were made by database searching of peptide ion fragments from LC-MS/MS or by MALDI-TOF MS PMF, the latter indicated by [ ] in the 'Score' column. The identifications were scored according to algorithms that take into account mass accuracy and peptide coverage. The search criteria used allowed +/- 50 ppm mass error and up to 2 missed cleavages. The identified proteins were partly verified by comparison of their theoretical molecular weights and pIs with gel position on the master gel.

The analysis of single hybrids in the first experiment showed that the overall differential expression was greatly reduced and the changes in abundance were significantly less; the largest change in protein abundance detected was 3.5-fold for an isoform of vimentin. Unlike with the analysis of the pools, there were no opposing expression changes identified between the two cell models and all of the changes were unique to one cell model or the other when using an average ≥ 1.5-fold (p <0.05, n=3) threshold. Notably, one gene product of Ch18 was identified (thioredoxin-like protein 1; up-regulated in 18-G-5). A number of the proteins identified in this analysis were also observed in the previous 2D-DIGE analysis of the hybrid pools, although their changes in abundance were not equivalent between the two experiments (Table 3.4). For example, annexin A1 was down-regulated in the TOV-112D hybrid pool and the single 18-D-22 clone (-2.25 and –2.83 fold, respectively) and cofillin was up-regulated in the TOV-112D hybrid pool and in the 18-G-5 clone (+3.1 and +1.87 fold respectively). However, adenosylhomocysteinase which was significantly up-regulated (+4.97 fold) in the TOV-21G pool and down-regulated (-1.9 fold) in the TOV-112D pool was moderately, but significantly, up-regulated in both the single 18-G-5 and 18-D-22 hybrid clones (+1.19 and +1.52 fold, respectively). This difference is not likely to be a product of poor reproducibility of the technique since 2D-DIGE has been proved to be a highly reproducible method (Gharbi, Gaffney et al. 2002) and is most likely to be accounted for by the heterogeneity of the clones. Proteins of interest included eukaryotic translation initiation factor 4E (EIF4E) and PIG3 which were up-regulated (1.86 and 1.67 fold respectively) in the 18-D-22/parental comparison as was peroxiredoxin 2 (1.51 fold), whilst basic transcription factor BTF3 isoform 1 was down-regulated (-1.55 fold). In

contrast, thioredoxin-like protein 1 displayed a significant increase in expression (1.59 fold) in the 18-G-5 hybrid clone, although annexin A1 was also identified from this protein spot with an equally high significance score. Notably, there were less similarities between the TOV-21G hybrid pool and the single 18-G-5 clone than in the other cell models, suggesting greater clonal variation in the clear cell model.

As previously observed there were few proteins identified showing the same directionality of altered expression in both parent:hybrid cell models. This was also evident in the second analysis of hybrid clones 18-D-23 and 18-G-1.26, where only endoplasmic reticulum protein ERp29 precursor displayed a decrease in average abundance in both hybrid cell lines, whilst heat-shock protein beta 1 (Hsp27) was up-regulated in both the 18-D-23 and 18-G-1.26 cell lines (Table 3.3B). In contrast to the previous comparison, only two proteins displayed opposite regulation in the two cell models. These were ubiquitin-conjugating enzyme E2-25 kDa isoform 1 which was down-regulated (-1.52 fold) in the 18-D-23 hybrid cell line and up-regulated (1.94 fold) in the 18-G-1.26 hybrid cell line, and an isoform of the intermediate filament protein vimentin, which was up-regulated in the 18-D-23 hybrid (1.67 fold) and down-regulated (-1.52 fold) in the 18-G-1.26 hybrid versus their parental cell lines. Of the 15 isoforms of vimentin identified, all except two were significantly down-regulated in the 18-G-1.26 hybrid cell line. Vimentin is known to be multiply phosphorylated and subject to protease cleavage, so these differential changes may be caused by PTMs.

In the comparison of the hybrid cell line 18-D-23 and its parental cell line TOV-112D, a total of 12 protein isoforms were identified from 11 protein features (Fig 3.3). Some of these changes were also observed in the 18-D-22 vs TOV-112D comparison. These included annexin A1 (down-regulated over two-fold in the 18-D-23 and 18-D-22 clones); retinol dehydrogenase 1 (down-regulated over two-fold in both clones) and a matched isoform of vimentin which was up-regulated by 1.67 fold in the 18-D-23 hybrid cell line and by 1.78 fold in the 18-D-22 hybrid cell line.

The comparison between the hybrid cell line 18-G1.26 and its parent cell line TOV-21G resulted in a total of 136 protein identifications from 123 distinct protein features. Of these, 91 displayed significant down-regulation and 34 displayed significant up-regulation. Eukaryotic translation initiation factor 5A-1 isoform 2 (EIF-5A2) and a fragment of stathmin 1 variant were identified from a gel feature which was down-regulated the most (5.4 fold). Stathmin was seen previously as being significantly up-regulated in the TOV-21G/hybrid pool. At this stage it is difficult to know whether the change observed is from EIF5A or stathmin, particularly since the predicted and measured pI's and MW's are not concordant for the stathmin and EIF5A identifications, respectively. This highlights a drawback of 2D-DIGE, but also implicates the detection of differential post-translational modifications. The most up-regulated protein feature also gave two different protein identifications. Membrane-associated progesterone receptor component 2 and proteasome subunit alpha type 5 were identified from a protein feature being up-regulated 3.49 fold. Both proteins have a similar Mw and pI.

Several proteins were identified from multiple gel features, calreticulin precursor was identified in 2 protein spots. Expression was significantly down-regulated in the 18-G-1.26/parental comparison (-1.65 and -2.06 fold). However, expression was only marginally down-regulated in only one of the gel spots of the 18-D-23/parental comparison. Calreticulin precursor is a calcium-binding chaperone promoting folding, oligomeric assembly and quality control in the ER via the calreticulin/calnexin cycle. Another protein identified twice and significantly down-regulated (-4.7 and -2.6 fold) in the 18-G-1.26/parental comparison was nucleophosmin. This abundant and highly conserved phosphoprotein shuttles between the nucleus and cytoplasm and is involved in ribosome biogenesis, centrosome duplication, protein chaperoning, histone assembly, cell proliferation and regulation of tumor suppressors TP53/p53 and ARF. Prohibitin was also identified in two gel spots and expression was shown to be significantly up-and down-regulated in each in the 18-G-1.26/parental comparison. A post-translational modification is the likely cause for contrasting expression for a protein found in two closely located gel-spots.

Other proteins of interest included proliferating cell nuclear antigen (PCNA) which was significantly up-regulated (1.85 fold) in the 18-G-1.26/parental comparison and protein DJ-1, which was found to be significantly down-regulated (-2.63 fold) in the 18-G-1.26/parental comparison. Of the identifications, several were proteins with structural functions. These included the actin binders cofilin, F-actin capping protein, macrophage capping protein, twinfilin 2, destrin, fascin, PDLIM1, ezrin, dynactin and septin. F-actin capping protein and fascin were up-regulated in the hybrid clone 18-G-1.26 whilst

macrophage capping protein displayed down-regulation (-2.24 fold) in the same hybrid clone. Destrin was identified from two closely located protein spots. These spots displayed differential regulation in the two hybrid clones under analysis. Although abundant proteins, these changes suggest changes to the actin skeleton in response to tumour suppression. Finally, von Hippel-Lindau binding protein 1 (VBP1) was identified and displayed down-regulation in hybrid clone 18-G-1.26. VBP1 binds Von Hippel-Lindau, a well known tumour suppressor protein and chaperones it to the nucleus or cytoplasm.

3.2.2 Common protein identifications and expression changes

A number of proteins were identified as common to all three experiments described in this chapter, including annexin Al, cofilin-1, peroxiredoxin 2, vimentin, PDI and ERp29 (Table 3.4). Annexin A1 displayed down-regulation (-2.25 fold) in the TOV-112D hybrid pool and up-regulation (2.28 fold) in the TOV-21G hybrid pool. In accordance, two isoforms were down-regulated in the 18-D-22 and 18-D-23 hybrid clones and a single isoform was up-regulated in the 18-G-5 hybrid clone. Cofilin displayed concordant up-regulation (3.1, 1.69 and 1.87 fold, respectively) in both hybrid pools and the single hybrid clone 18-D-22, whilst being down-regulated (-2.35 fold) in the hybrid clone 18-G-1.26. Peroxiredoxin 2 displayed down-regulation (-4.25 fold) in the TOV-112D hybrid pool and up-regulation (5.71 fold) in the TOV-21G hybrid pool, whilst being up-regulated (1.51 and 1.49 fold, respectively) in the hybrid clones 18-D-22 and 18-D-23

and down-regulated (-1.74 fold) in the hybrid clone 18-G-1.26. Vimentin was down-regulated (-2 and -1.94 fold, respectively) in the 18-G-5 and 18-G-1.26 hybrid clones, two isoforms of ERp29 displayed down-regulation in the hybrid clones 18-D-23 and 18-G-1.26 and adenosylhomocysteinase displayed up-regulation in the hybrid clones 18-D-22 and 18-G-5, whilst PDI showed no common changes in expression.

The lack of common changes in both clones of both cell lines makes selection of candidates for further testing very difficult and reveals the extensive variation between the cell models.

A .Data from pools

	112D hybrid pool /		21G hybrid pool /	
	Av. Ratio	**T-test**	**Av. Ratio**	**T-test**
Adenosylhomocysteinase	-1.9	0.021	4.97	0.00017
Annexin A1	-2.25	0.00071	2.75	0.00018
Cofilin-1	3.1	1.70E-05	1.69	0.00066
Peroxiredoxin 2	-4.25	0.00012	5.71	0.00014
Vimentin	-3.93	0.0011	1.73	0.00091
Vimentin	-1.84	7.80E-05	5.38	0.00029
Vimentin	-5.45	0.00021	1.58	0.013
Protein disulphide-isomerase	-1.12	0.0035	2.71	0.000043
ERp29	-1.46	0.00074	3.42	0.00024

B. Data from single clones

	18-D-22 /112D		18-D-23/112D		18-G-5/21G		18-G-1.26/21G	
	Av. Ratio	**T-test**	**Av. Ratio**	**T-test**	**Av. Ratio**	**T-test**	**Av. Ratio**	**T-test**
Adenosylhomocysteinase	1.52	0.017			1.19	0.024		
Annexin A1	-2.83	0.0059	-2.37	0.00064	-1.02	*0.75*	-1.07	*0.61*
Annexin A1	-3.05	0.0043			-1.15	*0.051*		
Annexin A1	-1.06	*0.68*			1.59	0.0051		
Cofilin-1	1.87	0.018	*1.15*	0.4	-1.09	*0.56*	-2.35	0.02
Peroxiredoxin 2	1.51	0.033	1.49	0.004	1	*0.97*	-1.74	0.0017
Vimentin	3.5	0.021	-1.15	0.64	-2	*0.21*	-1.94	0.046
Vimentin	1.78	0.002	1.14	0.63	-1.2	0.016	-1.68	0.0083
Protein disulphide-isomerase	-1.29	*0.13*	1.53	0.024	-1.1	*0.11*	-2.2	0.0021
ERp29			-1.31	0.000097			-1.67	1.2E-05
ERp29			-1.62	0.00025			-1.65	0.0016

Table 3.4 Comparison of protein expression for identified proteins seen in the pooled hybrid and single hybrid 2D-DIGE experiments. Table A. shows changes in protein abundance for the pools of hybrids compared with the parent cell lines. Table B. shows changes in protein abundance for proteins identified in the two hybrids pairs versus parental comparison. Red = up-regulated (>1.5 fold). Green = down-regulated (>-1.5 fold).

3.2.2 Conclusions

In summary, the whole cell lysate analysis of the single hybrid clones highlights the issue of clonal variation. In the case of the 18-G-5 and 18-G-1.26 cell lines the variation is dramatic; the 18-G-5/parental comparison resulted in 8 spots changing and the 18-G-

1.26/parental comparison resulted in 214 spots changing. Both comparisons were made under the same stringent experimental and statistical criteria. The 18-D-23/parental comparison more closely correlated with the 18-D-22/parental comparison, with the total number of spots changing being 28 for each and more overlap was observed in the proteins identified. For example, annexin A1, retinol dehydrogenase and vimentin were identified as displaying the same direction of altered expression when compared with the TOV-112D parental line. Weight could be attached to the significance of these identifications in light of the clonal variation discussed above. The region of chromosome 18 successfully inserted into each hybrid has clearly affected the proteomic expression signature displayed by each hybrid in a cell model. The aCGH analysis of the TOV-112D hybrid clones indicated that both hybrids acquired a small region comprising ~10 Mb spanning 18p11.21-18q11.2, whereas analysis of the TOV-21G hybrid clones revealed almost complete transfer in both hybrid clones (Chapter 1). This would help to account for the proteomic variation between the cell models and also provide a more focused approach to uncovering the tumour suppressor gene signatures in each cell model.

A number of proteins identified as differentially expressed have been previously implicated in tumourigenisis. For example, in the first analysis EIF4E was identified as an up-regulated protein in the 18-D-22 clone. This protein is involved in RNA binding and protein synthesis. It has been implicated in malignancy since increased mRNA levels have been reported in carcinomas of the bladder, head and neck, liver, colon and breast (Kerekatte, Smiley et al. 1995; Anthony, Carter et al. 1996; Li, Liu et al. 1997; Nathan, Franklin et al. 1999; Rosenwald, Chen et al. 1999; Crew, Fuggle et al. 2000; DeFatta,

Nathan et al. 2000; Haydon, Googe et al. 2000; Graff, Konicek et al. 2009) and EIF4E over-expression preferentially increases the expression of a number of oncogenes (De Benedetti and Harris 1999; Nathan, Franklin et al. 1999; Mamane, Petroulakis et al. 2004; Graff, Konicek et al. 2008; Konicek, Dumstorf et al. 2008). Its increased expression in one of the suppressed cell lines would however argue that EIF4E is not universally involved in promoting oncogenesis. Another protein, BTF3, forms a stable complex with RNA polymerase IIB and is required for transcriptional initiation. It has been found to be over-expressed in glioblastoma multiforme, sporadic colorectal cancer and pancreatic ductal adenocarcinoma. In the latter, BTF3 is involved in the regulation of genes involved in tumourigenesis (Kusumawidjaja, Kayed et al. 2007). Here, its down-regulation may promote the suppressed tumourigenic phenotype of the 18-D-22 clone versus its parental cell line. The antioxidant enzymes, peroxiredoxin 2, 3 and 6 and thioredoxin-like protein, were found to be differentially expressed. These enzymes regulate cellular redox state and protect against protein, lipid and DNA oxidation that can modulate cell proliferation and apoptosis and also speculated to be important in tumour development and invasion. The link between redox state and cancer is unclear. Whilst tumours adapt to hypoxic conditions by up-regulating angiogenesis and switching to anaerobic glycolysis (Warburg effect), oxidants may also up-regulate oncogenic mutation of DNA. Although clear roles for these antioxidant enzymes in tumour suppression are not apparent, it appears that redox balance in the hybrid clones is perturbed. Another protein involved in response to oxidative stress and irradiation was PIG3; up-regulated in 18-D-22. It is induced by the tumour suppressor p53 and is thought to be involved in p53 mediated cell death (Flatt, Polyak et al. 2000). These data implicate p53 in the suppressed phenotype of this clone.

Endoplasmic reticulum protein ERp29 displayed significant down-regulation in hybrid clones of both cell models. Levels of this protein have been found to be elevated in cancerous cells compared to normal cells (Cheretis, Dietrich et al. 2006). Prohibitin (PHB) expression was also down-regulated in the hybrid clone 18-G-1.26. PHB is an evolutionarily conserved gene that is ubiquitously expressed and is thought to be a negative regulator of cell proliferation (Mishra, Murphy et al. 2006). More recent research has shown that PHB interacts with p53 *in vivo* and *in vitro*, increasing p53 mediated transcription by enhancing its recruitment to promoters (Fusaro, Dasgupta et al. 2003). Also, PHB has been shown to interact with all of the Rb family of tumour suppressor proteins to negatively regulate cell proliferation (Wang, Nath et al. 1999). Its down-regulation in the model studied here would suggest that it does not play a role in suppressing tumourigenic phenotype in this system. PCNA acts as a subunit of DNA polymerase delta and thus associated with DNA replication. Its involvement in DNA replication and excision repair after sub-lethal damage has been reported (Umar, Buermeyer et al. 1996; Essers, Theil et al. 2005; Masih, Kunnev et al. 2008). PCNA has been shown to be a valuable prognostic and diagnostic marker in some cancers (al-Sheneber, Shibata et al. 1993; Mayer, Takimoto et al. 1993; Basolo, Pinchera et al. 1994; Inagaki, Ebisuno et al. 1997), including ovarian cancer (Thomas, Nasim et al. 1995). The elevated levels of PCNA observed in the 18-G-1.26 hybrid clone are surprising given its role in proliferation and the fact this clone grew more slowly than the parental cell line. Protein DJ-1 was originally identified as an oncogenic product that is able to transform cells weakly on its own and more strongly in combination with Ras (Nagakubo, Taira et al. 1997). Protein DJ-1 prevents cell death through its anti-oxidative activities and it has

been suggested that this provides a survival advantage in cancer cells (Taira, Saito et al. 2004; Kim, Peters et al. 2005; Davidson, Hadar et al. 2008). Its expression was down-regulated in the 18-G-1.26 clone, which would appear to reflect the tumourigenic suppression displayed by this cell line. Actin is necessary for a large number of cellular processes including cell division, cell migration, polarized growth, secretion and endocytosis. Finally, actin dynamics are tightly controlled by a number of actin binding proteins that interact with actin filaments and/or monomeric actin. De-regulation of actin-organization forms a critical element of the oncogenic and invasive potential of cancer cells. The actin binding proteins ezrin and fascin, for example, have been implicated in a host of cancers (Grothey, Hashizume et al. 2000; Martin, Harrison et al. 2003). The observed de-regulated expression of these proteins and other actin-binders in the hybrid clones suggest that changes to the actin cytoskeleton are functionally important in tumour suppression.

In conclusion, the analysis of protein changes associated with tumour suppression in the EOC Ch18 MMCT cell models has resulted in the identification of gene signatures of neoplastic suppression, but the picture is extremely complex and hampered by clonal variation. Despite this, it has provided numerous interesting findings that could be taken forward for validation, functional studies and investigations of biomarker potential in tumour tissue samples or sera from ovarian cancer cases and controls.

Chapter 4 2D-DIGE analysis of the secreted proteome of Ch18 MMCT models

Introduction

Many genetic alterations selected during malignant transformation disrupt signalling networks, resulting in the release of tumour cells from normal growth constraints or the establishment of new signalling pathways that confer growth and survival advantages on cancer cells. This is often facilitated by the improper expression of secreted proteins or their receptors. The study of secreted and cell surface proteins is regarded as the most promising area for biomarker discovery. This chapter concentrates on differential expression profiling of secreted proteins in the chromosome 18 MMCT epithelial ovarian cancer cell models using 2D-DIGE.

The diagnostic potential ascribed to serum and plasma is reflected in the huge efforts put into their characterisation worldwide such as the HUPO Plasma Proteome Project (http://www.hupo.org/research/hppp/). Multiple approaches to discover putative tumour biomarkers within the plasma or serum of cancer patients have been reported (Welsh, Sapinoso et al. 2003; Zhang, Bast et al. 2004; Ahmed, Oliva et al. 2005; Rai, Gelfand et al. 2005; Volmer, Stuhler et al. 2005; Wu, Chien et al. 2005; Lin, Lin et al. 2006). However, the complexity and the huge dynamic range of expression of the plasma and serum proteomes present a challenge for their analyses. Additionally, proteins derived

from tumours and present in the circulation are expected to be of low abundance and attempts to identify tumour markers in blood has largely resulted in the detection of changes in abundant serum proteins and immune-response proteins which lack specificity for disease detection. Working with tumour tissues or cell models to find secreted candidate markers is a promising alternative approach.

The release of proteins from tumour cells occurs as a result of a number of diverse mechanisms. Classical secretion is the most obvious mode of protein release and is expected to be relevant for proteins such as extracellular matrix molecules, proteases and protease inhibitors, as well as growth factors and cytokines. There is also the release of membrane proteins through proteolytic shedding of ectodomains or through cleavage of phospholipid membrane anchors. Exosomal release of proteins is a further mechanism by which cells may release proteins into the extracellular environment. Exosomes are membrane-coated vesicles derived from multivesicular bodies in the late endosomal compartment which fuse with the plasma membrane to expel their protein content. Proteins may also be released from cells due to apoptosis and necrosis or through physical disruption during handling.

4.1 Proteomic analysis of secreted proteins

To investigate the 'secretome' of proteins released *in vitro,* from ovarian cancer cell lines and their Ch18 MMCT hybrids, cells were grown in standard medium with 15% fetal calf serum until reaching a confluence of 80%. Cells were then washed to remove

contaminating serum proteins and were then cultured for 24 h in serum-free medium. The serum free media was then replenished and harvested after a further 24 h as conditioned media for analysis. The media was concentrated and then desalted using Millipore Centriplus devices, dried down and then resuspended in 2D lysis buffer. The secreted proteins were first assessed on a 1D gel (Fig 4.1) and then the cell culture was scaled up for 2D-DIGE analyses.

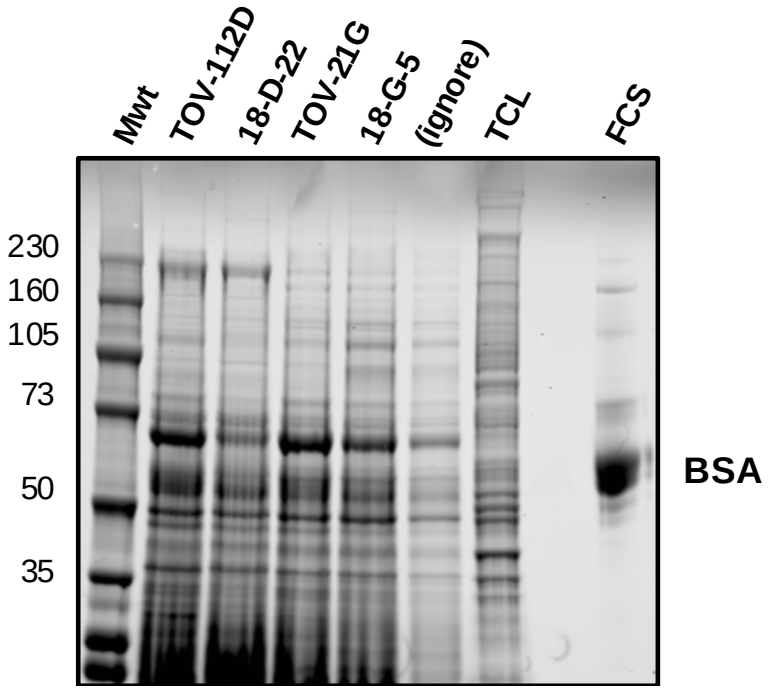

Figure 4.1 CCB-stained 1D gel of the secretome of the epithelial ovarian cancer cell lines. Proteins from conditioned media (10 µg), total cell lysate (TCL; 10 µg) and fetal calf serum (10 µg) were loaded for comparison of the extracted secretome of the two parental cell lines TOV-112D and TOV-21G and the hybrid cell lines 18-D-22 and 18-G-5.

This preliminary analysis showed the efficiency of secreted protein extraction from conditioned media before scaling up preparation for 2D-DIGE, but also suggested considerable contamination from serum proteins, particularly BSA. For 2D-DIGE, two experiments were run, each using media from four 15 cm tissue culture dishes per cell

line. In the first experiment 10 ml of media was used per dish. This made sample desalting and concentration quite time consuming. The yield of protein was only sufficient to load a total of 60 µg per gel (20 µg per sample). This gave rise to problems in identification due to low abundance. A second experiment used 5 ml of media per dish reducing the sample processing time and allowing the number of culture dishes to be doubled to improve protein yield. Samples from each parent and hybrid pair were labelled with Cy3 or Cy5 in triplicate. A pool of samples was also prepared as an internal standard and labelled with Cy2 to be run on all six gels. Samples were mixed appropriately and proteins separated by 2D electrophoresis. The gels from both experiments were curated and analysed in the BVA module of Decyder (Fig 4.2) as described in Materials and Methods.

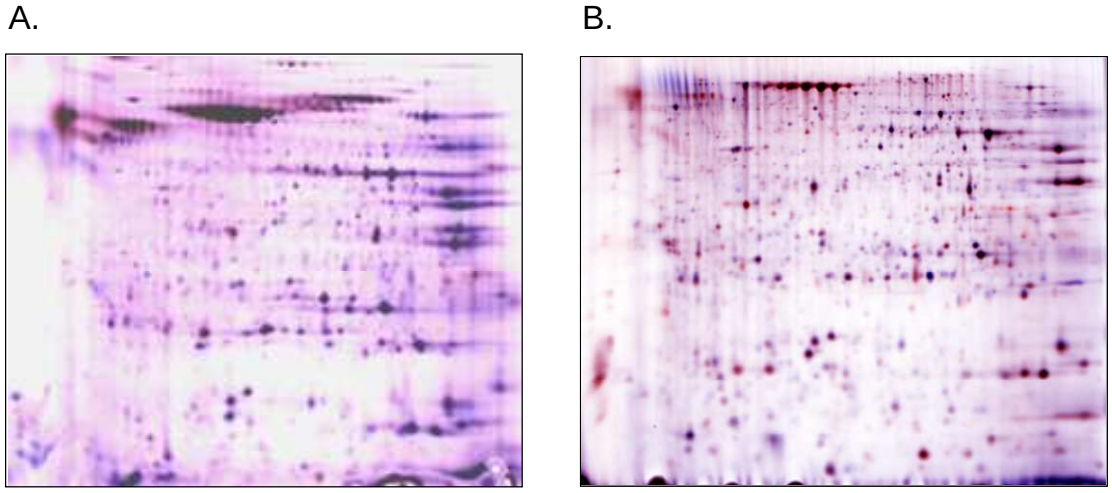

Figure 4.2 Master gel images for the two separate 2D-DIGE 'secretome' experiments. (A) In the first experiment the amount of secreted protein harvested allowed a maximum load of 60 µg of labelled secreted protein to be run on each gel. The label was increased to 8 pmol/µg of protein. (B) The experiment was repeated starting with more conditioned media. The total load per gel was 300 µg. Labelling was carried out at the usual 4 pmol of Cydye per 1 µg of protein. The superimposed images shown were created in Adobe Photoshop to show differentially expressed proteins in red and blue.

In the second experiment, differentially expressed proteins within each parent/hybrid comparison which displayed a change in average abundance of ≥ 2-fold (n=3, *p* value <0.05) were selected. The 18-D-22/TOV-112D comparison resulted in a total of 38 spots displaying differential expression. Of these, 23 were up-regulated and 15 down-regulated. The 18-G-5/TOV-21G comparison resulted in a total of 90 spots displaying differential expression. Of these 43 were up-regulated and 47 down-regulated (Fig 4.3).

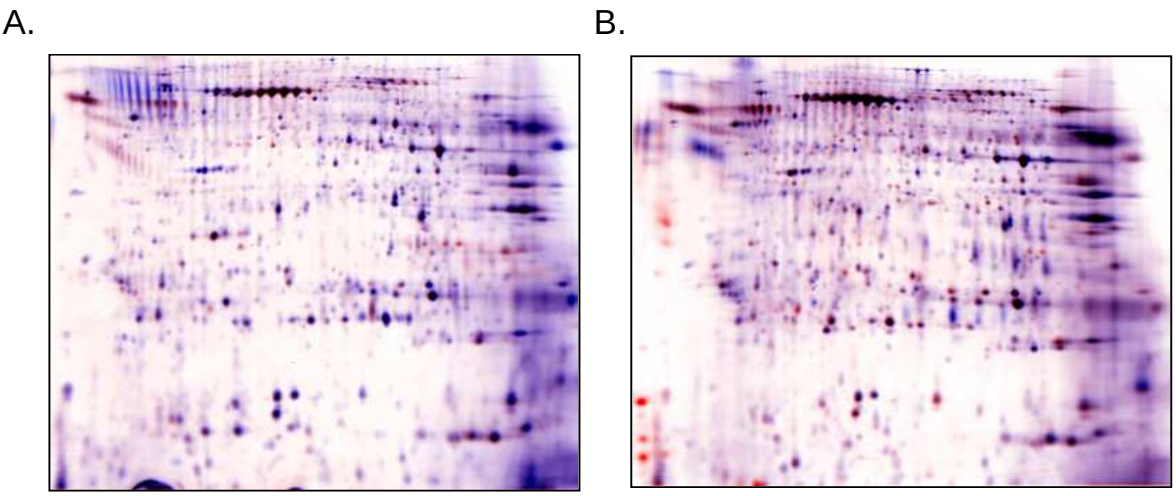

Figure 4.3 Differentially expressed proteins for parent/hybrid comparisons. (A) Example image of 18-D-22/TOV-112D comparison. (B) Example image of 18-G-5/TOV-21G comparison. Up-regulated spots are in red and down-regulated spots are in blue. Images were merged using Adobe Photoshop. 1654 common protein features were identified using Decyder software.

4.2 Identification of differentially expressed secreted proteins

In the second experiment, 43 of the 128 differentially expressed spots were identified by MALDI-TOF MS and/or LC-MS/MS. These represented 29 distinct gene products (Table 2.4). A large proportion of the proteins identified were cellular proteins, derived from the cytoplasm, nucleus, cytoskeleton, endoplasmic reticulum and mitochondrial matrix of cells. However, nine distinct gene products were identified as classically secreted proteins and were differentially expressed proteins not identified previously in our laboratory. The large proportion of proteins identified as cellular proteins may be present due to non-specific release through cell rupture and apoptosis. However, these proteins could also be released into the media from membrane vesicles such as exosomes or micro-particles. Around half of the proteins labelled with the fluorescent Cy dyes were also not visible by CCB staining and so were not picked. Whilst these are likely to be of low abundance, some secreted glycoproteins may be poorly detected by CCB due to their glycosylation (Zacharius, Zell et al. 1969). The scarcity of bovine proteins identified in the secretome underlines the effectiveness of the protocol of minimizing media contaminants. However, a later experiment revealed how ineffective washing of cells during sample preparation can result in significant and differential BSA contamination (see later).

Master No.	Name	IPI	HGNC Symbol	Chr.	18D22/112D Av. Ratio	18D22/112D T-test	18G5/21G Av. Ratio	18G5/21G T-test	pI	Mw	pI (pred)	Mw (pred)	Score	Cov%	Peptides	Function	Location
840	Acetyl-CoA acetyltransferase, cytosolic	IPI00291419	ACAT2	6	*-1.12*	*0.16*	-2.22	3.80E-05	7.15	72254	6.47	41838	164	45	12	Belongs to the thiolase family.	Cellular
916	Annexin A1	IPI00218918	ANXA1	9	*1.15*	*0.1*	-2.03	0.0011	7.06	65687	6.64	38787	101	44	9	Calcium/phospholipid-binding protein which promotes membrane fusion and is involved in exocytosis. This protein regulates phospholipase A2 activity.	Cellular
941	Annexin A1	IPI00218918	ANXA1	9	1.17	0.033	-3.02	0.00029	6.7	63230	6.64	38787	139	49	12	Calcium/phospholipid-binding protein which promotes membrane fusion and is involved in exocytosis. This protein regulates phospholipase A2 activity.	Cellular
1110	Annexin A1	IPI00218918	ANXA1	9	-1.24	0.026	-2.58	0.00029	8.21	48526	6.64	38787	108	37	9	Calcium/phospholipid-binding protein which promotes membrane fusion and is involved in exocytosis. This protein regulates phospholipase A2 activity.	Cellular
1099	Carboxy-propeptide of alpha 1 (III) procollagen	IPI00021033	COL3A1	2	-2.36	8.30E-06	-1.55	0.0094	5.12	49460	5.34	27904	189	51	20	Collagen type III occurs in most soft connective tissues along with type I collagen.	Secreted
1629	Chromosome 6 open reading frame 115 (predicted)	IPI00374316	C6orf115	6	*1.1*	*0.33*	-2.06	0.00023	5.85	6902	5.86	9108	75	46	5		
1470	Cofilin, non-muscle isoform	IPI00012011	CFL1	11	2.5	7.00E-06	-2.74	3.60E-06	6.68	16341	8.26	18588	76	38	6	It is the major component of intranuclear and cytoplasmic actin rods.	Cellular
1605	Galectin-1	IPI00219219	LGALS1	22	*-1.28*	*0.19*	-2.58	3.10E-05	4.5	6000	5.34	14917	123	66	8	Lactose-binding lectin 1	Secreted
443	Glucose-6-phosphate dehydrogenase	IPI00289800	G6PD	X	1.53	0.0011	-2.21	0.00018	7.2	108959	6.44	59553	132	25	12	Produces pentose sugars for nucleic acid synthesis and main producer of NADPH reducing power.	Cellular
1381	Heterogeneous nuclear ribonucleoprotein A1	IPI00797148	HNRNPA1	12	2.45	0.00022	*1.03*	*0.81*	8.1	27923	8.38	22316	107	45	9	Involved in the packaging of pre-mRNA into hnRNP particles	Nucleus/ Cytoplasm
981	Insulin-like growth factor binding protein 2 precursor	IPI00297284	IGFBP2	2	*1.29*	*0.058*	2.12	2.80E-05	7.16	60352	7.48	36198	178	45	15	IGF-binding proteins prolong the half-life of the IGFs and have been shown to either inhibit or stimulate the growth promoting effects of the IGFs on cell culture. They alter the interaction of IGFs with their cell surface receptors.	Secreted
1089	Insulin-like growth factor binding protein 2 precursor	IPI00297284	IGFBP2	2	-2.96	6.90E-06	*-1.19*	*0.27*	7.38	50411	7.48	36198	78	21	7	IGF-binding proteins prolong the half-life of the IGFs and have been shown to either inhibit or stimulate the growth promoting effects of the IGFs on cell culture. They alter the interaction of IGFs with their cell surface receptors.	Secreted
1169	Insulin-like growth factor binding protein 2 precursor	IPI00297284	IGFBP2	2	-1.56	0.00026	2.24	5.60E-05	7.3	50000	7.48	36198	86	28	6	IGF-binding proteins prolong the half-life of the IGFs and have been shown to either inhibit or stimulate the growth promoting effects of the IGFs on cell culture. They alter the interaction of IGFs with their cell surface receptors.	Secreted
962	Insulin-like growth factor binding protein 7 precursor	IPI00016915	IGFBP7	4	*-1.29*	*0.26*	3.52	4.10E-06	7.29	62564	8.25	30138	116	45	12	Binds IGF-I and IGF-II with a relatively low affinity. Stimulates prostacyclin (PGI2) production.	Secreted
991	Insulin-like growth factor binding protein 7 precursor	IPI00016915	IGFBP7	4	*1.36*	*0.14*	3.13	0.00025	7.67	60097	8.25	30138	105	47	11	Binds IGF-I and IGF-II with a relatively low affinity. Stimulates prostacyclin (PGI2) production.	Secreted
1108	Insulin-like growth factor binding protein 7 precursor	IPI00016915	IGFBP7	4	*-1.17*	*0.15*	2.23	0.00044	4.18	48321	8.25	30138	72	27	6	Binds IGF-I and IGF-II with a relatively low affinity. Stimulates prostacyclin (PGI2) production.	Secreted
1043	Insulin-like growth factor binding protein 7 precursor	IPI00016915	IGFBP7	4	1.46	0.015	2.12	0.00032	8.24	56279	8.25	30138	[107]	14	3	Binds IGF-I and IGF-II with a relatively low affinity. Stimulates prostacyclin (PGI2) production.	Secreted
1030	Insulin-like growth factor binding protein 7 precursor (IGFBP-7)	IPI00016915	IGFBP7	4	*-1.05*	*0.54*	4.35	3.40E-06	7.7	56878	8.25	30138	117	52	13	Binds IGF-I and IGF-II with a relatively low affinity. Stimulates prostacyclin (PGI2) production.	Secreted
1033	Insulin-like growth factor binding protein 7 precursor (IGFBP-7) (IBP-7)	IPI00016915	IGFBP7	4	1.81	0.001	3.54	8.80E-07	7.94	56758	8.25	30138	183	56	14	Binds IGF-I and IGF-II with a relatively low affinity. Stimulates prostacyclin (PGI2) production.	Secreted
787	Leukocyte elastase inhibitor	IPI00027444	SERPINB1	6	*1.91*	*0.21*	-2.16	0.00019	6.34	75699	5.9	42829	100	28	9	Regulates the activity of the neutrophil proteases elastase, cathepsin G and proteinase-3.	Secreted
193	Lumican precursor	IPI00020986	LUM	12	2.57	0.00019	*1.01*	*0.9*	4.6	128798	6.16	38747	129	32	10	Belongs to the small leucine-rich proteoglycan (SLRP) family. Class II subfamily	Secreted
1381	Peroxiredoxin 1	IPI00640741	PRDX1	1	2.45	0.00022	*1.03*	*0.81*	8.1	27923	6.41	19135	78	32	6	An antioxidant. Has a protective role in cells.	
1393	Peroxiredoxin 1	IPI00000874	PRDX1	1	2.84	1.50E-05	*-1.1*	*0.11*	8.44	26652	8.27	22324	145	41	11	Involved in redox regulation of the cell.	Cellular
1402	Peroxiredoxin 1	IPI00000874	PRDX1	1	-1.15	0.0032	-2.27	6.70E-05	7.97	26315	8.27	22324	165	71	14	Involved in redox regulation of the cell.	Cellular
1234	Phosphoglycerate mutase 2	IPI00218570	PGAM2	7	-1.75	0.0023	-3.96	1.30E-06	6.81	37241	9	28788	[96]	8	3	Interconversion of 3- and 2-phosphoglycerate with 2,3-bisphosphoglycerate as the primer of the reaction.	Cellular
624	Pigment epithelium-derived factor precursor	IPI00006114	SERPINF1	17	-3.05	1.40E-05	2.61	0.00039	5.46	93156	5.97	46484	124	28	12	Belongs to the serpin family.	Secreted
846	Placental thrombin inhibitor	IPI00514598	SERPINB6	6	*1.21*	*0.084*	-2.45	0.00017	5.02	71796	5.18	42904	105	28	8	Inhibits thrombin.	Cellular
1222	Platelet-activating factor acetylhydrolase IB beta subunit	IPI00026546	PAFAH1B2	11	*1.07*	*0.49*	-3.99	4.60E-06	5.6	38362	5.57	25724	74	33	7	Platelet-activating factor acetylhydrolase IB beta subunit	Cytoplasm
1361	Prolactin precursor (PRL)	IPI00000871	PRL	6	2.28	0.00013	-1.5	0.0074	6.97	28946	6.5	26258	166	73	19	Belongs to the somatotropin/prolactin family.	Secreted
121	Protein disulfide-isomerase A3 precursor	IPI00025252	PDIA3	15	*-1*	*0.95*	2.12	1.40E-05	7.65	138413	5.98	57146	79	30	17	Belongs to the protein disulfide isomerase family.	Endoplasmic reticulum lumen
425	Protein disulfide-isomerase A3 precursor	IPI00025252	PDIA3	15	*-1.05*	*0.38*	2.95	7.00E-05	5.76	110586	5.98	57146	134	30	17	Belongs to the protein disulfide isomerase family.	Endoplasmic reticulum lumen

607	Protein disulfide-isomerase A6 precursor	IPI00644989	PDIA6	2	*1.1*	*0.39*	2.22	2.30E-05	4.71	94347	4.95	48490	67	18	7	Catalyzes the rearrangement of -S-S- bonds in proteins.	Endoplasmic reticulum; endoplasmic reticulum lumen (By similarity)
1451	Vimentin	IPI00418471	VIM	10	-2.86	0.00014	2.04	0.0097	4.22	20410	5.06	53545	[149]	8	4	Vimentins are class-III intermediate filaments	Cellular
1282	Splice Isoform 2 of Triosephosphate isomerase	IPI00451401	TPI1	12	1.72	0.0057	-2.61	0.00016	7.78	34581	8.5	27320	81	39	7	Metabolic pathways.	Cellular
1282	Splice Isoform A2 of Heterogeneous nuclear ribonucleoproteins A2/B1	IPI00414696	HNRPA2B1	7	1.72	0.0057	-2.61	0.00016	7.78	34581	8.67	36041	72	25	8	Involved with pre-mRNA processing. Forms complexes (ribonucleosomes) with at least 20 other different hnRNP and heterogeneous nuclear RNA in the nucleous.	Nucleus. Component of ribonucleosomes.
1142	Splice Isoform Short of Proteasome subunit alpha type 1	IPI00016832	PSMA1	11	*-1.3*	*0.11*	3.25	0.00052	6.89	45443	6.15	29822	92	29	7	Involved in an ATP/ubiquitin-dependent non-lysosomal proteolytic pathway.	Cytoplasmic and nuclear
786	Stathmin	IPI00479997	STMN1	1	*1.09*	*0.24*	2.18	0.00028	6.98	76020	5.77	17161	124	51	9	It prevents assembly and promotes disassembly of microtubules.	Cellular
1492	Stathmin	IPI00479997	STMN1	1	1.26	0.012	-2.19	8.40E-05	5.5	20000	5.77	17161	[73]	10	2	It prevents assembly and promotes disassembly of microtubules.	Cellular
1169	Tissue inhibitor of metalloproteinase 1	IPI00642739	TIMP1	X	-1.56	0.00026	2.24	5.60E-05	7.3	50000	8.4	16560	88	52	6	Tissue inhibitor of metalloproteinase 1 (Erythroid potentiating activity, collagenase inhibitor).	Secreted
1199	Tissue inhibitor of metalloproteinase 1	IPI00642739	TIMP1	X	-2.36	0.003	1.3	0.047	7.92	40362	8.4	16560	86	65	8	Tissue inhibitor of metalloproteinase 1 (Erythroid potentiating activity, collagenase inhibitor).	Secreted
454	Tryptophanyl-tRNA synthetase	IPI00295400	WARS	14	1.26	0.011	-2.42	4.50E-05	6.3	107811	5.83	53474	80	24	11	Belongs to the class-I aminoacyl-tRNA synthetase family.	Cellular
539	Tubulin beta-2 chain	IPI00011654	TUBB	6	*-1.08*	*0.97*	2.57	0.00014	4.56	100535	4.78	50095	118	41	19	Tubulin is the major constituent of microtubules.	Cellular
1335	Ubiquitin carboxyl-terminal hydrolase isozyme L1	IPI00018352	UCHL1	4	*1.22*	*0.072*	2.9	0.00024	5.24	31041	5.33	25151	121	47	12	Ubiquitin-protein hydrolase involved both in the processing of ubiquitin precursors and of ubiquitinated proteins.	Cytoplasm

Table 4.1 Differentially expressed proteins in the secretome of the EOC cell models 18-D-22/TOV-112D and 18-G-5/TOV-21G identified by mass spectrometry. Protein features that were matched across all gels with a fold change ≥ 2 fold where $p \leq 0.05$ were identified by MS. Orange shading indicates an increase in expression in the hybrid clone verses parent and green indicates a decrease. Yellow shading indicates multiple identifications from a single gel spot. Protein identifications were made by database searching of peptide ion fragments from LC-MS/MS or by MALDI-TOF MS PMF (indicated by [ ] in the 'Score' column). The identifications were scored according to algorithms that take into account mass accuracy and peptide coverage. The search criteria used allowed +/- 50 ppm mass error and up to 2 missed cleavages. The identified proteins were partially verified by comparison of their theoretical molecular weights and pIs with gel position on the master gel.

Multiple isoforms of insulin-like growth factor-binding protein 2 (IGFBP2) and insulin-like growth factor binding protein 7 (IGFBP7) were identified (Grimberg and Cohen 2000; Zumkeller 2001). Of these secreted proteins, the former appears to stimulate cellular proliferation (Lee, Mircean et al. 2005; Chakrabarty and Kondratick 2006) and the latter inhibits proliferation by binding IGF1, IGF2 and insulin (Oh, Nagalla et al. 1996; Yamanaka, Wilson et al. 1997). Two isoforms of IGFBP2 were identified displaying down-regulation of expression in the 18-D-22 cell line. Conversely, one of these isoforms and a third were significantly elevated in the 18-G-5 hybrid clone (Fig 4.3). IGFBP2 has been previously found to be overexpressed in malignant ovarian tissues and in the serum and cystic fluid of ovarian cancer patients (Wang, Rosen et al. 2006) and appears to increase the invasive capability of ovarian cancer cells (Lee, Mircean et al. 2005; Wang, Rosen et al. 2006). Its expression level also seems to positively correlate with levels of the EOC serum marker CA125, and it is also overexpressed in a variety of other cancers (Quinn, Treston et al. 1996). Six isoforms of IGFBP7 were significantly up-regulated in the 18-G-5 cell line. IGFBP7 expression is down regulated in several types of cancer, and restoration of expression induces cellular senescence or apoptosis (Swisshelm, Ryan et al. 1995; Lopez-Bermejo, Buckway et al. 2000; Landberg, Ostlund et al. 2001; Mutaguchi, Yasumoto et al. 2003). The nature of the identified isoforms is unclear but may represent glycosylated or splice variant forms, including a very acidic form (Fig 4.4).

		18-D-22/112D		18-G-5/21G	
Master No.	Name	Av. Ratio	T-test	Av. Ratio	T-test
981	Insulin-like growth factor binding protein 2 precursor	*1.29*	*0.058*	2.12	2.80E-05
1089	Insulin-like growth factor binding protein 2 precursor	-2.96	6.90E-06	*-1.19*	*0.27*
1169	Insulin-like growth factor binding protein 2 precursor	-1.56	0.00026	2.24	5.60E-05
962	Insulin-like growth factor binding protein 7 precursor	*-1.29*	*0.26*	3.52	4.10E-06
991	Insulin-like growth factor binding protein 7 precursor	*1.36*	*0.14*	3.13	0.00025
1108	Insulin-like growth factor binding protein 7 precursor	*-1.17*	*0.15*	2.23	0.00044
1043	Insulin-like growth factor binding protein 7 precursor	1.46	0.015	2.12	0.00032
1030	Insulin-like growth factor binding protein 7 precursor	*-1.05*	*0.54*	4.35	3.40E-06
1033	Insulin-like growth factor binding protein 7 precursor	1.81	0.001	3.54	8.80E-07

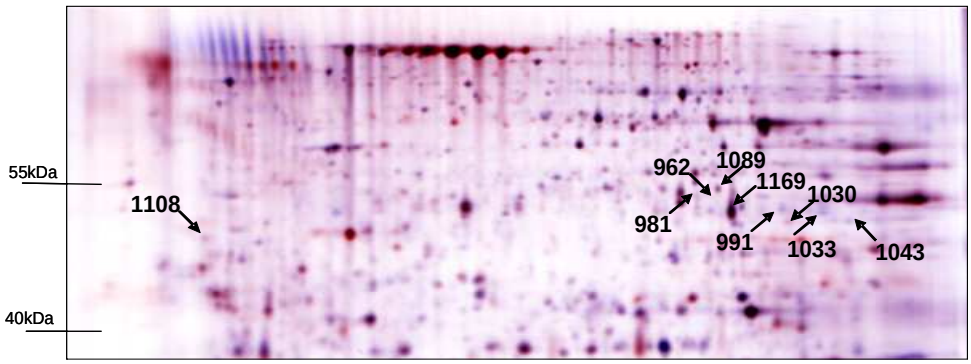

Figure 4.4 Change in protein expression of IGFBP2 and IGFBP7 isoforms. (A) Table displaying the fold-change in expression for the protein isoforms in each cell model. Orange indicates an increase and green a decrease in expression over 2-fold. (B) Gel image displaying each protein isoform of IGFBP2 and IGFBP7.

Galectin-1 was down-regulated in both hybrid clones compared to their parental lines (Fig 4.5A). Galectin-1 is a carbohydrate-binding protein and a component of the extracellular matrix thought to be involved in cell adhesion, cell proliferation and tumour progression. It has been reported that ovarian cancer antigen CA125 is a counter receptor for galectin-1, binding specifically to human galectin with high efficiency *in vitro* (Seelenmeyer, Wegehingel et al. 2003). Pigment epithelium-derived factor precursor

displayed a contrasting expression in the two cell line models (Fig 4.5B). Expression was significantly down-regulated (-3.05 fold) in the 18-D-22 cell line and up-regulated (2.61 fold) in the 18-G5 hybrid cell line. Pigment epithelium-derived factor has been shown to be a potent inhibitor of angiogenesis (Cheung, Au et al. 2006). Two isoforms of the protein tissue inhibitor metalloproteinase 1 (TIMP1) were identified which both displayed opposite changes in expression in the two cell models (Fig 4.5C/D) (Table 4.1). The family of tissue inhibitors of metalloproteinases (TIMPs) inhibit various matrix metalloproteinase (MMP) activities (Nelson, Fingleton et al. 2000) which are thought to be important for the creation and maintenance of a microenvironment that facilitates growth and angiogenesis of tumours. TIMP1 is reported to induce proliferation, promote angiogenesis and regulate apoptosis (Ikenaka, Yoshiji et al. 2003) (Reed, Koike et al. 2003). Finally, the hormone prolactin, which has been used in a multiplexed biomarker panel for ovarian cancer detection (Mor, Visintin et al. 2005) was found to be up-regulated (2.28 fold) in the 18-D-22 hybrid (Fig 4.5E).

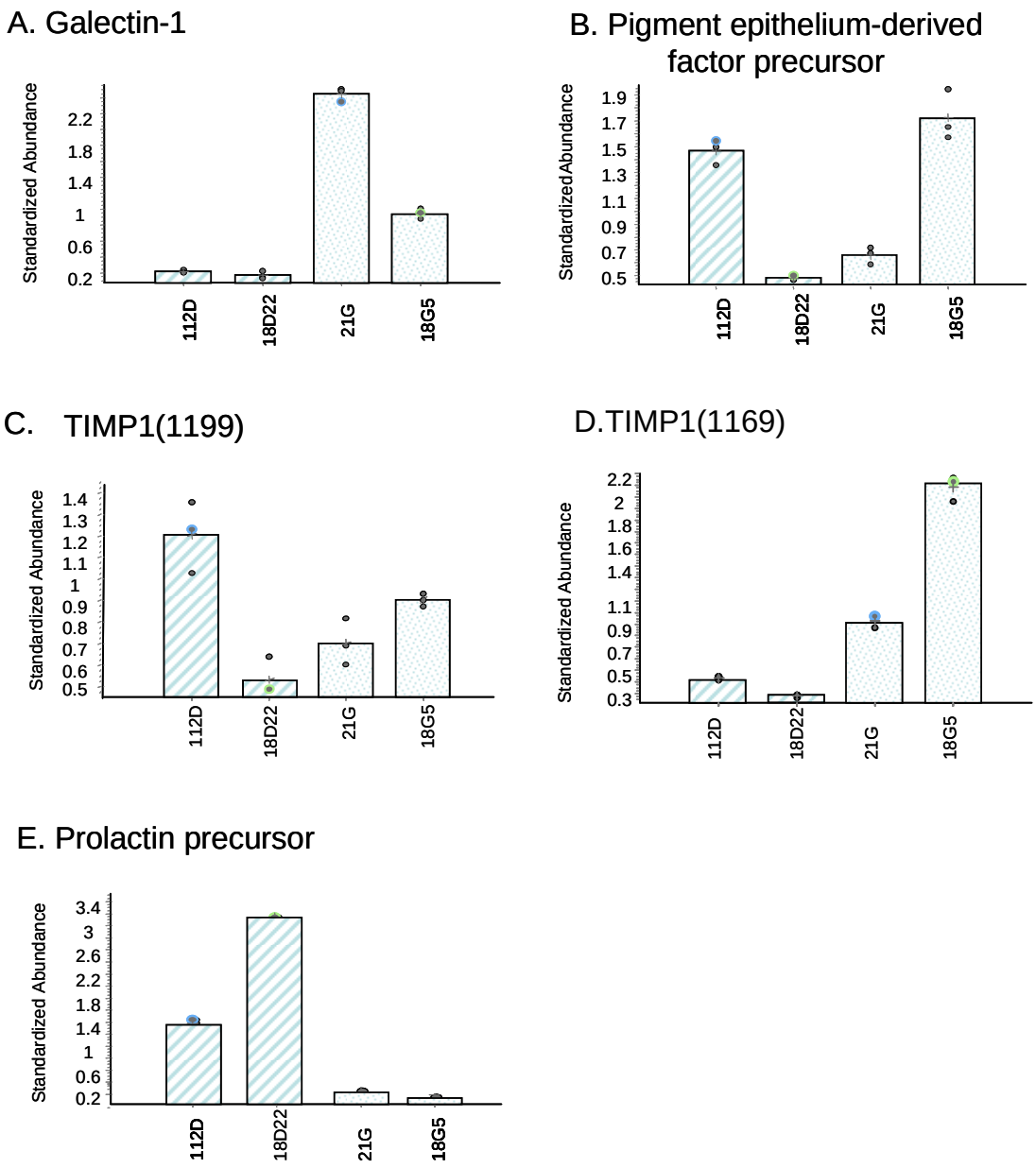

Figure 4.5 DeCyder analysis of differential protein expression in the 18-G-5/21G and 18-D-22/112D cell line comparisons for several of the identified secreted proteins. Graphical representations for selected proteins are shown as average standardised abundance (i.e. abundance versus the Cy2-labelled standard) for each condition with triplicate measurements. Where multiple isoforms were identified spot numbers are indicated in brackets.

4.3 2D-DIGE comparison of secreted proteins from two hybrid clones and parental cell lines

A 9 gel experiment was next undertaken involving a comparison between the two parent cell lines and both Ch18 hybrid clones displaying the most potent tumourigenic suppression (see Introduction, section). Secreted proteins were prepared as previously described from 8 x 15 cm plates using 5 ml media/plate. A total of 1779 distinct protein features were matched across the gels using Decyder image analysis software (Fig 4.6).

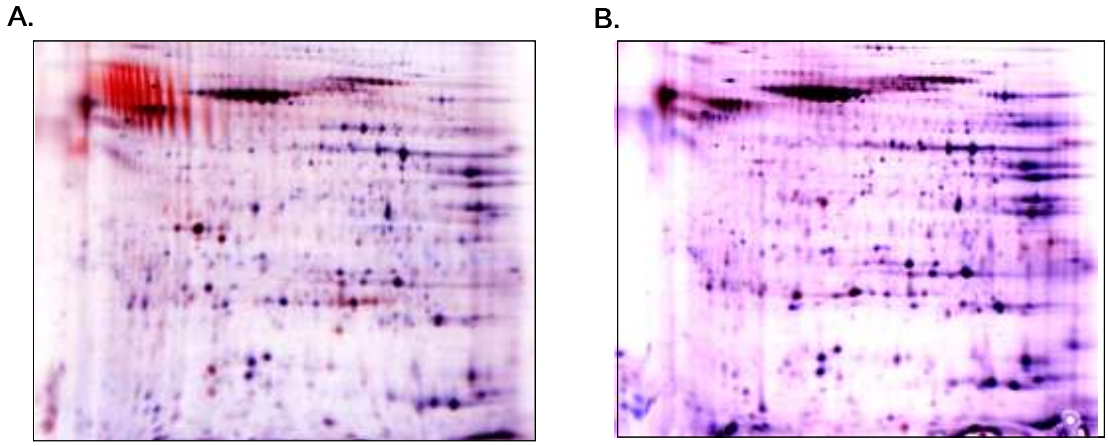

Figure 4.6 Representative superimposed gel images for parental:hybrid comparisons of secreted protein. 100 µg of secreted protein from each cell line was labelled in triplicate with either Cy3 or Cy5. The internal standard was created from a pool of all the cell lines and labelled with Cy2. (A) Example gel of 18-D22/TOV-112D comparison. The hybrid clone cell line is represented by blue and the parent cell line by red. (B) Example gel of 18-G1.26/TOV-21G comparison. The hybrid clone cell line is represented by blue and the parental cell line by red.

The comparison between the TOV-112D parental cell line and the 18-D-22 and 18-D-23 hybrid cell lines resulted in 122 and 63 protein features displaying significant differential expression, respectively (≥2 fold change; n=3; $p \leq 0.05$). For the comparison between the TOV-21G parental cell line and the 18-G-5 and 18-G-1.26 hybrid cell lines, 348 and 23 protein features displayed significant differential expression at the same threshold cut-offs. These protein spots were selected for picking and matched to a CCB stained gel image and spots excised and digested with trypsin for identification by mass spectrometry. A total of 384 spots were picked, and of these, 160 yielded confident identifications by LC-MS/MS using the same stringent criteria to search the NCBI and IPI databases.

Inspection of the gel images and identification of protein spots revealed a higher abundance of bovine serum albumin (BSA) and other serum proteins in the conditioned media from the 18-G-5 cells compared to the other cell lines (Fig 4.7).

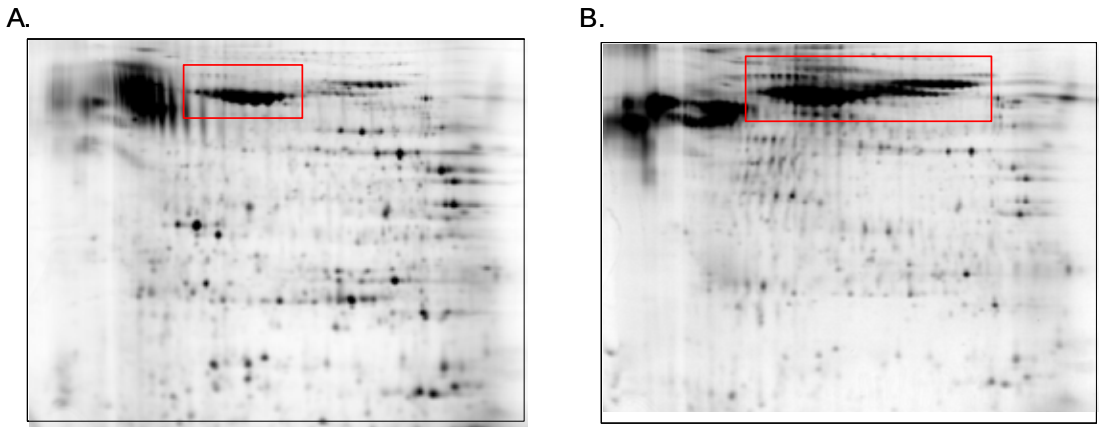

Figure 4.7 Gel images displaying higher abundance of bovine serum proteins in 18-G-5 cells. (A) Displays 18-G-1.26 secreted proteins (B) Displays 18-G-5 secreted proteins. The spots from the regions in red were identified as BSA and bovine serotranferrin.

This is most probably attributed to retention of serum proteins by the 18-G-5 cells at the washing and media swap stage during cell culture. The higher abundance of BSA and other serum proteins in this fraction led to a reduction in endogenous protein in the sample and is likely to have resulted in the much larger number of differences displayed by the 18-G-5 clone versus its parent in the analysis. Importantly, the levels of these serum proteins in the other cell lines were not altered and so the differentially expressed proteins identified could be used for data interpretation. This did not occur in the previous experiments, but highlights the difficulty in preparing secreted protein fractions from cells in culture. It is not sufficient to starve the cells and replenish with serum free media for collection in all cases. Different cell types may have higher affinity for binding/retaining serum proteins, thus making it more difficult to wash unwanted media

proteins from their surface. To differentiate proteins released into the media from cells protein and constituents of the serum utilized for culture, one can grow cells in the presence of [^{13}C]-labelled lysine and use the mass shift to differentiate cellular from serum-derived proteins (Faca, Ventura et al. 2008). Application iof heavy labellling in this study would prove too expensive given the number of cell lines under study and the scale of cell culture required for sufficient 'secreted' protein for 2D-DIGE analysis.

The experiment was thus repeated with more stringent washing. Image analysis revealed a total of 262 spots displaying a change in average abundance of $\geq$ 2 fold. These spots were picked from two Sypro-Ruby-stained gels, giving greater sensitivity. Identifications were made by LC-MS/MS on an LTQ Orbitrap XL linked to an Ultimate3000 nano-LC system (Table 4.2). The MS/MS peak lists were compared against theoretically expected tryptic peptide fragment masses in the IPI database submitted by the Mascot search engine including +2 and +3 peptide charge, mass tolerance of ± 30 ppm and a fragment mass tolerance of 0.1 Da. As before, identifications were accepted when at least two peptide sequences matched an entry with MOWSE scores above the p=0.05 homology threshold value.

4.3.1 Identification of differentially expressed proteins from two hybrid clones and parental cell lines

The direct comparison of the 18-D-22/TOV-112D secretome resulted in 228 differentially expressed protein spots, with 136 up-regulated and 82 down-regulated. For the 18-D-23/TOV-112D comparison, 143 were found to be differentially expressed with 124 up-regulated and 18 down-regulated. The comparison between 18-G-5/TOV-21G resulted in 32 differentially expressed spots with 7 up-regulated and 25 down-regulated. Finally, the 18-G-1.26/TOV-21G comparison resulted in 75 differentially expressed protein spots with 37 up-regulated and 38 down-regulated.

The number of differentially expressed spots was greater for each hybrid clone:parental comparison in this experiment compared to the previous, with the exception of the hybrid clone 18-G-5 where contamination in the previous experiment resulted in an exaggerated expression profile. However, the relative numbers changing between each comparison are comparable. This seems to be in contrast with the WCL analysis where the hybrid clones 18-G-5 and 18-G-1.26 displayed the greatest numbers of differentially expressed spots while the hybrid clones 18-D-22 and 23 displayed relatively few changes (see section 3.2.2). Additionally, the hybrid pairs in the secreted analysis displayed greater concordance in expression changes than that observed in the WCL analysis where only isoforms of two proteins, ALDH1A1 and LDHB, showed concordant expression in both hybrids and both cell models.

No gene products for chromosome 18 were reported. A good proportion (52%) of the identified proteins are known to be secreted and of these, IGFBP2, lumican, PEDGF/SERPINF1, prolactin, procollagen (III) and TIMP1 were previously identified as differentially expressed in the single hybrid clone versus parent comparison (section 4.2). It should be noted however that comparison of expression profiles between experiments is difficult because of the presence of multiple isoforms of each of the identified proteins and are hard to match. A number of secreted proteins not seen previously were also identified. These included apolipoprotein E, glucagon and IGFBP6. ApoE1 was significantly up-regulated in the 18-D-22/parental (2.99 fold) and 18-D-23/parental (3.54 fold) comparisons. This secreted protein mediates the binding, internalization and catabolism of lipoprotein particles. Functions seemingly unrelated to lipid transport have been reported for ApoE1 including the promotion of proliferation and survival in ovarian cancer cells (Chen, Pohl et al. 2005). IGFBP6 was also significantly up-regulated in the 18-D-22 (5.41 fold) and 18-D-23 (3.82 fold) hybrids compared to the parental TOV-112D cell line. In contrast, its expression was moderately down-regulated in both hybrid clones of the TOV-21G cell model. IGFBP6 is a member of the family of insulin-like growth factor binding proteins that regulate the functions of insulin-like growth factors which are important in cell survival and tumourigenesis (LeRoith and Roberts 2003). Three isoforms of glucagon, a hormone involved in carbohydrate metabolism, were identified, two displaying concordant up-regulation in the 18-D-22 and 18-D-23 cell lines and significant down-regulation in the 18-G-5 and 18-G-1.26 cell lines, whilst a third isoform displayed down-regulation in the 18-D-22 and 18-D-23 cell lines. Glycolytic rates are usually increased in cancer cells, the observed down-regulation of glucagon

secreted by the hybrid clones may be a consequence of the suppression of tumourigenic phenotype in these cell models. There were also differentially expressed proteins identified from the WCL analysis including ANXA1, ERp29, EIF5A, DLD, FSCN1, GRB2, LDHB, PDIA3, PRDX6, ALDH1A1 and UCHL1 where there was general agreement in direction of altered expression. For example, ERp29 was again down-regulated in the hybrid clones. This ER protein is involved in the processing of secretory proteins within the endoplasmic reticulum. It has been suggested that in the context of carcinogenesis, ERp29 facilitates secretion of proteins that mediate cross-talk between cancer cells and surrounding fibroblasts to confer a growth advantage (Mkrtchian, Baryshev et al. 2008). Thus, its down-regulation may participate in the observed suppression of neoplastic phenotype in these cell models. Two isoforms of lactate dehydrogenase B were identified. One isoform was conspicuous in that it displayed significant down-regulation in each of the hybrid clones of both cell models. However, the other isoform displayed moderate up-regulation in the 18-D-22 and 18-D-23 hybrid cell lines, but down-regulation in the 18-G-5 and 18-G-1.26 hybrid cell lines. This protein catalyses the reversible transformation of pyruvate to lactate, having a principal role in anaerobic cellular metabolism. It has been shown to be up-regulated in gynaecological malignancies and correlated with tumour grade (Simaga, Osmak et al. 2005; Koukourakis, Kontomanolis et al. 2008).

A number of isoforms of lumican were identified and all isoforms were significantly up-regulated in the 18-D-22 and 18-D-23 hybrid clones, but moderately down-regulated in the 18-G-5 and 18-G-1.26 hybrid clones versus their parental cell lines. Lumican belongs

to the family of small leucine rich repeat proteoglycans which constitute an important fraction of non-collagenous extracellular matrix proteins. Altered expression of lumican has been reported in a variety of cancers including breast, pancreatic and colorectal cancer (Vuillermoz, Khoruzhenko et al. 2004; Nikitovic, Katonis et al. 2008). Prolactin was again found to be significantly up-regulated (5.99 fold) in the 18-D-22/parental comparisons and in the 18-D-23/parental comparison (4.37 fold). Expression in the other hybrid cell lines was moderately down-regulated (<2 fold) compared to the parental TOV-21G cell line. Prolactin acts primarily in the mammary gland by promoting lactation. It has been shown to be linked to proliferation and survival in breast neoplasms (Manni, Wright et al. 1986) and to inhibit apoptosis in ovarian carcinoma (Asai-Sato, Nagashima et al. 2005). Also of note, were four isoforms of collagen alpha-1 (III) chain (COL3A1) displaying differential expression in the 18-D-22 and 18-D-23 hybrid cell lines. The different isoforms may arise as a result of differential glycosylation. It is likely that the most basic isoform, which was down-regulated compared to the other up-regulated forms, has a lower content of sialic acids and therefore different pI. The COL3A1 gene produces the components of type III collagen, where copies of this filament combine to make a molecule of type III procollagen. These triple stranded molecules are processed by enzymes outside the cell to remove protein segments from their ends. Once processed, they arrange themselves into long fibrils that become cross-linked providing strength and support around the cell. Levels of COL3A1 have been found to increase with the degree of malignancy in serous ovarian carcinomas (Tapper, Kettunen et al. 2001).

Master No.	Protein Name	HGNC	IPI	Chr.	18D22/122D Av. Ratio	18D22/122D T-test	18D23/112D Av. Ratio	18D23/112D T-test	18G5/21G Av. Ratio	18G5/21G T-test	18G126/21G Av. Ratio	18G126/21G T-test	Gel pI	Gel Mw	Pred pI	Pred Mwt	Score	% Cov	Function	Localisation
1318	3,2-trans-enoyl-CoA isomerase, mitochondrial (Isoform 1)	DCI	IPI00300567	16	-2.21	0.0012	-2.44	0.00012	-1.14	*0.18*	-1.2	0.037	6.45	28776	8.8	33080	118	8	Able to isomerize both 3-cis and 3-trans double bonds into the 2-trans form in a range of enoyl-CoA species.	Mitochondrion matrix.
1095	Annexin A1	ANXA1	IPI00218918	9	-4.57	0.00096	-5.16	0.00011	-1.11	*0.55*	1.3	*0.64*	8.44	38898	6.57	38918	574	35	Calcium/phospholipid-binding protein which promotes membrane fusion and is involved in exocytosis. This protein regulates phospholipase A2 activity. It seems to bind from two to four calcium ions with high affinity.	Cytoplasm
1061	Apolipoprotein E	APOE	IPI00021842	19	2.99	0.0081	3.54	0.0014	1.06	*0.69*	1.15	*0.34*	5.38	40028	5.65	36246	330	25	Mediates the binding, internalization, and catabolism of lipoprotein particles. It can serve as a ligand for the LDL (apo B/E) receptor and for the specific apo-E receptor (chylomicron remnant) of hepatic tissues.	Secreted
371	Collagen alpha-1(III) chain (Isoform 1)	COL3A1	IPI00021033	2	5.46	1.60E-06	3.63	0.00016	-1.28	*0.33*	1	*0.84*	4.17	73039	6.21	139733	63	1	Collagen type III occurs in most soft connective tissues along with type I collagen.	Secreted, extracellular space, extracellular matrix
512	Collagen alpha-1(III) chain (Isoform 1)	COL3A1	IPI00021033	2	-3.97	6.10E-05	-2.4	0.04	-1.49	*0.15*	-1.43	0.00059	8.99	67117	6.21	139733	639	10	Collagen type III occurs in most soft connective tissues along with type I collagen.	Secreted, extracellular space, extracellular matrix
1076	Collagen alpha-1(III) chain (Isoform 1)	COL3A1	IPI00021033	2	5.41	0.0047	3.82	0.0095	-1.32	0.0053	-1.68	0.0016	5.79	39432	6.21	139733	1289	7	Collagen type III occurs in most soft connective tissues along with type I collagen.	Secreted, extracellular space, extracellular matrix
1156	Collagen alpha-1(III) chain (Isoform 1)	COL3A1	IPI00021033	2	10.58	2.10E-05	6.2	5.00E-05	-1.41	0.0016	-1.68	0.00039	7.23	35598	6.21	139733	646	6	Collagen type III occurs in most soft connective tissues along with type I collagen.	Secreted, extracellular space, extracellular matrix
594	Dihydrolipoyl dehydrogenase, mitochondrial	DLD	IPI00015911	7	-3.52	7.70E-05	-1.85	0.0016	1.47	0.039	1.81	0.0026	9.06	63554	7.59	54686	464	19	Lipoamide dehydrogenase is a component of the glycine cleavage system as well as of the alpha-ketoacid dehydrogenase complexes.	Mitochondrial matrix
1318	Endoplasmic reticulum protein ERp29	ERP29	IPI00024911	12	-2.21	0.0012	-2.44	0.00012	-1.14	*0.18*	-1.2	0.037	6.45	28776	6.77	29032	112	29	Does not seem to be a disulfide isomerase. Plays an important role in the processing of secretory proteins within the ER, possibly by participating in the folding of proteins in the ER.	Endoplasmic reticulum lumen.
767	Enolase (Isoform alpha-enolase)	ENO1	IPI00465248	1	8.48	0.00027	5.15	0.00042	-1.34	0.0071	-1.82	0.00033	8.25	55528	7.01	47481	293	21	Multifunctional enzyme that, as well as its role in glycolysis, plays a part in various processes such as growth control, hypoxia tolerance and allergic responses. May also function in the intravascular and pericellular fibrinolytic system due to its ability to serve as a receptor and activator of plasminogen on the cell surface of several cell-types such as leukocytes and neurons.	Cytoplasm
1684	Eukaryotic translation initiation factor 5A-1 (Isoform 2)	EIF5A	IPI00376005	17	-1.15	*0.4*	1.31	0.042	-2.14	0.0012	-1.89	0.0037	4.86	13244	6.52	20442	426	41	Promotes the formation of the first peptide bond.	Nucleus
641	Fascin	FSCN1	IPI00163187	7	3.52	0.00013	2.2	3.80E-05	-1.18	*0.058*	-1.64	0.0039	6.01	61676	6.84	55123	246	23	Organizes filamentous actin into bundles with a minimum of 4.1:1 actin/fascin ratio.	Cytoplasm
990	Fructose-bisphosphate aldolase A	ALDOA	IPI00465439	16	-3.16	0.00019	-1.86	0.00053	1.04	*0.69*	1.63	0.0016	10.27	44279	8.3	39851	1297	50	D-fructose 1,6-bisphosphate = glycerone phosphate + D-glyceraldehyde 3-phosphate.	Cytoplasm
991	Fructose-bisphosphate aldolase A	ALDOA	IPI00465439	16	-3.39	0.00018	-1.97	0.0012	1.09	*0.47*	1.73	0.00066	10.43	44279	8.3	39851	732	37	D-fructose 1,6-bisphosphate = glycerone phosphate + D-glyceraldehyde 3-phosphate.	Cytoplasm
1710	Glucagon	GCG	IPI00306140	2	3.16	0.00074	3.29	0.00029	-8.14	2.50E-05	-9.13	0.00018	5.76	12941	5.84	20896	116	22	Glucagon plays a key role in glucose metabolism and homeostasis.	Secreted
1712	Glucagon	GCG	IPI00306140	2	3.61	0.00055	3.76	6.30E-05	-8.21	0.00022	-9.23	0.00028	5.28	12906	5.84	20896	1791	67	Glucagon plays a key role in glucose metabolism and homeostasis.	Secreted
1779	Glucagon	GCG	IPI00306140	2	-2.86	0.00011	-1.98	0.00094	-1	*0.99*	1.08	*0.49*	8.57	11446	5.84	20896	741	44	Glucagon plays a key role in glucose metabolism and homeostasis.	Secreted
1192	Glucosamine-6-phosphate isomerase 1	GNPDA1	IPI00009305	5	4.29	0.00031	2.75	0.001	-1.31	0.0063	-1.51	0.002	7.68	33986	6.42	32819	180	27	Seems to trigger calcium oscillations in mammalian eggs. These oscillations serve as the essential trigger for egg activation and early development of the embryo.	Cytoplasm
963	Glutaredoxin-3	GLRX3	IPI00008552	10	3.87	0.00081	2.45	0.0014	-1.16	*0.31*	-1.6	0.0029	5.2	45071	5.31	37693	91	8	May play a role in regulating the function of the thioredoxin system.	Cytoplasm, cell cortex. Under the plasma membrane. After PMA stimulation.
1267	Glutathione transferase omega-1	GSTO1	IPI00019755	10	-2.87	0.00075	-1.64	0.0026	-1.34	*0.17*	1.5	*0.095*	6.49	30765	6.23	27833	625	43	Exhibits glutathione-dependent thiol transferase and dehydroascorbate reductase activities.	Secreted
1412	Growth factor receptor-bound protein 2 (Isoform 1)	GRB2	IPI00021327	17	3.7	0.0016	2.53	0.0042	-1.45	0.0056	-1.48	0.0012	6.88	25314	5.89	25304	66	15	Isoform GRB3-3 does not bind to phosphorylated epidermal growth factor receptor (EGFR) but inhibits EGF-induced transactivation of a RAS-responsive element. Isoform GRB3-3 acts as a dominant negative protein over GRB2 and by suppressing proliferative signals, may trigger active programmed cell death.	Golgi apparatus (By similarity).
499	heat shock protein 60 kDa, mitochondrial	HSPD1	IPI00784154	2	6.42	0.00011	4.06	0.00035	-1.74	0.00095	-1.57	0.0065	5.01	67669	5.7	61187	92	8	Implicated in mitochondrial protein import and macromolecular assembly. May facilitate the correct folding of imported proteins. May also prevent misfolding and promote the refolding and proper assembly of unfolded polypeptides generated under stress conditions in the mitochondrial matrix.	Mitochondrial matrix.

1558	HNRPA2B1 protein	tNRNPA2B:	IPI00386854	7	-4.44	0.00046	-3.69	0.00073	1.07	*0.68*	-1.41	*0.24*	9.19	18984	4.79	28451	455	34	
1157	Insulin-like growth factor-binding protein 2	IGFBP2	IPI00297284	2	-1.3	0.048	1.19	*0.14*	-4.21	4.20E-05	-4.93	0.00011	5.42	35696	7.48	36198	375	30	IGF-binding proteins prolong the half-life of the IGFs and have been shown to either inhibit or stimulate the growth promoting effects of the IGFs on cell culture. They alter the interaction of IGFs with their cell surface receptors.	Secreted
1076	Insulin-like growth factor-binding protein 6	IGFBP6	IPI00029235	12	5.41	0.0047	3.82	0.0095	-1.32	0.0053	-1.68	0.0016	5.79	39432	8.15	26219	162	9	IGF-binding proteins prolong the half-life of the IGFs and have been shown to either inhibit or stimulate the growth promoting effects of the IGFs on cell culture. They alter the interaction of IGFs with their cell surface receptors.	Secreted
626	L-lactate dehydrogenase B chain	LDHB	IPI00219217	12	-2.29	0.00074	-2.31	0.0008	-3.77	0.0063	-3.43	0.0074	8.14	62183	5.71	36900	688	31	S)-lactate + NAD(+) = pyruvate + NADH.	Cytoplasm
743	L-lactate dehydrogenase B chain	LDHB	IPI00219217	12	1.98	0.00059	1.83	0.0016	-2.68	0.0055	-2	0.0034	6.27	56753	5.71	36900	170	14	S)-lactate + NAD(+) = pyruvate + NADH.	Cytoplasm
307	Lumican	LUM	IPI00020986	12	3.82	3.80E-05	2.29	1.10E-05	-1.26	0.018	-2.21	4.60E-05	8.34	75882	6.16	38747	375	18	Binds to laminin	Secreted, extracellular space, extracellular matrix
373	Lumican	LUM	IPI00020986	12	5.57	0.0027	3.53	0.01	-1.21	*0.41*	-1.55	*0.18*	4.45	72741	6.16	38747	155	14	Binds to laminin	Secreted, extracellular space, extracellular matrix
470	Lumican	LUM	IPI00020986	12	10.5	4.60E-05	6.58	0.00019	-1.74	0.00011	-1.52	0.0052	4.46	68411	6.16	38747	135	16	Binds to laminin	Secreted, extracellular space, extracellular matrix
472	Lumican	LUM	IPI00020986	12	10.05	8.60E-05	6.59	0.00014	-1.76	1.60E-05	-1.61	0.00021	4.56	68225	6.16	38747	181	25	Binds to laminin	Secreted, extracellular space, extracellular matrix
473	Lumican	LUM	IPI00020986	12	17.27	0.00013	10.42	0.00025	-1.71	0.00022	-1.61	0.0014	4.67	68132	6.16	38747	47	2	Binds to laminin	Secreted, extracellular space, extracellular matrix
499	Lumican	LUM	IPI00020986	12	6.42	0.00011	4.06	0.00035	-1.74	0.00095	-1.57	0.0065	5.01	67669	6.16	38747	157	15	Binds to laminin	Secreted, extracellular space, extracellular matrix
543	Lumican	LUM	IPI00020986	12	6.35	0.00068	3.8	0.00072	-1.3	0.0042	-1.6	0.012	4.62	65401	6.16	38747	182	13	Binds to laminin	Secreted, extracellular space, extracellular matrix
1045	N(G)-dimethylarginine dimethylaminohydrolase 1	DDAH1	IPI00220342	1	3.07	0.00045	2.59	0.00067	-1.31	0.046	-1.58	0.0055	5.81	40689	5.53	31444	607	44	Hydrolyzes N(G),N(G)-dimethyl-L-arginine (ADMA) and N(G)-monomethyl-L-arginine (MMA) which act as inhibitors of NOS. Has therefore a role in nitric oxide generation.	Cytoplasm
543	Nucleobindin-1	NUCB1	IPI00295542	19	6.35	0.00068	3.8	0.00072	-1.3	0.0042	-1.6	0.012	4.62	65401	5.15	53846	672	35	Major calcium-binding protein of the Golgi. May have a role in calcium homeostasis (By similarity).	Golgi apparatus, cis-Golgi network membrane; Peripheral membrane protein; Lumenal side.
1329	Peroxiredoxin-6	PRDX6	IPI00220301	1	3	0.0007	2.19	0.0028	-1.33	*0.16*	-1.31	*0.14*	8.5	28503	6	25133	979	63	Involved in redox regulation of the cell. Can reduce H(2)O(2) and short chain organic, fatty acid, and phospholipid hydroperoxides. May play a role in the regulation of phospholipid turnover as well as in protection against oxidative injury.	Cytoplasm
743	Pigment epithelium-derived factor	SERPINF1	IPI00006114	17	1.98	0.00059	1.83	0.0016	-2.68	0.0055	-2	0.0034	6.27	56753	5.97	46484	285	16	Neurotrophic protein; induces extensive neuronal differentiation in retinoblastoma cells. Potent inhibitor of angiogenesis. It exhibits no serine protease inhibitory activity.	Secreted
753	Pigment epithelium-derived factor	SERPINF1	IPI00006114	17	-3.41	7.40E-05	-2.77	0.00032	1.04	*0.85*	1.38	0.059	8.46	56521	5.97	46484	142	16	Neurotrophic protein; induces extensive neuronal differentiation in retinoblastoma cells. Potent inhibitor of angiogenesis. It exhibits no serine protease inhibitory activity.	Secreted
1409	Prolactin	PRL	IPI00000871	6	5.99	0.00037	4.37	0.00057	-1.47	0.012	-1.62	0.0033	6.4	25418	6.5	26329	489	36	Belongs to the somatotropin/prolactin family.	Secreted
1283	Proteasome subunit alpha type-4	PSMA4	IPI00299155	15	-2.68	0.00069	-1.71	0.0019	-1.24	*0.15*	1.02	*0.85*	9.69	29897	7.57	29750	334	25	The proteasome is a multicatalytic proteinase complex which is characterized by its ability to cleave peptides with Arg, Phe, Tyr, Leu, and Glu adjacent to the leaving group at neutral or slightly basic pH. The proteasome has an ATP-dependent proteolytic activity.	Cytoplasm. Nucleus.
1329	Proteasome subunit alpha type-6	PSMA6	IPI00029623	14	3	0.0007	2.19	0.0028	-1.33	*0.16*	-1.31	*0.14*	8.5	28503	6.34	27838	418	20	The proteasome is a multicatalytic proteinase complex which is characterized by its ability to cleave peptides with Arg, Phe, Tyr, Leu, and Glu adjacent to the leaving group at neutral or slightly basic pH. The proteasome has an ATP-dependent proteolytic activity.	Cytoplasm. Nucleus.
1412	Proteasome subunit beta type-4	PSMB4	IPI00555956	1	3.7	0.0016	2.53	0.0042	-1.45	0.0056	-1.48	0.0012	6.88	25314	5.89	25304	66	15	The proteasome is a multicatalytic proteinase complex which is characterized by its ability to cleave peptides with Arg, Phe, Tyr, Leu, and Glu adjacent to the leaving group at neutral or slightly basic pH. The proteasome has an ATP-dependent proteolytic activity.	Cytoplasm. Nucleus.
474	Protein disulfide-isomerase A3	PDIA3	IPI00025252	15	20.22	0.00066	12.3	0.0013	-1.72	2.00E-06	-1.59	0.0019	4.83	68225	5.98	57146	1742	31	Catalyzes the rearrangement of -S-S- bonds in proteins.	Endoplasmic reticulum lumen
575	Protein disulfide-isomerase A3	PDIA3	IPI00025252	15	4.65	0.0028	2.93	0.00013	-1.59	*0.078*	-1.99	0.0015	6.82	64251	5.98	57146	323	20	Catalyzes the rearrangement of -S-S- bonds in proteins.	Endoplasmic reticulum lumen
584	Protein disulfide-isomerase A3	PDIA3	IPI00025252	15	-3.06	8.30E-05	-2.76	4.20E-05	-1.06	*0.44*	-1.2	0.033	6.4	63902	5.98	57146	2272	42	Catalyzes the rearrangement of -S-S- bonds in proteins.	Endoplasmic reticulum lumen
497	Pyruvate kinase isozymes M1/M2 (Isoform M2)	PKM2	IPI00479186	15	-1.5	0.099	1.16	*0.34*	2	0.0023	3.8	4.50E-06	9.83	67301	7.96	58470	178	24	Glycolytic enzyme that catalyzes the transfer of a phosphoryl group from phosphoenolpyruvate to ADP, generating ATP.	Cytoplasm
631	Retinal dehydrogenase 1	ALDH1A1	IPI00218914	9	-3.87	0.00056	-2.38	0.0023	1.09	*0.73*	1.5	*0.19*	8.8	62352	6.3	55454	768	36	Binds free retinal and cellular retinol-binding protein- bound retinal. Can convert/oxidize retinaldehyde to retinoic acid (By similarity).	Cytoplasm

645	Retinal dehydrogenase 1	ALDH1A1	IPI00218914	9	-4.62	8.00E-06	-3.07	8.30E-05	-4.92	0.012	-10.15	3.70E-05	8.48	61844	6.3	55454	267	20	Binds free retinal and cellular retinol-binding protein- bound retinal. Can convert/oxidize retinaldehyde to retinoic acid (By similarity).	Cytoplasm
717	Retinal dehydrogenase 1	ALDH1A1	IPI00218914	9	2.29	0.011	1.94	0.018	-2.47	0.00012	-1.92	0.0026	5.85	57297	6.3	55454	986	55	Binds free retinal and cellular retinol-binding protein- bound retinal. Can convert/oxidize retinaldehyde to retinoic acid (By similarity).	Cytoplasm
1283	RSU1 Ras suppressor protein 1	RSU1	IPI00017256	10	-2.68	0.00069	-1.71	0.0019	-1.24	*0.15*	1.02	*0.85*	9.69	29897	8.57	31521	51	12	Potentially plays a role in the Ras signal transduction pathway. Capable of suppressing v-Ras transformation in vitro.	Cytoplasm
1684	SMT3 suppressor of mif two 3 homolog 2 isoform b precursor	SMT3	IPI00140827	X	-1.15	*0.4*	1.31	0.042	-2.14	0.0012	-1.89	0.0037	4.86	13244	5.32	10889	380	27	Involved in a variety of cellular processes, such as nuclear transport, transcriptional regulation, apoptosis, and protein stability. It is not active until the last two amino acids of the carboxy-terminus have been cleaved off.	Cytoplasm
1680	Superoxide dismutase [Cu-Zn]	SOD1	IPI00218733	21	2.6	0.00097	2.5	0.00018	-5.36	7.30E-05	-5.54	0.00092	6.58	13299	5.7	16154	854	35	Destroys radicals which are normally produced within the cells and which are toxic to biological systems.	Cytoplasm
444	T-complex protein 1 subunit alpha	TCP1	IPI00290566	6	6.76	0.001	3.63	0.0045	-1.46	0.011	-1.91	0.0019	6.91	70207	5.8	60819	70	4	Molecular chaperone; assists the folding of proteins upon ATP hydrolysis. Known to play a role, in vitro, in the folding of actin and tubulin.	Cytoplasm
1283	TIMP1 Metalloproteinase inhibitor 1	TIMP1	IPI00032292	X	-2.68	0.00069	-1.71	0.0019	-1.24	*0.15*	1.02	*0.85*	9.69	29897	8.46	23840	74	13	Complexes with metalloproteinases (such as collagenases) and irreversibly inactivates them. Also mediates erythropoiesis in vitro; but, unlike IL 3, it is species-specific, stimulating the growth and differentiation of only human and murine erythroid progenitors. Known to act on MMP-1, MMP-2, MMP-3, MMP-7, MMP-8, MMP-9, MMP-10, MMP-11, MMP-12, MMP-13 and MMP-16. Does not act on MMP-14.	Secreted
1217	Tropomyosin alpha-4 chain (Isoform 1)	TPM4	IPI00010779	19	-2.25	0.00082	-1.9	0.0064	1.32	*0.28*	1.38	0.034	4.32	32846	4.67	28619	1915	52	Binds to actin filaments in muscle and non-muscle cells. Plays a central role, in association with the troponin complex, in the calcium dependent regulation of vertebrate striated muscle contraction. Smooth muscle contraction is regulated by interaction with caldesmon. In non-muscle cells is implicated in stabilizing cytoskeleton actin filaments.	Cytoplasm
1401	Ubiquitin carboxyl-terminal hydrolase isozyme L1	UCHL1	IPI00018352	4	-1.6	0.017	1.11	*0.24*	-2.27	0.0091	-3.5	0.0013	5.57	25837	5.33	25151	1103	62	Ubiquitin-protein hydrolase involved both in the processing of ubiquitin precursors and of ubiquitinated proteins. This enzyme is a thiol protease that recognizes and hydrolyzes a peptide bond at the C-terminal glycine of ubiquitin. Also binds to free monoubiquitin and may prevent its degradation in lysosomes. The homodimer may have ATP-independent ubiquitin ligase	Cytoplasm
1318	Uncharacterized protein ENSP00000348237		IPI00453476	12	-2.21	0.0012	-2.44	0.00012	-1.14	*0.18*	-1.2	0.037	6.45	28776	6.67	29003	278	19	Belongs to the phosphoglycerate mutase family.	Cytoplasm
1076	Vesicular integral-membrane protein VIP36	LMAN2	IPI00009950	5	5.41	0.0047	3.82	0.0095	-1.32	0.0053	-1.68	0.0016	5.79	39432	6.46	40545	80	5	Plays a role as an intracellular lectin in the early secretory pathway. Interacts with N-acetyl-D-galactosamine and high-mannose type glycans and may also bind to O-linked glycans. Involved in the transport and sorting of glycoproteins carrying high mannose-type glycans (By similarity).	Membrane
611	Xaa-Pro dipeptidase	PEPD	IPI00257882	19	3.89	0.00013	2.35	5.20E-05	-1.37	0.01	-1.86	0.0024	6.53	62267	5.64	55311	92	5	Splits dipeptides with a prolyl or hydroxyprolyl residue in the C-terminal position. Plays an important role in collagen metabolism because the high level of iminoacids in collagen.	Cytoplasm
1614	Xaa-Pro dipeptidase	PEPD	IPI00257882	19	-3	0.00034	-2.05	0.00072	1.29	*0.14*	1.13	*0.19*	6.52	14852	5.64	55311	47	9	Splits dipeptides with a prolyl or hydroxyprolyl residue in the C-terminal position. Plays an important role in collagen metabolism because the high level of iminoacids in collagen.	Cytoplasm

Table 4.2 Differentially expressed proteins in the secretome of the EOC cell models identified by mass spectrometry. Protein features that were matched across all gels with a fold change ≥ 2 fold where $p \leq 0.05$ were identified by LC-MS/MS. Orange shading indicates an increase in expression and green indicates a decrease. Protein identifications were made by database searching of peptide ion fragments from LC-MS/MS generated peak lists. The search criteria used allowed +/- 30 ppm peptide mass error and up to 2 missed cleavages. The identified proteins were verified by comparison of their theoretical molecular weights and pIs with gel position on the master gel.

4.4 Conclusions

To answer one of the aims of this research, a method was developed to isolate the secreted proteome of cells in culture. Cells were grown in standard medium until reaching a confluence of 80%. These were then washed extensively to remove residual-serum proteins and were then cultured in serum-free medium before being harvested and cleared of dead and detached cells. A combination of ultrafiltration and subsequent desalting on columns resulted in a secreted protein extract amenable to 2D-DIGE analysis. In the analysis of conditioned medium, as expected, a proportion of classically secreted proteins were identified, however, there was some overlap with the WCL analyses as described earlier. Notable among the classically secreted proteins identified were the insulin-like growth factor binding proteins. These have a regulatory role in the insulin-like growth factor signalling system that is important in the growth and development of cells and thought to be particularly prominent in tumourigenesis (Lee, Mircean et al. 2005; Chakrabarty and Kondratick 2006). Of these, much work has been published on elevated levels of IGFBP2 in ovarian cancer and its value as a prognostic marker (Baron-Hay, Boyle et al. 2004). In this study, the less well characterised IGFBP6 and IGFBP7 were also identified as differentially expressed in the models of neoplastic suppression. The obvious importance of this family of proteins in tumourigenesis necessitates further understanding of the role that these two IGFBPs play. Their value as markers of neoplastic suppression cannot be ignored. Another secreted protein, pigment epithelium-derived factor precursor (PEDF), was identified as differentially expressed in both analyses and is reported to be involved in ovarian cancer development and

progression (Phillips, Ziegler et al. 1996). Its role in growth inhibition and apoptosis and observed decrease in expression in transformed cells has implicated PEDF as a potential tumour suppressor gene in ovarian cancers (Cheung, Au et al. 2006). Two isoforms were identified in one experiment, one displaying down-regulation in one hybrid pair and up-regulation in the other hybrid pair, whilst the second displayed the opposite. The secreted protein, galectin-1, identified as differentially expressed in one of the hybrid cell lines has been shown to interact specifically with CA125. A study has proposed a link between the expression of CA125 by tumour cells with the increased cell-surface expression of galectin-1 and further postulates a functional role for CA125 as a cargo protein. Undoubtedly, this emphasizes the potential of galectin-1 as a marker of neoplastic suppression in these models. Unfortunately, galectin-1 was only identified as differentially expressed in one hybrid cell-line; however, this does not mean expression is not altered in the other cell model. It is possible that the protein was differentially expressed but its identification was missed. Of the other secreted proteins identified as differentially expressed, all have been implicated in tumourigenesis, and roles in ovarian cancer have been suggested in the literature. These proteins include apolipoprotein E, involved in proliferation in ovarian cancer cells (Chen, Pohl et al. 2005); prolactin, involved in the inhibition of apoptosis in ovarian cancer (Asai-Sato, Nagashima et al. 2005); lactate dehydrogenase, found to be up-regulated in gynaecological malignancy (Yuce, Baykal et al. 2001); and TIMP1 and lumican, both of which have been implicated in the proliferation of cancer cells (Ping Lu, Ishiwata et al. 2002; Nakopoulou, Giannopoulou et al. 2003). Future work would be to assess the value of these candidate markers in the serum of women diagnosed with malignant ovarian cancer, benign disease

and matched healthy controls from the UKOPS (United Kingdom Ovarian Cancer Population Study) using immunoassays.

Chapter 5 Profiling of models of OC tumour suppression by 2D-LC-MS/MS with Tandem Mass Tags for Quantitation

Introduction

It has been over 30 years since O'Farrell introduced 2-dimensional polyacrylamide gel electrophoresis. Much improvement has been made to this technique over the years by researchers. However, 2DE still has limitations because it poorly resolves specific classes of proteins, such as very large and very small proteins, basic proteins and hydrophobic proteins. Considering the important functions these classes of proteins might have receptors, signal transducers and transporters etc) it is important that these proteins were not excluded in this study. Thus, although 2DE remains a standard tool for proteome research, improvements in chromatography-based separation linked to automated MS/MS have paved the way for new and exciting quantitative MS-based techniques.

Gel-free approaches have addressed the challenges presented by complex protein mixtures. In its simplest form, a complex mixture of proteins would be digested to peptides and separated over a gradient profile by charge and/or hydrophobic interactions and eluted peptides introduced to the mass spectrometer for automatic precursor ion detection and subsequent fragmentation carried out in a data dependent fashion for the

duration of the experiment. For complex mixtures one dimensional separation of peptides does not provide the necessary separating power to enable the mass spectrometer to process the hundreds of thousands of peptide species. Consequently, peptides derived from the low abundance protein components from within a complex mixture are often completely missed in the analysis. To address this challenge, multi-dimensional peptide separations have been developed coupling orthogonal separation methods to better resolve these complex mixtures and to increase the ability to detect low abundance protein components. The first chromatographic step is usually strong cation exchange, and the second is reversed-phase high performance liquid chromatography (HPLC) (Fig 5.1). This 2D method has demonstrated its ability to overcome the limitations of membrane protein analysis in 2DE separations, and significantly increases the proteomic coverage by allowing previously undetected low-abundance proteins to be identified in complex mixtures (Blonder, Chan et al. 2006). However, this technology does not provide quantitative information on its own and a number of MS-based quantitative methods exist that can be employed (Fig 5.1). These include label-free quantification including spectral counting and a variety of stable isotope labelling strategies which are explained in more detail in Chapter 1.5.1.

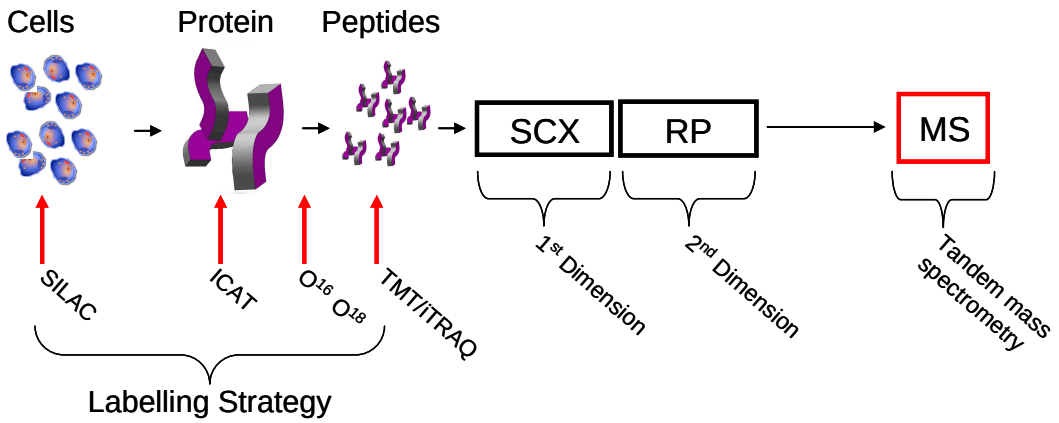

Figure 5.1 Quantitative MS-based labelling strategies coupled to 2D-LC-MS/MS. This figure shows SILAC labelling at the cellular level; ICAT labelling at the protein level; O^{16}-O^{18} labelling at proteolytic digestion; and isobaric mass tagging (e.g. TMT; iTRAQ) at the peptide level. Label-free quantitation can be carried out but requires multiple replicate runs for experimental robustness.

In this study, the recently commercialized TMT strategy was chosen for relative quantification of the EOC cell models by peptide 2D-LC. As described in the introduction, TMT labelling involves the tryptic digestion of samples prior to labelling, then pooling the labelled digests for 2D-LC separation coupled to MS/MS analysis (Fig 5.2). This strategy was applied to a WCL, secreted, crude membrane and surface labelled fraction as a complimentary approach to the 2D-DIGE profiling. The major aim was to identify proteins whose expressions were altered between each parental cell line and its pair of hybrid clones.

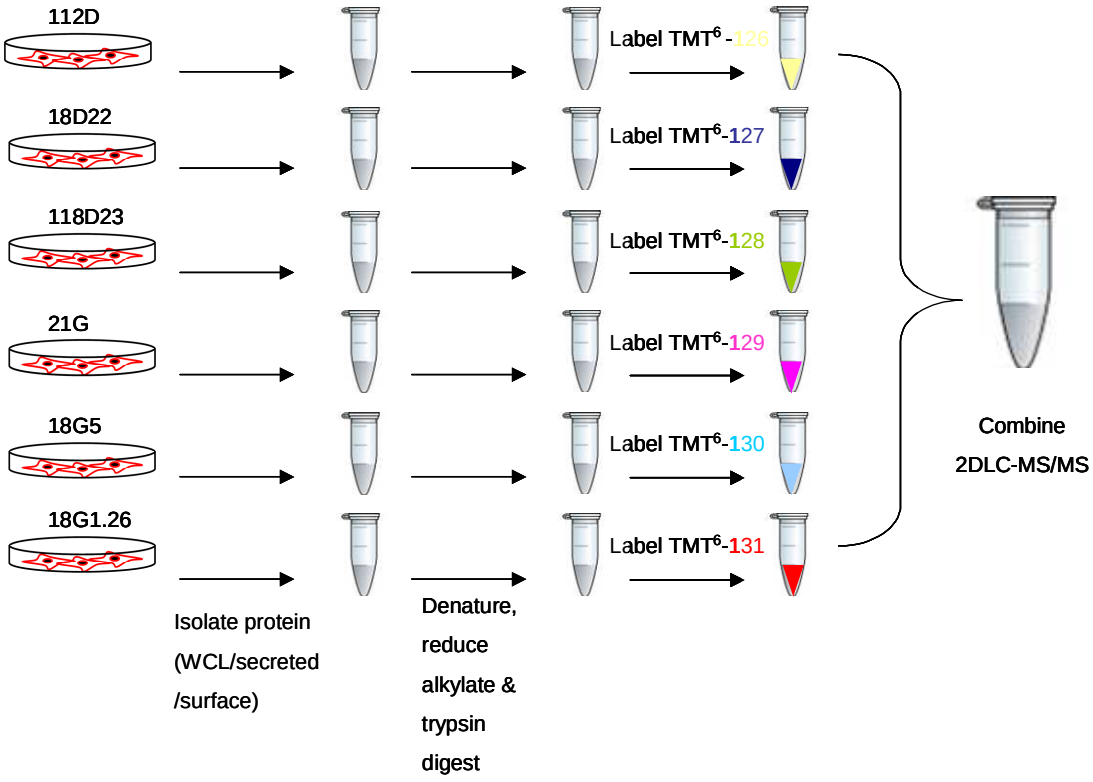

Figure 5.2 TMT labelling strategy. Protein was extracted from cells in culture. Amine-based buffers and salts were removed by precipitation and samples denatured, reduced and alkylated, before trypsin digestion. Samples were labelled with 6-plex TMT labels appropriately, combined, separated by SCX in the first dimension and RP chromatography in the second dimension before introduction to a mass spectrometer. Reporter ion intensities in the MS/MS spectra were used to determine relative peptide and protein abundances.

5.1.2 2D-LC-MS/MS

2D-LC had not previously been attempted in the laboratory and so set-up and optimisation was necessary. As described earlier, to achieve adequate resolution with complex mixtures of peptides, a combination of SCX and RP-HPLC can be employed. In this study a Polysulfoethyl SCX column (1 mm I.D x 15 cm, 5 µm, 300 Å) was used in the first dimension attached to the loading valve of an Ultimate 3000 HPLC system (Dionex). The column was chosen to be compatible with an off-line 2D-LC workflow to be performed entirely on the Ultimate 3000. The column is designed to work optimally within the flow rates (<100 µl/min) available on the loading pump of an Ultimate 3000. The differentially labelled digest mixture was separated using a salt gradient at pH 2-3, where carboxyl groups have lost their negative charge and nearly all peptides have a net positive charge. It is thought that approximately 65 % of peptides in a typical complex tryptic digest have a net charge of + 2 due to the basic N-terminus and the Lys or Arg at the C-terminus. Peptide digests were acidified (pH 2-3) with FA prior to separation over a gradient of 5-55% mobile phase B (95%/5% water/ACN v/v, 5 mM NaH_2PO_4 buffer pH 3.0, 1M NaCl) as recommended by the column manufacturer. The SCX column has a higher binding capacity (60 µg) than the RP column (3 µg) allowing more sample to be loaded and at a higher flow rate (50 µL/min). This versatility reduced chromatographic separation times and improved detection of low abundance proteins in complex mixtures. The gradient length and fraction number collected was optimised by RP-MS/MS analysis in the absence of a UV detector. A separation time of 30 min with fractions collected every 3 min after injection was found to be optimal (Fig 5.3).

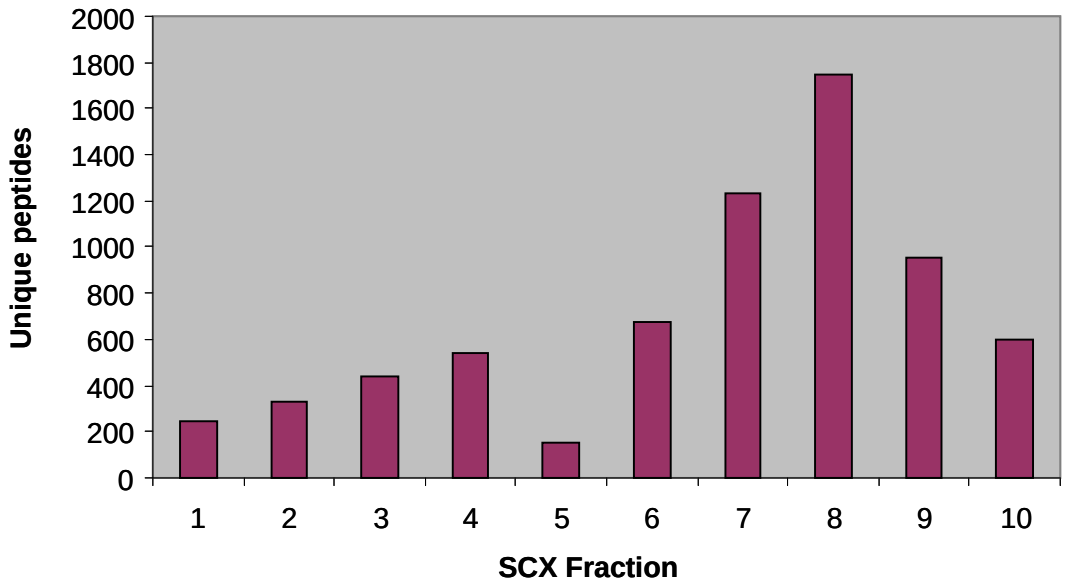

Figure 5.3 LC-MS/MS analysis of 10 SCX fractions. SCX fractions were collected every 3 min over a 30 min gradient of 5-55% mobile phase B. Fractions were dried down, Ziptipped, resuspended in 0.1% FA and injected for RP-LC-MS/MS analysis over a 60 min gradient. Spectra were processed using Proteome Discoverer and the IPI Human database interrogated using the Mascot search algorithm to identify peptide sequences. Fraction 5 yielded fewer peptides because of incomplete injection. ~6000 unique peptides were identified in this run.

The second dimension was carried out by RP-HPLC, in an automated fashion on an Ultimate 3000 HPLC (Dionex) linked to an LTQ-Orbitrap XL (Thermo Fisher) mass spectrometer with a PicoView ESI source. Each SCX fraction was dried down in a speedvac and desalted using Ziptips (see chapter 2.16), before resuspending in mobile phase A and injection. Separation was carried out on a C18 Pepmap column (75 µM x 150mm, 3 µm, 100 Å) with a linear gradient of 5-50% solvent B (20%/80% water/ACN v/v + 0.1% FA) over 90-120 min depending on sample complexity; the WCL fraction was separated over 120 minutes and the secreted, crude membrane and surface labelled fractions were separated over 90 minutes.

5.1.3 TMT-MS/MS

The TMT technology relies on accurate detection of low mass 'reporter ions' in MS/MS scans which are generated by fragmentation of the peptide tags. Mass spectrometers such as quadrupoles and TOF instruments have the capability of detecting low *m/z* fragment ions whereas for ion traps, detection is relatively poor. The MS platform used was an LTQ Orbitrap XL. This features a collision cell in which fragmentation is performed using higher energy collisional dissociation (HCD). This fragmentation technique produces rich 'triple-quad like' fragmentation patterns including fragments in the low *m/z* mass range. Ions fragmented by HCD in this extra octapole collision cell are returned to a C-trap and detected in the Orbitrap mass analyser. This provides very high mass accuracy and resolution of the reporter ions but at the possible expense of under sampling of precursor ions due to the longer MS/MS scan time.

The Orbitrap was operated using Xcalibur software and parameters were optimized for acquisition of high quality spectra for quantification and identification of TMT-tagged peptides. TMT-tagged peptides were detected in the Orbitrap at 60,000 resolution at *m/z* 400. A maximal ion accumulation of 1×10^6 ions in the Orbitrap was determined to be preferable with 1 second selected for all scan modes and automatic gain control selected to prevent over filling of the ion trap. A single microscan was deemed sufficient to produce high quality spectra whilst keeping the cycle time down. Fragmentation was optimal with HCD normalized collision energy set at 40%. Product ions were detected in the Orbitrap at a resolution of 7500. This resulted in prominent reporter fragment ions

and good sequence spectra from fragmented ions across the chromatographic separation. Ion detection in the Orbitrap alone increases the cycle time and so between three and five HCD spectra were acquired in a data dependent manner following each full scan in order to identify as many novel peptides with quantitative information as possible. Data dependent settings and lock masses were set as described in Chapter 2. Mascot 2.2 and Proteome Discoverer were then used for protein identification by searching the IPI human database. In each program, searches were carried out using carbamidomethylation of cysteine residues set as a fixed modification. In addition, TMT modification of peptide N-termini and lysine residues were set as fixed modifications. Methionine oxidation and N-terminal acetylation were set as variable modifications. A decoy database was searched under the same parameters to estimate a FDR. A peptide mass tolerance of 10 ppm and a fragment mass tolerance of 0.1 Da were selected for confident peptide matching.

5.2.1 Quantitative TMT profiling of the WCL

For the quantitative evaluation of protein expression profiles of the WCL of cell models of ovarian cancer neoplastic suppression, protein from each cell line was harvested and purified by acetone precipitation as described. 100 µg of each sample was denatured, reduced, alkylated, digested with trypsin and labelled appropriately with TMT labels (Fig 5.2). The labelled samples were combined and dried down in a speedvac. The sample was resuspended in SCX mobile phase A and acidified to pH 2.5. Approximately 50 µg of sample was injected onto a Polysulfoethyl SCX column for separation. 10 fractions were collected, dried down in a speedvac and desalted with Ziptips according to the

manufacturer's protocol. Each sample was further dried down and resuspended in 7 µl of 0.1 % formic acid (FA) and subjected to RP-LC-MS/MS. Each .Raw file produced in Xcalibur software (Thermo) was transferred to Mascot Daemon for processing by Mascot Distiller, where peak detection was carried out and datasets combined for Mudpit analysis, before searching against the IPI human database. The search parameters were set as described in Materials and Methods (Chapter 2). Search result filters were selected as follows; only "Mudpit scored" peptides with a score >20 and equal to or above the Mascot homology at a significance threshold of $p<0.05$ were included and single peptide identifications required a score equal to or above the Mascot identity threshold. MudPIT protein scoring is a more stringent scoring algorithm used for searches with more than 1000 spectra. It is determined from the excess of ions score over the homology threshold for each query plus the average of the thresholds used added to the score. In addition, for a given protein or peptide sequence the highest scoring and highest ranking respectively are highlighted in a Mascot report. This ensures that when a peptide belongs to another protein the most likely assignment is given preference. Quantitative information, calculated from reporter ion intensities, was only accepted for peptides with scores equal to or above the Mascot homology score and the median value was taken to compare protein ratios (Fig 5.4). Proteins with a ratio above 2 or below 0.5 in each comparison (127/126, 128/126, 130/129 and 131/129) were considered to be significantly different changes in expression.

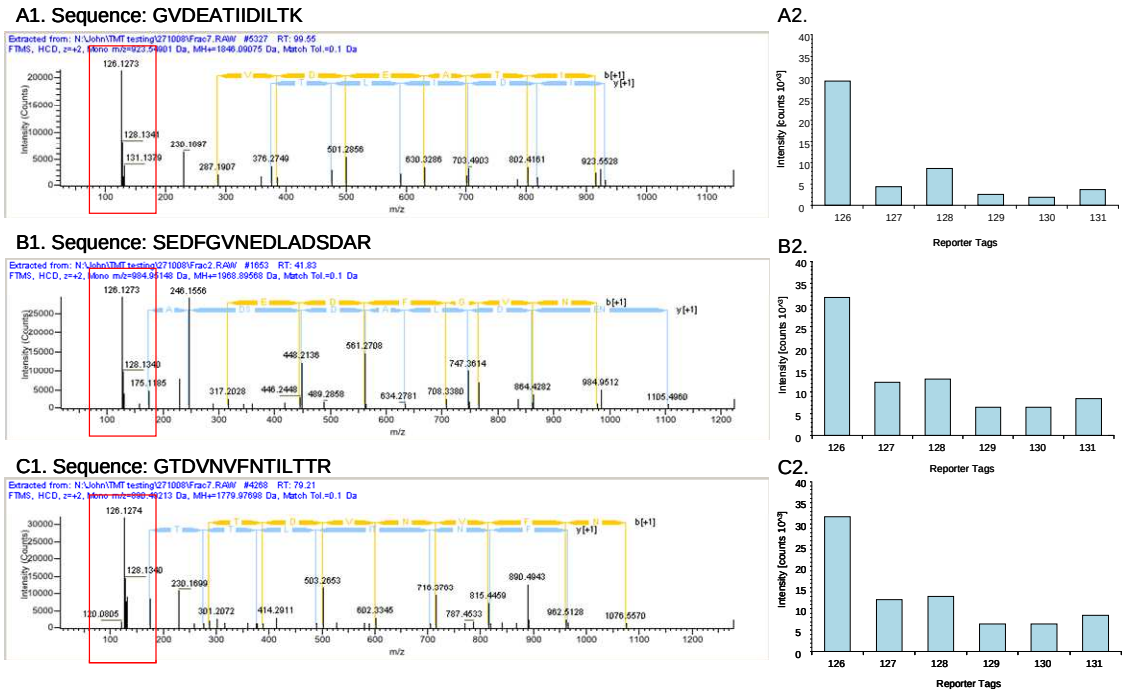

Figure 5.4 Representative annotated spectra and reporter ion intensities for three peptide sequence identifications from Annexin A1. A1) Annotated spectrum for sequence: GVDEATIIDILTK, identified with Mascot; ion score 75.68, Exp Value: 7.20E-07. A2) Reporter ion intensities for sequence: GVDEATIIDILTK, reporter tag 126 was labelled to TOV-112D; tag 127 labelled to 18-D-22; tag 128 labelled to 18-D-23; tag 129 labelled to TOV-21G; tag 130 labelled to 18-G-5 and tag 131 labelled to 18-G-1.26. B1) Annotated spectrum for sequence: SEDFGVNEDLADSDAR, identified with Mascot; ion score 80.28, Exp Value: 6.80E-08. B2) Reporter ion intensities for sequence: SEDFGVNEDLADSDAR. C1). Annotated spectrum for sequence: GTDVNVFNTILTTR, identified with Mascot; ion score 50.72, Exp Value 0.00029. C2) Reporter ion intensities for sequence: GTDVNVFNTILTTR. Annexin A1 displayed significant down-regulation in the hybrid clones 18-D-22 (median ratio 0.42) and 18-D-23 (median ratio 0.44) compared to the parent cell line TOV-112D. Reporter ions are boxed in red on the spectra. Data were generated using Proteome Discoverer.

5.2.2 Identification of differentially expressed WCL proteins

A total of 946 unique protein identifications were made from 2499 unique peptide matches using Mascot (Appendix 1A) .Of these, only 21 proteins were identified using a single, high-scoring peptide. The decoy database search resulted in 196 matches with a score equal to or above the Mascot peptide identity threshold compared to 4924 matches in the target database. For a peptide score equal to or above the homology threshold the decoy search resulted in 266 matches compared to 5435 matches in the target database resulting in a false discovery rate of 3.98% and 4.89% respectively which are considered acceptable for published data. The distribution of charge states of identified peptides was 94% +2, with only 6% of peptides displaying a charge state of +3. Database searches with the TMT modifications deselected determined the TMT labelling efficiency. The level of labelling was found to be in excess of 99% of peptides matches. The 2D-LC approach has proven to be competent at detecting proteins previously under-represented in the 2D-DIGE analysis. High and low molecular weight proteins; including spectrin beta chain (316 kDa) and thymosin beta-4-like protein 3 (7 kDa) respectively, and highly basic proteins, including histones and ribosomal proteins, were identified.

A total of 65 proteins were differentially expressed > 2 fold between a parental cell line and its corresponding hybrid clone. 36 proteins were found to be up-regulated and 2 down-regulated in the 18-D-22/TOV-112D comparison; 9 proteins were up-regulated and 3 down-regulated in the 18-D-23/TOV-112D comparison; 8 proteins were up-regulated

and 3 down-regulated in the 18-G-5/TOV-21G comparison and 2 up-regulated and 3 down-regulated in the 18-G-1.26/TOV-21G comparison. A total of 11 proteins displayed concordant expression changes (> 2 fold) in both hybrids compared to its parental cell line and these are shown in Table 5.1. The greatest change in expression was observed for Cytochrome b5 outer mitochondrial membrane precursor. Expression was changing 4.2 fold in the hybrid clone 18-D-22 and 3.7 fold in the hybrid clone 18-D-23.

Name	127/126	N	SD	128/126	N	SD	130/129	N	SD	131/129	N	SD
Annexin A1	**0.416**	32	NN	**0.441**	32	NN	0.787	30	NN	1.24	30	1.127
Cytochrome b5 outer mitochondrial membrane precursor	**4.2**	5	1.328	**3.704**	5	1.276	1.228	4	1.233	1.19	5	1.214
Caldesmon 1	**2.983**	2	1.007	**2.021**	2	1.031	1.274	2	1.196	0.859	2	1.041
Oxidation resistance protein 1	**2.864**	2	1.964	**2.1**	2	1.775	0.81	2	1.131	0.713	2	1.002
DNA-(apurinic or apyrimidinic site) lyase	**2.524**	2	1.347	**2.117**	2	1.347	0.983	2	1.377	0.877	2	1.099
PURINE NUCLEOSIDE P	**2.505**			**2.284**			1.31			1.295		
Integral membrane protein GPR177 1	**8.26**			**3.349**			0.964			0.792		
DNA polymerase epsilon subunit 4	**2.213**			**2.489**			0.885			0		
60S ribosomal protein L23a	1.197	2	1.011	0.92	2	1.036	**2.709**	2	3.617	**2.304**	2	3.304
Four and a half LIM domains 1 variant	0.686			**0.42**			**2.765**			**2.26**		

Table 5.1 Proteins displaying concordant expression changes in a hybrid pair compared to its parent cell line. Protein abundance is measured by peptide ratio. Significant up-regulation (>2 fold) is displayed in bold red and down-regulation (<0.5 fold) is displayed in bold blue. The reporter ions 127 and 128 are labelled to 18-D-22 and 18-D-23 and compared to the parental, TOV-112D, which is labelled with 126. Reporter ion 130 and 131 were labelled to 18-G-5 and 18-G-1.26 respectively, and each were compared to the parental TOV-21G, labelled with 129. Identifications in italic type were from a single peptide only. ('N' represents the number of labelled peptides (>1) used for ratio calculation, 'SD' is the geometric standard deviation of the peptide ratios for a given protein and 'NN' indicates the presence of a peptide ratio outside a normal distribution). Data were generated using Mascot with quantitation tool box.

Annexin A1 was the only concordantly expressed protein which was down-regulated by >2-fold in the 18-D-22 and 18-D-23 cell lines, compared to parental cell line TOV-112D. This protein was also identified in the 2D-DIGE analysis where its expression was also down-regulated in the pooled experiment and single hybrid clone comparisons.

Cytochrome b5 outer mitochondrial membrane precursor an electron carrier for several membrane bound oxygenases (Borgese, D'Arrigo et al. 1993) was significantly up-regulated in the hybrid cell lines 18-D-22 and 18-D-23 by ratios of 4.2 and 3.7 respectively. Caldesmon, an actin and myosin binding protein was up-regulated in hybrid cell lines 18-D-22 and 18-D-23 by ratios of 2.98 and 2.02, respectively. Oxidative resistance protein 1 is involved in protection from oxidative damage (Volkert, Elliott et al. 2000). This protein was up-regulated in the 18-D-22 and 18-D-23 hybrid cell lines by ratios of 2.86 and 2.1, respectively. DNA-(apurinic or apyrimidinic site) lyase (APE) was up-regulated in the 18-D-22 and 18-D-23 hybrid cell lines by ratios of 2.52 and 2.12, respectively. This protein repairs DNA damage and may have a role in protecting against lethal mutations. Purine nucleoside phosphorylase (PNP) was up-regulated in the 18-D-22 and 18-D-23 hybrid cell lines by ratios of 2.51 and 2.28, respectively. The 60S ribosomal protein L23a was the only concordantly regulated protein identified in the TOV-21G model and was up-regulated in the 18-G-5 and 18-G-1.26 cell lines by ratios of 2.71 and 2.3, respectively. Several other proteins displaying concordant expression in one of the cell models were identified using only a single, but highly significant peptide and should not be ignored. These included, PNP, integral membrane protein GPR1771, DNA polymerase epsilon 4 and four and a half LIM domains 1 variant. Whilst no protein changes were identified that were common to both cell models, numerous changes were identified that were also found in the 2D-DIGE analysis. Proteins included vimentin, annexin A1 (above), retinol dehydrogenase 1, laminin A/C, COL3A1, galectin-1 and ezrin. Generally there was agreement in the direction of altered expression between the experiments. For example, multiple isoforms of vimentin were identified from 2D-DIGE

gels with differing expression levels. The first single clone analysis of WCL by 2D-DIGE identified up-regulation of different vimentin isoforms in the 18-D-22 & 18-D-23 hybrid clones which is supported by the similar up-regulation of vimentin in this TMT analysis. However, the specific isoform of vimentin in the two analyses cannot be matched, highlighting the drawback of peptide-based analysis. Two isoforms of annexin A1 displayed down-regulation of expression in hybrid cell lines 18-D-22 and 18-D-23 compared to the parental cell line TOV-112D in the 2D-DIGE analysis of WCL. These findings are supported by the TMT analysis which identified annexin A1 as down-regulated -2.38 and -2.27 fold in hybrid clones 18-D-22 and 18-D-23, respectively. However, retinol dehydrogenase 1 did not display concordant expression between the two proteomic approaches. The TMT analysis of WCL identified up-regulation 2.2 fold in the hybrid clone 18-D-22, whereas the 2D-DIGE analysis identified down-regulation of an isoform by 2.63 fold and 2.04 fold in the hybrid clones 18-D-22 and 18-D-23, respectively. Galectin-1 was identified up-regulated 2.11 fold in hybrid clone 18-D-22 in the TMT analysis of WCL. This was previously identified in the 2D-DIGE analysis of the pooled hybrid clones displaying significant up-regulation of 4.93 fold in the TOV-112D which is consistent with the findings in this TMT analysis. Another differentially expressed protein also identified in the 2D-DIGE analysis of the pooled hybrid clones was purine nucleoside phosphorylase. The TMT analysis identified a single high scoring peptide displaying up-regulation in the hybrid clone 18-D-22 of 2.5 fold and the hybrid clone 18-D-23 of 2.3 fold. The 2D-DIGE analysis displayed contrasting down-regulation -2.79 fold in the TOV-112D hybrid clone pool. This possibly reflects the problems when dealing with pooled analyses discussed in Chapter 3.

5.3 Quantitative TMT profiling of secreted protein

TMT labelling combined with the 2D-LC-MS/MS strategy was applied to the secreted proteome of the cell models under study. The isolation of the secreted fraction was carried out in the same way as for the 2D-DIGE analysis (Chapter 2.4), although the extraction from conditioned medium was scaled down to reduce time. As a result, 25 µg of secreted protein from each cell line was recovered and labelled with the appropriate TMT tag before 2D-LC-MS/MS. The SCX step was carried out in exactly the same way as described earlier with 10 fractions collected over a gradient of 30 minutes. The RP gradient was reduced to 90 min to match the reduced complexity of the SCX fractions. Orbitrap raw data files were processed by Mascot distiller before merging and searching against the IPI human database. The search parameters were set as described earlier. Proteins were considered if the median value of the expression ratios for filtered peptides from that protein was >2 or <0.5 in the hybrid versus parental comparisons (and were significant, lying within a 95 % confidence interval).

5.3.1 Identification of differentially expressed secreted proteins

Analysis of the secreted fraction revealed a total of 223 unique protein identifications from 657 unique peptide matches (Appendix 1B). Of these, 45 proteins were identified by a single, high scoring peptide match. 76 proteins were differentially expressed > 2 fold in one or more of the hybrid clones and parental comparisons. The peptide charge distribution favoured +2 peptides making up 72.5% of peptide matches. 26.6% of peptides matches were +3 charged and the remainder +4. The labelling efficiency was found to be > 99% by searching the target database without the TMT mass modification addition. The decoy database search resulted in 229 peptide matches with a score equal to or above the Mascot peptide identity threshold compared to 1583 in the target database. For matches with a peptide score equal to or above the homology threshold the decoy database search resulted in 369 matches compared to 2178 matches in the target database, giving false discovery rates of 14.5 % and 16.9 %, respectively. These false discovery rates are quite high and not representative of the rates achieved for the analysis of the whole cell and membrane fractions (see later). This may have occurred since the data set comprised a relatively high number of repeat sequence identifications from a few highly abundant proteins. Bovine serum albumin peptides made up a large proportion of the peptide matches. A total of 489 peptide matches were identified from mass spectra, however, this represented only 8% of the total coverage. Many of the protein identifications came from a single peptide sequence observed repeated times which is common to MudPIT experiments analysing complex samples such as these. Additional

contaminants from the medium that were identified included alpha feto-protein, transferrin, growth-inhibiting protein 12 and serotransferrin. In addition, the incidence of 6-8 amino-acid peptide identifications were greater than observed for the WCL results, possibly because of a greater prevalence of lysine and arginine residues in secreted proteins. To conduct a decoy database search in Mascot, a random sequence of equal length is automatically generated and tested under the same search and filter parameters. Thus the combined effect of multiple repeats and shorter peptide sequence could result in the misrepresentation of decoy matches in the data set. To achieve a FDR < 5% for peptide matches with a score equal to or above the threshold for homology the significance threshold would have to be changed from 0.05 to 0.0099. At this level the number of unique proteins identified was reduced to 156 from 223 with the majority of the single peptide identifications from the previous search being excluded. Indeed, only 15 proteins were identified by a single high scoring unique peptide in this search. A comparison of protein identifications with gene ontology databases resulted in extracellular region, extracellular space and proteinaceous extracellular matrix proteins comprising 26% of the proteins identified (Fig 5.5). Furthermore, cell surface and membrane protein made up 8% of cellular proteins identified.

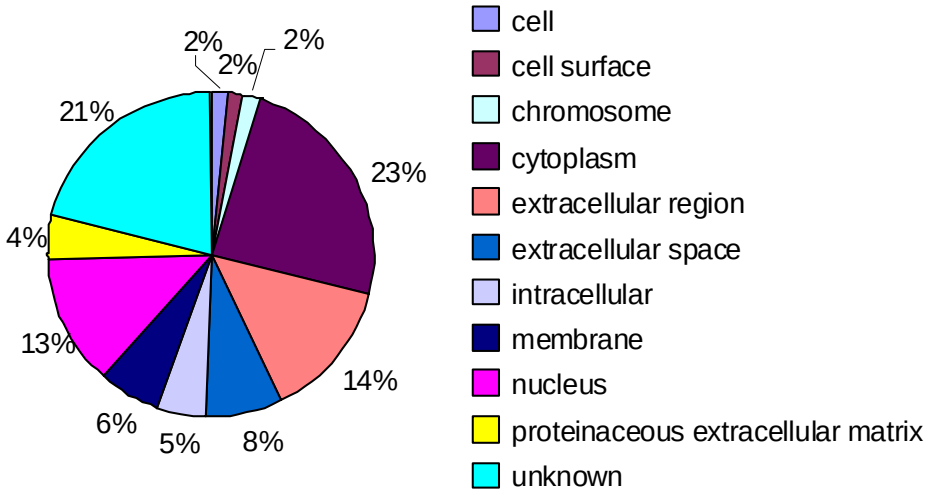

Figure 5.5 Cellular location of identified proteins in the secreted fraction determined from gene ontology databases. Some proteins represented multiple cellular components. The high number of 'unknown' assignments may again reflect the need for more thorough updating of gene ontology databases.

At the relaxed significance threshold, the comparison between the hybrid clone 18-D-22 and parent cell line TOV-112D, resulted in 19 up-regulated and 14 down-regulated proteins. The comparison between hybrid clone 18-D-23 and parent cell line TOV-112D resulted in 26 up-regulated and 14 down-regulated proteins. In the other cell model, comparison of hybrid clone 18-G-5 and parent cell line TOV-21G resulted in 20 up-regulated and 9 down-regulated proteins and for hybrid clone 18-G-1.26, 8 proteins were up-regulated and 54 down-regulated compared to its parent cell line TOV-21G. Of these, only calreticulin displayed concordant change in expression of >2 fold in both hybrids of both cell models and 7 displayed concordant expression > 1.5 fold. 18 proteins displayed >2 fold concordant changes in expression within a cell model (Table 5.2).

Name	127/126	N	SD	128/126	N	SD	130/129	N	SD	131/129	N	SD
Butyrophilin-like protein 3	**3.049**	1	---	**2.646**	1	---	**2.874**	1	---	**3.171**	1	---
Stromelysin-2	**2.957**	6	1.342	**2.782**	6	1.286	**2.157**	5	1.723	1.521	4	1.205
SECIS binding protein 2	1.839	16	1.108	**2.352**	16	NN	**1.997**	16	1.277	**2.11**	16	1.283
Midasin	1.856	11	1.139	**2.327**	11	1.089	**2.168**	2	1.045	**2.203**	2	1.268
TMEFF1	1.585	3	1.299	**2.036**	3	1.131	**2.438**	2	3.53	**2.48**	2	2.759
Creatine kinase M-type	**3.75**	3	1.09	**4.54**	3	1.034	**---**	0	---	**---**	0	---
Peptidyl-prolyl cis-trans isomerase B	**4.19**	2	1.23	**2.762**	2	1.117	1.337	2	1.012	0.568	2	1.191
C3 Complement C3 (Fragment)	**2.407**	12	1.601	**3.179**	13	1.539	1.208	10	1.325	1.038	10	NN
Calreticulin	**0.412**	5	1.597	**0.303**	2	1.417	**0.314**	3	1.523	**0.145**	3	NN
Calreticulin (Fragment)	**0.333**	2	1.243	**0.266**	2	1.18	**0.291**	2	1.048	**0.147**	2	1.079
Follistatin-related protein 1	**0.335**	7	2.16	0.513	8	2.195	**0.483**	9	NN	**0.328**	8	1.206
Reelin	1.554	4	1.119	1.34	4	1.313	**0.443**	5	NN	**0.289**	4	1.124
Histone H2B type 1-L	1.164	5	1.349	0.836	5	1.356	**0.495**	5	1.055	**0.427**	5	1.059
Heat shock protein, mitochondrial	0.933	6	1.388	0.824	6	1.423	**0.393**	8	1.101	**0.323**	8	1.278
Collagen alpha-1(XII) chain	0.879	1	---	1.332	1	---	**0.426**	1	---	**0.302**		
Serglycin	1.376	1	---	1.198	1	---	**0.389**	1	---	**0.184**		
Collagen alpha-1(III) chain	**0.398**	12	1.909	**0.276**	11	1.496	1.023	6	2.068	0.967	5	1.542
Insulin-like growth factor-binding protein 2	**0.264**	2	1.382	**0.487**	2	1.399	**---**	1	---	0.57	2	2.4

Table 5.2 Secreted proteins displaying concordant expression changes across all hybrid clones or in a hybrid pair compared to their parent cell line. Protein changes are shown as peptide reporter ion ratios for peptides matching that protein. Significant up-regulation >2 fold is displayed in bold red and down-regulation is displayed in bold blue. The reporter ions 127 and 128 were labelled to 18-D-22 and 18-D-23 and compared to their parental (TOV-112D), which was labelled with 126. Reporter ions 130 and 131 were labelled to 18-G-5 and 18-G-1.26 respectively, and each were compared to their parental (TOV-21G), labelled with 127. Identifications in italic type were from a single peptide only. 'N' represents the number of labelled peptides used, 'SD' the geometric standard deviation of the peptide ratios for a given protein and 'NN' indicates the presence of a peptide ratio outside a normal distribution. Proteins in red type displayed concordant expression changes in both cell models. Data were generated using Mascot with quantitation tool box.

Butyrophilin-like protein 3 displayed up-regulation > 2 fold in all four hybrid clones compared to their parental cell lines, although this membrane protein involved in lipid metabolism was identified by only a single high scoring peptide match. Stromelysin-2, a

secreted matrix-metalloproteinase (MMP10), displayed >2 fold up-regulation in all hybrid clone/parental comparisons except in the 18-G-1.26 hybrid clone compared to its parental cell line TOV-21G (1.52 fold). SECIS binding protein displayed up-regulation in all the hybrid clones. Expression was only marginally under the 2-fold cut-off in the 18-D-22 hybrid clone (1.86 fold) parent comparison. Midasin displayed up-regulation in all hybrid clones with only 18-D-22 expression just below the 2-fold level. This protein has been implicated as a chaperone involved in the assembly/disassembly of macromolecular complexes in the nucleus. Tomoregulin-1 (TMEFF1) displayed up-regulation over 2-fold in all but the 18-D-22 hybrid clone when compared to the parental cell lines. This transmembrane protein with EGF-like and one follistatin-like domain is speculated to be involved in growth factor signalling (Eib, Holling et al. 2000). TMEFF1 has been reported as a tumour suppressor gene in brain cancers (Gery, Yin et al. 2003). Up-regulation in the hybrid clones may promote the suppressed tumourigenic phenotype in these clones versus the parental cell lines. Calreticulin and a fragment of calreticulin were both identified as displaying significant down-regulation in all four hybrid clones compared to their parental cell lines. The fragment is distinguished by a unique peptide (sequence: EPAVYFK). Calreticulin is an ER and cytoplasmic protein involved in calcium binding and was identified in the 2D-DIGE analysis of WCL of the hybrid clones 18-D-22 and 18-G-1.26 where its expression was also found to be down-regulated. Follistatin-related protein 1 (FRP) displayed significant down-regulation in all hybrid clones except 18-D-23 with a change in expression of 0.51-fold (Fig 5.6). This secreted protein is predicted to modulate the action of TGFß superfamily members on cell proliferation and differentiation. Reelin displayed down-regulation in hybrid clones 18-

G-5 (0.44 fold) and 18-G-1.26 (0.29 fold) compared to parental cell line TOV-21G. This secreted protein is involved in modulating cell adhesion.

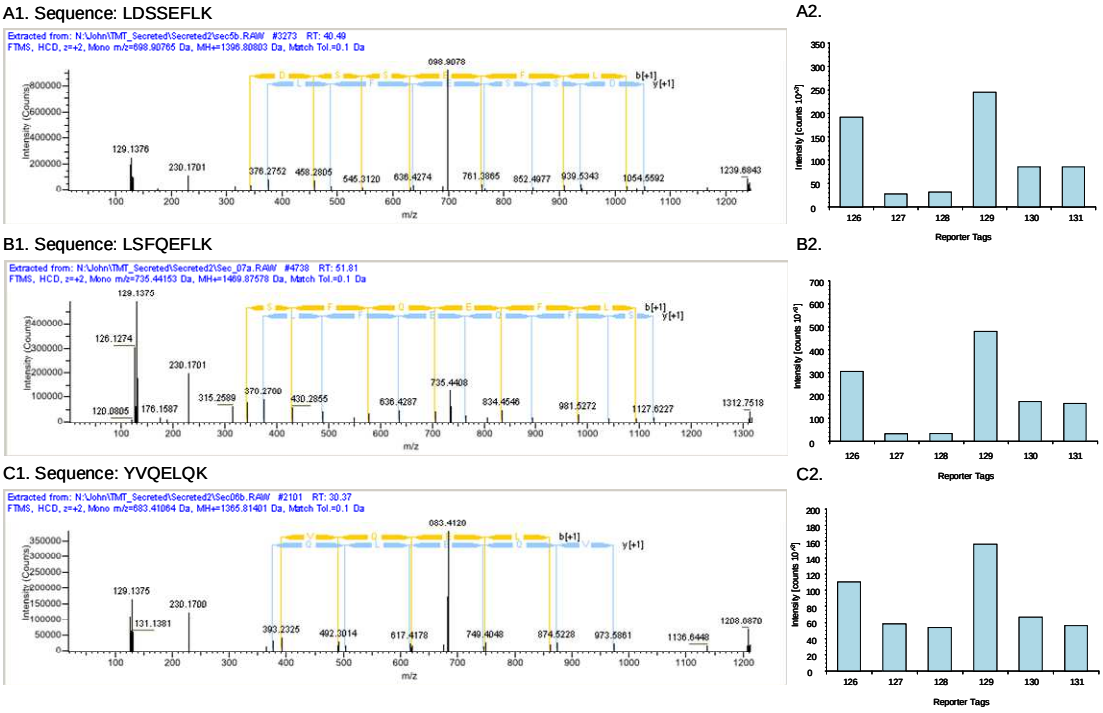

Figure 5.6 Representative annotated spectra and reporter ion intensities for three peptide sequence identifications from Follistatin-related protein 1. A1) Annotated spectrum for sequence: LDSSEFLK identified in Mascot; ion score 45.8, Exp Value 0.00081. A2) Reporter ion intensities for peptide sequence: LDSSEFLK. Tag 126 is labelled to TOV-112D, tag 127 to 18-D-22, tag 128 to 18-D-23, tag 129 to TOV-21G, tag 130 to 18-G-5 and tag 131 to 18-G-1.26. B1) Annotated spectrum for sequence: LSFQEFLK identified in Mascot; ion score 45.89, Exp Value 0.00074. B2) Reporter ion intensities for sequence: LSFQEFLK. C1) Annotated spectrum for sequence: YVQELQK identified in Mascot; ion score 34.45, Exp Value 0.014. C2) Reporter ion intensities for sequence: YVQELQK. Follistatin-related protein 1 displayed significant down-regulation in both hybrid clone pair. Data were generated using Proteome Discoverer.

Two secreted proteins displaying down-regulation in hybrid clones 18-D-22 and 18-D-23 were collagen alpha-1 (III) chain (COL3A) and IGFBP2. Four isoforms of COL3A were identified in the 2D-DIGE analysis, three of which displayed significant up-regulation and the fourth down-regulation in hybrid cell lines 18-D-22 and 18-D-23. The TMT result correlates with the fourth isoform identified in the 2D-DIGE analysis. A number of isoforms of IGFBP2 were identified in the 2D-DIGE analyses of secreted proteins. Expression of all were down-regulated in hybrid clones 18-D-22 and 18-G-1.26 compared to their respective parental cell lines. Contrasting up and down-regulation was observed in hybrid clone 18-G-5 and no significant change was observed in hybrid clone 18-D-23. The TMT analysis identified down-regulation in hybrid clone 18-D-22 correlating with the expression change observed in the 2D-DIGE analysis.

A number of other secreted and non-secreted proteins that were identified as changing > 2 fold in at least one hybrid clone in the TMT analysis were also identified in the 2D-DIGE experiments. These included lactate deydrogenase, lumican, IGFBP7, glucagon and TIMP1. For example, three isoforms of glucagon were identified in the 2D-DIGE analysis, two of which displayed significant up-regulation in the hybrid clones 18-D-22 and 18-D-23 and down-regulation in hybrid clones 18-G-5 and 18-G-1.26. The third isoform displayed moderate down-regulation in hybrid clones 18-D-22 and 18-D-23, possibly suggesting a post-translational modification. The TMT analysis indicated down-regulation of glucagon in the hybrid clone 18-D-22 (0.47 fold), correlating only with the expression change displayed by the third isoform in the 2D-DIGE analysis, this again highlights one of the drawbacks of peptide analysis where information on isoform

distribution is lacking. Finally, TIMP1 was identified in two separate 2D-DIGE experiments displaying down-regulation -2.68 and -2.36 fold in the hybrid clone 18-D-22. This correlates strongly with the change in expression -2.19 fold observed in the TMT analysis in the same hybrid clone.

5.4 Quantitative TMT profiling of membrane protein

The plasma membrane is a cellular compartment that provides a physical boundary between the cell and its environment. Membrane proteins are integral components of the plasma membrane and positioned at the interface between the cell and the surrounding environment. These proteins are involved in key biological function, such as cell-to-cell recognition, adhesion and the transport of ions and solutes. In addition, they act as receptors for relaying diverse intracellular and extracellular signals. Defining the surface membrane proteome is key to understanding the role of membrane proteins in these fundamental biological processes and the development of cancer (Santoni, Molloy et al. 2000). For example, levels of the type I EGF transmembrane protein receptor are elevated in 50% of ovarian cancers, which is associated with poor prognosis. Importantly, membrane proteins are particularly under-represented in conventional proteomic analyses using 2D, owing to their low abundance and hydrophobicity, although they are predicted to represent ~30% of the human genome.

In order to examine the expression changes of membrane proteins in the tumour suppression models, a crude membrane fractionation was prepared from cells in culture

(Chapter 2.5). Cells were harvested in a hypotonic lysis buffer, homogenised and the nuclear fraction cleared before ultracentrifugation at 100,000xg for 1 hour. The membrane-enriched fraction was suspended in RIPA buffer and the protein content determined by BCA assay. 100 µg of protein from each cell line was precipitated in ice-cold acetone overnight for digestion and subsequent TMT labelling before 2D-LC-MS/MS analysis as described earlier.

5.4.1 Identification of differentially expressed membrane proteins

A total of 432 unique protein identifications were made from 1392 unique peptide matches (Appendix 1C). Of these, 82 proteins were identified by a single, high scoring peptide match. 101 proteins were differentially expressed > 2 fold. The decoy database search resulted in 76 matches with a score equal to or above the Mascot peptide identity threshold compared to 2053 matches against the target database; a false discovery rate of 3.7%. For matches with a peptide score equal to or above the homology threshold the decoy database search resulted in 140 matches compared to 2681 matches against the target database which resulted in a false discovery rate of 5.22%. The distribution of charge state among the peptides identified was 62% +2 and 36% +3 with the remainder +4. Peptide labelling with the TMT tags was in excess of 99%. A comparison of protein identifications with gene ontology databases resulted in 11% of the crude membrane preparation proteins identified as *bona fide* membrane protein (Fig 5.7). There was poor depletion of nuclear, chromosome and cytoplasmic localised proteins, which made up a

significant proportion (70%) of the crude membrane fraction. Thus Ultra-centrifugation on its own is not sufficient for the recovery of membrane proteins and a more sophisticated approach including sucrose density gradients may reduce the contamination from non-membrane proteins (see below).

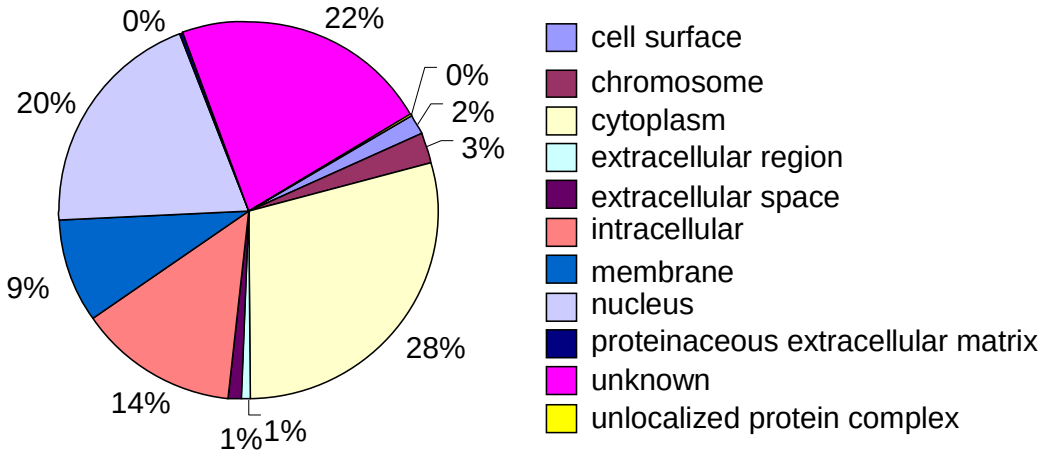

Figure 5.7 Cellular location of identified proteins in the crude membrane fraction determined from gene ontology databases. Some proteins represented multiple cellular components. The high number of 'unknown' assignments may again reflect the need for more thorough management and updating of gene ontology databases.

As with the previous TMT analyses, quantitative information was only accepted for peptides with scores equal to or above the Mascot homology score and the median value calculated from peptides matching a particular protein to compare protein ratios. Peptides displaying a change in expression >2-fold or <0.5-fold were considered as displaying differential expression. In hybrid clone 18-D-22, 10 proteins were up-regulated and 16 down-regulated compared to parental cell line TOV-112D; in the hybrid clone 18-D-23, 20 proteins were up-regulated and 7 down-regulated compared to parental cell line TOV-112D; in hybrid clone 18-G-5, 1 protein was up-regulated and 12 down-regulated

compared to the parental cell line TOV-21G; and in hybrid clone 18-G-1.26, no proteins were observed up-regulated, whereas 64 were down-regulated compared to parental cell line TOV-21G. In total, 14 proteins displayed differential expression of >2-fold in a pair of hybrid clones when compared to their parental cell line (Table 5.3).

Name	127/126	N	SD	128/126	N	SD	130/129	N	SD	131/129	N	SD
Heat shock protein 90kDa alpha	**0.453**	31	1.4	**0.375**	29	1.4	0.953	32	NN	1.427	32	NN
Endoplasmin	**0.491**	15	1.3	**0.349**	15	NN	0.799	14	1.1	1.241	15	1.3
HLA-B associated transcript 1	**0.27**	2	1.1	**0.365**	2	1.1	0.798	2	1.2	0.796	2	1.2
T-complex protein 1 subunit beta	**0.417**			**0.48**			0.695			0.936		
Prolyl 3-hydroxylase 3	**2.079**	3	1.2	**2.355**	3	NN	0.636	3	1.2	1.502	3	NN
Vimentin	**2.438**	32	NN	**4.624**	32	1.4	0.601	29	1.6	**0.416**	26	1.5
Protein tyrosine phosphatase-like protein	**2.13**	2	1	**2.918**	2	1.2	**0.302**	2	1.1	**---**	1	---
Cytochrome b5 outer mitochondrial membrane precursor	**5.509**	2	1.1	**6.665**	2	1.3	**0.205**	2	1	**0.157**	2	1.2
Voltage-dependent anion-selective channel protein 3	**2.051**	3	1.2	1.505	3	1.2	**0.447**	3	1.5	**0.207**	3	1.5
Nucleolin	0.866	8	1.3	1.759	8	NN	**0.438**	9	NN	**0.384**	9	NN
Prohibitin	1.212	4	1.1	1.83	4	1.2	**0.406**	4	1.1	**0.267**	4	1.2
Prohibitin-2	1.26			1.86			**0.298**			**0.196**		
Translocase 2	1.165			1.383			**0.462**			**0.343**		
Phosphatidylinositide phosphatase SAC1	1.635			1.665			**0.392**			**0.302**		

Table 5.3 Proteins from a crude membrane extraction displaying concordant expression >2-fold in a hybrid pair compared to their parent cell line. Protein abundance change is measured by median peptide ratio. Up-regulation is displayed in bold red and down-regulation is displayed in bold blue. The reporter ions 127 and 128 were labelled to 18-D-22 and 18-D-23, respectively and compared to the parental, TOV-112D, which was labelled with 126. Reporter ions 130 and 131 were labelled to 18-G-5 and 18-G-1.26 respectively, and each were compared to the parental, TOV-21G, labelled with 129. Identifications in italic type were from a single peptide only. 'N' represents the number of labelled peptides used for median protein ratio calculation and 'SD' the geometric standard deviation of the peptide ratios for a given protein. If there was no reporter ion information, dashes are displayed. If a peptide ratio appeared outside a normal distribution (not normal) 'NN' is displayed. Proteins in red type displayed concordant expression in both clones of a cell model.

None of the proteins identified displayed a concordant change in expression in both cell models. The hybrid pair, 18-D-22 and 18-D-23 displayed down-regulation of four

proteins; heat shock protein 90kDa alpha, endoplasmin, HLA-B associated transcript 1 and T-complex protein 1 subunit beta. Heat shock protein 90 alpha is a molecular chaperone found in the cytoplasm and is involved in mediating stress responses and importantly in promoting the active conformation of signalling proteins (Yonehara, Minami et al. 1996; Liang and MacRae 1997). Endoplasmin is also a molecular chaperone that functions in the processing of secreted proteins and is localised in the lumen of the endoplasmic reticulum. HLA-B associated transcript 1 is a membrane protein involved in the presentation of foreign antigens to the immune system. T-complex protein 1β is a molecular chaperone located in the cytoplasm which is involved in protein folding including actin and tubulin complex assembly. Prolyl 3-hydroxylase 3 (an oxidoreducatase found in the endoplasmic reticulum), was up-regulated in hybrid clones 18-D-22 and 18-D-23, three other proteins displayed up-regulation of expression in hybrid clones 18-D-22 and 18-D-23, but also displayed contrasting expression in one or both hybrids of the other cell model. Vimentin, up-regulated in hybrid clones 18-D-22 and 18-D-23 but down-regulated in 18-G-1.26, was identified previously in the 2D-DIGE analysis of WCL where its expression was also up-regulated in clones 18-D-22 and 18-D-23. Protein tyrosine phosphatase-like protein (PTPLAD1) displayed up-regulation in hybrid clones 18-D-22 and 18-D-23, but down-regulation in hybrid clone 18-G-5. PTPLAD1 is a membrane protein involved in Rac-1-mediated modulation of gene expression (Courilleau, Chastre et al. 2000). Cytochrome b5 outer membrane precursor (CYB5B) displayed significant up-regulation in hybrid clones 18-D-22 and 18-D-23 (5.51- and 6.67-fold, respectively), but was down-regulated 0.21- and 0.16-fold in the 18-G-5 and 18-G-1.26 clones. CYB5B is a mitochondrial membrane bound hemoprotein and

was also observed to be up-regulated in the 18-D-22 and 18-D-23 clones in the TMT analysis of WCL.

Finally, 6 proteins were identified displaying down-regulation in both of the hybrid clones 18-G-5 and 18-G-1.26 compared to their parental cell line TOV-21G and were mostly mitochondrial membrane proteins. These were voltage-dependent anion-selective channel protein 3, nucleolin, prohibitin, prohibitin-2, translocase 2 and phosphatidylinositide phosphatase SAC 1 (SACM1L). Voltage-dependent anion-selective channel protein 3 displayed up-regulation in the single hybrid clone 18-D-22 and contrasting down-regulation in hybrid clones 18-G-5 and 18-G-1.26. This protein forms a channel through the mitochondrial membrane that allows diffusion of small hydrophilic molecules. Nucleolin is a multifunctional protein thought to be involved in pre-rRNA transcription, ribosome assembly and transcriptional elongation. As mentioned previously prohibitin has a role in down-regulating proliferation and is located in the mitochondrial inner membrane. Prohibitin was previously identified in the 2D-DIGE analysis of WCL where two undefined isoforms displayed contrasting expression changes in hybrid cell line 18-G-1.26 (Chapter 3). Prohibitin-2 is also located on the mitochondrial inner membrane and acts as a mediator of transcriptional repression. Translocase 2 catalyses the exchange of ADP and ATP across the mitochondrial inner membrane. SACM1L is localised in the ER membrane and functions in vesicular trafficking through its hydrolysis of PI lipids (Kiss, Kedra et al. 2001).

5.4.2 Profiling of the cell surface proteome of EOC cell models

In order to better 'probe' membrane proteins, a strategy was devised for the enrichment of cell surface proteins (Fig 5.8). Live cells in culture were biotinylated using sulfo-NHS-SS-biotin for 30 min at 37 °C. The labelling is based on the reaction of primary amines in cell membrane proteins with the labelling reagent at pH 8. The biotinylation reagent is water soluble, but membrane impermeable and is therefore expected to only label cell surface and extracellular proteins which are then purified using immobilised avidin (Zhao, Zhang et al. 2004).

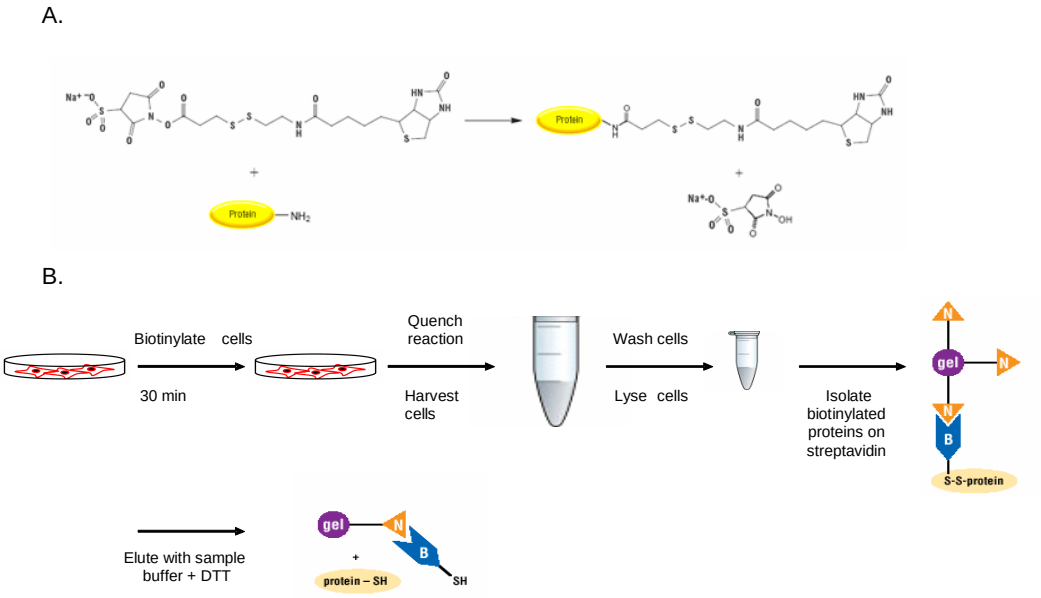

Figure 5.8 Cell surface protein labelling and enrichment strategy. A. Chemical structure of Sulfo-NHS-SS-Biotin [sulfosuccinimidyl-2-(biotinamido)ethyl-1,3-dithiopropionate]. B. Labelling method. Cells are washed with PBS to remove serum proteins then labelled for 30 min. The reaction is quenched and the cells gently harvested into a 50 ml falcon tube and washed with TBS before lysis. Biotinylated proteins are captured on streptavidin, washed then eluted in sample buffer with reductant (DDT) at 95 °C for 5 min.

Firstly, in order to test the enrichment strategy, a 1D gel was loaded with total cell lysate (TCL), the depleted fraction and the eluant (enriched labelled protein) from two different elution steps (Figure 5.9).

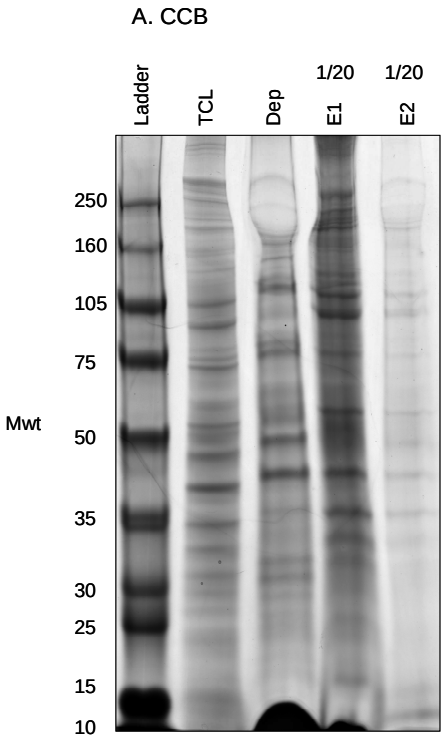

Figure 5.9 Enrichment of cell surface proteins. CCB stained gel image of 10µg of TCL and depleted fraction and 1/20 of eluates 1 & 2. E1 was from an incubation with 400 µL of Sample Buffer (SB) containing DTT for 60 minutes at room temperature. E2 was a subsequent incubation with SB and DTT, but with heating at 95 ºC for 5 minutes.

This preliminary analysis showed that there were distinct protein features not present in the TCL or depleted lanes, however, a proportion appeared to match. The second elution step (E2) showed that material could still be eluted from the beads, suggesting that the first elution was not complete. Boiling on the beads is preferable for complete

detachment of biotinylated protein from the avidin substrate. Elution, by cleavage of the disulphide bond, in the presence of DTT was only found to yield poor recovery of proteins and so elution was carried out in the presence of sample buffer also, although this created complications for TMT-labelling (see below). The gel lane was cut into 60 bands of approximately 2 mm each and diced into smaller pieces. The protein bands were digested with trypsin and analysed by LC-MS/MS as described in Materials and Methods (Chapter 2).

In total, 281 proteins were identified in the streptavidin-enriched sample from TOV-21G cells. Firstly, there was a significant number of non-membrane proteins detected. Of the proteins identified only 15% are classified as membrane proteins and two of the proteins were chromosome 18 gene products. The high proportion of non-membrane proteins may be attributed to experimental procedure and non-specific binding. Cellular material from dying cells may also be labelled and enriched. The label maybe internalised to a small degree during labelling, accounting for the recovery of abundant housekeeping cytoplasmic proteins. However, some of these non-membrane proteins may infact be targeted to the cell surface by as yet unexplained mechanisms. Previous research employing surface labelling by biotinylation and enrichment with streptavidin has shown similar proportions of non-membrane proteins amongst the total identified (Shin, Wang et al. 2003). For example, heat shock proteins (HSPs) have been found that do not encode transmembrane domains or signal sequences within their genomic structures. It is uncertain how these proteins are targeted to the cell surface, but it is unlikely that they utilize the classical secretory pathway from the ER via the golgi to the plasma membrane

(Multhoff and Hightower 1996). Labelling on ice was thus implemented from this point on to slow down possible label internalization and labelled cells were first fractionated into a crude membrane-enriched sample by hypotonic lysis and centrifugation to reduce possible non-specific binding of intracellular proteins to the streptavidin beads.

This technique for profiling of the cell surface proteome was then adapted for quantitative analysis of expression in the EOC models. This involved the use of TMT labels as before, although the enriched fractions from each cell line were run onto the top of a 20% polyacrylamide gel as a discrete band, fixed, stained and excised prior to digestion with trypsin and TMT labelling. This was introduced as a clean-up step because the surface fractions were better eluted in sample buffer rather than DTT alone as hoped. The digests were TMT labelled and separated into ten fractions by SCX for identification and quantification by RPLC-MS/MS (see Chapter 5.1).

5.4.3 Identification of differentially expressed surface labelled proteins

A total of only 93 unique protein identifications were made from 147 unique peptide matches. The decoy database search resulted in 10 matches with a score equal to or above the Mascot peptide identity threshold compared to 146 matches against the target database; a false discovery rate of 6.8%. For matches with a peptide score equal to or above the homology threshold the decoy database search resulted in 55 matches

compared to 247 matches against the target database which resulted in a false discovery rate of 22.3%. The charge distribution among the identified peptides was 43.8% +2, 52.1% +3 and 4.2 % +4. The proportion of TMT-labelled peptides was 7.7% with none changing significantly, calculated by database searching with and without TMT-6plex modifications. Database searching without TMT-6plex (N-term/K) modifications resulted in 441 proteins identified from 1418 unique peptide matches. The decoy database search resulted in 75 matches with a score equal to or above the Mascot peptide identity threshold compared to 1342 matches against the target database; a false discovery rate of 5.6%. For matches with a peptide score equal to or above the homology threshold the decoy database search resulted in 125 matches compared to 1869 matches against the target database which resulted in a false discovery rate of 6.7%. The charge distribution among the matched peptides was 76.1% +2, 23.5 % +3 and 0.34% +4.

Thus despite careful preparation of the surface-labelled protein digests, TMT labelling had not been successful. The method required an equal amount of surface labelled lysate from each cell line to be captured on streptavidin beads. After washing, captured protein was eluted in sample buffer and DTT and loaded onto a gel. This may have introduced contaminants which reduced the TMT-labelling. In addition a Speedvac was used to concentrate the sample prior to TMT labelling and results in heating of the sample over prolonged periods and was difficult to resolubilise. It is possible that freeze drying would have improved the TMT labelling although, unfortunately, a freeze dryer was unavailable at the time of the experiment and there was insufficient time on the project to repeat and optimize the experiment.

5.5 Conclusions

The TMT-6plex labelling approach allowed the simultaneous relative quantitation of proteins from extracts of the six cell lines under study, which included whole cell, secreted and crude-membrane fractions. This application was optimised on an Orbitrap XL resulting in sensitive and accurate protein identification with quantification. Importantly, the application of 2D-LC with TMT labelling has addressed the fundamental limitations of the 2D-DIGE method for detecting proteins of low-abundance, poor solubility, very small or large size and extreme pIs that were previously under-represented in the earlier analyses. Unfortunately the application of surface labelling with 2D-LC MS/MS in combination with TMT was unsuccessful. Adjustments to the protein extract preparation prior to labelling would certainly improve the TMT labelling. However, due to time constraints the experiments could not be repeated in this study. The protein identifications were useful in assessing the performance of the surface labelling strategy.

A total of 1601 proteins identifications with quantitative information were obtained by 2D-LC with TMT labelling from the whole cell, secreted and crude membrane fractions, with 242 differentially expressed proteins (> 2-fold) found between at least one parental cell line and its corresponding hybrid clone. Functional classification of the differentially expressed proteins using gene ontology databases showed that the majority were involved with cell differentiation (11%), followed by multi-cellular organismal development (9%) and cell death (7%) (Fig 5.10). Cellular differentiation is important for dividing cells to

achieve a set of structural and functional characteristics specific to a tissue. This process appears to be controlled by a combination of genetics and external stimuli, whilst the organisation of differentiated cells is maintained by proteins involved in multicellular organismal development. The processes of cellular differentiation and organization are key to understanding mechanisms of cellular transformation where failure in these processes can lead to abnormal growth and division of cells. Proteins that are involved in cell death are vitally important in maintaining quality control and repair mechanisms by elimination of unwanted genetically damaged cells. Evasion of apoptosis is a hallmark of cancer. Despite these functional classifications, many of the identified differentially expressed proteins have unknown biological functions, and it is tempting to speculate these as having roles in tumour promotion or suppression

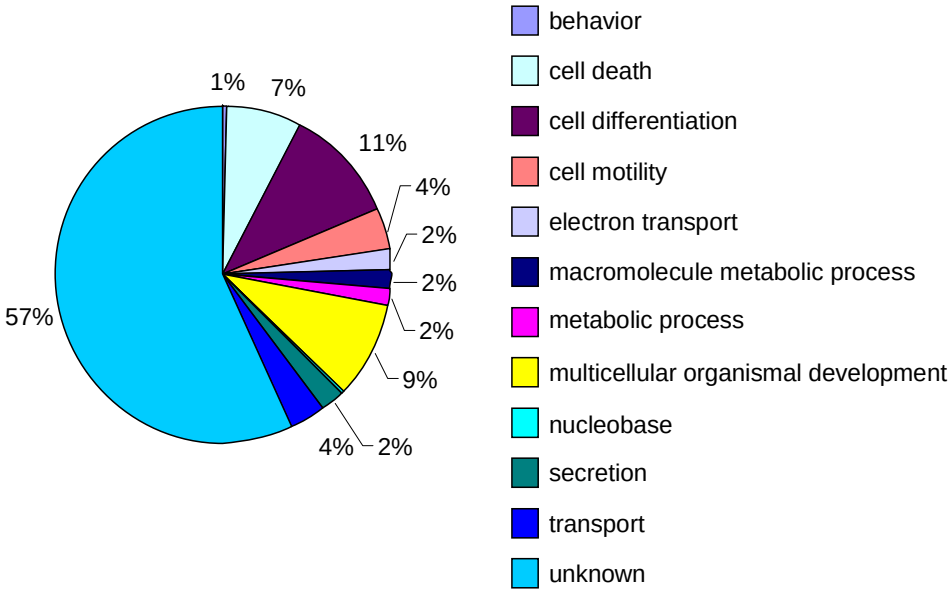

Figure 5.10 Biological function based on gene ontology databases of proteins identified displaying differential expression > 2 fold in at least a single hybrid clone. Individual proteins may have multiple functions assigned. The high proportion of assignments as 'unknown' possibly reflects the need for databases to be managed and updated more thoroughly as functional data is generated.

As seen in the 2D-DIGE analyses there was little overlap between the cell models in terms of protein changes identified. Again this possibly reflects the different molecular atiologies of endometrioid versus clear cell carcinomas from which the two parental cell lines were derived. Additionally, few proteins displayed concordant expression within a hybrid pair due to the possible clonal variation described earlier. Those proteins whose expression was concordant across both cell models or at least within a hybrid pair were considered to be the most interesting as potential biomarkers of neoplastic suppression and possibly functionally involved in tumour suppression.

A single protein, annexin A1, displayed concordant down-regulation (> 2 fold) in the 18-D-22 and 18-D-23 cell lines, compared to parental cell line TOV-112D in the whole cell lysate analysis. Annexin A1, a protein involved in cell differentiation, is a calcium and phospholipid binding protein with roles in maintenance of the cytoskeleton and extracellular matrix integrity, but may have other cellular functions and has been linked with reduced cell proliferation through regulation of the ERK/MAPK signalling pathway (Alldridge and Bryant 2003). Expression of annexin A1 has been observed to be down-regulated in head and neck, prostate, oesophagus and gastric cancer (Paweletz, Ornstein et al. 2000; Xia, Hu et al. 2002; Garcia Pedrero, Fernandez et al. 2004; Inokuchi, Lau et al. 2009), but up-regulated in pituitary, pancreatic, breast and hepatocellular cancer (Masaki, Tokuda et al. 1996; Pencil and Toth 1998; Bai, Ni et al. 2004; Mulla, Christian et al. 2004). The up-regulation of annexin A1 seems to occur predominantly in hormonally regulated cancers (Zhao, Hashiguchi et al. 2002). Annexin A1 was down-regulated in the hybrid clones used in this study and this was observed in both the 2D-DIGE and 2D-LC-MS/MS with TMT labelling analyses. Thus, it is tempting to speculate that annexin A1 may normally promote OC progression, and that it is down-regulated in the hybrid clones as a consequence of neoplastic suppression. Another protein identified in the whole cell lysate involved in cell differentiation, is galectin-1, a ubiquitously expressed protein (Camby, Le Mercier et al. 2006). Galectin-1 lacks a recognisable secretion signal sequence and does not pass through the ER/Golgi pathway and so must be secreted by another as yet undetermined process. In tumour development, galectin-1 has been shown to interact with the oncogene *H-RAS* and contributes to its membrane anchorage and transforming capacity (Paz, Haklai et al. 2001). Furthermore, galectin-1

has been shown to promote cell growth, cell adhesion and cell migration (Yang and Liu 2003; Rabinovich 2005). Interestingly, while the endogenously expressed protein is implicated as a growth-promoting factor, exogenously added galectin-1 was shown to inhibit neuroblastoma cell proliferation (Kopitz, von Reitzenstein et al. 2001). Galectin-1 was previously identified as down-regulated in clone 18-G-5 by 2D-DIGE analysis of secreted protein. This result would seem to correlate with the suppressed tumourigenic phenotype exhibited by this hybrid clone. However, analysis by 2D-LC-MS/MS with TMT quantification identified a significant up-regulation of galectin-1 in the hybrid clone 18-D-22 with a limited change observed in the other hybrid clones. It must be noted that the origin of the extract is different for this comparison.

Among the whole cell lysate proteins functionally classified as involved in cell motility was caldesmon. Cell motility is important in cancer cells as migration is critical in tumour invasion and metastasis. Caldesmon is an actin and tropomyosin binding protein that has been shown to be a potent repressor of podosome/invadopodium and cell invasion in cancer cell lines (Yoshio, Morita et al. 2007). The up-regulation of this protein in the hybrid clones 18-D-22 and 18-D-23 may reflect the suppression of tumourigenic phenotype in these clones as evidenced by their relatively poor growth in soft agar.

The fractionation of secreted proteins from conditioned medium was examined previously by 2D-DIGE analysis with some success. For the same fraction, 2D-LC-MS/MS approach would be expected to identify an overlapping set of secreted proteins plus others, potentially of lower abundance or not amenable to 2DE analysis. The cellular

location of identified proteins were determined from gene ontology databases (Fig 5.5). The success of the fractionation technique was highlighted by the numbers of proteins assigned to the extracellular region, extracellular space and proteinaceous extracellular matrix representing 26% of the cellular protein identified. In addition, 8% of identifications were assigned to membrane and cell surface proteins. These classes of proteins would be considered good candidate serum markers.

The secreted fraction yielded a significantly increased response in protein expression changes compared to the WCL fraction with some proteins displaying concordant expression across both cell models. Calreticulin (CRT) and a fragment of CRT, displayed significant down-regulation of expression in both cell models. This calcium binding protein has a high capacity for buffering Ca^{2+} and behaves as a Ca^{2+} signalling regulator. It is located most abundantly in the lumen of the ER and can be presented at the surface of cells where it is thought to induce an immunogenic response (Chaput, De Botton et al. 2007; Obeid, Tesniere et al. 2007; Obeid, Tesniere et al. 2007); an association with ERp57 at the surface of cells has been identified as a signal for phagocytosis (Johnson, Michalak et al. 2001). CRT fragments have also been found in the serum of patients with pancreatic cancer (Hong, Misek et al. 2004). The decrease in CRT expression observed in all the hybrid clones under analysis may reflect that these cells have been rescued from a state of lethality by incorporation of chromosome 18 and its tumor suppressive effect. It has also been shown that tumour cells treated with anthracyclins expose CRT on their cell surface, which marks them for removal by the immune system (Obeid, Tesniere et al. 2007).

Another protein displaying significant down-regulation was follistatin-related protein 1 (FRP), also known as FSTL1 and TSC-36. This is an extracellular glycoprotein containing a follistatin-like sequence containing 10 conserved cysteine residues. Follistatin is a specific inhibitor of the biosynthesis and secretion of pituitary follicle stimulating hormone. FRP may regulate the action of some growth factors in cell proliferation and differentiation. Expression has been shown to be increased by TGFβ1, a potent inhibitor of cell growth (Shibanuma, Mashimo et al. 1993). Furthermore, it appears to play a role in the altered phenotype of transformed cells, including negative regulation of their growth (Liu, Wang et al. 2006; Chan, Ngan et al. 2009). Levels of FRP are also decreased in V-ras transformed NTH3T3 (DT) fibroblastic cells (Mashimo, Maniwa et al. 1997). Moreover, when FRP was transfected into a NSCLC cell line, the transfectants displayed decreased growth rate and a change in cell morphology (Sumitomo, Kurisaki et al. 2000) and in the ovarian cancer cell line Ovca420 and endometrial cancer cell line AN3CA, cell migration and invasive capability were reduced (Chan, Ngan et al. 2009). It has also been shown to inhibit the invasiveness of rat fibroblasts transformed with v-fos (Johnston, Spence et al. 2000). Clearly, FRP has a tumour suppressive effect on a spectrum of cancer cell types. The down-regulation displayed in the hybrid cell lines compared to their parental cells does not indicate a suppressive role in the OC models used here. The down-regulation of expression could possibly reflect the hybrid cells return to more normal cell growth and proliferation, therefore FRP is not causative to the suppressed phenotype.

The secreted protein, stromelysin-2 (MMP10), displayed significant up-regulation in all but one of the hybrid clones under analysis. This protein is one of a family of 24 matrix-metalloproteinases (MMPs) that degrade the protein constituents of the connective tissue thereby facilitating invasion. MMP activity is tightly controlled by transcriptional activation of tissue inhibitors of metalloproteinases (TIMPs). MMP10 activity has been implicated in carcinogenesis and its over-expression has been observed in NSCLC compared to normal lung tissues (Gill, Kirwan et al. 2004; Zhang, Zhu et al. 2007), in human bladder transitional cell carcinoma (Seargent, Loadman et al. 2005), renal cell carcinoma (Miyata, Iwata et al. 2007) and lymphoid tumours (Van Themsche, Alain et al. 2004). Furthermore, MMP10 along with MMP9 have been shown to confer protection from PKC/p53-mediated apoptosis in human colon adenocarcinoma cell lines (Meyer, Vollmer et al. 2005). However, it is becoming apparent that MMPs also play a critical role in physiological processes such as regulation of the growth factors, chemokines, cytokines and cell surface adhesion receptors and proteoglycans involved in cell communication. The dys-regulation of these molecules may promote carcinogenesis. It would appear that MMP10 may also play a role in neoplastic suppression, as evidenced by its up-regulation in the OC cell models used here.

The membrane protein, protein tyrosine phosphatase-like protein (PTPLAD1), was identified from the crude membrane extract displaying concordant changes in the TOV-112D cell model. PTPLAD1 is involved in *RAC-1* signalling leading to the modulation of gene expression (Courilleau, Chastre et al. 2000). The observed up-regulation of this protein in the 18-D-22 and 18-D-23 hybrid cell lines may reflect an inhibitory control

over cell proliferation, differentiation and transformation through apoptosis in which this poorly characterised protein may play a role.

Another protein identified in the crude membrane extract displaying a significant change in expression was nucleolin, an abundant RNA- and protein-binding protein that is ubiquitously expressed. In the nucleus it controls DNA and RNA metabolism. In the cytoplasm it chaperones protein into the nucleus and also regulates mRNA activity. On the cell surface it can serve as an attachment protein for several ligands (Storck, Shukla et al. 2007). The ligands of nucleolin have been found to play an important role in tumourigenesis and angiogenesis. Nucleolin binds to laminin-1 that induces differentiation of cells (Turck, Lefebvre et al. 2006) and hepatocyte growth factor that regulates angiogenesis and the invasion and growth of cancer cells (Tate, Isotani et al. 2006). Surface levels of nucleolin have been reported to be increased in cells stimulated with VEGF (Huang, Shi et al. 2006) and it has been identified as an ErbB receptor interactor in breast cancer cells (Di Segni, Farin et al. 2008) It is also reported to reduce levels of the tumour suppressor protein p53 by inhibiting translation of the p53 mRNA (Takagi, Absalon et al. 2005). The down-regulation of expression of nucleolin observed in the hybrid cell lines 18-G-5 and 18-G-1.26 could reduce the potential of the cells to respond to growth ligands and/or promote p53 expression and thus suppresses their tumourigenic phenotype.

Another ubiquitously expressed protein displaying reduced expression in one of the cell models was prohibitin. Studies have shown that overexpression of prohibitin promotes

cell survival in ovarian cancer cells by inhibiting the cell cycle and blocking apoptosis whilst silencing has the opposite effect (Gregory-Bass, Olatinwo et al. 2008). The down-regulation of its expression observed in the hybrid cell lines 18-G-5 and 18-G1.26 may thus contribute to the reduced transformed phenotype of these cells.

Finally, heat shock protein 90α (HSP90A) was identified as displaying a significant reduction in expression in the TOV-112D cell model. This molecular chaperone regulates protein interactions by facilitating normal protein folding and its expression in cells under stress is an adaptive response to promote cell survival (Zhao, Hashiguchi et al. 2002). In cancer cells, the ability to prevail over stressful environments is vital for their survival and their ability to tolerate mutations in critical signalling molecules that would otherwise be lethal ((Isaacs, Xu et al. 2003; Neckers 2007; Tsutsumi, Beebe et al. 2009). HSP90 performs these twin roles through interaction with key protein kinase signalling molecules and its potential as a target for anti-cancer agents has been realised (e.g. 17AAG (Maloney, Clarke et al. 2007) currently on trial). The down-regulation of expression of HSP90A in the hybrid clones 18-D-22 and 18-D-23 is likely to reflect the tumourigenic suppression observed in these hybrid clones compared to their parental cancer cell line and as such may make a useful marker in OC.

It has not been possible to comment on all the proteins found to be differentially expressed, but these may well have roles in generating the tumourigenic suppression phenotype. However, it is difficult to assess from this work which of these changes are causative and which are a consequence. This will require further functional studies.

Chapter 6 Validation of protein changes observed by proteomic profiling

Introduction

The differential expression of protein candidates identified by 2D-DIGE and 2D-LC-MS/MS + TMT analysis were further validated in the TOV-112D and TOV-21G models by immunoblotting where antibodies were available. Additional clones were also examined, as were revertant cell lines, where the normal Ch18 material has been lost, and a panel of ovarian cancers and NOSE cell lines. Candidates were selected based on expression profile and putative role in cancer. Furthermore, the potential of one candidate (MMP10) as a biomarker was assessed by measuring the level of this protein in serum from cases of malignant and benign OC and healthy controls. Finally, to further assess if any of the candidates were linked to aberrant growth factor signalling, the activation of downstream signalling was assessed in the cell models following EGF treatment.

6.1 Validation by immunoblotting

Tumour protein p53-inducible gene 3 (PIG3) expression was up-regulated in hybrid clone 18-D-22 and 18-G-5 in the 2D-DIGE analysis of whole cell lysates (Fig 6.1A). In western blot analysis the PIG3 signal was elevated in hybrid clone 18-G-5 and slightly less so in hybrid clone 18-G-1.26 compared to the parental cell line TOV-21G (Fig 6.2A). Notable,

PIG3 expression was also elevated in the other 18-G-clones, and importantly reverted in revertant clones where normal Ch18 material transferred into TOV-21G has been lost due to removal of the antibiotic selection. The elevated signal in hybrid clone 18-G-5 compared to its parental cell line TOV-21G was thus in agreement with the 2D-DIGE data. Its consistent behaviour in the other clones, reduced expression in the revertants and p53-inducible nature support its functional role as a tumour suppressor in this model.

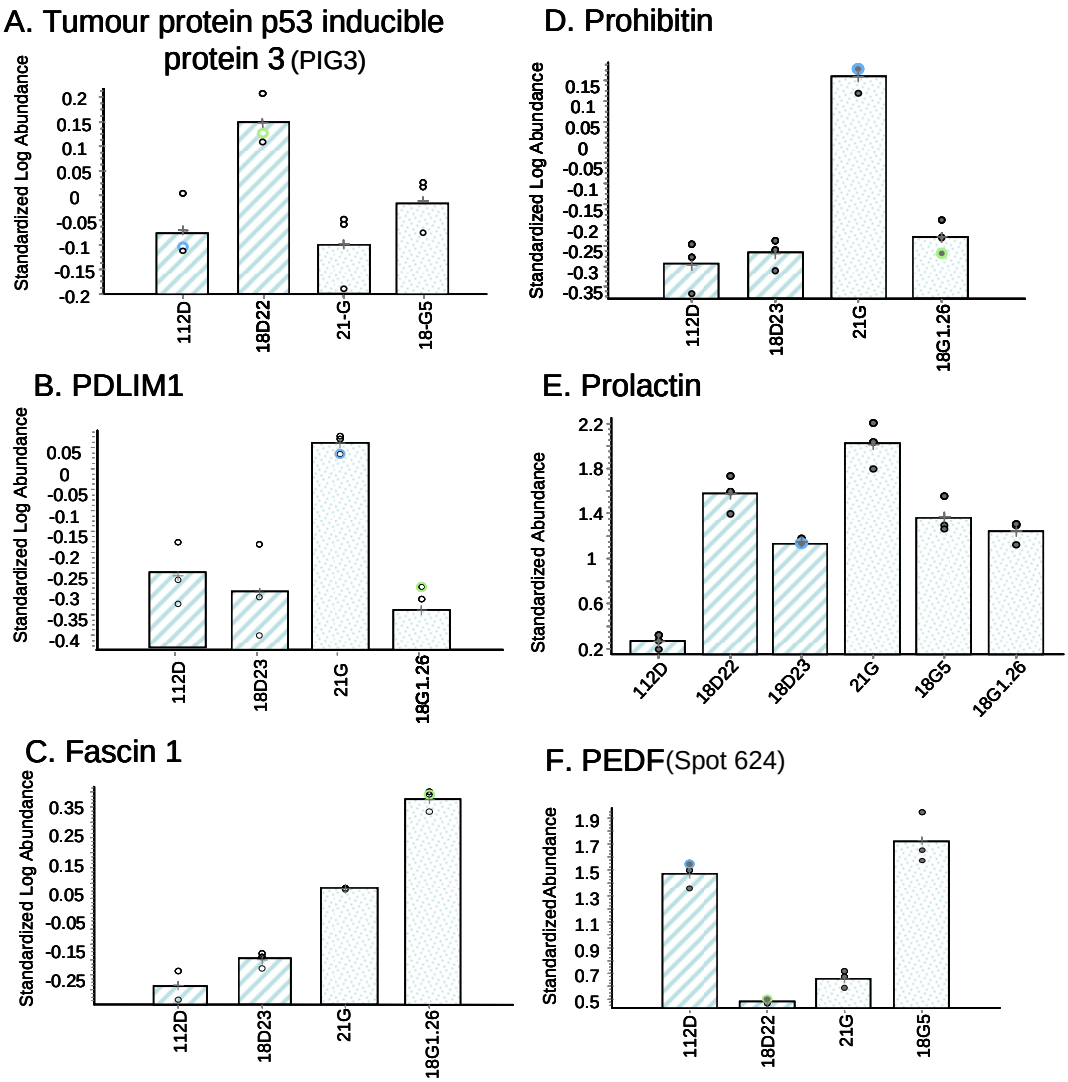

Figure 6.1 DeCyder analysis of differential protein expression. Graphical representations for selected proteins are shown as average standardized abundance (i.e. abundance versus the Cy2-labelled standard) for each condition with triplicate measurements. Isoforms of PEDF are distinguished by spot number in brackets.

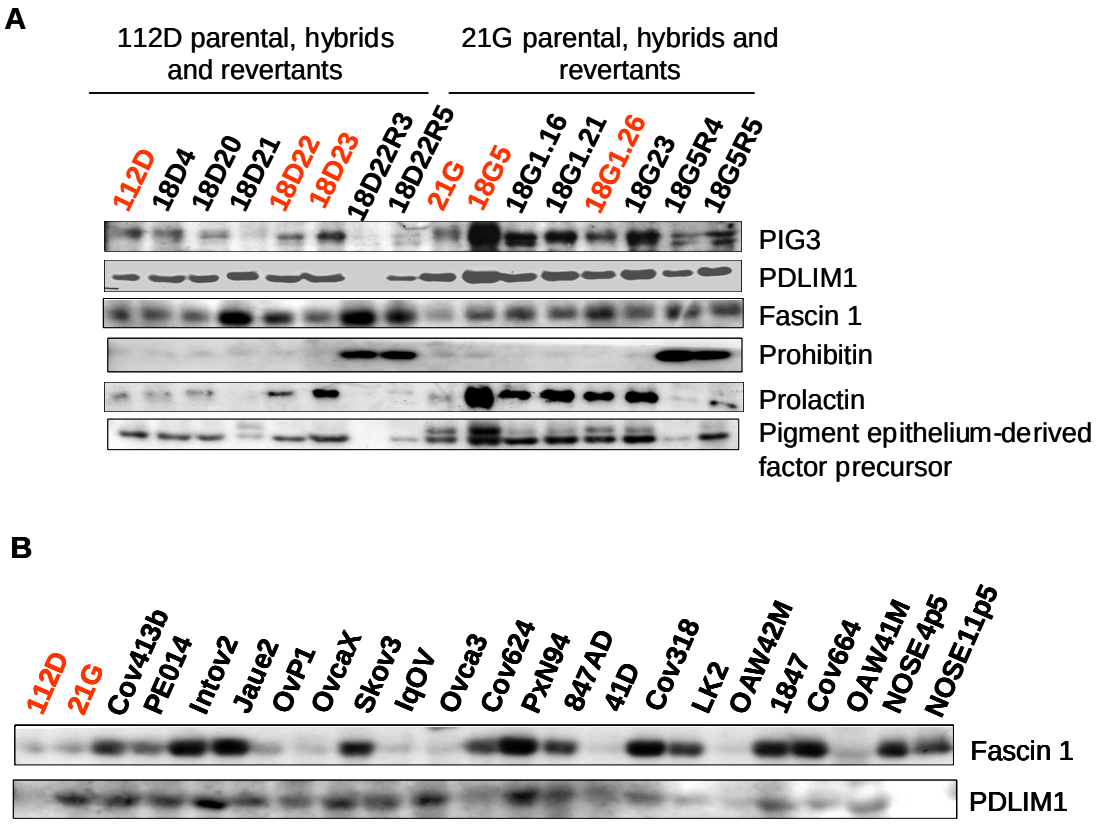

Figure 6.2 Western Blot analyses of A. Models of EOC tumour suppression and revertants, and B. OC cell lines and normal ovarian surface epithelium cell lines. Equal amounts of protein extract were loaded onto a 12% SDS-PAGE gel and processed for western blotting with the indicated antibodies. Highlighted in red are the cell lines used for proteomic screening in this study. Clones 18-D-22R3, R5 and 18-G-5R4,R5 are revertants of the 18-D-22 and 18-G-5 hybrid clones, where normal Ch18 material has been lost.

PDZ and LIM domain protein 1 (PDLIM1), a cytoskeletal protein, was found to be down-regulated in hybrid clone 18-G-1.26 in the 2D-DIGE analysis of the whole cell lysate (Fig 6.1B). Levels were fairly consistent for all cell lines in the western blot analysis except in hybrid clone 18-G-5 where it was up-regulated and revertant 18-D-22-R3, where no

signal was detected (Fig 6.2A). The differentially expressed protein spot identified as PDLIM1 in the 2D-DIGE analysis could represent a specific isoform, while western blot analysis detected total PDLIM1 protein and may explain the difference in results between the two methods.

Fascin 1 organises actin filaments, this protein was up-regulated in hybrid clone 18-G-1.26 (Fig 6.1C) and is consistent with the robust signal in the western blot analysis (Fig 6.2A). Expression of fascin 1 was also elevated in all of the TOV-21G hybrid clones compared to their parental cell line, although this expression change appeared not to be reverted by loss of Ch18 material. In the other cell model, signals were elevated in hybrid clone 18-D-22, although, this was not observed in the 2D-DIGE analysis, where as expression in clone 18-D-23 was.

Prohibitin, a regulator of proliferation was identified in the 2D-DIGE and TMT analyses as being down-regulated in hybrid clones 18-G-1.26 (Fig 6.1D) and 18-G-5. Surprisingly, the western blot analysis displayed strong signals for all revertant cell lines tested, although its expression appeared to be down-regulated in 18-G-1.26 versus its parental (Fig 6.2A). Expression of prohibitin has obviously been altered further by the removal of incorporated chromosome 18 in these cells.

The 2D-DIGE analysis of secreted proteins identified prolactin and PEDF as differentially expressed proteins. Prolactin, a hormone belonging to the somatotrophin

family, displayed up-regulation in hybrid clones 18-D-22 and 18-D-23 (Fig 6.1E). This was consistent with the western blot analysis, where signals were elevated in these two cell lines compared to the parental, TOV-112D (Fig 6.2A). The revertant cell lines behaved as would be expected and exhibited a similar signal to their parental cell lines. In the other cell model, levels were also elevated in all hybrid clones, though this was not detected in the 2D-DIGE analysis where the prolactin isoform was moderately decreased in the two TOV-21G hybrid clones examined. Three isoforms of the neurotrophic protein, pigment epithelium-derived factor (PEDF), were identified by 2D-DIGE/MS displaying contrasting expression possibly due to the presence of different PTMs. The up-regulation of expression in hybrid clone 18-G-5 observed in gel spot 624 (Fig 6.1F) is consistent with the increased signal detected by western blot analysis in this cell line. Notably, its expression was reduced in the revertants, adding weight to its choice as a candidate biomarker for further characterization.

Fascin 1 and PDLIM1 were differentially expressed in the 2D-DIGE analysis of whole cell lysate. Antibodies for these were used to probe the whole cell lysates of a panel of OC cell lines and normal ovarian surface epithelium (NOSE) cell lines (Fig 6.2B). Fascin 1 expression fluctuated between very low signal to robust signal in the OC cell lines. Levels in the two NOSE cell lines examined were elevated in comparison to the TOV-112D and TOV-21G cancer cell lines. Whilst this suggests fascin may play a role in tumour suppression, its down-regulation is not a general feature in all ovarian cancers. PDLIM1 displayed a more consistent level of expression in the OC cell lines, while the signal was conspicuously absent in the two NOSE cell lines. This suggests that PDLIM1

may be generally elevated in ovarian cancers, and thus may play a role in promoting tumourigenic phenotype.

Unfortunately, not all the promising candidates could be validated by immunoblotting because some antibodies that were tested proved to be non-specific or resulted in no signal at the correct molecular weight or antibodies could not be found against them. These included IGFBP7, galectin-1, TIMP1 and FRP.

6.2 Validation by ELISA

A commercially available ELISA kit has been developed for MMP10, therefore the level of this secreted protein was examined in serum as a potential biomarker of EOC. Serum samples collected from women diagnosed with malignant ovarian cancer, benign disease and matched healthy controls from the UKOPS (United Kingdom Ovarian Cancer Population Study) were tested using this MMP10 immunoassay for validation. Serum samples from 43 malignant, 22 benign and 22 healthy controls were examined. The ovarian cancer serum samples came from a representative selection of histological subtypes and were split by stage resulting in 24 stage I + II and 19 stage III + IV cases. The MMP10 immunoassay (Quantikine) is a sandwich enzyme immunoassay carried out in a 96 well plate format as described in Chapter 2. Levels of MMP10 were marginally elevated in the ovarian cancer cases. A stage wise comparison showed a significant elevation of MMP10 ($p=0.041$) in stage III + IV versus healthy whilst none of the other comparisons were statistically significant (Figure 6.3).

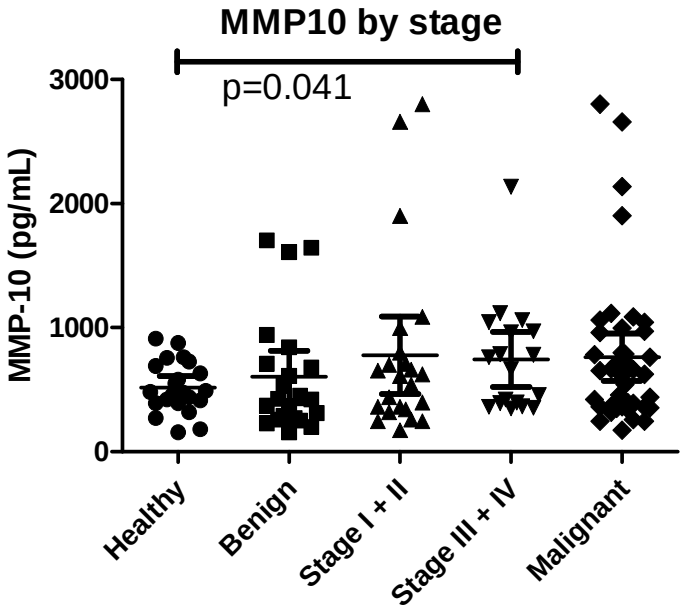

Figure 6.3 Serum levels of MMP10 in malignant and benign cases of OC and healthy controls. Bars indicate median and upper and lower quartiles.

The up-regulation of MMP10 in the hybrid clones found in the TMT analysis suggested a potential role of this protein as a tumour suppressor. However, the contrasting expression in the immunoassay suggests an alternative role. MMP10 would not be valuable as an early detection biomarker for OC, however, elevated levels in stage III + IV OC cases were significantly different to healthy controls, indicating it as a potential prognostic marker. Thus functional characterisation of this protein should be considered, as well as further testing in larger cohorts, of ovarian cancer cases and controls with correlation to follow-up clinical data.

6.3 Examination of EGF-dependent signalling

Cellular proliferation is a tightly regulated process carried out by a complex inter-play of growth factors, growth factor receptors and signalling components. The role of growth factor driven signalling has been recognized for a long time as important in the pathogenesis of human cancer. Many proto-oncogenes code for proteins that are involved in intracellular signal transduction. For instance, the epidermal growth factor receptor (EGFR) family has a critical role in the pathogenesis and progression of many cancers. EGFR is a glycoprotein and tyrosine kinase that is expressed on the cell surface and it functions as a receptor for a family of ligands including EGF. It is involved in regulating cellular proliferation, survival, migration and differentiation. Approximately 50% of ovarian cancers have elevated levels of EGFR which is associated with a poor prognosis (Nicholson, Gee et al. 2001; Yarden 2001). Akt and Erk are downstream targets of EGFR that form part of a survival and mitogen activated protein kinase (MAPK) signalling cascade, respectively. Phosphorylation and activation of these kinases drives proliferation and survival, and signalling through these kinases has been intricately linked with the pathogenesis of human cancer (Hanahan and Weinberg 2000; Deb, Su et al. 2001; Vivanco and Sawyers 2002). Akt, a component of the PI3K signalling pathway, is activated in response to receptor-driven PIP3 production that drives Akt membrane recruitment through binding to its pleckstrin homology domain, and activating phosphorylation at Thr308 and Ser473. The Erk (MAPK) signalling cascade is activated downstream of numerous tyrosine kinase receptors in response to ligand binding and Ras activation and regulates many cellular processes, including proliferation and survival.

The expression and activation of these proteins in the parental and hybrid cell lines was examined by western blotting to ascertain the level of disruption to these signalling pathways, if any. The EOC cell lines were starved of serum and then stimulated with EGF and cells harvested at different time points. Protein concentration was measured and equal amounts of sample were separated by 1D SDS-PAGE and transferred onto membranes. The effect of EGF stimulation was analysed by western blotting with antibodies against Akt and Erk and their phosphorylated activated forms. The membranes were probed with the phospho-specific antibodies and then reprobed with the respective pan antibody. Epidermal growth factor receptor (EGFR) levels were also examined (Fig 6.4).

Anti-EGFR immunoblotting revealed virtually no signal in the TOV-112D cell line or its Ch18 MMCT hybrids 18-D-22 and 18-D-23, suggesting that this cell line expresses low levels of the receptor (Fig 6.4). In comparison, EGFR was detected at a much higher level in the TOV-21G and 18-G-1.26 cell lines, but less so in clone 18-G-5. This data suggests that EGFR may be over-expressed in this cancer cell line, and its expression lowered in at least one Ch18 MMCT clone, possibly explaining its suppressed tumourigenic phenotype. Upon stimulation with EGF, EGFR expression declined over time in the TOV-21G cell line consistent with ligand-induced receptor internalisation and degradation as reported in many cell systems (Oksvold, Huitfeldt et al. 2002). However, in the 18-G-1.26 cell line, EGFR expression was less dependent on EGF ligand triggering.

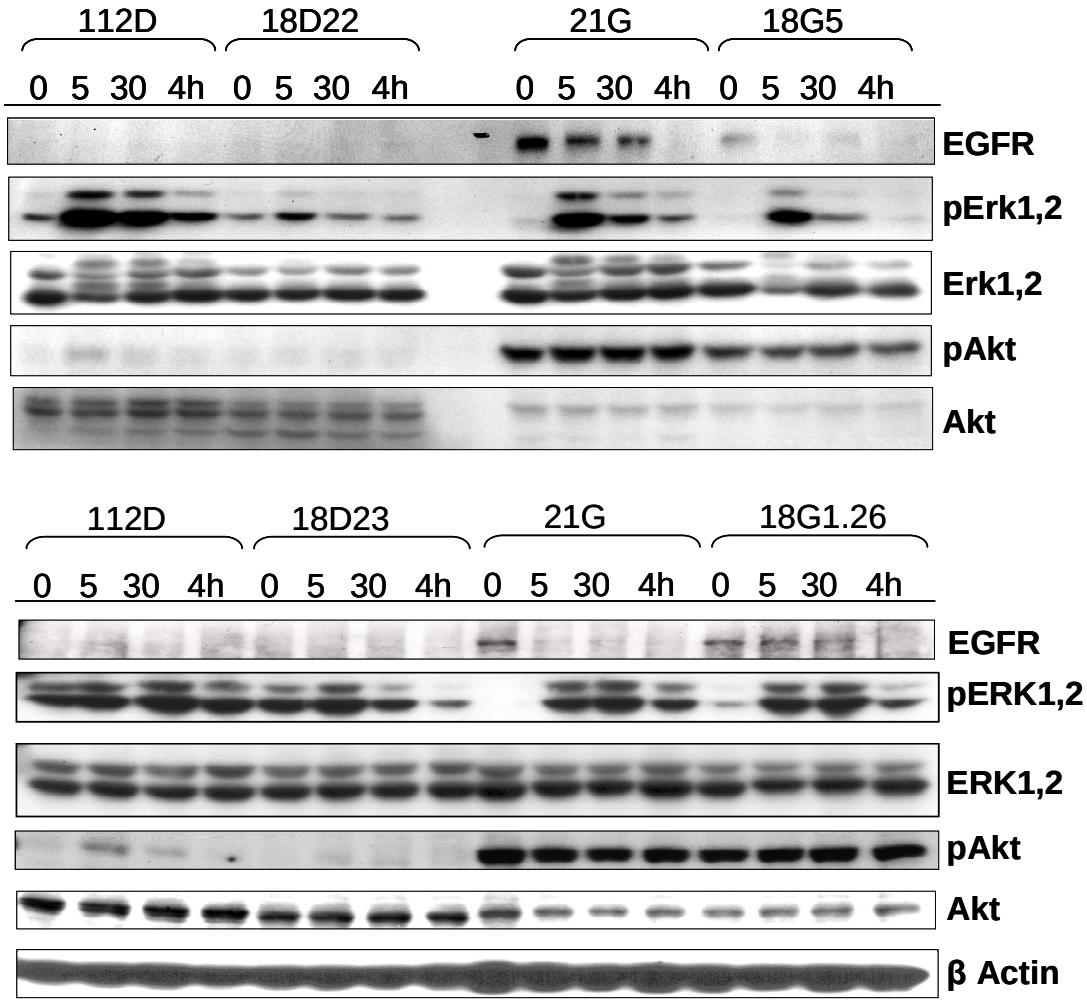

Figure 6.4 Response of parental EOC cell lines and their Ch 18 MMCT hybrids to EGF stimulation. Serum starved cells were harvested at 0, 5, 30 and 240 minutes after stimulation with 10 nM EGF. Targets are EGFR; a cell surface receptor involved in regulating cellular growth and differentiation, Akt and Erk; proteins that form part of a survival and MAPK signalling cascade respectively. Their phosphorylated forms drive proliferation and survival and have been linked with pathogenesis in human cancer.

The phosphorylation and activation of Akt was relatively unresponsive to EGF in both cell models, although it was constitutively elevated in the TOV-21G parental and derived hybrid cells, but less so in the 18-G-5 clone. The levels of total Akt remained constant

over the time course, but were higher in TOV-112D cells and its hybrid clones. Erk1/2 phosphorylation was rapidly and transiently activated by EGF in all cases, but was noticeably abrogated in hybrid clone 18-D-22. Total Erk1/2 levels remained unchanged with the mobility shift due to phosphorylation, clearly visible in one set of blots.

The fact that Erk was phosphorylated in the TOV-112D cells indicated that EGFR is indeed expressed in these cells, albeit at lower levels that the TOV-21G cells. It is clear from this preliminary data that the parental cell lines appear to have diverse and potentially disrupted signalling pathways. This may be expected in cell lines derived from tumours. For example, the apparent constitutive activation of Akt in the TOV-21G cells suggests deregulated PI3K signalling. This important signalling pathway has been reported to be activated in ~30% of all ovarian cancers and 45% of endometrioid and clear cell subtypes due to mutation and activation of PI3K itself or loss of the lipid phosphatase and tumour suppressor gene PTEN (Kurose, Zhou et al. 2001; Vivanco and Sawyers 2002). The hybrids also appeared to show some differences from their parental cell lines in both receptor levels and their response to EGF stimulation, suggesting that genes on Chromosome 18 may have the capacity to suppress these pathways. The alterations in the activation of these pathways may result in some of the observed protein changes deleted using the proteomic profiling technologies reported herein. These would occur through regulated transcription or protein turnover and it will be interesting to test this level of regulation using specific kinase inhibitors of Akt and ERK signalling, as well as to test the effect of acute EGF stimulation on the expression of candidate proteins. This however is beyond the scope of this study.

6.4 Conclusions

A number of proteins have been validated by immunoblotting. Candidates whose expression was found to be reverted in the revertant cell lines are especially promising. However, the effect of clonal variation is a problem when interpreting findings. Validation of more candidates has been hampered by reagent availability and lack of specificity of antibodies that were tested. MMP10 was found to be a marker in serum that could significantly discriminate between healthy and late stage ovarian cancer cases. Although not consistent with the TMT profiling data, where MMP10 was up-regulated in the Ch18 MMCT hybrids, this serum data is interesting and warrants further validation and needs to be repeated on a larger sample cohort. In addition, further candidates from the proteomic profiling should be tested in this manner to establish if they have biomarker potential.

Chapter 7 Discussion

Identifying molecular markers of disease may provide novel approaches to screening and diagnosis and could enable targeted treatment and/or lead to the design of novel therapies. The biological and molecular basis of epithelial ovarian tumour development remains poorly understood. The development of models of tumour suppression in EOC cell lines offers an alternative method for identifying potential markers for ovarian cancer and for understanding the molecular mechanisms of tumourigenesis.

The focus of this study has been the investigation of the protein expression profiles of two parental EOC cell lines and their MMCT Chromosome 18 hybrid cell lines to identify protein signatures of neoplastic suppression. The insertion of whole or partial normal chromosomal material into a cell has the potential for far reaching effects throughout the cell. In order to identify as many components of the complex biological processes occurring within these cell models, a large scale proteomic investigation was preferred. To achieve this, a combination of cellular fractionation, quantitative 2D-DIGE, affinity chromatography and 2D-LC-MS/MS were employed to examine the whole cell, secreted, membranous and cell surface proteomes.

The first approach was based on a differential two-dimensional gel electrophoresis pattern analysis between protein samples. This technique gives additional molecular information such as isoelectric point and molecular weight alterations arising from PTMs, providing further insight into possible protein activities. The drawbacks of this method included limited analysis of low-abundance, high molecular weight and hydrophobic proteins, and also time consuming and labour-intensive manipulation of gels. The second approach was a gel-free mass spectrometry-based peptide analysis technique that used isobaric amino-group-specific mass tags to compare the peptide intensities between samples to infer quantitative values for the proteins from which they are derived. This method is advantageous in that it can be completely automated and there is reduced bias against low-abundance proteins. The disadvantages include a bias towards high molecular weight proteins, lack of protein mass or pI information and hence loss of information about specific isoforms and reduced through-put due to extended analysis times.

In a comparison of the two proteomic platforms, nearly 400 protein changes were identified in the whole cell and secreted fractions of the two cell models by 2D-DIGE, while over a 1000 proteins were identified and quantified in the TMT analyses resulting in ~250 protein changes being identified. A typical pH 3-10 NL gel is capable of resolving over 2000 protein isoforms, a number comparable (until recently) with non-gel 2D-LC-MS/MS approaches. 2D-LC-MS/MS is still improving in terms of the identification of greater numbers and lower abundance proteins from a single sample (Nagele, Vollmer et al. 2004). With these advances, the use of isobaric tags has become increasingly popular for protein quantification between multiple samples. While 2D-LC-

MS/MS techniques identify as many peptides as possible before the quantitative information can be determined, 2D-DIGE has the advantage that only significantly altered protein isoforms are selected for identification. Although labour intensive, image analysis software such as DeCyder, quickly identifies protein spots that are differentially expressed above a determined threshold for picking and identification by MS. The need for more convoluted HPLC and MS identification and analysis is negated. The quantitative information in gel-free platforms is only 'unlocked' once complicated analysis of MS data has been performed. For this reason, there is a lot of redundancy in the data-sets produced. Due to the large number of proteins identified, more stringent approaches for selecting proteins of interest must be employed. In the present study, the list of protein identifications was extensive (see Appendix) and so only proteins displaying a change of expression in both hybrid clones of at least one cell model were reported in the results sections.

Using the gel-based platform, protein products from a single gene were identified in multiple distinct protein spots. For example, IGFBP7 was identified by 2D-DIGE/MS as 6 differentially expressed isoforms. As noted in Chapter 4, these isoforms may represent glycosylated and/or splice variant forms, including a very acidic form. Although this gives us information on the chemistry of certain isoforms and their abundance, it also poses challenges for quantitation. For example, IGFBP2, identified in the same experiment, displayed 3 distinct isoforms. These isoforms behaved differently in each cell line comparison. Interpretation of these kinds of features must be carefully undertaken. It should not be assumed that it is possible to determine overall protein regulation when it is

represented by a number of different protein isoforms. This was less problematic in the gel-free platform with TMT labelling, where quantitation is assessed at the peptide level, although isoform-specific information is usually lost. Another feature of 2D-DIGE that affects interpretation of differential expression is the co-migration of proteins. For co-migrated proteins, DeCyder is not robust enough to identify unambiguously the boundaries of each protein form, so assignment of the altered protein is not possible. In the present study, multiple cases of 2 and 3 unique protein identifications were observed in a single spot. 2D-DIGE quantitation works best where a proteome has been resolved to the extent that a single spot will represent one protein. This can be done by introducing fractionation steps to reduce the complexity of the sample before 2D-separation. The use of different pH gradients in the first dimension and gradient gels in the second dimension could also be used to improve separation, although this would be labour intensive and costly. In the present study the use of both gel-based and 2D-LC-MS/MS platforms together was complimentary and generated a large dynamic spectrum of protein changes with putative roles in neoplastic suppression. Indeed, there was little overlap between the two approaches, although importantly, those proteins identified by both approaches generally displayed concordant changes in expression level. Those protein changes that did not, could be explained by differential PTMs exhibited by multiple isoforms.

Preliminary experiments examined whole cell lysates of parental cell lines versus hybrid pools using 2D-DIGE. Five hybrid clones derived from each parental cell line were chosen for their potent suppression of tumourigenicity *in vitro* and *in vivo*. This was considered to be the best way to analyse a large number of hybrids without incurring the

high costs of running many 2D-DIGE gels. The results showed that there was little overlap between the cell models with many proteins being oppositely regulated and all but one being a chromosome 18 gene product. The lack of overlap in protein expression between the two cell models may reflect the fact that the cell lines are derived from endometrioid and clear cell ovarian carcinomas respectively, which presumably display different molecular aetiologies. However, the differences will also reflect the considerable clonal variation that was apparent. Following on from this, a single hybrid clone from each pool was selected for direct comparison with its parental cell line under the same experimental conditions. The number of protein spots displaying a significant change in expression was reduced. This difference compared to the pooled analysis indeed reflects the heterogeneity of the hybrid cells selected for each pool. Despite this, common changes were identified across the two experiments and between the two cell models. Two further hybrid clones from each pool were then selected for comparison in the same way. These also displayed potent suppression of tumourigenic phenotype *in vitro* and *in vivo* and further candidate proteins involved in suppression were identified.

Microsatellite repeat analysis and CGH array analysis showed a ~10 Mb region had been transferred in the TOV-112D hybrid cell lines. The proteomic signatures of these hybrid clones were relatively equivalent, as would be expected. A full copy of chromosome 18 was transferred into the TOV-21G hybrid cell lines. The proteomic signatures of these hybrid clones were vastly different from the TOV-112D clones and could be attributed to the difference in Ch18 incorporation. In addition, CGH array also identified other gross differences in the chromosomal material (Chapter 1). Particularly, the TOV-112D hybrid

clones had additional genetic changes including deletion of chromosome 8q and part deletion of chromosome 9q in both hybrids, and deletion of the majority of chromosome 12q in hybrid clone 18-D-23. The TOV-21G hybrid clones revealed almost complete transfer of Ch18 without other gross changes. These changes may also explain the observed differences between the hybrid clones of each cell model. Despite broad coverage of the genome, few chromosome 18 gene products were identified as being differentially expressed. Thus, a proportion of the expression changes measured must be secondary effects of Ch18 insertion, where Ch18-encoded genes regulate the expression of genes on other chromosomes. This reveals the complexity of gene and protein regulation in this system.

Functional classification by gene ontology database searching revealed that the most represented classes of proteins were structural proteins involved in maintaining and modulating the cytoskeleton and ECM. Stress response and chaperone proteins were also highly represented. This is perhaps not surprising as many of these are abundant cellular components. Structural proteins and cytoskeletal regulators identified included; vimentin, collagen, fascin, PDLIM1, F-actin capping protein, twinfillin-2, cofilin, actin and tubulin. The rearrangement of extracellular matrix proteins and cytoskeletal microfilaments induces major cellular morphological alterations in transformed cells (Yamazaki, Kurisu et al. 2005). The action of actin cross-linking, severing and polymerisation factors serves to potentiate the invasiveness of tumour cells. The differential expression of these cytoskeletal and associated proteins would be expected to confer the distinct growth characteristics observed in the parental cell lines and the Ch18 hybrids on soft agar and in

nude mice (Dafou, Ramus et al. 2009). Whilst actin and tubulin were up-regulated in hybrid clone 18-G-1.26, the other structural proteins were generally down-regulated, suggesting these proteins may participate in the observed suppression of neoplastic phenotype in this cell line. In future, it will be necessary to test the function of these proteins in affecting cell morphology, cell migration and invasion by targeted knockdown of their expression.

Oxidative stress is primarily a result of the generation of reactive oxygen species (ROS) in the mitochondrion during production of adenosine triphosphate. ROS in cells profoundly affects numerous critical cellular functions and the absence of efficient cellular detoxification mechanisms which remove these ROS may contribute to cancer and other diseases. ROS are thought to be tumourigenic because of their ability to damage DNA and initiate tumour development through mutagenesis. ROS may also increase cell proliferation, survival and cellular migration and it is now accepted that certain ROS such as H_2O_2 are signalling intermediates that provide a permissive environment for receptor tyrosine kinase signalling (Finkel 2000; Rhee, Kang et al. 2005). ROS, however, can induce senescence and cell death and so may also function in tumour suppression. Proteins associated with regulating the redox status of the cell include superoxide dismutases, thioredoxins, peroxiredoxins, glutaredoxins and glutathione transferases. This class of proteins were highly represented in the present study, displaying differential expression between the parent and hybrid cell lines. However, their regulation was somewhat varied between the cell models making it difficult to draw conclusions about the redox status of cells in relation to neoplastic

suppression. The adaptation of tumour cells to hypoxia and acidification of the tumour micro-environment is also known to promote their survival over normal cells. When tumour cells experience stressful conditions such as oxygen deprivation, the accumulation of mis-folded proteins can induce the over-expression of chaperones such as heat-shock proteins. Heat shock proteins (HSP) are expressed at high levels in a variety of tumours (Calderwood, Khaleque et al. 2006). In the majority of cancers, increased levels of HSP is attributed to mutation of the tumour suppressor p53, which releases the transcriptional repression of HSP genes (Lee, Montebello et al. 1994; Gandour-Edwards, Trock et al. 1998). The observed differential expression of HSPs and other chaperones in ovarian cancer cell models again cannot be linked to a specific cellular effect owing to the heterogeneity of the effects, although many of the chaperone/HSPs were down-regulated in clone 18-G-1.26, which was the most different of the clones examined in terms of its proteomic profile.

A strategy was developed to analyse secreted proteins from cells grown in culture. This was successful with the identification of numerous differentially expressed secreted proteins by 2D-DIGE/MS and 2D-LC-MS/MS with TMT labelling. Secreted proteins identified by both technologies displayed consistent regulation (e.g. IGFBP2) giving increased confidence in the results. It is immediately apparent that the analysis of the secretome has identified a number of proteins involved in tumourigenesis that have already been characterised to some extent as diagnostic or prognostic markers of cancer. Among these were IGFBP2, IGFBP7, PEDF, prolactin, lactate dehydrogenase, lumican, TIMP1 and galectin-1. It is encouraging that these proteins were identified in the models

of neoplastic suppression used in this study. In addition, the secreted protein MMP10 identified by 2D-LC with TMT, displayed promise as a potential biomarker. These identifications highlight the effectiveness of fractionation combined with two complimentry proteomic platforms to probe deeper into the proteome in search of suitable diagnostic and/or prognostic markers of OC. Future work will involve confirming these changes in the cell models used herein, and then testing their expression in tissue or serum samples from ovarian cancer cases and healthy controls, as was done for MMP10. Indeed MMP10 could significantly discriminate between healthy and late stage OC cases and may therefore have potential as a prognostic marker rather than a diagnostic marker. Further to this, and for poorly characterised gene products, their functions could be tested by knocking down their expression using RNAi and assessing the effect this has on proliferation, growth on soft agar and invasion.

The development of a membrane enrichment strategy combined with TMT labelling for quantification requires further work. The suitability of 2D-LC with TMT labelling for the analysis of membrane protein fractions is evidenced by the identification of surface and membrane proteins in this study, however problems were encountered at the TMT-labelling stage and further optimization work is required.

7.5 Future prospects

The proteomic analysis of neoplastic suppression presented here represents a starting point for the selection of candidate proteins to be assessed for their potential as future

biomarkers of ovarian cancer. Further validation of differentially expressed proteins by quantitative immunochemistry in normal ovarian and cancer cell lines and in the serum from malignant and benign cases of ovarian cancer and healthy controls is necessary. While, their value as markers is evaluated, functional characterisation studies would improve our understanding of the mechanisms of neoplastic suppression. Gene silencing to alter the expression of specific gene products of interest, using double stranded interfering RNAs (Downward 2004), could be usefully applied in this model system. Additionally, candidate proteins could be over expressed in the parental cell lines using transfected constructs which overexpress the target proteins to assess their roles in suppressing tumourigenic phenotype. A combination of soft agar colony forming, MTT proliferation, transwell migration/invasion assays and tumour formation in nude mice assays would improve our understanding of the role of these candidates in ovarian cancer biology.

A shortlist of 20 candidate proteins has been selected for further study based on the expression profiling performed in this study. Protein identifications that displayed concordant expression in a hybrid pair in either the 2D-DIGE and/or 2D-LC-MS/MS analysis were considered. Despite heterogeneity between the cell models and the clonal variation between the hybrid clones, calreticulin, MMP10 and follistatin-related protein displayed concordant expression in both cell models and represent the most promising candidates. In addition, proteins from novel genes and those that were secreted or surface proteins were considered more desirable as potential biomarkers. Example candidates include; galectin-1, TIMP1, pigment epithelium-derived factor precursor, IGFBP2,

IGFBP7, prolactin, tomoregulin-1 and procollagen (III). Finally, their functional importance and links to cancer in the literature were also considered, for example PIG3, annexin A1 and prohibitin are examples with strong links to cancer progression, whilst prolactin has been previously used in a biomarker panel for the detection of early stage ovarian cancer (Visintin, Feng et al. 2008) and shown to transform NOSE cells (Levina, Nolen et al. 2009).

7.6 Conclusions

Understanding the biology of ovarian cancer is limited because little is known about the processes governing neoplastic transformation and suppression. Differential protein expression analysis of cell models of neoplastic suppression using a combination of complimentry proteomic techniques has identified a number of proteins of interest with regard to their potential in mediating tumourigenic suppression or being altered as a consequence of suppression. As such they represent candidate biomarkers of ovarian cancer. This has been possible despite the problems associated with the complexity of the model systems used due to the fact that the cell types were derived from endometrioid and clear cell carcinomas with different molecular aetiologies and the effects of clonal variation.

References

Adib, T. R., S. Henderson, et al. (2004). "Predicting biomarkers for ovarian cancer using gene-expression microarrays." Br J Cancer **90**(3): 686-92.

Aebersold, R. and M. Mann (2003). "Mass spectrometry-based proteomics." Nature **422**(6928): 198-207.

Aggarwal, K., L. H. Choe, et al. (2006). "Shotgun proteomics using the iTRAQ isobaric tags." Brief Funct Genomic Proteomic **5**(2): 112-20.

Ahmed, N., K. T. Oliva, et al. (2005). "Proteomic tracking of serum protein isoforms as screening biomarkers of ovarian cancer." Proteomics **5**(17): 4625-36.

al-Sheneber, I. F., H. R. Shibata, et al. (1993). "Prognostic significance of proliferating cell nuclear antigen expression in colorectal cancer." Cancer **71**(6): 1954-9.

Alldridge, L. C. and C. E. Bryant (2003). "Annexin 1 regulates cell proliferation by disruption of cell morphology and inhibition of cyclin D1 expression through sustained activation of the ERK1/2 MAPK signal." Exp Cell Res **290**(1): 93-107.

Altinoz, M. A. and R. Korkmaz (2004). "NF-kappaB, macrophage migration inhibitory factor and cyclooxygenase-inhibitions as likely mechanisms behind the acetaminophen- and NSAID-prevention of the ovarian cancer." Neoplasma **51**(4): 239-47.

Amanchy, R., D. E. Kalume, et al. (2005). "Phosphoproteome analysis of HeLa cells using stable isotope labeling with amino acids in cell culture (SILAC)." J Proteome Res **4**(5): 1661-71.

Anderson, N. L. and N. G. Anderson (1998). "Proteome and proteomics: new technologies, new concepts, and new words." Electrophoresis **19**(11): 1853-61.

Anthony, B., P. Carter, et al. (1996). "Overexpression of the proto-oncogene/translation factor 4E in breast-carcinoma cell lines." Int J Cancer **65**(6): 858-63.

Asai-Sato, M., Y. Nagashima, et al. (2005). "Prolactin inhibits apoptosis of ovarian carcinoma cells induced by serum starvation or cisplatin treatment." Int J Cancer **115**(4): 539-44.

Auersperg, N., M. I. Edelson, et al. (1998). "The biology of ovarian cancer." Semin Oncol **25**(3): 281-304.

Auersperg, N., S. L. Maines-Bandiera, et al. (1997). "Ovarian carcinogenesis and the biology of ovarian surface epithelium." J Cell Physiol **173**(2): 261-5.

Auersperg, N., J. Pan, et al. (1999). "E-cadherin induces mesenchymal-to-epithelial transition in human ovarian surface epithelium." Proc Natl Acad Sci U S A **96**(11): 6249-54.

Auersperg, N., A. S. Wong, et al. (2001). "Ovarian surface epithelium: biology, endocrinology, and pathology." Endocr Rev **22**(2): 255-88.

Aunoble, B., R. Sanches, et al. (2000). "Major oncogenes and tumor suppressor genes involved in epithelial ovarian cancer (review)." Int J Oncol **16**(3): 567-76.

Bailly, M. and G. E. Jones (2003). "Polarised migration: cofilin holds the front." Curr Biol **13**(4): R128-30.

Bantscheff, M., M. Boesche, et al. (2008). "Robust and sensitive iTRAQ quantification on an LTQ Orbitrap mass spectrometer." Mol Cell Proteomics **7**(9): 1702-13.

Baron-Hay, S., F. Boyle, et al. (2004). "Elevated serum insulin-like growth factor binding protein-2 as a prognostic marker in patients with ovarian cancer." Clin Cancer Res **10**(5): 1796-806.

Basolo, F., A. Pinchera, et al. (1994). "Expression of p21 ras protein as a prognostic factor in papillary thyroid cancer." Eur J Cancer **30A**(2): 171-4.

Bast, R. C., Jr., D. Badgwell, et al. (2005). "New tumor markers: CA125 and beyond." Int J Gynecol Cancer **15 Suppl 3**: 274-81.

Bell, D. A. (2005). "Origins and molecular pathology of ovarian cancer." Mod Pathol **18 Suppl 2**: S19-32.

Bengtsson, S., M. Krogh, et al. (2007). "Large-scale proteomics analysis of human ovarian cancer for biomarkers." J Proteome Res **6**(4): 1440-50.

Bjellqvist, B., K. Ek, et al. (1982). "Isoelectric focusing in immobilized pH gradients: principle, methodology and some applications." J Biochem Biophys Methods **6**(4): 317-39.

Blonder, J., K. C. Chan, et al. (2006). "Identification of membrane proteins from mammalian cell/tissue using methanol-facilitated solubilization and tryptic digestion coupled with 2D-LC-MS/MS." Nat Protoc **1**(6): 2784-90.

Borgese, N., A. D'Arrigo, et al. (1993). "NADH-cytochrome b5 reductase and cytochrome b5 isoforms as models for the study of post-translational targeting to the endoplasmic reticulum." FEBS Lett **325**(1-2): 70-5.

Bottari, P., R. Aebersold, et al. (2004). "Design and synthesis of visible isotope-coded affinity tags for the absolute quantification of specific proteins in complex mixtures." Bioconjug Chem **15**(2): 380-8.

Bouchal, P., T. Roumeliotis, et al. (2009). "Biomarker discovery in low-grade breast cancer using isobaric stable isotope tags and two-dimensional liquid chromatography-tandem mass spectrometry (iTRAQ-2DLC-MS/MS) based quantitative proteomic analysis." J Proteome Res **8**(1): 362-73.

Boyce, E. A. and E. C. Kohn (2005). "Ovarian cancer in the proteomics era: diagnosis, prognosis, and therapeutics targets." Int J Gynecol Cancer **15 Suppl 3**: 266-73.

Bozzetti, C., B. Bortesi, et al. (2004). "Loss of heterozygosity (LOH) in ovarian cancer." Int J Gynaecol Obstet **85**(3): 294-5.

Breedlove, G. and C. Busenhart (2005). "Screening and detection of ovarian cancer." J Midwifery Womens Health **50**(1): 51-4.

Calderwood, S. K., M. A. Khaleque, et al. (2006). "Heat shock proteins in cancer: chaperones of tumorigenesis." Trends Biochem Sci **31**(3): 164-72.

Camby, I., M. Le Mercier, et al. (2006). "Galectin-1: a small protein with major functions." Glycobiology **16**(11): 137R-157R.

Candiano, G., M. Bruschi, et al. (2004). "Blue silver: a very sensitive colloidal Coomassie G-250 staining for proteome analysis." Electrophoresis **25**(9): 1327-33.

Chakrabarty, S. and L. Kondratick (2006). "Insulin-like growth factor binding protein-2 stimulates proliferation and activates multiple cascades of the mitogen-activated protein kinase pathways in NIH-OVCAR3 human epithelial ovarian cancer cells." Cancer Biol Ther **5**(2): 189-97.

Chan, Q. K., H. Y. Ngan, et al. (2009). "Tumor suppressor effect of follistatin-like 1 in ovarian and endometrial carcinogenesis: a differential expression and functional analysis." Carcinogenesis **30**(1): 114-21.

Check, E. (2004). "Proteomics and cancer: running before we can walk?" Nature **429**(6991): 496-7.

Chen, Y. C., G. Pohl, et al. (2005). "Apolipoprotein E is required for cell proliferation and survival in ovarian cancer." Cancer Res **65**(1): 331-7.

Cheretis, C., F. Dietrich, et al. (2006). "Expression of ERp29, an endoplasmic reticulum secretion factor in basal-cell carcinoma." Am J Dermatopathol **28**(5): 410-2.

Cheung, L. W., S. C. Au, et al. (2006). "Pigment epithelium-derived factor is estrogen sensitive and inhibits the growth of human ovarian cancer and ovarian surface epithelial cells." Endocrinology **147**(9): 4179-91.

Choe, L. H. and K. H. Lee (2000). "A comparison of three commercially available isoelectric focusing units for proteome analysis: the multiphor, the IPGphor and the protean IEF cell." Electrophoresis **21**(5): 993-1000.

Chrambach, A. and D. Rodbard (1971). "Polyacrylamide gel electrophoresis." Science **172**(982): 440-51.

Christoph, F., C. Kempkensteffen, et al. (2006). "Methylation of tumour suppressor genes APAF-1 and DAPK-1 and in vitro effects of demethylating agents in bladder and kidney cancer." Br J Cancer **95**(12): 1701-7.

Claessens, H. A. and M. A. van Straten (2004). "Review on the chemical and thermal stability of stationary phases for reversed-phase liquid chromatography." J Chromatogr A **1060**(1-2): 23-41.

Coghlin, C., B. Carpenter, et al. (2006). "Characterization and over-expression of chaperonin t-complex proteins in colorectal cancer." J Pathol **210**(3): 351-7.

Courilleau, D., E. Chastre, et al. (2000). "B-ind1, a novel mediator of Rac1 signaling cloned from sodium butyrate-treated fibroblasts." J Biol Chem **275**(23): 17344-8.

Crew, J. P., S. Fuggle, et al. (2000). "Eukaryotic initiation factor-4E in superficial and muscle invasive bladder cancer and its correlation with vascular endothelial growth factor expression and tumour progression." Br J Cancer **82**(1): 161-6.

Dafou, D., S. J. Ramus, et al. (2009). "Chromosomes 6 and 18 induce neoplastic suppression in epithelial ovarian cancer cells." Int J Cancer **124**(5): 1037-44.

Daly, R. J., M. D. Binder, et al. (1994). "Overexpression of the Grb2 gene in human breast cancer cell lines." Oncogene **9**(9): 2723-7.

Dankort, D., B. Maslikowski, et al. (2001). "Grb2 and Shc adapter proteins play distinct roles in Neu (ErbB-2)-induced mammary tumorigenesis: implications for human breast cancer." Mol Cell Biol **21**(5): 1540-51.

Davidson, B., R. Hadar, et al. (2008). "Expression and clinical role of DJ-1, a negative regulator of PTEN, in ovarian carcinoma." Hum Pathol **39**(1): 87-95.

Davies, B. R., I. A. Steele, et al. (2003). "Immortalisation of human ovarian surface epithelium with telomerase and temperature-sensitive SV40 large T antigen." Exp Cell Res **288**(2): 390-402.

Dayon, L., A. Hainard, et al. (2008). "Relative quantification of proteins in human cerebrospinal fluids by MS/MS using 6-plex isobaric tags." Anal Chem **80**(8): 2921-31.

De Benedetti, A. and A. L. Harris (1999). "eIF4E expression in tumors: its possible role in progression of malignancies." Int J Biochem Cell Biol **31**(1): 59-72.
Deb, T. B., L. Su, et al. (2001). "Epidermal growth factor (EGF) receptor kinase-independent signaling by EGF." J Biol Chem **276**(18): 15554.
DeFatta, R. J., C. O. Nathan, et al. (2000). "Antisense RNA to eIF4E suppresses oncogenic properties of a head and neck squamous cell carcinoma cell line." Laryngoscope **110**(6): 928-33.
Di Segni, A., K. Farin, et al. (2008). "Identification of nucleolin as new ErbB receptors-interacting protein." PLoS One **3**(6): e2310.
Doherty, A. M. and E. M. Fisher (2003). "Microcell-mediated chromosome transfer (MMCT): small cells with huge potential." Mamm Genome **14**(9): 583-92.
Downward, J. (2004). "Use of RNA interference libraries to investigate oncogenic signalling in mammalian cells." Oncogene **23**(51): 8376-83.
Dubeau, L. (1999). "The cell of origin of ovarian epithelial tumors and the ovarian surface epithelium dogma: does the emperor have no clothes?" Gynecol Oncol **72**(3): 437-42.
Duggan, B. D. and L. Dubeau (1998). "Genetics and biology of gynecologic cancer." Curr Opin Oncol **10**(5): 439-46.
Eschenbruch, M. and R. R. Burk (1982). "Experimentally improved reliability of ultrasensitive silver staining of protein in polyacrylamide gels." Anal Biochem **125**(1): 96-9.
Essers, J., A. F. Theil, et al. (2005). "Nuclear dynamics of PCNA in DNA replication and repair." Mol Cell Biol **25**(21): 9350-9.
Esteller, M. (2005). "Dormant hypermethylated tumour suppressor genes: questions and answers." J Pathol **205**(2): 172-80.
Everley, P. A., J. Krijgsveld, et al. (2004). "Quantitative cancer proteomics: stable isotope labeling with amino acids in cell culture (SILAC) as a tool for prostate cancer research." Mol Cell Proteomics **3**(7): 729-35.
Fenn, J. B., M. Mann, et al. (1989). "Electrospray ionization for mass spectrometry of large biomolecules." Science **246**(4926): 64-71.
Finkel, T. (2000). "Redox-dependent signal transduction." FEBS Lett **476**(1-2): 52-4.
Flatt, P. M., K. Polyak, et al. (2000). "p53-dependent expression of PIG3 during proliferation, genotoxic stress, and reversible growth arrest." Cancer Lett **156**(1): 63-72.
Folsom, A. R., J. P. Anderson, et al. (2004). "Estrogen replacement therapy and ovarian cancer." Epidemiology **15**(1): 100-4.
Fusaro, G., P. Dasgupta, et al. (2003). "Prohibitin induces the transcriptional activity of p53 and is exported from the nucleus upon apoptotic signaling." J Biol Chem **278**(48): 47853-61.
Gagne, J. P., C. Ethier, et al. (2007). "Comparative proteome analysis of human epithelial ovarian cancer." Proteome Sci **5**: 16.
Gagne, J. P., P. Gagne, et al. (2005). "Proteome profiling of human epithelial ovarian cancer cell line TOV-112D." Mol Cell Biochem **275**(1-2): 25-55.
Gandour-Edwards, R., B. J. Trock, et al. (1998). "Heat shock protein and p53 expression in head and neck squamous cell carcinoma." Otolaryngol Head Neck Surg **118**(5): 610-5.

Garcia Pedrero, J. M., M. P. Fernandez, et al. (2004). "Annexin A1 down-regulation in head and neck cancer is associated with epithelial differentiation status." Am J Pathol **164**(1): 73-9.

Garinis, G. A., G. P. Patrinos, et al. (2002). "DNA hypermethylation: when tumour suppressor genes go silent." Hum Genet **111**(2): 115-27.

Gerber, S. A., A. N. Kettenbach, et al. (2007). "The absolute quantification strategy: application to phosphorylation profiling of human separase serine 1126." Methods Mol Biol **359**: 71-86.

Gerber, S. A., J. Rush, et al. (2003). "Absolute quantification of proteins and phosphoproteins from cell lysates by tandem MS." Proc Natl Acad Sci U S A **100**(12): 6940-5.

Gery, S., D. Yin, et al. (2003). "TMEFF1 and brain tumors." Oncogene **22**(18): 2723-7.

Gharbi, S., P. Gaffney, et al. (2002). "Evaluation of two-dimensional differential gel electrophoresis for proteomic expression analysis of a model breast cancer cell system." Mol Cell Proteomics **1**(2): 91-8.

Gorg, A., C. Obermaier, et al. (1999). "Recent developments in two-dimensional gel electrophoresis with immobilized pH gradients: wide pH gradients up to pH 12, longer separation distances and simplified procedures." Electrophoresis **20**(4-5): 712-7. [pii].

Gortzak-Uzan, L., A. Ignatchenko, et al. (2008). "A proteome resource of ovarian cancer ascites: integrated proteomic and bioinformatic analyses to identify putative biomarkers." J Proteome Res **7**(1): 339-51.

Goshe, M. B. and R. D. Smith (2003). "Stable isotope-coded proteomic mass spectrometry." Curr Opin Biotechnol **14**(1): 101-9.

Graff, J. R., B. W. Konicek, et al. (2008). "Targeting the eukaryotic translation initiation factor 4E for cancer therapy." Cancer Res **68**(3): 631-4.

Graff, J. R., B. W. Konicek, et al. (2009). "eIF4E activation is commonly elevated in advanced human prostate cancers and significantly related to reduced patient survival." Cancer Res **69**(9): 3866-73.

Griffin, T. J., S. P. Gygi, et al. (2001). "Quantitative proteomic analysis using a MALDI quadrupole time-of-flight mass spectrometer." Anal Chem **73**(5): 978-86.

Gril, B., M. Vidal, et al. (2007). "Grb2-SH3 ligand inhibits the growth of HER2+ cancer cells and has antitumor effects in human cancer xenografts alone and in combination with docetaxel." Int J Cancer **121**(2): 407-15.

Grimberg, A. and P. Cohen (2000). "Role of insulin-like growth factors and their binding proteins in growth control and carcinogenesis." J Cell Physiol **183**(1): 1.

Grothey, A., R. Hashizume, et al. (2000). "Fascin, an actin-bundling protein associated with cell motility, is upregulated in hormone receptor negative breast cancer." Br J Cancer **83**(7): 870-3.

Gunawardana, C. G., N. Memari, et al. (2009). "Identifying novel autoantibody signatures in ovarian cancer using high-density protein microarrays." Clin Biochem **42**(4-5): 426-9.

Gygi, S. P. and R. Aebersold (2000). "Mass spectrometry and proteomics." Curr Opin Chem Biol **4**(5): 489-94.

Ha, P. K. and J. A. Califano (2006). "Promoter methylation and inactivation of tumour-suppressor genes in oral squamous-cell carcinoma." Lancet Oncol **7**(1): 77-82.

Han, E. K., M. Begemann, et al. (1996). "Increased expression of cyclin D1 in a murine mammary epithelial cell line induces p27kip1, inhibits growth, and enhances apoptosis." Cell Growth Differ **7**(6): 699-710.
Han, X., A. Aslanian, et al. (2008). "Mass spectrometry for proteomics." Curr Opin Chem Biol **12**(5): 483-90.
Hanahan, D. and R. A. Weinberg (2000). "The hallmarks of cancer." Cell **100**(1): 57-70.
Hanash, S. (2003). "Disease proteomics." Nature **422**(6928): 226-32.
Havilio, M. and A. Wool (2007). "Large-scale unrestricted identification of post-translation modifications using tandem mass spectrometry." Anal Chem **79**(4): 1362-8.
Haviv, I. and I. G. Campbell (2002). "DNA microarrays for assessing ovarian cancer gene expression." Mol Cell Endocrinol **191**(1): 121-6.
Haydon, M. S., J. D. Googe, et al. (2000). "Progression of eIF4e gene amplification and overexpression in benign and malignant tumors of the head and neck." Cancer **88**(12): 2803-10.
Hazama, H., H. Nagao, et al. (2008). "Comparison of mass spectra of peptides in different matrices using matrix-assisted laser desorption/ionization and a multi-turn time-of-flight mass spectrometer, MULTUM-IMG." Rapid Commun Mass Spectrom **22**(10): 1461-6.
Henzel, W. J., T. M. Billeci, et al. (1993). "Identifying proteins from two-dimensional gels by molecular mass searching of peptide fragments in protein sequence databases." Proc Natl Acad Sci U S A **90**(11): 5011-5.
Hernandez, E., N. B. Rosenshein, et al. (1984). "Tumor heterogeneity and histopathology in epithelial ovarian cancer." Obstet Gynecol **63**(3): 330-4.
Hillenkamp, F. and M. Karas (1990). "Mass spectrometry of peptides and proteins by matrix-assisted ultraviolet laser desorption/ionization." Methods Enzymol **193**: 280-95.
Hillenkamp, F., M. Karas, et al. (1991). "Matrix-assisted laser desorption/ionization mass spectrometry of biopolymers." Anal Chem **63**(24): 1193A-1203A.
Hu, Q., R. J. Noll, et al. (2005). "The Orbitrap: a new mass spectrometer." J Mass Spectrom **40**(4): 430-43.
Hu, W., P. D. McCrea, et al. (2000). "Increased expression of fascin, motility associated protein, in cell cultures derived from ovarian cancer and in borderline and carcinomatous ovarian tumors." Clin Exp Metastasis **18**(1): 83-8.
Huang, Y., H. Shi, et al. (2006). "The angiogenic function of nucleolin is mediated by vascular endothelial growth factor and nonmuscle myosin." Blood **107**(9): 3564-71.
Ichikawa, Y., S. J. Lemon, et al. (1999). "Microsatellite instability and expression of MLH1 and MSH2 in normal and malignant endometrial and ovarian epithelium in hereditary nonpolyposis colorectal cancer family members." Cancer Genet Cytogenet **112**(1): 2-8.
Ikenaka, Y., H. Yoshiji, et al. (2003). "Tissue inhibitor of metalloproteinases-1 (TIMP-1) inhibits tumor growth and angiogenesis in the TIMP-1 transgenic mouse model." Int J Cancer **105**(3): 340-6.
Inagaki, T., S. Ebisuno, et al. (1997). "PCNA and p53 in urinary bladder cancer: correlation with histological findings and prognosis." Int J Urol **4**(2): 172-7.

Inokuchi, J., A. Lau, et al. (2009). "Loss of annexin A1 disrupts normal prostate glandular structure by inducing autocrine IL-6 signaling." Carcinogenesis **30**(7): 1082-8.
Jacobs, I. J., S. J. Skates, et al. (1999). "Screening for ovarian cancer: a pilot randomised controlled trial." Lancet **353**(9160): 1207-10.
James, P., M. Quadroni, et al. (1993). "Protein identification by mass profile fingerprinting." Biochem Biophys Res Commun **195**(1): 58-64.
Jensen, O. N. (2004). "Modification-specific proteomics: characterization of post-translational modifications by mass spectrometry." Curr Opin Chem Biol **8**(1): 33-41.
Jochumsen, K. M., Q. Tan, et al. (2007). "Gene expression in epithelial ovarian cancer: a study of intratumor heterogeneity." Int J Gynecol Cancer **17**(5): 979-85.
Johnson, S., M. Michalak, et al. (2001). "The ins and outs of calreticulin: from the ER lumen to the extracellular space." Trends Cell Biol **11**(3): 122-9.
Jones, M. B., H. Krutzsch, et al. (2002). "Proteomic analysis and identification of new biomarkers and therapeutic targets for invasive ovarian cancer." Proteomics **2**(1): 76-84.
Kenrick, K. G. and J. Margolis (1970). "Isoelectric focusing and gradient gel electrophoresis: a two- dimensional technique." Anal Biochem **33**(1): 204-7.
Kerekatte, V., K. Smiley, et al. (1995). "The proto-oncogene/translation factor eIF4E: a survey of its expression in breast carcinomas." Int J Cancer **64**(1): 27-31.
Khalique, L., A. Ayhan, et al. (2007). "Genetic intra-tumour heterogeneity in epithelial ovarian cancer and its implications for molecular diagnosis of tumours." J Pathol **211**(3): 286-95.
Kim, R. H., M. Peters, et al. (2005). "DJ-1, a novel regulator of the tumor suppressor PTEN." Cancer Cell **7**(3): 263-73.
Kiss, H., D. Kedra, et al. (2001). "The LZTFL1 gene is a part of a transcriptional map covering 250 kb within the common eliminated region 1 (C3CER1) in 3p21.3." Genomics **73**(1): 10-9.
Kloor, D. and H. Osswald (2004). "S-Adenosylhomocysteine hydrolase as a target for intracellular adenosine action." Trends Pharmacol Sci **25**(6): 294-7.
Konicek, B. W., C. A. Dumstorf, et al. (2008). "Targeting the eIF4F translation initiation complex for cancer therapy." Cell Cycle **7**(16): 2466-71.
Kopitz, J., C. von Reitzenstein, et al. (2001). "Negative regulation of neuroblastoma cell growth by carbohydrate-dependent surface binding of galectin-1 and functional divergence from galectin-3." J Biol Chem **276**(38): 35917-23.
Koukourakis, M. I., E. Kontomanolis, et al. (2008). "Serum and Tissue LDH Levels in Patients with Breast/Gynaecological Cancer and Benign Diseases." Gynecol Obstet Invest **67**(3): 162-168.
Kruger, M., M. Moser, et al. (2008). "SILAC mouse for quantitative proteomics uncovers kindlin-3 as an essential factor for red blood cell function." Cell **134**(2): 353-64.
Kudoh, K., M. Takano, et al. (2000). "[Comparative genomic hybridization for analysis of chromosomal changes in cisplatin-resistant ovarian cancer]." Hum Cell **13**(3): 109-16.
Kurose, K., X. P. Zhou, et al. (2001). "Frequent loss of PTEN expression is linked to elevated phosphorylated Akt levels, but not associated with p27 and cyclin D1

expression, in primary epithelial ovarian carcinomas." Am J Pathol **158**(6): 2097-106.
Kusumawidjaja, G., H. Kayed, et al. (2007). "Basic transcription factor 3 (BTF3) regulates transcription of tumor-associated genes in pancreatic cancer cells." Cancer Biol Ther **6**(3): 367-76.
Landberg, G., H. Ostlund, et al. (2001). "Downregulation of the potential suppressor gene IGFBP-rP1 in human breast cancer is associated with inactivation of the retinoblastoma protein, cyclin E overexpression and increased proliferation in estrogen receptor negative tumors." Oncogene **20**(27): 3497-505.
Lee, C. S., J. Montebello, et al. (1994). "Overexpression of heat shock protein (hsp) 70 associated with abnormal p53 expression in cancer of the pancreas." Zentralbl Pathol **140**(3): 259-64.
Lee, E. J., C. Mircean, et al. (2005). "Insulin-like growth factor binding protein 2 promotes ovarian cancer cell invasion." Mol Cancer **4**(1): 7.
LeRoith, D. and C. T. Roberts, Jr. (2003). "The insulin-like growth factor system and cancer." Cancer Lett **195**(2): 127-37.
Levina, V. V., B. Nolen, et al. (2009). "Biological significance of prolactin in gynecologic cancers." Cancer Res **69**(12): 5226-33.
Li, B. D., L. Liu, et al. (1997). "Overexpression of eukaryotic initiation factor 4E (eIF4E) in breast carcinoma." Cancer **79**(12): 2385-90.
Lin, Y. W., C. Y. Lin, et al. (2006). "Plasma proteomic pattern as biomarkers for ovarian cancer." Int J Gynecol Cancer **16 Suppl 1**: 139-46.
Liotta, L. A. and E. F. Petricoin (2006). "Serum peptidome for cancer detection: spinning biologic trash into diagnostic gold." J Clin Invest **116**(1): 26-30.
Liu, H., D. Lin, et al. (2002). "Multidimensional separations for protein/peptide analysis in the post-genomic era." Biotechniques **32**(4): 898, 900, 902 passim.
Liu, J., G. Yang, et al. (2004). "A genetically defined model for human ovarian cancer." Cancer Res **64**(5): 1655-63.
Lopez-Bermejo, A., C. K. Buckway, et al. (2000). "Characterization of insulin-like growth factor-binding protein-related proteins (IGFBP-rPs) 1, 2, and 3 in human prostate epithelial cells: potential roles for IGFBP-rP1 and 2 in senescence of the prostatic epithelium." Endocrinology **141**(11): 4072-80.
Makarov, A., E. Denisov, et al. (2006). "Performance evaluation of a hybrid linear ion trap/orbitrap mass spectrometer." Anal Chem **78**(7): 2113-20.
Makarov, A., E. Denisov, et al. (2006). "Dynamic range of mass accuracy in LTQ Orbitrap hybrid mass spectrometer." J Am Soc Mass Spectrom **17**(7): 977-82.
Mamane, Y., E. Petroulakis, et al. (2004). "eIF4E--from translation to transformation." Oncogene **23**(18): 3172-9.
Mann, M., P. Hojrup, et al. (1993). "Use of mass spectrometric molecular weight information to identify proteins in sequence databases." Biol Mass Spectrom **22**(6): 338-45.
Manni, A., C. Wright, et al. (1986). "Promotion by prolactin of the growth of human breast neoplasms cultured in vitro in the soft agar clonogenic assay." Cancer Res **46**(4 Pt 1): 1669-72.
Martin, T. A., G. Harrison, et al. (2003). "The role of the CD44/ezrin complex in cancer metastasis." Crit Rev Oncol Hematol **46**(2): 165-86.

Martoglio, A. M., B. D. Tom, et al. (2000). "Changes in tumorigenesis- and angiogenesis-related gene transcript abundance profiles in ovarian cancer detected by tailored high density cDNA arrays." Mol Med **6**(9): 750-65.

Mashimo, J., R. Maniwa, et al. (1997). "Decrease in the expression of a novel TGF beta1-inducible and ras-recision gene, TSC-36, in human cancer cells." Cancer Lett **113**(1-2): 213-9.

Masih, P. J., D. Kunnev, et al. (2008). "Mismatch Repair proteins are recruited to replicating DNA through interaction with Proliferating Cell Nuclear Antigen (PCNA)." Nucleic Acids Res **36**(1): 67-75.

Mayer, A., M. Takimoto, et al. (1993). "The prognostic significance of proliferating cell nuclear antigen, epidermal growth factor receptor, and mdr gene expression in colorectal cancer." Cancer **71**(8): 2454-60.

Mei, F. C., T. W. Young, et al. (2005). "RAS-Mediated epigenetic inactivation of OPCML in oncogenic transformation of human ovarian surface epithelial cells." Faseb J.

Menon, U., A. Gentry-Maharaj, et al. (2008). "Recruitment to multicentre trials--lessons from UKCTOCS: descriptive study." BMJ **337**: a2079.

Meyer, E., J. Y. Vollmer, et al. (2005). "Matrix metalloproteinases 9 and 10 inhibit protein kinase C-potentiated, p53-mediated apoptosis." Cancer Res **65**(10): 4261-72.

Meyer, T. S. and B. L. Lamberts (1965). "Use of coomassie brilliant blue R250 for the electrophoresis of microgram quantities of parotid saliva proteins on acrylamide-gel strips." Biochim Biophys Acta **107**(1): 144-5.

Mills, K., P. Morris, et al. (2005). "Measurement of urinary CDH and CTH by tandem mass spectrometry in patients hemizygous and heterozygous for Fabry disease." J Inherit Metab Dis **28**(1): 35-48.

Mishra, S., L. C. Murphy, et al. (2006). "The Prohibitins: emerging roles in diverse functions." J Cell Mol Med **10**(2): 353-63.

Mkrtchian, S., M. Baryshev, et al. (2008). "ERp29, an endoplasmic reticulum secretion factor is involved in the growth of breast tumor xenografts." Mol Carcinog **47**(11): 886-92.

Mor, G., I. Visintin, et al. (2005). "Serum protein markers for early detection of ovarian cancer." Proc Natl Acad Sci U S A **102**(21): 7677-82.

Mukherjee, K., V. Syed, et al. (2005). "Estrogen-induced loss of progesterone receptor expression in normal and malignant ovarian surface epithelial cells." Oncogene **24**(27): 4388-400.

Multhoff, G. and L. E. Hightower (1996). "Cell surface expression of heat shock proteins and the immune response." Cell Stress Chaperones **1**(3): 167-76.

Mutaguchi, K., H. Yasumoto, et al. (2003). "Restoration of insulin-like growth factor binding protein-related protein 1 has a tumor-suppressive activity through induction of apoptosis in human prostate cancer." Cancer Res **63**(22): 7717-23.

Naaby-Hansen, S., M. D. Waterfield, et al. (2001). "Proteomics--post-genomic cartography to understand gene function." Trends Pharmacol Sci **22**(7): 376-84.

Nagakubo, D., T. Taira, et al. (1997). "DJ-1, a novel oncogene which transforms mouse NIH3T3 cells in cooperation with ras." Biochem Biophys Res Commun **231**(2): 509-13.

Nagele, E., M. Vollmer, et al. (2004). "2D-LC/MS techniques for the identification of proteins in highly complex mixtures." Expert Rev Proteomics **1**(1): 37-46.
Nathan, C. O., S. Franklin, et al. (1999). "Expression of eIF4E during head and neck tumorigenesis: possible role in angiogenesis." Laryngoscope **109**(8): 1253-8.
Neesham, D. (2007). "Ovarian cancer screening." Aust Fam Physician **36**(3): 126-8.
Nelson, A. R., B. Fingleton, et al. (2000). "Matrix metalloproteinases: biologic activity and clinical implications." J Clin Oncol **18**(5): 1135-49.
Neuhoff, V., N. Arold, et al. (1988). "Improved staining of proteins in polyacrylamide gels including isoelectric focusing gels with clear background at nanogram sensitivity using Coomassie Brilliant Blue G-250 and R-250." Electrophoresis **9**(6): 255-62.
Neuhoff, V., R. Stamm, et al. (1990). "Essential problems in quantification of proteins following colloidal staining with coomassie brilliant blue dyes in polyacrylamide gels, and their solution." Electrophoresis **11**(2): 101-17.
Nicholson, R. I., J. M. Gee, et al. (2001). "EGFR and cancer prognosis." Eur J Cancer **37 Suppl 4**: S9-15.
Nikitovic, D., P. Katonis, et al. (2008). "Lumican, a small leucine-rich proteoglycan." IUBMB Life **60**(12): 818-23.
Nishizuka, S. (2006). "Profiling cancer stem cells using protein array technology." Eur J Cancer **42**(9): 1273-82.
Obeid, M., A. Tesniere, et al. (2007). "Calreticulin exposure dictates the immunogenicity of cancer cell death." Nat Med **13**(1): 54-61.
Oh, Y., S. R. Nagalla, et al. (1996). "Synthesis and characterization of insulin-like growth factor-binding protein (IGFBP)-7. Recombinant human mac25 protein specifically binds IGF-I and -II." J Biol Chem **271**(48): 30322-5.
Oksvold, M. P., H. S. Huitfeldt, et al. (2002). "UV induces tyrosine kinase-independent internalisation and endosome arrest of the EGF receptor." J Cell Sci **115**(Pt 4): 793-803.
Oktem, O. and K. Oktay (2007). "A novel ovarian xenografting model to characterize the impact of chemotherapy agents on human primordial follicle reserve." Cancer Res **67**(21): 10159-62.
Olsen, J. V., L. M. de Godoy, et al. (2005). "Parts per million mass accuracy on an Orbitrap mass spectrometer via lock mass injection into a C-trap." Mol Cell Proteomics **4**(12): 2010-21.
Olsen, J. V., B. Macek, et al. (2007). "Higher-energy C-trap dissociation for peptide modification analysis." Nat Methods **4**(9): 709-12.
Ong, S. E., B. Blagoev, et al. (2002). "Stable isotope labeling by amino acids in cell culture, SILAC, as a simple and accurate approach to expression proteomics." Mol Cell Proteomics **1**(5): 376-86.
Ouellet, V., M. C. Guyot, et al. (2006). "Tissue array analysis of expression microarray candidates identifies markers associated with tumor grade and outcome in serous epithelial ovarian cancer." Int J Cancer **119**(3): 599-607.
Parazzini, F., C. La Vecchia, et al. (1989). "Menstrual factors and the risk of epithelial ovarian cancer." J Clin Epidemiol **42**(5): 443-8.
Patterson, S. D. and R. H. Aebersold (2003). "Proteomics: the first decade and beyond." Nat Genet **33 Suppl**: 311-23.

Patton, W. F. (2000). "A thousand points of light: the application of fluorescence detection technologies to two-dimensional gel electrophoresis and proteomics." Electrophoresis **21**(6): 1123-44.
Paweletz, C. P., D. K. Ornstein, et al. (2000). "Loss of annexin 1 correlates with early onset of tumorigenesis in esophageal and prostate carcinoma." Cancer Res **60**(22): 6293-7.
Paz, A., R. Haklai, et al. (2001). "Galectin-1 binds oncogenic H-Ras to mediate Ras membrane anchorage and cell transformation." Oncogene **20**(51): 7486-93.
Pedrero, J. M. G., M. P. Fernandez, et al. (2005). "Annexin A1 Down-Regulation in Head and Neck Cancer Is Associated with Epithelial Differentiation Status." American Journal of Pathology **164** (1): 73.
Peng, J. and S. P. Gygi (2001). "Proteomics: the move to mixtures." J Mass Spectrom **36**(10): 1083-91.
Perry, R. H., R. G. Cooks, et al. (2008). "Orbitrap mass spectrometry: instrumentation, ion motion and applications." Mass Spectrom Rev **27**(6): 661-99.
Petricoin, E. F., A. M. Ardekani, et al. (2002). "Use of proteomic patterns in serum to identify ovarian cancer." Lancet **359**(9306): 572-7.
Petricoin, E. F. and L. A. Liotta (2004). "SELDI-TOF-based serum proteomic pattern diagnostics for early detection of cancer." Curr Opin Biotechnol **15**(1): 24-30.
Phillips, N. J., M. R. Ziegler, et al. (1996). "Allelic deletion on chromosome 17p13.3 in early ovarian cancer." Cancer Res **56**(3): 606-11.
Purdie, D. M., C. J. Bain, et al. (2003). "Ovulation and risk of epithelial ovarian cancer." Int J Cancer **104**(2): 228-32.
Quaglia, M., C. Pritchard, et al. (2008). "Amine-reactive isobaric tagging reagents: requirements for absolute quantification of proteins and peptides." Anal Biochem **379**(2): 164-9.
Quaye, L., H. Song, et al. (2009). "Tagging single-nucleotide polymorphisms in candidate oncogenes and susceptibility to ovarian cancer." Br J Cancer.
Quinn, K. A., A. M. Treston, et al. (1996). "Insulin-like growth factor expression in human cancer cell lines." J Biol Chem **271**(19): 11477-83.
Rabilloud, T. (1990). "Mechanisms of protein silver staining in polyacrylamide gels: a 10-year synthesis." Electrophoresis **11**(10): 785-94.
Rabilloud, T. (1992). "A comparison between low background silver diammine and silver nitrate protein stains." Electrophoresis **13**(7): 429-39.
Rabilloud, T. (1994). "Two-dimensional electrophoresis of basic proteins with equilibrium isoelectric focusing in carrier ampholyte-pH gradients." Electrophoresis **15**(2): 278-82.
Rabilloud, T. (1999). "Silver staining of 2-D electrophoresis gels." Methods Mol Biol **112**: 297-305.
Rabilloud, T., J. M. Strub, et al. (2001). "A comparison between Sypro Ruby and ruthenium II tris (bathophenanthroline disulfonate) as fluorescent stains for protein detection in gels." Proteomics **1**(5): 699-704.
Rabinovich, G. A. (2005). "Galectin-1 as a potential cancer target." Br J Cancer **92**(7): 1188-92.
Rae, M. T. and S. G. Hillier (2005). "Steroid signalling in the ovarian surface epithelium." Trends Endocrinol Metab **16**(7): 327-33.

Rai, A. J., C. A. Gelfand, et al. (2005). "HUPO Plasma Proteome Project specimen collection and handling: towards the standardization of parameters for plasma proteome samples." Proteomics **5**(13): 3262-77.

Ramus, S. J., P. D. Pharoah, et al. (2003). "BRCA1/2 mutation status influences somatic genetic progression in inherited and sporadic epithelial ovarian cancer cases." Cancer Res **63**(2): 417-23.

Ramus, S. J., R. A. Vierkant, et al. (2008). "Consortium analysis of 7 candidate SNPs for ovarian cancer." Int J Cancer **123**(2): 380-8.

Reed, M. J., T. Koike, et al. (2003). "Inhibition of TIMP1 enhances angiogenesis in vivo and cell migration in vitro." Microvasc Res **65**(1): 9-17.

Rhee, S. G., S. W. Kang, et al. (2005). "Intracellular messenger function of hydrogen peroxide and its regulation by peroxiredoxins." Curr Opin Cell Biol **17**(2): 183-9.

Roberts, P. C., E. P. Mottillo, et al. (2005). "Sequential molecular and cellular events during neoplastic progression: a mouse syngeneic ovarian cancer model." Neoplasia **7**(10): 944-56.

Rodriguez, G. (2003). "New insights regarding pharmacologic approaches for ovarian cancer prevention." Hematol Oncol Clin North Am **17**(4): 1007-20, x.

Rosenwald, I. B., J. J. Chen, et al. (1999). "Upregulation of protein synthesis initiation factor eIF-4E is an early event during colon carcinogenesis." Oncogene **18**(15): 2507-17.

Rossing, M. A., K. L. Cushing-Haugen, et al. (2007). "Menopausal hormone therapy and risk of epithelial ovarian cancer." Cancer Epidemiol Biomarkers Prev **16**(12): 2548-56.

Sakai, W., E. M. Swisher, et al. (2008). "Secondary mutations as a mechanism of cisplatin resistance in BRCA2-mutated cancers." Nature **451**(7182): 1116-20.

Sakamoto, M., H. Sakamoto, et al. (1996). "[CGH (comparative genomic hybridization)]." Nippon Rinsho **54**(4): 933-43.

Santoni, V., M. Molloy, et al. (2000). "Membrane proteins and proteomics: un amour impossible?" Electrophoresis **21**(6): 1054-70. [pii].

Schildkraut, J. M., E. Bastos, et al. (1997). "Relationship between lifetime ovulatory cycles and overexpression of mutant p53 in epithelial ovarian cancer." J Natl Cancer Inst **89**(13): 932-8.

Seargent, J. M., P. M. Loadman, et al. (2005). "Expression of matrix metalloproteinase-10 in human bladder transitional cell carcinoma." Urology **65**(4): 815-20.

Seelenmeyer, C., S. Wegehingel, et al. (2003). "The cancer antigen CA125 represents a novel counter receptor for galectin-1." J Cell Sci **116**(Pt 7): 1305-18.

Shevchenko, A., M. Wilm, et al. (1996). "Mass spectrometric sequencing of proteins silver-stained polyacrylamide gels." Anal Chem **68**(5): 850-8.

Shibanuma, M., J. Mashimo, et al. (1993). "Cloning from a mouse osteoblastic cell line of a set of transforming-growth-factor-beta 1-regulated genes, one of which seems to encode a follistatin-related polypeptide." Eur J Biochem **217**(1): 13-9.

Shin, B. K., H. Wang, et al. (2003). "Global profiling of the cell surface proteome of cancer cells uncovers an abundance of proteins with chaperone function." J Biol Chem **278**(9): 7607-16. Epub 2002 Dec 18.

Simaga, S., M. Osmak, et al. (2005). "Quantitative biochemical analysis of lactate dehydrogenase in human ovarian tissues: correlation with tumor grade." Int J Gynecol Cancer **15**(3): 438-44.

Sinha, P., G. Hutter, et al. (1998). "Increased expression of annexin I and thioredoxin detected by two-dimensional gel electrophoresis of drug resistant human stomach cancer cells." J Biochem.Biophys.Methods **37**(3): 105.

Skates, S. J., N. Horick, et al. (2004). "Preoperative sensitivity and specificity for early-stage ovarian cancer when combining cancer antigen CA-125II, CA 15-3, CA 72-4, and macrophage colony-stimulating factor using mixtures of multivariate normal distributions." J Clin Oncol **22**(20): 4059-66.

Soufir, N., S. Queille, et al. (2007). "Inactivation of the CDKN2A and the p53 tumour suppressor genes in external genital carcinomas and their precursors." Br J Dermatol **156**(3): 448-53.

Spurrier, B., P. Honkanen, et al. (2008). "Protein and lysate array technologies in cancer research." Biotechnol Adv **26**(4): 361-9.

Suehiro, Y., M. Sakamoto, et al. (2000). "Genetic aberrations detected by comparative genomic hybridization in ovarian clear cell adenocarcinomas." Oncology **59**(1): 50-6.

Sumitomo, K., A. Kurisaki, et al. (2000). "Expression of a TGF-beta1 inducible gene, TSC-36, causes growth inhibition in human lung cancer cell lines." Cancer Lett **155**(1): 37-46.

Swisshelm, K., K. Ryan, et al. (1995). "Enhanced expression of an insulin growth factor-like binding protein (mac25) in senescent human mammary epithelial cells and induced expression with retinoic acid." Proc Natl Acad Sci U S A **92**(10): 4472-6.

Taira, T., Y. Saito, et al. (2004). "DJ-1 has a role in antioxidative stress to prevent cell death." EMBO Rep **5**(2): 213-8.

Tapper, J., E. Kettunen, et al. (2001). "Changes in gene expression during progression of ovarian carcinoma." Cancer Genet Cytogenet **128**(1): 1-6.

Tate, A., S. Isotani, et al. (2006). "Met-Independent Hepatocyte Growth Factor-mediated regulation of cell adhesion in human prostate cancer cells." BMC Cancer **6**: 197.

Tavani, A., E. Ricci, et al. (2000). "Influence of menstrual and reproductive factors on ovarian cancer risk in women with and without family history of breast or ovarian cancer." Int J Epidemiol **29**(5): 799-802.

Taylor, C. F., R. S. Charlton, et al. (2003). "Genomic deletions in MSH2 or MLH1 are a frequent cause of hereditary non-polyposis colorectal cancer: identification of novel and recurrent deletions by MLPA." Hum Mutat **22**(6): 428-33.

Thomas, H., M. M. Nasim, et al. (1995). "Proliferating cell nuclear antigen (PCNA) immunostaining--a prognostic factor in ovarian cancer?" Br J Cancer **71**(2): 357-62.

Timms, J. F., E. Arslan-Low, et al. (2007). "Preanalytic Influence of Sample Handling on SELDI-TOF Serum Protein Profiles." Clin Chem **53**(4): 645-656.

Tonge, R., J. Shaw, et al. (2001). "Validation and development of fluorescence two-dimensional differential gel electrophoresis proteomics technology." Proteomics **1**(3): 377-96.

Tress, M. L., P. L. Martelli, et al. (2007). "The implications of alternative splicing in the ENCODE protein complement." Proc Natl Acad Sci U S A **104**(13): 5495-500.

Turck, N., O. Lefebvre, et al. (2006). "Effect of laminin-1 on intestinal cell differentiation involves inhibition of nuclear nucleolin." J Cell Physiol **206**(2): 545-55.

Tyers, M. and M. Mann (2003). "From genomics to proteomics." Nature **422**(6928): 193-7.

Uitto, P. M., B. K. Lance, et al. (2007). "Comparing SILAC and two-dimensional gel electrophoresis image analysis for profiling urokinase plasminogen activator signaling in ovarian cancer cells." J Proteome Res **6**(6): 2105-12.

Umar, A., A. B. Buermeyer, et al. (1996). "Requirement for PCNA in DNA mismatch repair at a step preceding DNA resynthesis." Cell **87**(1): 65-73.

Unlu, M., M. E. Morgan, et al. (1997). "Difference gel electrophoresis: a single gel method for detecting changes in protein extracts." Electrophoresis **18**(11): 2071-7.

Unwin, R. D., D. L. Smith, et al. (2006). "Quantitative proteomics reveals posttranslational control as a regulatory factor in primary hematopoietic stem cells." Blood **107**(12): 4687-94.

Van Themsche, C., T. Alain, et al. (2004). "Stromelysin-2 (matrix metalloproteinase 10) is inducible in lymphoma cells and accelerates the growth of lymphoid tumors in vivo." J Immunol **173**(6): 3605-11.

Villanueva, J., D. R. Shaffer, et al. (2006). "Differential exoprotease activities confer tumor-specific serum peptidome patterns." J Clin Invest **116**(1): 271-84.

Visintin, I., Z. Feng, et al. (2008). "Diagnostic markers for early detection of ovarian cancer." Clin Cancer Res **14**(4): 1065-72.

Vivanco, I. and C. L. Sawyers (2002). "The phosphatidylinositol 3-Kinase AKT pathway in human cancer." Nat Rev Cancer **2**(7): 489.

Volkert, M. R., N. A. Elliott, et al. (2000). "Functional genomics reveals a family of eukaryotic oxidation protection genes." Proc Natl Acad Sci U S A **97**(26): 14530-5.

Volmer, M. W., K. Stuhler, et al. (2005). "Differential proteome analysis of conditioned media to detect Smad4 regulated secreted biomarkers in colon cancer." Proteomics **5**(10): 2587-601.

Vuillermoz, B., A. Khoruzhenko, et al. (2004). "The small leucine-rich proteoglycan lumican inhibits melanoma progression." Exp Cell Res **296**(2): 294-306.

Vuong, G. L., S. M. Weiss, et al. (2000). "Improved sensitivity proteomics by postharvest alkylation and radioactive labelling of proteins." Electrophoresis **21**(13): 2594-605.

Walsh, N., P. Dowling, et al. (2008). "Aldehyde dehydrogenase 1A1 and gelsolin identified as novel invasion-modulating factors in conditioned medium of pancreatic cancer cells." J Proteomics **71**(5): 561-71.

Wang, G., W. W. Wu, et al. (2006). "Label-free protein quantification using LC-coupled ion trap or FT mass spectrometry: Reproducibility, linearity, and application with complex proteomes." J Proteome Res **5**(5): 1214-23.

Wang, H., D. G. Rosen, et al. (2006). "Insulin-like growth factor-binding protein 2 and 5 are differentially regulated in ovarian cancer of different histologic types." Mod Pathol **19**(9): 1149-56.

Wang, K. L., T. T. Wu, et al. (2006). "Expression of annexin A1 in esophageal and esophagogastric junction adenocarcinomas: association with poor outcome." Clin Cancer Res **12**(15): 4598-604.

Wang, S., N. Nath, et al. (1999). "Prohibitin, a potential tumor suppressor, interacts with RB and regulates E2F function." Oncogene **18**(23): 3501-10.
Watanabe, T., N. Shinohara, et al. (2000). "Significance of the Grb2 and son of sevenless (Sos) proteins in human bladder cancer cell lines." IUBMB Life **49**(4): 317-20.
Welcsh, P. L., M. K. Lee, et al. (2002). "BRCA1 transcriptionally regulates genes involved in breast tumorigenesis." PNAS **99**(11): 7560-7565.
Welcsh, P. L., K. N. Owens, et al. (2000). "Insights into the functions of BRCA1 and BRCA2." Trends Genet **16**(2): 69-74.
Welsh, J. B., L. M. Sapinoso, et al. (2003). "Large-scale delineation of secreted protein biomarkers overexpressed in cancer tissue and serum." Proc Natl Acad Sci U S A **100**(6): 3410-5.
Wolf, N. G., F. W. Abdul-Karim, et al. (1999). "Analysis of ovarian borderline tumors using comparative genomic hybridization and fluorescence in situ hybridization." Genes Chromosomes Cancer **25**(4): 307-15.
Wu, C. C., K. Y. Chien, et al. (2005). "Cancer cell-secreted proteomes as a basis for searching potential tumor markers: nasopharyngeal carcinoma as a model." Proteomics **5**(12): 3173-82.
Wu, W., W. Hu, et al. (2002). "Proteomics in cancer research." Int J Gynecol Cancer **12**(5): 409-23.
Xia, S. H., L. P. Hu, et al. (2002). "Three isoforms of annexin I are preferentially expressed in normal esophageal epithelia but down-regulated in esophageal squamous cell carcinomas." Oncogene **21**(43): 6641-8.
Xue, L. Y., L. H. Teng, et al. (2007). "[Expression of annexin I in different histological types of carcinomas]." Zhonghua Zhong Liu Za Zhi **29**(6): 444-8.
Yamanaka, Y., E. M. Wilson, et al. (1997). "Inhibition of insulin receptor activation by insulin-like growth factor binding proteins." J Biol Chem **272**(49): 30729-34.
Yamazaki, D., S. Kurisu, et al. (2005). "Regulation of cancer cell motility through actin reorganization." Cancer Sci **96**(7): 379-86.
Yang, R. Y. and F. T. Liu (2003). "Galectins in cell growth and apoptosis." Cell Mol Life Sci **60**(2): 267-76.
Yarden, Y. (2001). "Biology of HER2 and its importance in breast cancer." Oncology **61**(Suppl 2): 1-13.
Yi, E. C. and D. R. Goodlett (2004). "Quantitative protein profile comparisons using the isotope-coded affinity tag method." Curr Protoc Protein Sci **Chapter 23**: Unit 23 2.
Yoshio, T., T. Morita, et al. (2007). "Caldesmon suppresses cancer cell invasion by regulating podosome/invadopodium formation." FEBS Lett **581**(20): 3777-82.
Young, T., F. Mei, et al. (2005). "Proteomics analysis of H-RAS-mediated oncogenic transformation in a genetically defined human ovarian cancer model." Oncogene **24**(40): 6174-84.
Yu, K. H., C. G. Barry, et al. (2009). "Stable isotope dilution multidimensional liquid chromatography-tandem mass spectrometry for pancreatic cancer serum biomarker discovery." J Proteome Res **8**(3): 1565-76.
Yuce, K., C. Baykal, et al. (2001). "Diagnostic and prognostic value of serum and peritoneal fluid lactate dehydrogenase in epithelial ovarian cancer." Eur J Gynaecol Oncol **22**(3): 228-32.

Zacharius, R. M., T. E. Zell, et al. (1969). "Glycoprotein staining following electrophoresis on acrylamide gels." Anal Biochem **30**(1): 148-52.

Zhang, Y., A. Wolf-Yadlin, et al. (2005). "Time-resolved mass spectrometry of tyrosine phosphorylation sites in the epidermal growth factor receptor signaling network reveals dynamic modules." Mol Cell Proteomics **4**(9): 1240-50.

Zhang, Z., R. C. Bast, Jr., et al. (2004). "Three biomarkers identified from serum proteomic analysis for the detection of early stage ovarian cancer." Cancer Res **64**(16): 5882-90.

Zhao, C., A. Hashiguchi, et al. (2002). "Exogenous expression of heat shock protein 90kDa retards the cell cycle and impairs the heat shock response." Exp Cell Res **275**(2): 200-14.

Zhao, Y., W. Zhang, et al. (2004). "Proteomic analysis of integral plasma membrane proteins." Anal Chem **76**(7): 1817-23.

Zumkeller, W. (2001). "IGFs and IGFBPs: surrogate markers for diagnosis and surveillance of tumour growth?" Mol Pathol **54**(5): 285-8.